Université de Montréal

The roles of Protein Phosphatase 2A in nuclear envelope reformation after mitosis in *Drosophila*

Par

Haytham Mehsen

Faculté de Médecine

Thèse présentée en vue de l'obtention du grade de Doctorat en biologie moléculaire, Option biologie des systèmes.

Décembre 2019

Résumé

Pendant le bris de l'enveloppe nucléaire, la kinase dépendante des cyclines liée à la cycline B (CDK1-cycline B) et d'autres kinases phosphorylent des protéines nucléaires conduisant au désassemblage des complexes de protéines de l'enveloppe nucléaire. Les protéines nucléaires phosphorylées sont ensuite déphosphorylées par un groupe de phosphatases en sortie mitotique. La protéine phosphatase 2A en complexe avec la sous-unité régulatrice B55 (PP2A-B55) est connue pour être la principale phosphatase à déphosphoryler les protéines critiques à la fin de la mitose. Cependant, les substrats nucléaires déphosphorylés par PP2A-B55 à la sortie mitotique sont peu connus.

En utilisant des cellules de drosophile en culture, nous avons démontré que PP2A-B55 est nécessaire pour le recrutement de protéines de l'envelope nucléaire telles que BAF, la protéine de lamina nucléaire Lamin B et la nucléoporine Nup107. De plus, nous avons trouvé que les œufs de femelles des drosophiles hétérozygotes pour une mutation dans les gènes codant pour la Lamine B et Tws (B55 chez la drosophile) n'éclosent pas. Ces œufs présentent divers défauts au stade de la méiose et des divisions nucléaires de l'embryon syncytial. De plus, des tests *in vitro* et d'autres analyses biochimiques indiquent que PP2A-Tws se lie et déphosphoryle BAF. J'ai d'autres résultats qui suggèrent un rôle de la protéine Ankle2 dans la régulation du recrutement de BAF pour réassembler les noyaux à la sortie mitotique. Mes résultats suggèrent également que Ankle2 en complexe avec PP2A est responsable de la bonne progression mitotique. Mes résultats mettent en évidence l'utilité de la drosophile comme système modèle dans l'étude de différents aspects du cycle cellulaire. Ils démontrent également un rôle de PP2A dans la reformation de l'enveloppe nucléaire en fin de mitose.

Mots clés: PP2A-B55, Ankle2, reformation d'enveloppe nucléaire, *Drosophile*, mitose.

Abstract

During nuclear envelope breakdown, the cyclin-dependent kinase 1 bound to Cyclin B (CDK1-Cyclin B) and other kinases phosphorylate a number of nuclear proteins leading to the disassembly of nuclear envelope protein complexes. Phosphorylated nuclear proteins are then dephosphorylated by a group of phosphatases at mitotic exit. The protein phosphatase 2A in complex with the regulatory subunit B55 (PP2A-B55) is known to be the major phosphatase to dephosphorylate critical proteins at the end of mitosis. However, little was known about the nuclear substrates dephosphorylated by PP2A-B55 at mitotic exit. Using *Drosophila* cells in culture, we demonstrated that PP2A-B55 is required for the recruitment of nuclear envelope proteins such as BAF, the nuclear lamina protein Lamin B, and the nucleoporin Nup107. Also, eggs from *Drosophila* females heterozygous for a mutation in genes coding for Lamin B and Tws (B55 in *Drosophila*), didn't hatch. These eggs showed various defects during the nuclear division stage and meiosis. Moreover, *in vitro* assays and other biochemical analyses indicate that PP2A-B55 binds and dephosphorylates BAF. I have other results that suggest a role of the protein Ankle2 in regulating BAF recruitment to reassembling nuclei at mitotic exit. My results also suggest that Ankle2 in complex with PP2A is responsible for the proper mitotic progression. Our results highlight the importance of *Drosophila* in investigating different aspects of the cell cycle. It also demonstrates a role of PP2A in the nuclear envelope reformation at the end of mitosis.

Key words: PP2A-B55, Ankle2, nuclear envelope reformation, *Drosophila*, mitosis.

Table of contents

Figures list

Tables

List of Abbreviations

MTOC: Microtubule Organizing Center

NE: Nuclear envelope

NEBD: Nuclear envelope breakdown

NER: Nuclear envelope reformation

CDK: Cyclin dependent kinase

CAK: Cyclin activating kinase

KAP: Kinase-interacting phosphatase

CKI: CDK inhibitor proteins

APC: Anaphase promoting complex

PLK: Polo-like kinases

PP2A: Protein phosphatase 2A

GWL: Greatwall kinase

ER: Endoplasmic reticulum

NPC: Nuclear pore complex

NLS: Nuclear localization signal

NES: Nuclear export signal

Nup: Nucleoporin

KASH domain: (Klarsicht, Anc-1, Syne-1, homology) domain

SUN domain: (Sad1p/UNC-84) domain

LEM domain: (LAP2, Emerin, and MAN1) domain

LBR: Lamin B receptor

DNA: Deoxyribonucleic acid

RNA: Ribonucleic acid

RRM: RNA recognition motif

BAF: Barrier-to-autointegration-factor

PIC: Pre-integration complex

RNAi: RNA interference

PKC and PKA: Protein kinase C and A

OA: Okadaic acid

UAS: upstream activating sequence

SAC: Spindle assembly checkpoint

cGAS: Cyclic GMP-AMP synthase

STING: stimulator of Interferon Genes (STING)

Acknowledgments

I would like to start by thanking Dr. Vincent Archambault for accepting me as a student in his laboratory. During the time in his lab, I always felt that he was not only a supervisor but an older brother. He was always available to teach me various techniques and to give me feedback whenever I asked for it. He also helped me in writing my paper and my scholarship applications. With his help, my English writing improved a lot. It would be very difficult to forget the time I spent in his laboratory.

I would also like to thank all the lab members, especially Karine Normandin. In addition, in helping me to improve my French skills, she helped me a lot during my experiments and my work in the laboratory, and I enjoyed talking to her. I like to thank Damien Garrido, Mohammed Bourouh, David Kachaner, and Myreille Larouche. It was great working with all of you. I cannot forget to thank Laia Jordana, who helped me a lot towards the end of my project. She is great and hardworking, and I am sure she will accomplish great things in the laboratory. I also would like to thank Maissa Babouder who gave me a lot of nice ideas and support.

I am also thankful for all my committee members, Dr. Sebastien Carreno, Dr. Philippe Roux, and Dr. Jose Teodoro, for all their feedback and for spending time to look at my work. I also want to thank Dr. Marc Therrien, Gregory Emery, and all the fly lab members for their feedback. I also would like to thank Christian Charbonneau for his help in working on the microscopes and analyzing my images.

Finally, I would like to thank my wife Kamar, who gave me unlimited support and was always there for me when I needed her. I cannot forget mentioning my daughter Jasmine

who will always be in my heart and mind. I also want to thank my mother and my father. I hope they will be proud of me for what I accomplished.

Chapter 1: General Introduction

Background and Organization of the Chapters

As I am writing these words, I remember how this project was born. During my first meeting with Dr. Vincent Archambault in 2013 to discuss my master's project, he told me that the only thing we know is that there is a potential interaction between the gene *lamin* (expresses the protein Lamin B of the nuclear lamina) and the gene *tws (*expresses the B55 regulatory subunit of the protein phosphatase 2A (PP2A). From that point, we became interested in whether PP2A-B55 plays a role in regulating nuclear envelope reformation during the exit from mitosis. Many results showed that a significant number of proteins are phosphorylated at the beginning of mitosis, principally by the cyclin-dependent kinase 1 bound to cyclin B (CDK1-cyclin B). However, little is known about the nature of the phosphatase that dephosphorylates these proteins when the cell exits mitosis. Recent publications suggested a role of PP2A-B55 in dephosphorylating CDK1-cyclin B substrates. Following a genetic screen performed in the laboratory, we found a possible genetic interaction between *tws* and several genes expressing nuclear envelope proteins. Therefore, my project was to discover the potential role of PP2A-B55 in the nuclear envelope reformation (NER) at the end of mitosis.

I will start my thesis by an introduction in **Chapter 1** were I first explain the different stages of the cell cycle and the different events taking place during mitosis in **section 1.1.** Since I used the fruit fly *Drosophila melanogaster* as the model organism in my project, I talk about the life cycle of this organism and discuss its importance in research in **section 1.2.** In **section 1.3**, I talk about the cell cycle control system, which is composed of cyclin-dependent kinases bound to proteins called cyclins. I discuss the roles of these enzymes and how they are regulated during the cell cycle. Since my project is principally about mitosis, I talk about the different events taking place during mitotic entry in **section 1.4** and mitotic exit in **section 1.5.** In addition, in these sections, I also discuss the kinases regulating mitotic entry and the phosphatases regulating mitotic exit. In **section 1.6**, I describe the different components of the nuclear envelope. I also focus on describing the role of the different proteins in each part of the nuclear envelope. Then, I describe the processes of nuclear envelope breakdown (NEBD) and reformation in sections **1.7** and **1.8**. I focus more on discussing previous publications about the role of the different kinases and phosphatases in the process of NEBD and NER, concentrating more on the role of

PP2A-B55 in the reformation process. I end the introduction by raising questions about the role of PP2A-B55 in the NER process and the role of a new protein called Ankle2 in this mechanism.

In **Chapter 2**, I present my work published in JCB in 2018, where we showed that PP2A-B55 promotes NER by dephosphorylating a small protein called BAF and possibly other nuclear envelope proteins.

In **Chapter 3,** I show strong evidence of the role of the protein Ankel2 in NER. In addition, I show results from *in vivo* experiments about the role of Ankle2 in mitotic progression during early fly embryo development.

In **Chapter 4**, I discuss the major questions that need to be answered in this project and experiments that are required to be done to answer these questions. I also discuss how my project will help in the advancement of knowledge in the cell cycle field. I also mention how results from my project might help in finding new targets for cancer drug discovery.

1.1 The Cell Cycle

One of the essential properties of the cell is its ability to divide. Cell division is a requirement for a multicellular organism to develop and grow. During development, the fertilized egg (zygote) divides successively to give rise to a new multicellular organism. Moreover, cells of an organism need to divide repeatedly to renew old or dead cells for maintaining tissue integrity [1]. The cell cycle is a series of events by which a mother cell divides, giving rise to two genetically identical daughter cells. In eukaryotic cells, the cell cycle is composed of interphase (consisting of G1, S, and G2 phases) and M-phase (consists of mitosis and cytokinesis) (**Fig 1.1**) [2]. I will be discussing the processes taking place during interphase and M-phase in more detail below.

1.1.A. Interphase

The interphase is the most prolonged phase of the cell cycle. The first period of interphase is called the Gap 1 phase or G1 (**Fig. 1.1**). The G1 phase is critical for preparing chromosomes for DNA replication and starts when the cell manufactures all RNAs and proteins required for DNA synthesis [3]. These events are not induced spontaneously but triggered by external stimuli. In the absence of growth factors, the cell is in a quiescent phase known as the G0 phase. When growth factors are present, the cell exits G0 and enters G1. A restriction point called the R point is also present between both phases and determines whether the cell stays in G0 or progresses to G1 [4]. When the cell crosses this point, it enters G1 independent of external stimuli [2, 4]. The second period of interphase is the DNA synthesis phase or S phase. During this phase, the cell also expresses proteins required for DNA repair, thus maintaining DNA integrity during

replication. In addition to DNA replication, centrosomes are duplicated during the S phase. These structures are crucial for cell division, as they are the principal Microtubule Organizing Centers (MTOC) from which most cell microtubules nucleate. These microtubules serve as an essential requirement during the process of mitosis [5]. The last phase of interphase is another Gap phase known as the G2 phase, in which the cell grows and prepares for division (**Fig. 1.1**). During this phase, duplicated centrosomes start to separate to opposite cell poles [5], and the cell expresses proteins required for mitosis.

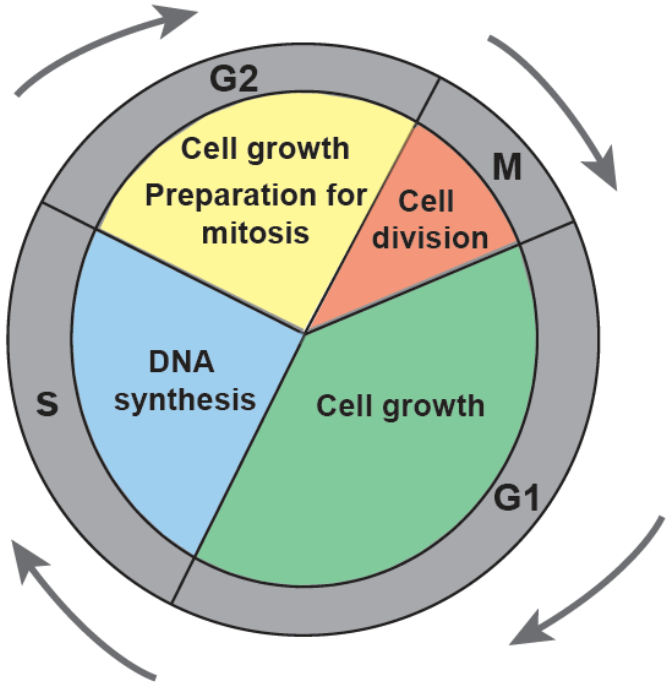

Figure 1.1: Different stages of the cell cycle. Briefly, the cell cycle is composed of interphase which consists of G1, S and G2 phase, and M-phase which consists of mitosis (nuclear division) and cytokinesis (cytoplasmic division).

1.1.B. Mitosis

Mitosis is known to be composed of five events: prophase, prometaphase, metaphase, anaphase, and telophase. Each of these events constitutes a set of different processes (**Fig 1.2**). The most important events that occur during prophase are chromatin condensation to chromosomes and cytoskeleton reorganization to form the mitotic spindle [2]. The thread-like structured chromatin twists around proteins called histones to form an

octamer structure. This process takes place during the S phase. At early mitosis, several twisting events of chromatin follow, and mitotic chromosomes are constructed [6]. These chromosomes constitute of two sister chromatids attached at the centromere. In the cytoplasm, the mitotic spindle, consisting of microtubules, assembles between the two centrosomes [7]. This process is also maintained through the help of microtubule-dependent motor proteins called kinesins [2, 8]. Microtubules of the mitotic spindle are divided into three categories: Astral microtubules, kinetochore microtubules, and overlap microtubules, each of which serves a specific function during cell division. After chromosome condensation and mitotic spindle assembly, the nuclear envelope breakdown (NEBD) marks the end of prophase (**Fig 1.2**). This process takes place during prometaphase. Various proteins of the nuclear envelope (NE) disassemble and are soluble in the cytoplasm [9]. During prometaphase, also, centrosomes continue to separate and are found at opposite poles of the cell, and microtubules are now ready for division (**Fig 1.2**). The attachment of kinetochore microtubules to kinetochores also takes place during prometaphase. Kinetochores are protein complexes of about 100 polypeptides that assemble and bind to each chromatid of a chromosome [6, 10]. After binding of microtubules to kinetochores, chromosomes start to move and align to the cell equatorial plate during metaphase (**Fig 1.2**). Metaphase is a quick process and is sometimes hard to specify since some chromosomes do not stay at the equator. However, it is easier to notice the end of metaphase, as it happens when the first sister chromatid separates, and the cell enters anaphase [6]. Early anaphase, known as anaphase A, starts when microtubules shorten to decrease the distance between chromosomes and the poles (**Fig 1.2**). During late anaphase or anaphase B, the spindle elongates to push the chromosomes to the poles [6]. Astral and overlap microtubules are the types of

microtubules known to function during anaphase A and B. The last step of mitosis is telophase, where the spindle elongation persists, pushing more chromosomes to the poles. Also, proteins of the NE start to assemble around chromosomes to mark the start of nuclear envelope reformation (NER) (**Fig 1.2**). Chromosomes then decondense to chromatin, and the cell prepares for its physical separation or cytokinesis [6] (**Fig 1.2**).

1.1.C. Cytokinesis

Cytokinesis is the process by which the cytoplasm of a dividing cell splits into two daughter cells. It first starts with the formation of the central spindle, a region of antiparallel overlapping microtubules, at the equatorial zone of the cell. A molecular signaling pathway, that depends on the function of the protein RhoA between the cortex and the anaphase spindle, is known to induce the formation of the contractile ring [11]. After The contractile ring is composed of other types of filamentous proteins such as myosin, actin, and anillin. These structural proteins create forces that further constrict the ring to form the midbody region. Finally, a complex of filamentous proteins called ESCRT-III catalyzes the cell membrane scission to generate the two daughter cells (**Fig 1.2**). This process is also known as abscission [11].

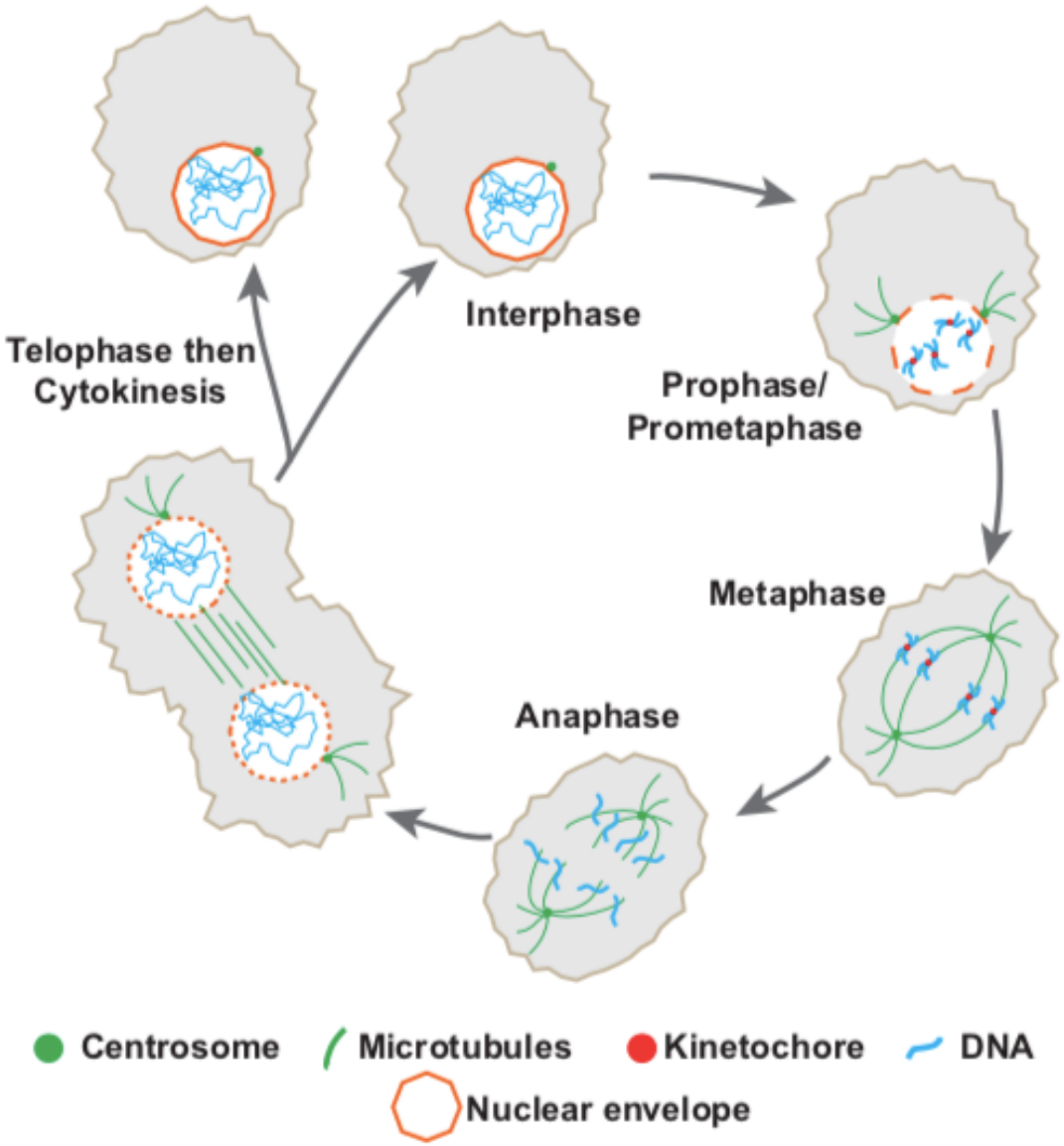

Figure 1.2: Different events occurring during M-phase. During prophase/prometaphase, chromatin condenses to chromosomes and the nuclear envelope breaks down. Chromosomes align at the equatorial plate at metaphase. At anaphase, sister chromatids separate to opposite poles. Chromosomes decondense and the nuclear envelope reforms at telophase. Two daughter cells form during cytokinesis.

1.2 *Drosophila melanogaster* as a model

1.2.A. The fruit fly model, its short life cycle and advantages:

The *Drosophila melanogaster*, or the fruit fly, is one of the known model organisms currently used in biomedical research. The fruit fly has also been extensively used in the past for many genetic investigations [12]. The first interest in using the fruit fly as a model organism was the discovery of polytene chromosomes found in the fruit fly salivary glands [13]. Then, the fruit fly was used to investigate complex developmental processes and important developmental genes were identified. Scientists use *Drosophila* because of its ease of manipulation, a small number of chromosomes (4 chromosomes), a short life cycle, and a small well-sequenced genome [12, 14]. Also, most of the fruit fly genome is well conserved through evolution. For example, about 61% of the fruit fly genome is present in the human genome, and about 75% of human disease-causing genes also exist in *Drosophila* [15]. At 25 ^{0}C, the life cycle of the fruit fly from the moment when the egg is laid to become an adult is 10 days (**Fig 1.3)**. One day after the egg hatches, the first instar larva forms which then increases in size to become a third instar larva after two days. Three days after that, the larva sticks on a surface, and turns into a pupa. Then, after about four days, all the organs and the tissues of the fly in the pupa are completely formed, and the adult fly is now ready to exit the pupa case (**Fig 1.3)** [14].

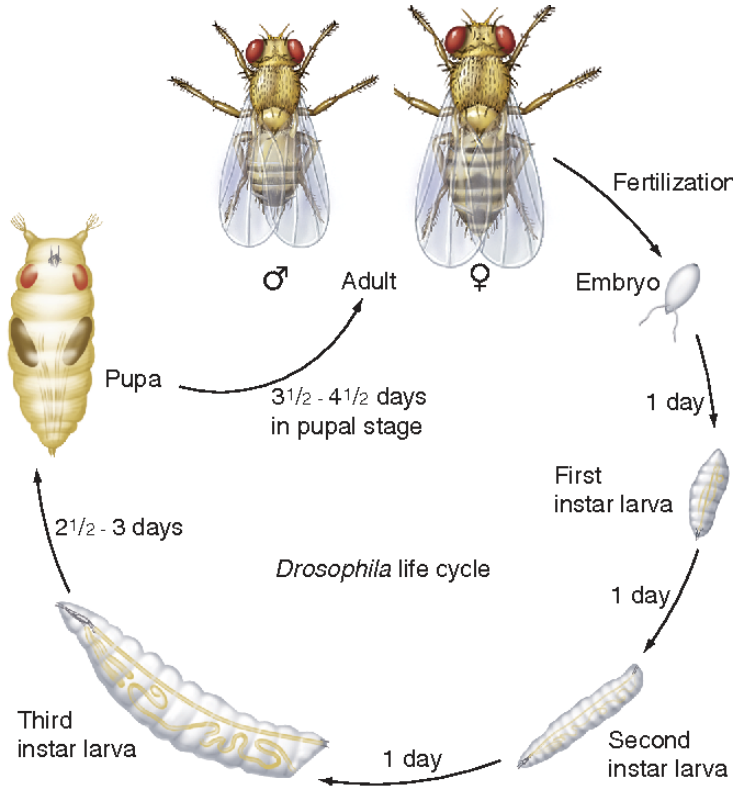

Figure 1.3: The life cycle of the *Drosophila melanogaster*. Following egg fertilization, an embryo starts to develop to reach the third instar larva after three days. After another two to three days, a pupa is formed. An adult fly then exits the pupa after about four days. The figure was taken from [16], with permission from McGraw-Hill.

1.2.B. The fruit fly as a tool in research

The great advantage of using *Drosophila melanogaster* as a model organism is the vast number of different approaches that could be developed. Regarding genetic approaches, the existence of P-element and chemically generated mutations made it possible to perform different genetic screens. P-elements are transposable DNA pieces that are inserted in genes to modify their function. However, some P-elements fail to affect the gene function, and the protein expressed by that gene remains functional [17]. Hence, null mutations are more powerful than gene mutations created by P-element insertions. In addition, and due to the presence of the Gal4/UAS system, expressing an external DNA fragment is possible [18, 19]. The system had been previously discovered in yeast [19]. The Gal4 protein binds to the upstream activating sequence (UAS) promoter to induce the

expression of the downstream gene. With that system, a gene or a dsRNA could be placed downstream of the UAS promoter and inserted in the fly genome [18]. Also, the Gal4 protein could be inserted in another fly where it would be expressed. Interestingly, a drug-inducible or tissue-specific promoter could be placed upstream of the DNA sequence coding for Gal4 [19]. Then, the fly expressing Gal4 is crossed with another fly having the UAS sequence with the transgene, and the transgene is expressed in the F1 generation [18].

The most exciting aspect of the fruit fly is the ability to be used for performing genetic screens. One of the best-known types of genetic screens that are performed using *Drosophila* is the one used to identify recessive lethal genes [20]. Flies are either exposed to UV or fed with a mutagen to create mutations at different sites of the genome. Then, after multiple crosses, flies homozygous for a lethal gene die, and a recessive lethal gene is identified. Since the identified gene is homozygous lethal, it is difficult to maintain that fly line over time. For this, balancer chromosomes now exist to maintain fly lines with recessive lethal mutants [20]. These chromosomes are homozygous-lethal and possess several chromosomal inversions, which make it impossible for meiotic recombination to take place, thus maintaining one copy of the mutant gene in the fly line [20].

The Bloomington stock center contains a massive number of fly stocks with genes mutations and chromosomal deletions covering the whole fly genome. Now, specialized companies exist to produce transgenic lines that might be difficult to produce in the laboratory. Also, other companies provide services to generate a fly with a CRISPR/Cas9 knockout genes [21]. In addition, an RNAi screen library is also available to be tested in fly cells in culture. Immunofluorescence could be easily applied either on fly embryos, ovaries, or any other fly tissue. Recent studies showed that it is also possible to inject

embryos with inhibitors, dyes, or specific proteins followed by live imaging. For our research, the fruit fly is an excellent model organism to study different aspects of cell division.

1.2.C. Meiosis and mitosis in *Drosophila*

When a fly egg is ovulated in the female ovary, the egg is arrested in metaphase 1 of the first meiotic division. After the egg is laid, meiosis proceeds and four meiotic products are formed next to the egg cortex [22]. One of the four products come to proximity with the male pronucleus, and NEBD takes place (**Fig 1.4)**. The genetic content of both pronuclei divide separately, and the first mitotic nuclear division occurs. The other four meiotic products fuse and form a polar body. Following this division, thirteen cycles of fast nuclear divisions take place in a syncytium [22]. These divisions are a series of S and M phases without Gap phases (**Fig 1.4)** [22]. The stage of development where these divisions occur is called the syncytial embryo development stage.

Drosophila mitosis during these nuclear divisions is semi-closed since a complete NEBD does not take place before prometaphase. Instead, small invaginations in the NE takes place near the poles, to allow astral microtubules to enter the nucleus [23]. Other than the absence of NEBD in the *Drosophila* nuclear division during early development, centrosome duplication doesn't take place during prophase but only during anaphase. Cytokinesis only occurs after the thirteenth cycle of nuclear division during a process called cellularization [24]. Since the RNA and proteins implicated in these thirteen nuclear divisions are maternally contributed, the role of a specific gene in these divisions can be investigated by modifying the female genome.

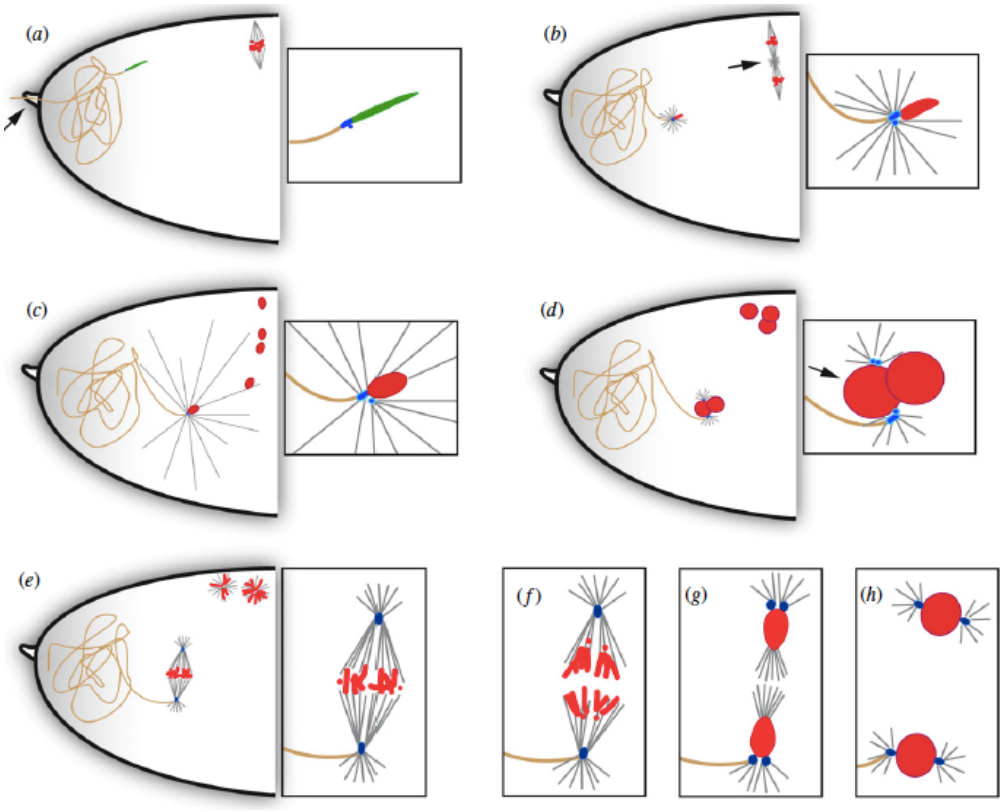

Figure 1.4: Meiosis and mitosis during early fly development. (a) When the egg is laid, it is arrested at the metaphase of the first meiotic division. (b) and (c) Meiosis completes until the formation of four meiotic products. d. The sperm fertilizes one of the four products and mitosis takes place in (e) and the three other meiotic products form a polar body. Figure taken from [22].

1.3 The cell cycle control system

For ensuring that the different processes of the cell cycle occur properly, a cell cycle control system, composed of a large group of proteins, exists. This control system works on three stages or checkpoints of the cell cycle: The G1/S transition which controls S phase and DNA replication, the G2/M which regulates the entry into mitosis, and the metaphase-anaphase transition that is important for completion of mitosis [25].

1.3.A. The cyclin-dependent kinases (CDKs) are master elements of the cell cycle control system

The cyclin-dependent kinases (CDKs) are serine/threonine kinases that are the critical components of the cell cycle control system. The name of these kinases comes from the fact that they are only active once they bound to a regulatory subunit called “cyclin.” These kinases are well conserved throughout evolution. For example, the cell cycle is controlled by CDK1 in both fission and budding yeast, CDK1, and CDK2 in *Xenopus*, CDK1, CDK2, and CDK4 in *Drosophila*, and CDK1, CDK2, CDK4, and CDK6 in humans [26]. Most of these CDKs are involved in regulating cell cycle events. However, other CDKs exist that either indirectly regulate the cell cycle (CDK7) or regulate other different processes such as gene transcription (CDK11) [26] and nerve cell differentiation (CDK5) [27]. CDK7 or cyclin activating kinase (CAK) is known to regulate the cell cycle by phosphorylating different CDKs leading to their activation. CDKs are responsible for phosphorylating a significant number of substrates. Following an extensive proteomic study, CDKs are known to favorably phosphorylate substrates on serine/threonine (S/T) followed by a proline (P) followed by any amino acid (X) and an arginine (R) and a lysine (K) [27, 28].

1.3.B. Mechanisms for Cyclin-dependent kinases activation

Activation of these kinases do not depend on their cellular concentration, but mostly on variable cyclin levels during each checkpoint of the cell cycle. Once present at high levels, cyclin binds tightly to CDKs to induce a conformational change leading to their activation. In the absence of cyclin binding, a stretch of amino acids found at the carboxy-

terminal lobe of CDK called the T-loop, blocks the substrate binding to the CDK active site [29, 30]. Each CDK can bind several types of cyclins which are expressed and degraded at a specific stage of the cell cycle (**Fig 1.5**). Some cyclins are expressed during G1, while others are encoded at G1/S, S phase, or M-phase, and hence are called G1 cyclins, G1/S cyclins, S cyclins, and M cyclins respectively. For example, in human cells, G1 cyclins are cyclin D1,2, and 3, G1/S cyclin is cyclin E, S cyclin is cyclin A at S, and M cyclin is cyclin B (**Fig 1.5**) [2, 27]. Due to their importance in the control of the cell cycle, these cyclins are conserved among different organisms. Also, other forms of cyclins are present. For instance, cyclin B3 is a well-conserved cyclin and is critical for the metaphase-to-anaphase transition both in mitosis and meiosis [31, 32]. Moreover, a recent study in female mice shows that cyclin B3 is essential for a proper progression of oocyte meiosis [33].

The cyclin binding to CDK is not only essential for its activation but also helps in the ability of CDK to recognize specific substrates. For instance, a hydrophobic patch, found on the surface of cyclin A, is necessary for the cyclin interaction with another hydrophobic patch called the RXL motif found in the substrate [34]. When the substrate-cyclin patches interact, the substrate-kinase affinity increases, leading to an increase in the rate of substrate phosphorylation. Moreover, cyclin binding to CDK is also crucial to target the CDK-cyclin complex to specific subcellular regions. For example, before NEBD in an animal cell, CDK1-cyclin B is found in the cytoplasm [35]. When the cell enters mitosis, CDK1-cyclin B translocates to the nucleus to phosphorylate NE substrates to induce NEBD [35].

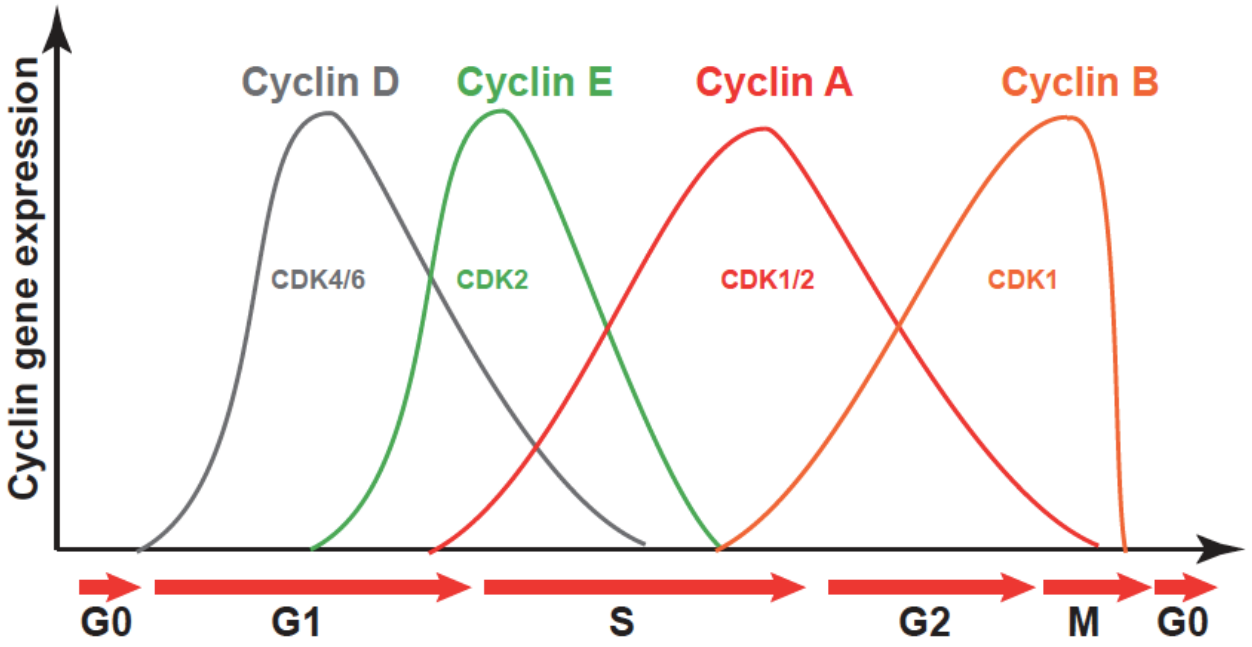

Figure 1.5: The level of expression of different cyclins in a eukaryotic cell during different stages of the cell cycle. Cyclin D expression is maximal during G1 and becomes in complex with CDK4/6. Cyclin E expression is high during the G1/S transition and is in complex with CDK2. Cyclin A expression peaks during S phase and becomes in complex with CDK1/2. Cyclin B expression is maximal during M phase and is in complex with CDK1.

Cyclin binding to CDKs is the first step in their partial activation, but other requirements are critical for their full activation. The first indispensable requirement is the phosphorylation of CDK on a Thr residue at positions 160/161 (depending on the type of CDK) next to its kinase active site [29, 36]. CDK7-cyclin H or CAK is the kinase responsible for phosphorylating these sites. Another requirement for full CDK activation is the dephosphorylation of Thr14 and Tyr15 residues next to the ATP-binding pocket. The kinase Wee1 phosphorylates these sites leading to CDK inhibition, possibly by affecting ATP binding to the ATP-binding pocket. Another kinase is also responsible for phosphorylation of these sites exits in vertebrates and is called Myt1 [29, 36]. To fully

activate the CDK-cyclin complex, the phosphatase Cdc25 dephosphorylates CDK on Thr14 and Tyr15. The dephosphorylation of these sites leads to a conformational change exposing the ATP-binding site to ATP for full CDK-cyclin activation. It is interesting to know that CDK1-cyclin M regulates Wee1 and Cdc25 activities at early mitosis. The active CDK1-cyclin M complex inhibits Wee1 and activates Cdc25 creating a positive feedback loop for further CDK1-cyclin M activation [36].

1.3.C. Mechanisms for of Cyclin-dependent kinases inhibition

At critical periods of the cell cycle, different mechanisms exist to inhibit the cell cycle control system or at least prevent its excessive activation. These mechanisms mainly inhibit CDK-cyclin complexes. One of the simplest ways to inhibit CDKs is to dephosphorylate Thr160/161 next to the kinase domain. Studies in human cells show that the kinase-interacting phosphatase (KAP), is responsible for the dephosphorylation of Thr160 on the human CDK2 monomer [37]. Also, the phosphatase PP2C is known to be capable of dephosphorylating CDK2 on Thr160 and CDK6 on an unknown site [38]. However, the nature of the phosphatase(s) dephosphorylating other CDKs remains unexplored.

Moreover, the inhibition by CDK inhibitor proteins (CKIs) is another mechanism responsible for reducing CDK-cyclins activity. These proteins inhibit the cell cycle control system by inhibiting CDK-cyclin complexes for maintaining a stable G1 or inducing a cell cycle arrest, such as in the case of DNA damage [39]. They do so by inhibiting CDK-cyclins S and M activity before G1. Like all elements of the cell cycle control system, CKIs are widely conserved through evolution, but their number varies between organisms. For example, two CKIs exit in *Drosophila* and about seven in humans. Two different families

of CKIs are known: Cip/Kip and INK4 family. The Cip/Kip family of CKIs inhibits CDK-cyclin complexes required for the G1/S transition and S phase [40]. Interestingly, inhibitors such as those of the Cip/Kip family can function to activate some CDK-Cyclin complexes. Members of the Cip/Kip family can bind to CDK4/CD6-cyclin D complexes and help in their assembly [39]. The other CKI family, INK4, lacks this feature and is mainly responsible for inhibiting the assembly of CDK4/CDK6 with their respective cyclins. Due to their vital role, different mechanisms are available to tightly regulate the activity of these CKIs. For instance, CKIs are phosphorylated by CDKs and destroyed by the proteasome to reduce the inhibition of CDK-cyclins S when the cell passes G1 [39].

Another, though more crucial mechanism for inhibiting the cell cycle control system is through protein degradation taking place at the G1/S phase and metaphase-to-anaphase transition. During the G1/S phase, CDK inhibitors are first ubiquitinated by a ubiquitin-protein ligase called SCF. This enzyme is composed of the subunits Skp1, cullin, and, the F-box protein [41]. The former two proteins are core subunits required for SCF activity. The latter component of the SCF enzyme is the most critical one as it confers substrate specificity [41]. For example, the binding of the F-box protein Cdc4 to the CKI inhibitor Sic1 in *Saccharomyces cerevisiae* leads to the start of the S phase after CDK-S cyclin activation. When SCF is active, it can ubiquitinate several CKIs. However, the ubiquitination and the destruction of such CKI are not random but are time specific. For the S phase to start, CDK-cyclin G1/S is active and phosphorylate Sic1 leading to its ubiquitination by SCF and its degradation by the proteasome [42]. Another ubiquitin-protein ligase is present during the cell cycle and is called the anaphase-promoting complex (APC). The APC is a massive E3 ubiquitin ligase complex that regulates the metaphase-to-anaphase transition and the stability of the G1 phase [43]. During the

metaphase-to-anaphase transition, a complex called the spindle assembly checkpoint (SAC) ensures correct attachment of sister chromatids to kinetochores [44]. When this happens, the SAC activates the APC [44] to ubiquitinate a protein called securin, leading to its proteolytic degradation. When securin is degraded, a protease called separase is active and releases the cohesion from sister chromatids leading to their separation at anaphase [43]. Also, the APC promotes S and M cyclin degradation to inactivate CDK-cyclin S and M, thus driving the cell to exit mitosis. APC targets such as securin and cyclins contain specific amino-acid motifs that are important for their ubiquitination and degradation. APC substrates targeted for degradation possess two motifs known as the D-box and the Ken-box that are required for APC-substrate recognition [43]. The targeting of the APC to its specific substrates doesn't depend on their phosphorylation as it is the case for SCF but requires the APC to bind to specific proteins called activator subunits. Two known proteins, Cdc20 and Cdh1, are known as APC activator subunits and are essential for APC activity during the cell cycle. The activation of APC by CDK phosphorylation induces Cdc20 binding leading to securin and M cyclins degradation and the exit from mitosis. On the other hand, and to stabilize the G1 phase, Cdh1 binds the APC complex, which continuously works on ubiquitinating S and M cyclins to target them to the proteasome [43]. During cell preparation for another division, CDKs phosphorylates Cdh1 releasing it from the APC. This event deactivates the APC until the metaphase-to-anaphase transition of the second cycle [43].

1.4 Regulation of mitotic entry

1.4.A. Cyclin-dependent kinases: Master regulators of mitotic entry

As explained before, the significant events occurring during the entry into mitosis are chromatin condensation, mitotic spindle assembly, and NEBD. During mitotic exit, chromatin decondenses, the mitotic spindle disassembles, and the NER takes place [45]. These processes are tightly regulated both in time and in space. Most substrates implicated in these events of mitotic entry were shown to be phosphorylated by CDK-cyclins M at mitotic entry [45]. When active, these CDK-M cyclins complexes phosphorylate multiple mitotic substrates to induce entry to mitosis [46, 47]. At the end of mitosis, M-cyclins are degraded by the APC, leading to CDK inactivation [48]. Phosphorylated mitotic substrates are then dephosphorylated by several phosphatases for the cell to exit mitosis [2, 45]. The major CDK implicated in the process of mitotic entry is CDK1, although some studies show that CDK2 could perform some mitotic functions in mammals [49]. As for all CDKs, CDK1 activates once bound to its respective cyclin. M-cyclins are widely conserved in evolution, and most organisms possess at least one M cyclin. For example, budding yeast contains six versions of cyclin B, four of which, when bound to CDK1, are implicated in mitotic entry regulation [50]. Fission yeast, on the other hand, composes three versions of cyclin B, where only one has mitotic functions [51]. The fruit fly contains three M cyclins: cyclin A, B, and B3 [32, 52]. When bound to CDK1, both cyclin A and B are essential in regulating specific major events of mitotic entry in *Drosophila*, whereas cyclin B3 contributes more in mitotic exit [31] and meiosis [33]. As in *Drosophila*, cyclin A and B are crucial in regulating entry to mitosis in vertebrates, and each of these cyclins is found in two versions: A1, A2, and B1, B2. Most studies performed

in human cells show that CDK1-cyclin B1 is vital in regulating major events of mitotic entry, though CDK1-cyclin A seems to be important in regulating critical mechanisms during prophase [53]. As mentioned before, cyclin binding to CDK is not enough to fully activate the CDK-cyclin complex. Indeed, cdc25 must dephosphorylate the sites Thr14 and Tyr15 on CDK1, initially phosphorylated by Wee1, for the full activation of the CDK1-M cyclin complex.

As my project is focusing on the mechanisms occurring after prophase, I will focus more on the role of CDK1-cyclin B and not CDK1-cyclin A. To induce events of mitotic entry, CDK1-cyclin B phosphorylates a vast repertoire of critical mitotic substrates. In *Xenopus*, CDK1 phosphorylates an essential microtubule-associated protein called XMAP215, an event that is essential for spindle assembly during mitosis. When CDK1 was incubated with XMAP215 *in vitro*, the rate of elongation of tubulin increased by more than 4-folds [54], suggesting that spindle assembly at mitotic entry requires XMAP215 phosphorylation by CDK1. The cytoskeleton disassembly is another event occurring at mitotic entry. In a study done using mouse cells, CDK1 phosphorylates the protein vimentin, an intermediate filament protein, found in the cell cytoskeleton. The phosphorylation of vimentin by CDK1 leads to its disassembly and thus contributes to cytoskeleton disassembly at the entry to mitosis [55]. Moreover, CDK1 is best known to regulate NEBD. After prophase, CDK1-cyclin B localizes to the NE and phosphorylates multiple NE proteins. We will discuss this in more detail in the following sections. CDK1-cyclin B also phosphorylates PRC1 [56], a microtubule-bundling protein [57], that is essential for spindle elongation at anaphase. This phosphorylation prevents PRC1 activity before anaphase [56]. Another fundamental substrate of CDK1-cyclin B is the APC complex. To activate the APC, CDK1-cyclin B first phosphorylates several members of

the complex. This phosphorylation induces the binding of Cdc20 to APC, leading to the full APC activation [58]. Then, the APC ubiquitinates cyclin B and induces its degradation by the proteasome, thus inactivating CDK1-cyclin B at the end of mitosis [59].

1.4.B. Other kinases also function in mitotic entry regulation

The importance of CDK-M cyclins in the regulation of mitotic entry has been highlighted long ago through studies performed in different model organisms. However, other kinases have been found to regulate some processes of mitotic entry. A genome-wide screen was conducted to identify kinases required for cell cycle progression. In this study, many kinases other than CDKs were found to regulate different phases of mitosis [60]. However, two of these kinases, the polo-like kinases (PLKs) and aurora kinase A and B, were shown to be important kinases for regulating mitotic entry.

PLKs contain an N-terminal kinase domain, required for their catalytic activity. In their C-terminal region, PLKs contain a domain called the Polo-box domain, which confers substrate specificity and targets the protein to different cellular locations [61]. To highlight their functional diversity, most PLKs localize to different subcellular compartments [62]. For example, the *Drosophila* PLK called Polo is diffused in the cytoplasm in interphase cells. During prophase, polo concentrates on centrosomes and kinetochores. Then, it localizes to the central spindle at anaphase and to the midbody during cytokinesis [62]. Most PLKs phosphorylates a wide range of substrates required for different mitotic events. For example, during cytokinesis, human Plk1 was shown to phosphorylate the protein Ect2. When phosphorylated, Ect2 binds the protein CYK4 to initiate a signaling cascade that leads to the initiation of the formation of the contractile ring during early cytokinesis [63]. Also, Plk1 phosphorylates PRC1 on a site different from that phosphorylated by

CDK1, to prevent early midzone formation before cytokinesis [64]. Due to its important role, PLKs are tightly regulated during mitosis. For example, human Plk1 is phosphorylated during mitosis on Ser 137 and Thr 210. These sites might be either phosphorylated by the kinases the Ser20-like kinase (SLK) or the polo-like kinase kinase 1 (xPlkk1). In mammalian cells, SLK phosphorylates and activates the mammalian Plk1 during the G2/M transition [65]. The *Xenopus* xPlkk1 is important for phosphorylating Plk1 during the G2/M transition, as the injection of xPlkk1 in *Xenopus* oocytes leads to a quick entry to mitosis [66]. Interestingly, the phosphorylation of Plk1 on Ser 137 and Thr 210 is sensitive to DNA damage, as the phosphorylation of Plk1 on these sites was inhibited during DNA damage, possibly through a Chk2-dependent mechanism [67, 68].

Aurora kinases are another type of kinases that regulate mitotic entry events. Aurora kinases are composed of an N-terminal kinase domain and another domain that confers substrate specificity and protein localization [69]. Two aurora kinases, A and B, are essential during mitotic entry [69]. Studies performed in different models, such as *Drosophila*, *C. elegans,* and human cells, showed that the aurora kinase A functions to assemble and stabilize the bipolar spindle during early mitosis [69, 70]. On the other hand, the aurora kinase B has roles in controlling the structure and segregation of sister chromatids, where it functions in stabilizing the interaction between kinetochores and the mitotic spindle [69, 71]. The activation of aurora kinases not only relies on their phosphorylation state but also on their binding to regulatory proteins for their subcellular localization. For example, the aurora A kinase binds a protein called TPX2, required for targeting the kinase to microtubules [70]. Also, a study in yeast and human cells showed that the phosphatase inhibitor-2 is also vital for aurora A activation [72]. For aurora B activation, the kinase first binds to the proteins INCENP and survivin, which are members

of the chromosomal passenger complex [73]. When attached to these proteins, aurora B translocates to its respective locations to perform its function.

1.5 Regulation of mitotic exit

When the APC complex triggers the degradation of cyclin B, CDK1-cyclin B is inactivated to prevent the overphosphorylation of mitotic substrates and to prepare the cell for mitotic exit [74]. On the other hand, different events that occur at mitotic entry needs to be reversed. For example, the mitotic spindle should disassemble, the NE should reform, and chromosomes must decondense [2]. For these events to occur, a wide range of substrates that were phosphorylated at mitotic entry are dephosphorylated by multiple phosphatases at mitotic exit [74, 75]. Among the vital phosphatases implicated in the dephosphorylation of mitotic substrates is the protein phosphatase 2A carrying the regulatory subunit B55 (PP2A-B55) and PP1 [76]. However, many other phosphatases also contribute to this process. In this section, we will be discussing the role of these phosphatases in mitotic exit and the mechanisms of their regulation.

1.5.A. The protein phosphatase 2A: An important regulator of mitotic exit

1.5.A.a. The structure of the PP2A complex

PP2A belongs to the PPP protein phosphatase family, the largest family of serine/threonine phosphatases that is found in eukaryotes. The family includes, in addition to PP2A and PP1, PP2B, PP4, PP5, PP6, and PP7 [76]. As other protein phosphatases, PP2A is not functional in its monomeric form but is only active when it forms a

heterotrimeric complex. The complex composes of a catalytic subunit (PP2AC), a scaffolding subunit (PP2AA), and a regulatory B subunit that is essential for PP2A substrate specificity and subcellular localization [76] (**Fig 1.6**). The regulatory subunits in mammals are diverse and grouped in four families based on the similarity of their amino acid sequence and their three-dimensional structure. The four families of the PP2A regulatory subunits are B55 (PR55/B), B56 (PR61, B'), B72 (PR72/B''), and Striatin (PR93/B''') [76]. Both the B55 and B56 subunits play essential roles in regulating events of mitotic exit, while other subunits have other functions in the organism. B55 and B56 also exist in different isoforms in mammals. The B55 subunit is present in the α, β, γ, and δ isoforms, while B56 exists in α, β, γ,δ, and ε [76]. All of the different subunits of PP2A are present in various species, though in varying numbers. The PPP2AC in mammals and *Xenopus* is also named PPH21 in budding yeast [77], mts in *Drosophila* [78], and let-92 in *C.elegans* [79]. The scaffolding subunit PPP21RB in mammals and *Xenopus* is also named TPD3 in budding yeast [77], Pp2A-29 in *Drosophila* [78], and ppa-1 in *C.elegans* [79]. The B55 and the B56 regulatory subunits are not present in different isoforms in other species. The B55 subunit is found in one isoform called Twins (Tws) in *Drosophila* [78], Cdc55 in budding yeast [77], and sur-6 in *C.elegans* [79]. The B56 subunit is present in two isoforms called widerborst (wdb) and well-rounded (wrd) in *Drosophila* [80], and pptr-1 and pptr-2 in *C.elegans* [79]. No B56 subunit is present in budding yeast, and multiple isoforms of both B55 and B56 are present in *Xenopus*.

The assembly of the heterotrimeric structure of PP2A is a multi-step process. In mammals, both the catalytic and the scaffolding subunits form a dimer. To build a trimeric structure, B subunits bind both the catalytic and the scaffolding subunits of PP2A (**Fig 1.6**). For the binding to the various regulatory subunits, the scaffolding subunit contains a

stretch of 15 repeats called the HEAT repeat [81, 82]. The B56 subunit structure also includes a similar HEAT repeat structure that helps in recognizing and binding the PP2A scaffolding subunit [82]. The structure of the B55 subunit consists of a seven β-propellers and a β-hairpin-like structure which are essential in binding to the PP2A scaffolding subunit and substrates [83] (**Fig 1.6**).

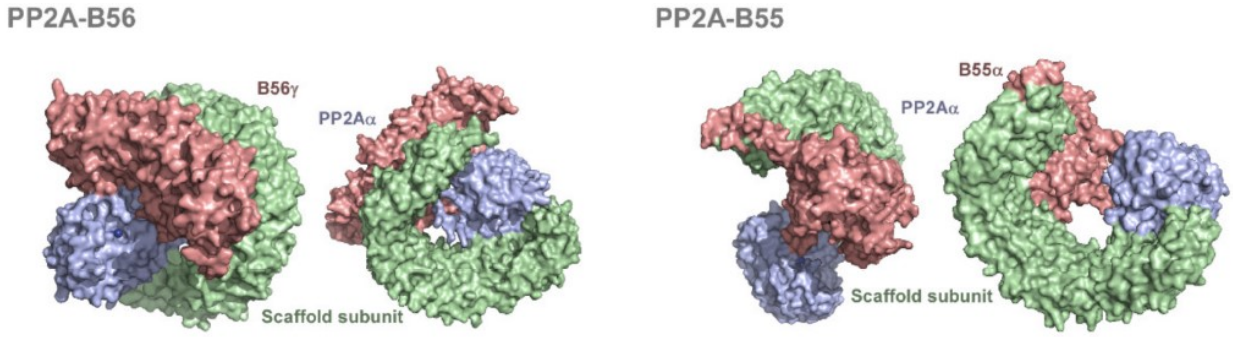

Figure 1.6: The structural composition of PP2A-B56 and PP2A-B55. PP2A is a trimeric complex composed of a catalytic subunit (green), scaffolding subunit (purple), and a regulatory subunit (red). Figure taken from [75].

1.5.A.b. The functions of PP2A-B55 during mitotic exit

As mentioned above, the PP2A in complex with the B55 and B56 regulatory subunits have an essential function during mitotic exit, though PP2A-B55 is more critical in this process. Studies in *Drosophila*, *Xenopus* egg extracts, and human cells show that PP2A-B55 dephosphorylate substrates at mitotic exit, that were initially phosphorylated by CDK1-cyclin B. Extracts from *Drosophila* females with *tws* mutant brains were unable to dephosphorylate histone H1 previously phosphorylated by CDK1-cyclin B [84]. In two recent studies using *Xenopus* egg extracts, authors show that PP2A-B55δ is essential for dephosphorylating multiple substrates previously phosphorylated by CDK1-cyclin B [85, 86]. Moreover, human PP2A-B55α seems to be essential for PRC1 dephosphorylation

initially phosphorylated by CDK1-cyclin B [87]. In the same study, PP2A-B56 also dephosphorylates PRC1, but on a different site previously phosphorylated by Plk1 [87]. These findings suggest that PP2A-B56 can dephosphorylate substrates that were not phosphorylated by CDK1-cyclin B.

Studies in different model organisms show that PP2A-B55 is essential for regulating different processes during mitotic exit. In a screen done in human cells, PP2A-B55δ was found to be critical for regulating spindle disassembly and NER [88]. Also, PP2A-Tws (PP2A-B55 in flies) regulates mechanisms that are essential for centrosome attachment to nuclei during early embryo development [89]. Embryos laid by females heterozygous for a *tws* mutation show clear centrosome attachment defects to nuclei [89]. However, the identity of the PP2A-Tws substrates required for this mechanism is still elusive. More recently, a proteomic-based screen using *Xenopus* egg extracts discovered more than 100 binding partners of B55α and B55β responsible for cell division, DNA replication, DNA repair, and cell signaling [90]. From the screen, authors found that PP2A-B55 interacts with the DNA-binding protein complex RPA, previously shown to be phosphorylated by CDK2 during replicative stress. Interestingly, the levels of B55α increased upon replicative stress [90]. These results made the authors suggest that PP2A-B55 can regulate RPA functions under replicative stress. However, the exact mechanism for this regulation was not investigated in this study.

It has now become evident that PP2A-B55 preferably dephosphorylates phospho-sites previously phosphorylated by CDK1-cyclin B, which is S/TP. However, an in-depth proteomic analysis identified recognition signals that control PP2A substrate dephosphorylation during mitotic exit [91]. In this study, PP2A-B55 seems to favorably dephosphorylate sites containing S/TP that are flanked by polybasic amino acids, which

are thought to bind to the negative patches on B55 [91]. Sites on PP2A-B55 substrates flanked with more basic amino acids are dephosphorylated more rapidly than those containing few basic amino acids. In the same study, PP2A-B55 was able to dephosphorylate spindle proteins (with sites flanked by many basic amino acids) more rapidly than NE proteins (with sites flanked by few basic amino acids) [91]. Dephosphorylation kinetics is not only controlled by the presence of polybasic amino acids near dephosphorylation sites, but also by the PP2A catalytic subunit preference towards the sites phospho-T or phospho-S [92]. PP2A-B55 dephosphorylates substrates more rapidly with phospho-T than those with phospho-S sites [92]. These results suggest that PP2A-B55 would dephosphorylate substrates with phospho-T flanked with more basic amino acids during early mitotic exit, while it will dephosphorylate substrates with phospho-S flanked by less basic acids during late mitotic exit.

1.5.A.c. The regulation of PP2A-B55 during mitosis

Since PP2A-B55 opposes CDK1-cyclin B by dephosphorylating its substrates, an active PP2A-B55 at mitotic entry can lead to premature substrate dephosphorylation and an early exit from mitosis. For this, PP2A-B55 should be inactivated at mitotic entry and must get fully active only once the cell is ready to exit mitosis. PP2A-B55 inactivation occurs at the beginning of mitosis through a mechanism that depends on the Ser/Thr kinase greatwall (Gwl) and the small proteins ENSA and Arpp19 [93]. The regulation mechanism is simple. At mitotic entry, CDK1-cyclin B phosphorylates MASTL (Gwl in human cells) at the site Thr207 at its kinase domain [93, 94]. After being phosphorylated, the autophosphorylation of MASTL takes place at the Ser875 site leading to its full activation. Following its activation, Gwl phosphorylates ENSA on Ser67 and Arpp18 on

Ser62 [75, 87, 93, 95]. However, CDK1-cyclin B is also capable of phosphorylating Arpp19 on a different site than the one phosphorylated by MASTL [96]. The phosphorylation of ENSA and Arpp19 allows their binding to PP2A-B55, leading to its inhibition at mitotic entry [75, 87, 93, 97]. At mitotic exit, Gwl, ENSA, and Arpp19 are dephosphorylated, which causes a release of ENSA and Arpp19 from PP2A-55, leading to its activation at mitotic exit [75, 87] (**Fig 1.7**).

The mechanism of inactivation of PP2A-B55 at mitotic entry has been extensively examined in different model organisms [98]. In fly cells in culture, for instance, Gwl is present in the nucleus [99]. After being phosphorylated by CDK1-cyclin B, Gwl translocates to the cytoplasm [99], where it phosphorylates endos (ENSA in *Drosophila*), which exits the cytoplasm (**Fig 1.7**). PP2A-Tws, found in the cytoplasm, is then inhibited by the phosphorylated endos, leading to its inhibition at mitotic entry [99]. Surprisingly, no ortholog of Gwl has been identified in *C. elegans*, although ENSA is present in this organism [97], which raises the question of the mechanism by which PP2A-B55 is inactivated in worms.

The mechanisms by which PP2A-B55 reactivates at mitotic exit has also been studied. The degradation of cyclin B partially activates PP2A-B55, where it partially dephosphorylates ENSA and Arpp19 [75, 100]. Therefore, ENSA and Arpp19 are PP2A-B55 substrates and inhibitors [101]. By this “unfair competition” mechanism, ENSA and Arpp19 are dephosphorylated [101], and PP2A-B55 can now bind and dephosphorylate various mitotic substrates. Another study shows that ENSA/Arpp19 could also be phosphorylated by the RNA polymerase II carboxy-terminal domain phosphatase, also known as Fcp1 [100]. For Gwl dephosphorylation, a study in *Drosophila* shows that the partially active PP2A-Tws dephosphorylates Gwl on a site next to a nuclear localization

signal (NLS) initially phosphorylated by CDK1-cyclin B [102]. This dephosphorylation activates the NLS in Gwl, leading to its translocation to the nucleus to prevent endos phosphorylation and to fully activate PP2A-Tws at mitotic exit [102] (**Fig 1.7**).

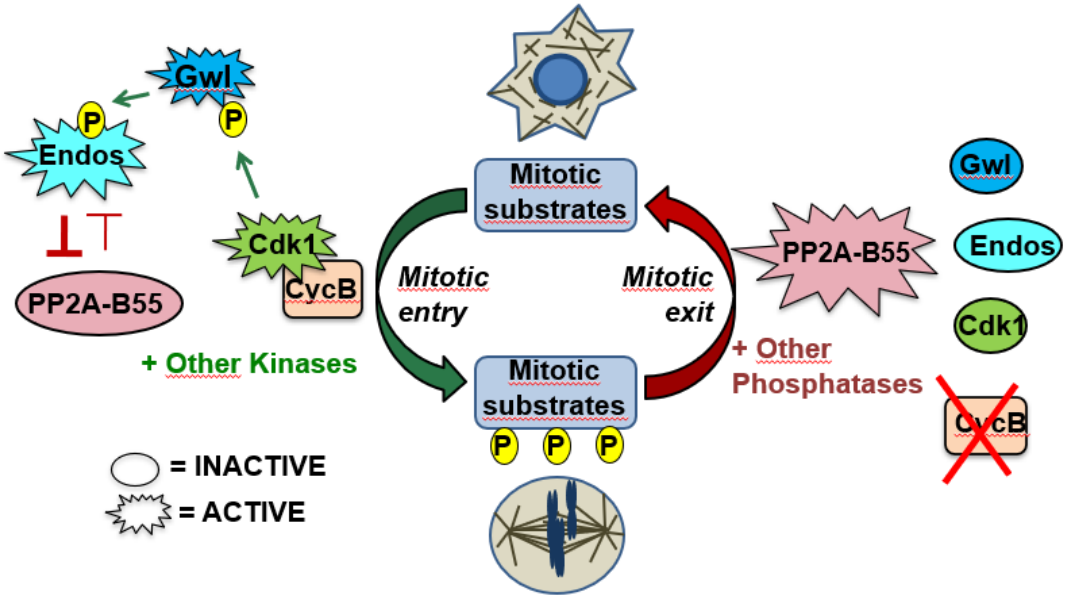

Figure 1.7: The regulation of PP2A-B55 (PP2A-Tws) in *Drosophila* during mitosis. During mitotic entry, active CDK1-cyclin B and other kinases phosphorylate a myriad of mitotic substrates. These substrates are then dephosphorylated during mitotic exit mainly by active PP2A-B55. PP2A-B55 is inactive during mitotic entry. CDK1-cyclin B phosphorylates Gwl (MASTL in mammals), which then phosphorylates Endos (ENSA or ARP19 in mammals). Phosphorylated Endos binds to and inhibits PP2A-B55 at mitotic entry. Gwl and Endos are dephosphorylated at mitotic exit, and PP2A-B55 is active. Figure provided by Vincent Archambault.

1.5.A.d. PP2A-B55 and Cancer

A cell in an organism does not operate individually but is subjected to external signals from neighboring cells that order the cell to act during different situations. These signals can order the cell to divide, differentiate, or die [103]. This notion of cell collaboration is essential to keep tissues and thus, the whole organism alive. However, an unrepairable mutation in a gene of a cell in a tissue may lead to the development of a

new behavior that other cells in the tissue do not have. One example of a gene mutation is a one that leads to an increase in cell proliferation [103].

Multiple mutations in a gene, either due to a heritable cause [104] or an exposure to a carcinogen (a cancer leading agent) [105], followed by natural selection [106], will form an individual cell clone which will abnormally utilize nutrients available for other cells, and hence affects the viability of the whole tissue and then the whole organism [103]. These are the general events that lead to the formation of a cancerous tumor or neoplasm. In this tumor, several critical cellular processes are affected, such as cell proliferation and division, differentiation, apoptosis, migration, and others. These are also known as the hallmarks of cancer [107]. Different genes regulating these processes are found to be mutated in multiple cancer types. These genes are known as cancer-critical genes. Mutation in these genes could either be gain-of-function or loss-of-function mutations. Genes, where a gain-of-function mutation induces cancerous cell formation, are called oncogenes, such as the genes *KRAS*, *cyclin D1* and *cyclin E1*, and *HER* [108]. Whereas genes, where a loss-of-function mutation increases the risk of a cancerous cell formation, are called tumor-suppressor genes, such as *p53*, *INK4* and, *PTEN* [108].

As cancer is now among the leading death-causing diseases worldwide [109], many efforts are being made to treat cancer patients using diverse strategies. One of the approaches is to kill cancer cells by targeting mitosis. Many studies indicate that multiple cell division regulatory proteins are either defective or overexpressed in several cancer types, such as PLKs, cyclins, and aurora kinases [110, 111]. For targeting mitotic entry, scientists identified drugs that could be either microtubule poisons, such as Taxol, or drugs targeting the kinases controlling mitotic entry such as CDKs and PLKs [112, 113]. Although this strategy was efficient in killing cells, some cells were able to escape the drug

effect through a mechanism called mitotic slippage [112, 114]. Moreover, in some cases, these drugs were being resisted by cells, making them inefficient for being a part of cancer chemotherapy [115]. However, drugs that were targeting proteins regulating mitotic exit, such as proteins of the APC(Cdc20) [116], blocked cells at the metaphase-to-anaphase transition leading to cell death [112]. Hence, it seems that finding strategies to target other mitotic exit proteins could be promising for future cancer treatment.

After treating tumors with okadaic acid (OA), a PP2A/PP1 inhibitor [117], tumor growth increased, suggesting that PP2A is a tumor suppressor gene [118, 119]. Therefore, identifying drugs that activate PP2A instead of stopping it might be a good strategy for cancer treatment. Different members of the PP2A trimeric complex show abnormal levels of expression in various cancer types. The level of expression of B56γ was high in metastatic cells from a B16 mouse melanoma model [119]. Moreover, the level of expression of B55α was very low in patients with acute myeloid leukemia [120]. Also, mutations in the scaffolding subunit PPP2R1A and PPP2R1B were present in both ovarian and cervical cancer, and a deletion in gene expressing B55 was found in breast, prostate, and ovarian cancer [121]. Since PP2A-B55 is an essential regulator of mitotic exit, it is critical to identify substrates it dephosphorylates and mechanisms regulating its activity. Understanding the role and the regulation of PP2A-B55 in mitotic exit will enable scientists to develop drugs that target PP2A-B55 and could be part of combinatorial cancer therapy.

1.5.A.e. Other phosphatases regulating events of mitotic exit

Other than PP2A-B55, PP1 is also known to play essential roles in the regulation of mitotic exit. The PP1 enzyme is composed of a catalytic subunit but lacks a scaffolding subunit. To be active, PP1 must bind to a regulatory subunit, of which more than two hundred exist. The most studied PP1 regulatory subunits are Sds22, Repo-man, KI-67, PNUTS, and AKAP149 [122]. PP1-Sds22 localizes at kinetochores and dephosphorylates the cytoskeleton proteins ezrin/radixin/moesin, also known as ERM proteins. These proteins play critical roles in linking actin filaments to the plasma membrane [123]. The dephosphorylation of ERM proteins by PP1-Sds22 induces cortical relaxation, thus facilitating the process of anaphase elongation and proper cell division [123]. The subunit Repo-man recruits the PP1 catalytic subunit to late anaphase chromosomes, where PP1 is thought to be important in the early reassembly of the Nup107 complex at mitotic exit [75, 124]. However, whether PP1-Repo-man dephosphorylates any nucleoporin is still unknown. For KI-67, the only piece of evidence indicating its role as a PP1 regulatory subunit is the ability to recruit PP1 to chromosomes at anaphase [125]. KI-67 depletion leads to a reduced localization of PP1 to anaphase chromosomes with normal cell division[126]. These results might also suggest that KI-67 is redundant with Repo-man. However, data that show this kind of redundancy are still missing. The regulatory subunit PNUTS targets PP1 to reforming nuclei for the regulation of chromatin decondensation [127], although PP1 substrates implicated in this process are still unknown. Finally, the transmembrane-domain-containing protein AKAP149 also recruits the PP1 to reassembling nuclei and is thought to be essential for PP1 function in Lamin B dephosphorylation at mitotic exit [128].

PP2A-B55 and PP1 are not the only phosphatases implicated in regulating events during mitotic exit. An RNAi phosphatase screen performed in *Drosophila* S2 cells identified the roles of several phosphatases with mitotic functions [129]. Phosphatases such as PP4, PP2C, and PTP seem to function in regulating some events during mitotic entry and exit [129].

1.6 The nuclear envelope structure

The nuclear envelope, found in eukaryotic cells, is a lipid bilayer that separates the cytoplasm from the genetic material found in the nucleus. The envelope consists of an inner nuclear membrane (INM), and an outer nuclear membrane (ONM), both of which are continuous with the endoplasmic reticulum (ER) [130]. The envelope also includes large complex spanning both membranes, required for the nucleo-cytoplasmic transport, called the nuclear pore complex (NPC) [131]. The inner part of the INM consists of a fibrous-like structure called the nuclear lamina that provides strength and rigidity for the whole envelope [130, 132]. Chromatin in the nucleus connects to the nuclear envelope through various proteins that bind both DNA and proteins in the envelope [130]. In this section, we will be describing the different structures of the NE, the proteins that make these structures, and the functions of these proteins (**Fig. 1.8**).

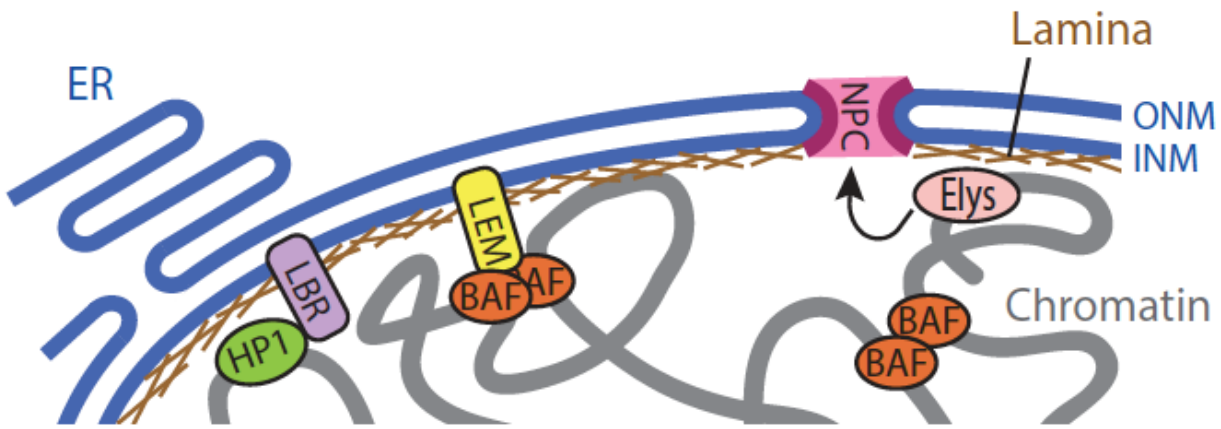

Figure 1.8: The structure of the nuclear envelope. The nuclear envelope is composed of the outer and inner nuclear membranes (ONM and INM), the nuclear lamina, nuclear and pore complexes. The envelope is connected to chromatin via different proteins such as Elys, BAF, and HP1. Figure provided by Vincent Archambault.

1.6.A. The nuclear lamina

1.6.A.a. The nuclear lamina and lamins

The nuclear lamina is a filamentous structure found at the inner part of the INM and composed of intermediate filament proteins called lamins [133] (**Fig. 1.8**). As it gives stability to the NE, the nuclear lamina is present in almost all invertebrate and vertebrate cells [133]. In interphase cells, lamins play crucial roles in chromatin organization, gene expression, and structural and functional organization of the nucleus [132-137]. Lamins are also important for organism development [138], as a mutation in lamin expressing genes was found with patients suffering from laminopathy diseases, one of which is striated muscle laminopathy [139].

In mammalian cells, three types of closely related lamins, having a size between 65- 70 kDA, exist termed lamins A, B, and C [132, 139]. While Lamins A and C are soluble in the cytoplasm during cell division, B-type lamins associate with membranes [139]. Other

organisms such as birds have lamins A, B1 and, B2, while five types of lamins exist in *Xenopus* [134, 136]. The human genome contains three lamin genes synthesizing seven different lamin proteins [129]. In *Drosophila*, it was thought that only one type of lamin, called Lamin Dm0, exists in the nuclear lamina [133]. However, other studies found that Lamin C also exists, but expressed at later stages of the fly development [136] [140]. This is also the case for mammals, as B-type lamins are constitutively expressed in all body cells, while Lamins A and C are only expressed in differentiated cells [132]. It is important to note that in most organisms, one gene expresses Lamin B, and another one expresses both Lamins A and C. The slight differences between the amino acid sequence of Lamin A and C are likely because both gene products arise from alternative splicing [133].

1.6.A.b. Lamin structure

As most intermediate filaments, the structure of lamins consists of an N-terminal head domain, a central α-helical central region, and a C-terminal tail domain [132-134]. These domains are essential for the proper dimerization of lamin molecules, a process that is important for the construction of the nuclear lamina. The central region of lamins is composed of four coiled-coil domains and is responsible for the early lamin assembly process [133]. The head and the tail domains are subjected to various modifications that are essential for the late stages of lamin assembly. The C-terminal domain of lamins contains an NLS, a feature not present in other intermediate filament proteins, which is critical for lamin import to the nucleus through the NPC [132]. The C-terminal domain also consists of a CAAX box, which is necessary to link lamin molecules to the INM [132] [133] [137, 139]. This process does not occur spontaneously with newly formed lamin molecules but requires further processing steps. After lamin synthesis, the C-terminal domain of

lamin is trimmed by peptidases and then isoprenylated at a cysteine residue [132] [136, 137]. These processing steps enable new lamins to associate with the INM [137]. This C-terminal isoprenyl group is maintained on Lamin B molecules and cleaved from Lamin C molecule [132]. These observations explain why Lamin B molecules link membranes during mitosis, while Lamin C molecules are soluble in the cytoplasm.

1.6.A.c. The nuclear lamina assembly

The nuclear lamina assembly is a multi-step process. First, two lamin monomers, of a 50 nm length, assemble through their central region [134]. This dimerization step occurs through hydrophobic interactions between the two central regions of the lamin monomers [132]. The second step of assembly is the literal head-to-tail association of lamin dimers to form a 70 nm structure, where tails are present inside the structure, and heads are kept outside the structure [134]. It is thought that during mitosis, the nuclear lamina disassembles into these 70 nm structures [134]. The third step is the lateral stacking of several 70 nm structures to form another 10 nm width structure. These newly formed structures from the third step can also bind longitudinally to create a more extended paracrystalline structure, which is the central part of the nuclear lamina [134]. Both the N-terminal and C-terminal domains of lamins are necessary for their assembly process, as the deletion of one of the two domains leads to an increase in lamin solubility *in vitro* [132]. The disassembly and the reassembly of the nuclear lamina during mitotic entry and exit depend on the phosphorylation state of the molecules of the nuclear lamina. Different kinases and phosphatases play vital roles in the disassembly and reassembly of the nuclear lamina during mitosis. We will be discussing these kinases and phosphatases in the subsequent sections.

1.6.B. The nuclear pore complex

Traversing both the ONM and INM are large protein complexes, that act as gates between the cytoplasm and the nucleus, termed nuclear pore complexes (NPCs) [133] (**Fig. 1.8, 1.9**). NPCs, with a molecular size between 40 and 60 MDA, contain a set of more than 30 different proteins called nucleoporins [141]. The NPC is an eight-fold symmetrical structure [142] with a diameter of 80 nm [133] that exists in all NEs of eukaryotic cells and is conserved from yeast to mammals [133, 142]. The most critical function of the NPC is to mediate the transport of cargos, most of which are mRNA and proteins, between the cytoplasm and the nucleus [143]. However, lately, the NPC seems to be essential in performing other functions such as the regulation of gene expression, cell differentiation, epigenetic and heterochromatin regulation, cell development, DNA repair, and the assembly of the mitotic spindle [141, 143].

1.6.B.a. The structure of the NPC

The NPC consists of different subcomplexes that constitute a cytoplasmic and a nuclear ring found on opposite sides of the complex, a transmembrane and an inner ring, nuclear basket composed of nuclear filaments, a central channel that maintains selective permeability, and cytoplasmic fibrils [144] (**Fig. 1.9**). The cytoplasmic, nuclear, and the inner rings are essential for forming the central channel of the complex. Although cytoplasmic fibrils extend from the outer cytoplasmic rings as seen by electron microscopy, it is still controversial whether these fibrils are part of the NPC [144]. As mentioned before, the NPC is composed of different nucleoporins (Nups) (**Fig. 1.9**). These proteins exist in different subcomplexes of the NPC based on their amino acid composition. Nups can be classified as transmembrane, scaffold (outer and inner rings),

linker, and Phe-Gly (FG) [144]. Three transmembrane Nups, GP210, NDC1, and POM121 in vertebrates, are building blocks of the transmembrane ring and are critical in linking the NPC to nuclear membranes. Nups that are part of the outer and inner rings that form the central channel are biochemically stable and conserved Nups essential for assembling the NPC [144]. Nups that assemble the outer ring belongs to the vertebrate Nup107 complex, while those that are a part of the inner ring belong to the vertebrate Nup155 complex [144]. FG Nups, such as vertebrate Nup98 and Nup62, are present in their unfolded state and are critical for the transport mechanism. Linker Nups, such as vertebrate Nup93 and Nup88, link the scaffold to the FG Nups [144].

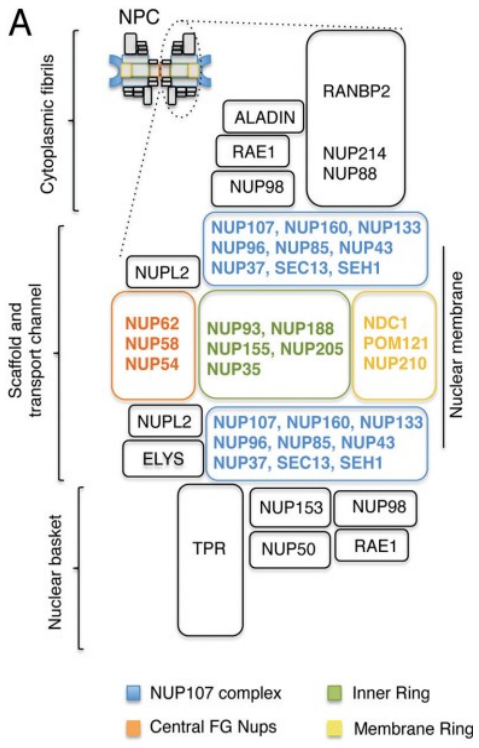

Figure 1.9: The structure of the nuclear pore complex. The NPC is composed of scaffold and transport channel, nuclear basket and cytoplasmic fibrils. Each of these structures is made of a set of different nucleoporins. Figure taken from [141].

1.6.B.b. The disassembly and assembly of the NPC

During mitosis, the NPC disassembles in the cytoplasm. Studies using different model organisms show that the disassembly process is a step-wise synchronous mechanism [142]. For instance, in starfish oocytes, the disassembly process starts with the removal of Nups of the nuclear basket and cytoplasmic fibrils, which leads to a loss in nuclear permeability [142]. A similar process exists in *Drosophila*, and the proteins of the Nup107 complex disassembles after the removal of nuclear basket Nups. In budding yeast, where no NEBD takes place, the process of NPC disassembly is absent. However, in budding yeast with closed mitosis, partial disassembly of NPC takes place by the removal of some FG Nups during prophase [142]. This partial disassembly of NPC increases complex permeability allowing different mitotic regulators to pass to the nucleus [142]. The disassembly of NPC is shown to depend on phosphorylation. Several kinases play an essential role in this process. We will discuss this in the following sections.

During mitotic exit, more specifically at early anaphase, the NPC should assemble back on newly formed nuclei [142]. Similar to NPC disassembly, the NPC assembly process is also a stepwise controlled mechanism. The first step of assembly starts with the recruitment of the large DNA binding protein ELYS/Mel-28 to chromatin [142, 145]. ELYS/Mel-28 binding to chromatin induces the recruitment and binding of the Nup107 complex to form what is known as the pre-pore complex [141]. Then, the Nup107 complex binds the nuclear membrane via the transmembrane Nup, POM121 [145]. After binding to the nuclear membrane, other NPC complexes assemble starting by the Nup155 complex, linker Nups such as Nup88, FG Nups such as Nup62, and other Nups that form the nuclear basket and cytoplasmic fibrils[145]. For the initiation of the NPC assembly

process, critical Nups are dephosphorylated. We will discuss this in detail in the following sections.

1.6.B.c. The nuclear transport machinery and mechanism

The primary role of the NPC is to transport cargos between the cytoplasm and the nucleus. Cargos such as ions and molecules having a size less than 40 kDA can easily diffuse through the NPC. However, larger proteins are actively transported by a large family of proteins called karyopherins [142]. Karyopherins can be importins that import cargos through the NPC to the nucleus, or exportins that carry cargos through the NPC to the cytoplasm (**Fig. 1.10**). Proteins targeted to the nucleus possess an NLS in their amino acid sequence, while those that need to exit the nucleus might have a nuclear export signal (NES). Since it is an active transport mechanism, a source of energy is required for this process [146]. This energy comes from the small GTPases Ran. The energy that comes from GTP hydrolysis is not essential for the translocation through the NPC but is critical to trigger the assembly and disassembly of transport complexes in the cytoplasm and the nucleus. For instance, in the cytoplasm, importins bind cargos with an NLS only following Ran-GTP hydrolysis to Ran-GDP by a Ran-GAP (**Fig. 1.10**). Then, after the importin-cargo complex passes through the NPC, a Ran-GEF transfers Ran-GDP to Ran-GTP. Importin releases the cargo in the cytoplasm when it binds cytoplasmic Ran-GTP [146] (**Fig. 1.10**). On the other hand, high Ran-GTP in the nucleus helps in the binding of exportins to their cargo. After the exportin-cargo complex passes to the cytoplasm, it releases its cargo after binding to Ran-GDP in the cytoplasm [146] (**Fig. 1.10**). Although it seems that Ran-GTP, Ran-GDP, Ran-GEF, and Ran-GAP are only soluble in the cytoplasm or the nucleus, these molecules also bind at different sites on the

NPC. Some of these molecules bind the Nup 358 [146] found on the cytoplasmic part of the NPC, while others bind to the Nup 153 [147] that exists at the nucleocytoplasmic portion of the NPC.

In addition to their importance in the nucleo-cytoplasmic transport machinery of the NPC, importins, and Ran-GTP can play other functions, specifically during mitosis. One of the roles of importins and Ran-GTP is during NPC assembly at the end of mitosis. To prevent their interaction with chromatin and other Nups, ELYS/Mel-28 and the Nup107 complex bind importins before the start of the NPC assembly mechanism [142]. After binding to Ran-GTP, known to bind chromosomes during mitosis, importins release ELYS/Mel-28 and the Nup107 complex, which are now able to bind chromatin and initiate the NPC assembly process [142]. Another vital role of importins takes place during the contractile ring assembly at early cytokinesis. Anillin, a protein of the contractile ring, binds importin-β through its C-terminal NLS and localizes to the cortex of mammalian cells. This mechanism is critical both for cortical polarity and cytokinesis [148].

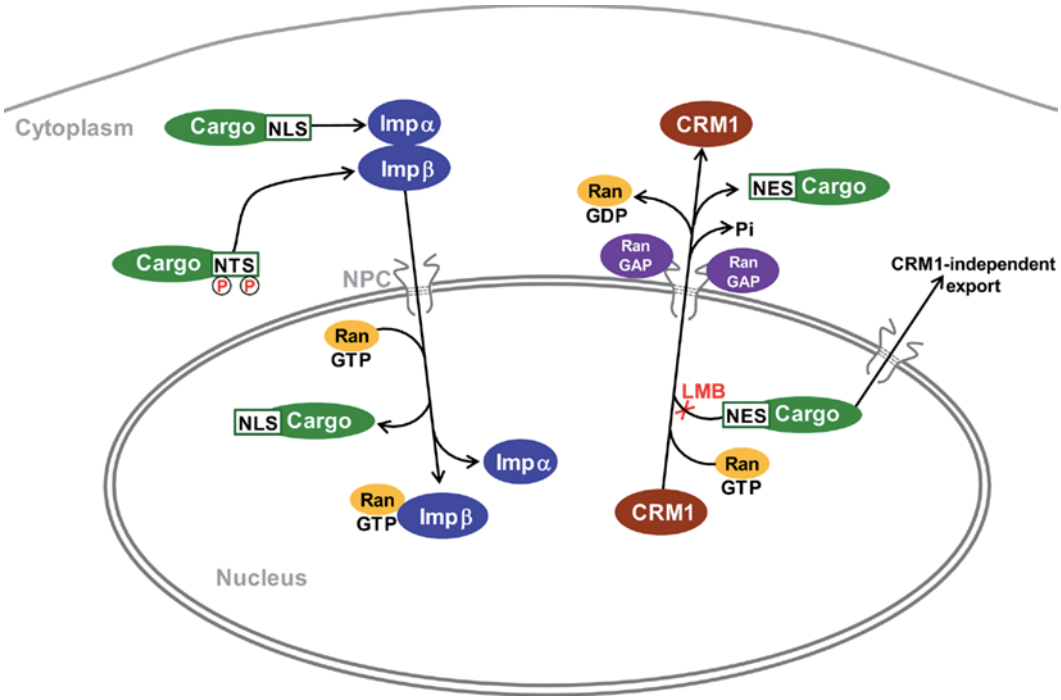

Figure 1.10: The nucleo-cytoplasmic transport mechanism in the cell. Importins such as importin α and β transport cargo from the cytoplasm to the nucleus. CRM1 is an exportin that carry cargo from the nucleus to the cytoplasm. RanGTP hydrolysis is required for this transport mechanism. LMB (Leptomycin B) is an export inhibitor. Figure taken from [149].

1.6.B.d. Nuclear pore complexes are also present on annulate lamellae

Annulate lamellae (AL) are organelles present in the cytoplasm as membrane sheets containing NPCs, and are also known to be subdomains of the ER [150, 151]. Like NPCs bound to NE, those bound to AL consist of more than 30 different types of Nups. However, they lack the Nups ELYS/Mel-28, POM121, and Tpr. AL are found in cells with high dividing capacity such as germ cells and embryos during early development in frogs, fruit flies, worms, and humans [150, 151]. However, the exact function of these structures in the cells is still under investigation. In a study using HeLa cells, the number of AL in the cells seems to be critical for the nuclear transport mechanism [150]. An upregulation of

AL increases the number of NPCs on AL and decreases those found on the NE. This affects the distribution of transport proteins such as importins causing a decrease in the nuclear export and import rate [150]. This suggests that these structures act as a control of the nucleo-cytoplasmic process. Also, a recent study shows that AL are essential for immature and pre-assembled NPC insertion in the NE during syncytial embryo development in *Drosophila* [151]. This model of AL function gave one of the important explanations to how the INM is continuous with cell ER [151]. More investigation is required to reveal the roles of these structures on normal cell function under various conditions.

1.6.C. The outer nuclear membrane

The ONM is a lipid bilayer that contains transmembrane proteins and serves in several developmental processes. The integral proteins of the ONM share an N-terminal KASH (Klarsicht, Anc-1, Syne-1, homology) domain. These proteins bind INM proteins having SUN (Sad1p/UNC-84) domains to mediate different functions [130, 152]. In addition, proteins of the nuclear lamina bind proteins with a SUN domain found on the INM [153]. This binding is essential for the processes of nuclear migration and cellular polarization. ONM proteins such as nesprin also interact with the cell actin cytoskeleton through an N-terminal actin domain [152]. By connecting to both the nuclear lamina and the actin cytoskeleton, ONM proteins with KASH domains provide a connection between the nuclear envelope and the MTOC [138]. This connection is critical for different cellular processes such as nuclear migration of photoreceptor cells during *Drosophila* eye development [138].

As mentioned above, the ONM continues and links with both the smooth and the rough ER, and some ribosomes bind different regions of the ONM [154]. However, other functions of the ONM are still unexplored. Therefore, more efforts should be made to uncover new ONM proteins and investigate their functions.

1.6.D. The inner nuclear membrane, a site for binding chromatin

1.6.D.a. Proteins of the inner nuclear membrane, structure and, functions

The INM is a critical region of the NE, as it plays vital roles in gene expression and DNA metabolism [130]. It also provides a site of contact between the NE and both the nuclear lamina and chromatin. Transmembrane proteins are present on the entire INM. Most of the proteins that exist in the INM are known to share a 40 amino acid conserved globular module called the LEM domain. The 3D structure of the domain consists of two parallel α-helices that are connected by a loop [155]. The name of the domain comes from the first letter of first discovered INM protein families called LAP2, Emerin, and MAN1. Other LEM-domain proteins, such as LEM2, LEM3, LEM4, LEM5, and the *Drosophila* proteins Otefin and Bocksbeutel, also exist [155]. The known function of most of these proteins is to interact with a small conserved protein called the barrier-to-autointegration-factor (BAF) and to proteins of the nuclear lamina. For example, the lamina-associated polypeptide-2 (LAP2) family consists of different isoforms. The N-terminal region of most of the proteins in the LAP2 family consists of two domains, a LEM domain that can bind the chromatin indirectly via its interaction with BAF, and a LEM-like domain which can directly interact with chromatin [155]. The C-terminal domain of proteins of this family includes a lamina-binding domain which helps in binding lamins, most of which are A-type lamins [139]. Regarding the protein MAN1, its N-terminal domain consists of a conserved

LEM domain, and the C-terminal domain composes an RNA recognition motif (RRM) [155]. MAN1 also binds lamins, and its role is critical in chromosome segregation and cell division [139]. Emerin is another INM protein with a typical LEM domain on its N-terminus. The Emerin gene (*EMD)* is present on the X-chromosome of the human genome and expresses a 34 kDA protein [139]. Other than its ability to interact with BAF, Emerin binds several lamin proteins, but favorably binds Lamin C [139]. Emerin is critical for cell survival and development, and mutations in the *EMD* had been linked with patients having Emery-Dreifuss muscular dystrophy [139]. There are three LEM domain proteins in *Drosophila*: Otefin, MAN1, and Bocks [156]. The functions of these proteins are not well understood, but their ability to bind BAF is conserved. Interestingly, flies with a single mutant for a gene that encodes one of the LEM domain proteins are viable. However, flies with double mutant genes that expresses two LEM domain proteins failed to hatch, suggesting that LEM domain proteins are functionally redundant [156].

Other INM proteins also exist, but in contrast to INM proteins described above, these INM proteins lack a conserved LEM domain. An example of such protein is the Lamin B receptor protein or LBR. As all INM proteins, LBR also binds lamins, and can also associate with chromatin by a BAF-independent process. In addition to binding chromatin, LBR can interact through its N-terminal domain with the heterochromatin specific protein 1 (HP1) [139, 157]. This interaction also helps to link chromatin to the NE.

1.6.D.b. BAF, its structure, and functions in linking the NE to chromatin

As discussed above, multiple sites of attachment between the NE and chromatin exist. However, the most critical attachment is the one taking place between proteins with LEM domains and BAF (barrier-to-autointegration factor). BAF is a small protein of a size

between 10 and 20 kDA that is widely conserved among different metazoans [158, 159]. The name BAF comes from its role in the biogenesis of the Molony Murine Leukemia Virus (MoMLV). When MoMLV infects a cell, the reverse transcription complex reverse transcribes the viral RNA into DNA [158]. This viral dsDNA is present in the cell cytoplasm as a nucleoprotein called the pre-integration complex (PIC). BAF is recruited to the PIC during complex formation and protects viral DNA from its autointegration in the cell genome [158]. Failure of BAF recruitment to the PIC complex leads to viral DNA autointegration and viral self-destruction. By binding DNA, BAF prevents the viral DNA from being inaccessible to viral integrases and thus to viral DNA integration to the host genome [158]. Previous studies showed that BAF forms dimers that bind DNA in a non-sequence specific manner. After binding DNA, BAF dimers undergo a 3D-conformational change that enhances BAF binding to other proteins such as LEM domain proteins or lamins [158]. The 3D structure of the DNA unbound BAF monomer and BAF dimer bound to DNA is already present. The BAF monomer consists of a non-specific DNA binding motif composed of two helix-hairpin-helix structure. This DNA binding motif is located on opposite surfaces of the BAF dimer [160].

The most critical function of BAF is to regulate nuclear assembly during mitosis. BAF regulates proper nuclear assembly by binding various NE proteins. In interphase cells, BAF is present in the cytoplasm and on the NE where it binds LEM domain proteins, lamins, and histones. During early anaphase, LEM domain proteins such as LAP2α bind a fraction of BAF at the telomere region [158]. Then, during early telophase, the BAF-LAPα complex spread on the surface of the central zone of telophase chromosomes proximal to the mitotic spindle, known as the core region [158]. Then, other NE proteins assemble to complete the NER process. However, these studies failed to explain the role

of the free BAF fraction during the exit from mitosis. Recently, in a study performed in HeLa cells, the depletion of BAF by RNAi leads to the formation of nuclei fragments (known as micronuclei) [161]. These micronuclei are vulnerable to DNA damage and are assumed to cause genome instability and cancer formation. In this study, BAF seems to create a stable anaphase chromosome structure, which is necessary to shape a single nucleus at late mitosis [161]. This study contradicts previous studies showing that BAF accumulation at the core region is essential to recruit LEM domain proteins during nuclear assembly. However, the role of BAF seems essential for linking the different scattered chromosomes, rather than binding LEM domains [161]. This conclusion was made after observing that BAF mutants that fail to bind DNA are unable to bind LEM domain proteins, whereas BAF mutants that fail to bind LEM domain proteins can still bind DNA [161]. Moreover, BAF binding to DNA is critical to protect the mass of anaphase chromosomes from being invaded by LEM domain proteins. This conclusion is due to the fact that LAP2β-GFP strongly accumulated at the inner-chromosomal regions in cells depleted from BAF [161]. The importance of the role of BAF in nuclear assembly was also noticed in other model organisms. BAF depletion in *C. elegans* leads to the formation of anaphase bridges and to mislocalization of LEM domain proteins and lamins on the NE [158]. In *Drosophila*, BAF-null mutant flies lay eggs having dead larvae with small brains and missing imaginal discs [162]. Brain tissues from these larvae showed improper chromatin reorganization of interphase cells, improper nuclei shapes, unusual distribution of lamin, and abnormal M-phase progression [162]. This suggests that BAF plays an essential role both in chromatin organization and proper shaping of the nucleus. The binding event of BAF to DNA is not random but is tightly regulated by phosphorylation. We will discuss the regulatory mechanism of BAF-DNA binding in the following sections.

In addition to its role in nuclear assembly at the end of mitosis, BAF functions in regulating gene expression [158]. BAF plays critical roles in the formation of heterochromatin formation, by its ability to bridge-DNA and to bind the core histone H3 [158]. Through its binding to LEM domain proteins, BAF indirectly regulates the expression of several genes. For instance, LAP2α binds several transcription factors such as the retinoblastoma protein pRB, to inhibit E2F activity [158]. It seems that BAF regulates gene expression by competing with pRB for binding to LEM domain proteins such as LAP2α.

1.7 The nuclear envelope breaks down in early mitosis

1.7.A. The general process of nuclear envelope breakdown

In organisms with open mitosis, the process of NEBD is critical for the mitotic spindle to gain access to condensed chromosomes. In mammalian cells, this process starts at late prophase by the disassembly of NPCs and which finishes within minutes [163]. Following NPC disassembly, microtubules found at the external face of the NE exerts pulling forces that create NE invagination [163]. This process is essential in finalizing mitotic spindle assembly, lamina stretching, and getting rid of NE membranes bound to chromosomes. The next step is the completion of lamina depolymerization, which initiates in early prophase. The last step is the detachment of INM proteins and lamins from chromatin, mainly by the dissociation of these proteins from BAF [163]. As most of the NE proteins disassemble, their fate and localization during mitosis were always under question. In the past decade, there was a great interest in the role of the ER during NEBD. At mitotic entry, and in mammalian cells, the ER reorganizes and forms a

tubular-like network [163]. Disassembled proteins such as INM and lamins reabsorb into the ER, while Nups are mostly released in the cytoplasm [130]. The formation of the tubular-like structure of the ER during mitosis is still under investigation. For instance, in *C.elegans* and some mammalian cells, the ER is present in the form of a cisterna that localizes at the cell cortex and doesn't form a tubular-like structure during mitosis as in most mammalian cells [163]. More efforts are necessary to solve this contradiction in the role of the ER during NEBD.

1.7.B. CDK1, a principal kinase phosphorylating NE protein during NEBD

For triggering events of NEBD, multiple kinases phosphorylate a myriad of NE proteins. Kinases such as CDK1, Plk1, Aurora A, PKC, and others play an essential role in this process [132, 163]. However, among these, CDK1 is the most critical kinase that triggers NEBD [163] (**Fig. 1.11**). Proteomic analysis of samples from HeLa cells arrested in M-phase identified more than 1000 proteins, most of which were phosphorylated on S/TP, the known consensus sequence phosphorylated by CDK1. Many of these 1000 proteins were nucleoporins, LEM domain proteins, and lamina proteins [46]. Although CDK1-cyclin B is the principal kinase triggering NEBD, depletion of cyclin A2 from HeLa cells delayed the process of NEBD, suggesting that CDK1-cyclin A2 might be implicated in that process [164].

Many studies showed that CDK1-cyclin B phosphorylate several Nups, such as members of the Nup107 and Nup53 complexes, to induce NPC disassembly and detachment from the NE [163] (**Fig. 1.11**). Peptides from these Nups from M-phase arrested HeLa cells were mostly phosphorylated on S/TP, although phosphorylation of other sites was also present [46], suggesting that other kinases could phosphorylate these

Nups. It would be interesting to mutate some of these sites to determine their effect on the process of NPC disassembly at mitotic entry.

As for Nups, CDK1 is also responsible for phosphorylating lamina proteins to induce their disassembly at early mitosis. *In vivo* and *in vitro* experiments performed in different model organisms identified different CDK1 phosphorylation sites on lamina proteins (**Fig. 1.11**). For instance, the head-to-tail disassembly of chicken Lamin B2 polymers seems to depend on the various phosphorylation events on S/TP sites present mostly on the N and C-terminus of the protein [137]. In another study, the incubation of CDK1 with isolated chicken nuclei *in vitro* induced their disassembly by phosphorylating the sites found on the N-terminal region of Lamin B2 [137]. Also, bacterially purified Lamin C filaments incubated with active CDK1 induced disassembly of these filaments [165]. Head-to-tail disassembly of *Drosophila* Lamin Dmo also depends on the phosphorylation on an N-terminal Ser 24 [135] and a site in the C-terminal region by CDK1 [166]. Moreover, human cells expressing two serine phospho-mutants, Ser22 and Ser392 found on the N and C-terminal part of Lamins A and C respectively showed exciting phenotypes [167]. Cells expressing these mutants were unable to disassemble their nuclear lamina leading to failure in chromosome segregation and mitotic arrest [167]. These results suggest that phosphorylation of sites within the N and C-terminal part of lamins is sufficient to induce lamina disassembly. Other phosphorylation sites might be important for the detachment of lamins from other NE proteins during NEBD [167].

CDK1 activity is also necessary for phosphorylating several INM proteins during NEBD. In normal rat kidney epithelial cells (NRK), LAP2α dissociates from chromosomes during metaphase. LAP2α dissociation from chromosomes might depend on its phosphorylation by CDK1 since multiple CDK1 consensus sites exist in the LAP2α amino

acid sequence [168]. Indeed, in a study using a mouse neuroblastoma cell line, CDK1 was responsible for phosphorylating LAP2β on Thr 74 and Thr 159 [169]. CDK1 also phosphorylates LBR for its dissociation from lamina proteins. Studies using chicken cells identified Ser 71 [170] and Thr 188 [171] as the sites phosphorylated by CDK1 during mitosis. More recently, another study using HeLa cells, revealed that Ser 71 is the principal site in LBR being phosphorylated by CDK1. Also, CDK1 might be responsible for the interaction between LEM domain proteins and BAF. A study using the *Xenopus* egg cell-free system identified multiple phosphorylation sites on Emerin that are crucial for its dissociation from BAF during mitosis. Among these sites, Ser 49 was the only identified site followed by a proline [172]. The identity of the kinase implicated in the Emerin-BAF dissociation mechanism is still unknown.

1.7.C. Other kinases also participate in phosphorylating NPC, lamina, and INM proteins

As already mentioned, kinases such as Plk1 and aurora A are also essential for inducing NEBD. The depletion of Plk1 in *C. elegans* leads to NEBD defects in worm oocytes before ovulation [173] (**Fig. 1.11**). Also, treating HeLa cells with the Plk1 inhibitor, BI 2536, strongly delayed NEBD [174]. However, the identity of the NE substrates phosphorylated by Plk1 was still unknown. Recently, a study performed using HeLa cells showed that the inhibition of Plk1 localizes importin β and some Nups to condensed chromosomes instead of being diffused in the cytoplasm, while the localization of Lamin A/C was not affected [175]. These results and others in that study made the authors suggest that Plk1 is responsible for NPC but not lamina disassembly during NEBD. Moreover, in a quantitative phospho-proteomic study, phospho-peptides from multiple

Nups were enriched in BI 2356 treated cells confirming the role of Plk1 in phosphorylating members of the NPC [176]. In the same study, phospho-peptides of some Nups were enriched upon aurora kinase inhibition [176]. However, these results seem to contradict data that shows no effect on NPC disassembly following aurora B inhibition [175]. In contrast, the depletion of aurora A [177] in *C. elegans* delayed NEBD. Time-lapse experiments in worm embryos depleted from AIR-1 (aurora A in *C. elegans*) showed a delay in the disassembly of lamina and NPC proteins [177]. Whether aurora kinases are necessary for lamina and NPC disassembly in organisms other than *C. elegans* remains unexplored. However, recently, HeLa cells treated with ZM447439, an aurora B inhibitor, showed a delay in the dissociation of LBR from chromosomes [178]. It remains to be seen whether aurora B phosphorylates LBR, and whether this phosphorylation is necessary for LBR dissociation from HP1 or chromatin during NEBD.

Other kinases, though with less importance, phosphorylate various NE substrates during NEBD. In the past decades, many *in vitro* assays were performed using purified Lamin B and Lamin C from various model organisms. These experiments show that the protein kinases A and C (PKA and PKC) [132], the S6 kinase II [165], and the CAM kinase II [132], have the ability to phosphorylate multiple sites both on the N and C-terminal regions of Lamin B and C. Also, some kinases are responsible for phosphorylating INM proteins. Among these kinases, the RS kinase can phosphorylate LBR on multiple sites *in vitro* [170]. However, *in vivo* studies showing the role of these kinases in the phosphorylation of lamins and INM proteins are still absent. Moreover, multiple kinases participate in phosphorylating several Nups. *In vitro* and *in vivo* studies in yeast showed that the casein kinase Hrr25p binds to and phosphorylates Nup53 [179]. Since no role of Hrr25p in phosphorylating NPC proteins in other organisms exist, the role of Hrr25p seems

restricted to yeast. Also, the kinases PKA and the glycogen synthase kinase can phosphorylate Nup 62 *in vitro* [180]. However, the specificity of these *in vitro* assays should be taken into consideration.

1.7.D. BAF dissociation from chromatin and NE proteins during NEBD depends on phosphorylation by VRK1

During NEBD, BAF dissociates from chromatin, LEM domain proteins, and lamins. The dissociation of BAF from these structures during NEBD depends on its phosphorylation by the human vaccinia-related kinase 1 (VRK1) (**Fig. 1.11**). The first discovered role of VRK1 was its ability to phosphorylate histone H2A *in vitro*. VRK1 is widely conserved through evolution. One VRK1, called NHK-1, is found in *Drosophila*, one VRK1 in *C. elegans*, and three, VRK1,2,3, in mammals [181]. In human cells, the overexpression of VRK1 weakens the interaction between BAF and chromatin [182]. In an *in vitro* assay from the same study, VRK1 phosphorylates three sites located on the N-terminal region of BAF [182]. Moreover, the expression of a phospho-Ser 4 deficient mutant form of BAF leads to abnormal localization of Emerin to the NE [183]. Also, VRK1 depletion decreased the cytoplasmic portion of GFP-BAF compared with control cells. However, in contrast with previous studies, VRK1 depletion had no effect on the localization of Emerin and Lamin A/C in interphase cells [184]. These observations might be due to the incomplete loss of VRK1 by RNAi in these cells. Taken together, these results indicate that VRK1 phosphorylates BAF on Ser 4 for its dissociation from LEM domain proteins and chromatin during NEBD **(Fig. 1.11)**.

The mechanism of VRK1 phosphorylation of BAF, leading to its dissociation from chromatin and LEM domain proteins is also present in *Drosophila*. During the early stages

of fly oogenesis, meiotic chromosomes scatter the whole oocyte nucleus [181]. Chromosomes then form a compact structure in the middle of the oocyte nucleus at later stages of fly oogenesis called the karyosome. In the fly ovaries, the fly oocyte is blocked at the first metaphase of the first meiotic division [22]. When the female fly lays the egg, meiosis completes and four meiotic products form. The male sperm joins one of these meiotic products, while the other three form a polar body [22].

Interestingly, the karyosome in oocytes from females heterozygous for an *NHK-1* mutation, which reduces NHK-1 expression by about 20%, was less compact and meiotic chromosomes were found near the NE [181]. Purified wild type NHK-1, but not a kinase-dead mutant, was able to phosphorylate BAF in fly ovary extracts, indicating that BAF is a substrate of NHK-1 [181]. To test whether the phosphorylation of BAF is essential in karyosome formation, the authors designed a phospho-deficient BAF mutant by replacing three known phosphorylation sites on the N-terminal region of BAF by alanine [181, 182]. The expression of this phospho-deficient BAF mutant in flies leads to a less compact karyosome with meiotic chromosomes near the NE of oocytes [181]. This phenotype was weaker than the phenotype seen in oocytes from *NHK-1* mutant female flies, probably due to the presence of the wild type BAF in flies expressing the phospho-deficient BAF mutation. Moreover, the expression of this mutant increased the level of the fly LEM domain protein on the NE, indicating the BAF phosphorylation by NHK-1 is necessary for the dissociation of BAF from LEM domain proteins in flies [181]. It would be interesting to investigate the different phenotypes in syncytial embryos from females heterozygous for *NHK-1*.

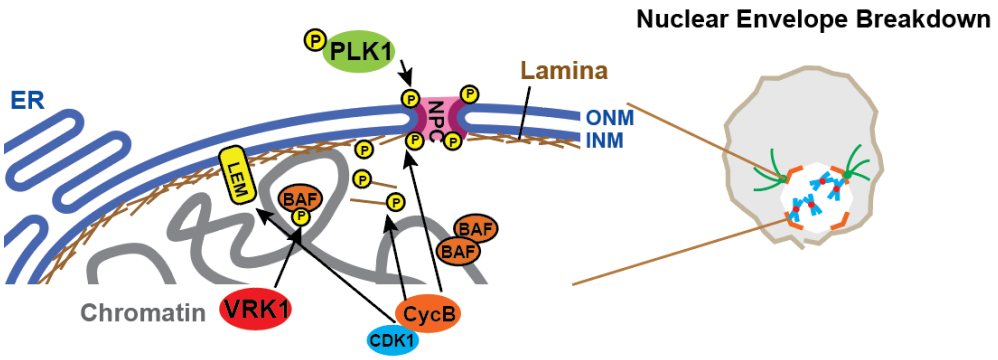

Figure 1.11: The regulation of nuclear envelope disassembly. Various kinases are implicated in phosphorylating nuclear envelope proteins to induce nuclear envelope disassembly. CDK1-cyclin B is known to phosphorylate several NE proteins such as proteins of the nuclear lamina and nucleoporins. Plk1 was also shown to phosphorylate nucleoporins. VRK1 is mostly known to phosphorylate BAF leading to its disassembly from LEM domain proteins such as LBR, Emerin, and MAN1.

1.8 The nuclear envelope reassembles at the end of mitosis

1.8.A. The general process of nuclear envelope reformation

The NER starts at late anaphase and finishes at the end of telophase. The first essential step in initiating NER is chromatin decondensation and nucleus shaping [122]. Many mechanisms are involved in this process. The first mechanism for chromatin decondensation depends on microtubule dynamics and occurs mostly in mouse oocytes and early embryos [185]. The chromokinesin KID is a plus-end-directed DNA binding motor that seems to be necessary during nuclear reassembly as its loss results in the formation of micronuclei in mouse oocytes [185]. Although the exact contribution of KID in the process of nuclear reassembly is still unexplored, it is thought that the KID-DNA

complex slides on microtubules to form a compact chromatin structure at anaphase of mouse oocyte meiosis. The second mechanism of chromatin decondensation relies on the AAA+ ATPase and the ubiquitin-dependent chaperone p97 [186]. This ubiquitin chaperone activates when it binds to its known cofactors, NPL4 and UFD1 [186]. During nuclear reassembly, and following ATP hydrolysis, the complex binds and removes polyubiquitinated aurora B found on chromatin [186, 187]. The removal of aurora B from chromatin is necessary to release its inhibitory effect on chromatin decondensation and NER. However, the identity of the aurora B substrates required for such an inhibitory role is still obscure. The final mechanism that is critical for shaping the nucleus during NER depends on the function of the small protein BAF. This mechanism was already discussed in section **1.6.B.c.**

After chromatin decondensation, NE membranes and proteins are recruited to the properly shaped nucleus. The ER provides an essential source of the NE membrane during the process of NER. In section **1.7.A**, we discussed that during NEBD, the ER forms a tubular-like structure where most NE proteins reside following NE disassembly. During NER, the ER extends toward the chromatin forming tips of ER tubules on the chromatin surface [188]. Integral proteins that are present within the ER membrane are also targeted to the chromatin surface and help in ER binding to chromatin [189, 190]. Once ER tips are bound to chromatin, more membranes are recruited to form a flat sheet of membranes that covers the chromatin and forms the NE [191]. During this process, more NE proteins, such as Emerin, LAP2β, and Lamin A, bind to the chromatin core region through a BAF-dependent mechanism [192, 193]. Other proteins such as Lamin B, some nucleoporins, and LBR are present at the noncore chromatin region [194]. ELYS/MEL-28 is one of the proteins that bind to the noncore region initiating NPC reassembly.

ELYS/Mel-28 binding to chromatin recruits members of the Nup107 complex to form the pre-pore complex [195]. More nucleoporins are recruited to complete the NPC assembly, as discussed in section **1.6.B.b.** During the NPC assembly, the complex is also being anchored to the formed nuclear membrane. Two models of NPC anchoring to membranes have been proposed [145]. The first model, also known as the insertion model, proposes that during NPC assembly, the complex anchors between two membrane sheets of the NE [145]. The other model, called the enclosure model, suggests that the assembly first starts by binding of nucleoporins to chromatin, during which nuclear membranes enclose the anchored NPC [145]. It is thought that the anchorage of the assembled NPC to the NE could take place through each of the two proposed models. As already discussed in section **1.6.B.b**, the function of the nucleoporin POM121 is critical to mediate the interaction between nuclear membranes and the NPC [196].

Following NPC membrane anchorage and the formation of nuclear membrane sheets over the chromatin, some gaps are still present in some regions of the NE. The process of NE sealing takes place to close these gaps, and is critical for perfect compartmentalization of the NE [122]. Several protein complexes are known to be implicated in the process of NE sealing. A group of proteins known as SNAREs, discovered in *Xenopus* extracts, seem to be required for NE sealing, as removal of these proteins from extracts leads to NER inhibition [197]. Also, the addition of an antibody that blocked SNARE activity in these extracts, accumulated vesicles on the chromatin surface and prevented NE sealing [197]. However, how do SNARE contribute to NE sealing and what are the specific SNARE proteins implicated in this mechanism are all questions that need to be answered. The ESCRT-III complex is another complex implicated in the process of NE sealing [198]. This complex is mostly known in the process of membrane

scission at the late stages of cytokinesis. It seems that this complex functions to cut the small pieces of membranes that might form at the end of NER [198].

The final step in NER is the reassembly of the nuclear lamina. We already explained that some ER tubules recruit some lamins to the chromatin surface. However, these lamins are not sufficient to assemble the whole lamina structure. When the NER finishes and the transport through NPC initiates, several karyopherins import lamins to the nucleus, and the lamina assembly begins [199]. The assembly of lamins to form the lamina depends on their dephosphorylation by phosphatases [122]. We will discuss the regulation of nuclear lamina reassembly and NER as a whole in the following section. When assembled, the nuclear lamina establishes several connections with regions of the NE. An interaction between the nuclear lamina and members of NPC is well demonstrated. By performing GST-pulldowns and other assays *in vitro*, the Nup 153 was found to strongly associate with nuclear lamina proteins such as Lamin A and Lamin B [200] A similar association also exists between Nup 88 and Lamin A, but not Lamin B1 and B2 [201]. By performing *in vivo* experiments in HEK cells and *in vitro* assays, it is clear that the N-terminal part of Nup 88 binds tightly to the tail region of Lamin A [201]. Another interaction takes place between the nuclear lamina and ONM proteins. The interaction between the nuclear lamina and ONM proteins having a KASH domain (section **1.6-C**), which is lost during NEBD, reestablishes at the end of NER. The interaction between the nuclear lamina and the ONM is critical for the association of the nucleoskeleton with the cytoskeleton [122].

1.8.B. PP2A-B55 and PP1 as principal regulators of NER

Since many kinases phosphorylate a large group of substrates to induce NEBD, NER fails to occur if these substrates were not dephosphorylated. Several phosphatases are known to dephosphorylate these substrates. However, the phosphatases PP2A-B55 and PP1 are critical regulators of the process of NER, since the treatment of cells with OA delayed the process of NER [71]. Interestingly, human cells depleted from B55α also delayed nuclear reassembly [88]. Moreover, worm embryos depleted from Let-92, the catalytic subunit of PP2A in *C. elegans*, resulted in embryos with abnormally shaped nuclei [202]. These results suggest that PP2A-B55 and PP1 are essential for the process of NER. For instance, PP1-Repo-man localizes to mitotic chromosomes during anaphase and prevents chromatin condensation [203]. Also, PP1-PNUTS locates to reassembling nuclei and is thought to function in chromatin decondensation [127]. However, the proteins dephosphorylated by PP1-Repo-man and PP1-PNUTs to inactivate chromatin condensation and activate chromatin decondensation respectively are not known. PP2A and PP1 are also required for NPC reassembly. The injection of OA in *Drosophila* fly embryos prevents the reassembly of the NPC [203]. As discussed in section **1.6.B.c,** PP1-Repo-man is necessary for NPC reassembly at the end of mitosis (**Fig. 1.12**). It remains to be seen whether some Nups are dephosphorylated by PP1-Repo-man. For PP2A-B55, a proteomics-based study identified high confidence PP2A-B55 dependent substrates. Among those identified, PP2A-B55 dephosphorylates sites on Nup98, Nup153, Nup107, and POM121 [91] (**Fig. 1.12**). However, the implication of the dephosphorylation of these Nups by PP2A-B55 is unknown. For instance, are all these dephosphorylation events essential for NPC reassembly at mitotic exit? It would be interesting to mutate some of these sites to identify the Nup (s) that is critical for NPC assembly at the end of mitosis.

PP1 is also thought to be a Lamin B phosphatase. Using multiple biochemical assays to measure different Lamin B phosphatase activities, the study shows that PP1 but not PP2A is responsible for Lamin B dephosphorylation *in vitro*. Also, *in vitro* experiments show that the PP1 regulatory subunit AKAP149 recruits PP1 to reassembling nuclei for Lamin B dephosphorylation [128] (**Fig. 1.12**). Loss of AKAP149 fails to recruit PP1 to the NE leading to failure in nuclear lamin reassembly and abolishment of NER [128]. However, *in vivo* results showing the role of PP1 and not PP2A in Lamin B reassembly, are still missing. For example, what is the effect of depleting PP1, PP2A, or B55 on Lamin B reassembly in cells? Do PP1 and PP2A work together to promote NER? What are the Lamin B sites dephosphorylated by PP1 or PP2A? How is Lamin B dephosphorylation linked with NER? We will answer all of these questions in **Chapter two** of this thesis. We will also discuss the credibility of results showing that PP1 is a Lamin B phosphatase in **Chapter four** of this thesis.

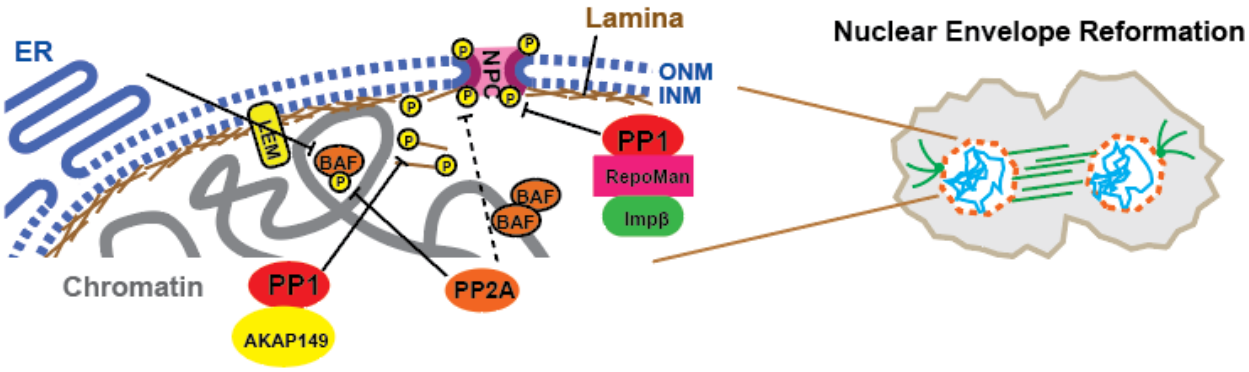

Figure 1.12: The regulation of nuclear envelope reassembly. At the end of mitosis, PP2A-B55 dephosphorylates BAF and might also dephosphorylate proteins of the nuclear lamina and nucleoporins. PP1-AKAP149 is also known to dephosphorylate proteins of the nuclear lamina. PP1-Repo-man dephosphorylate nucleoporin. These and other dephosphorylation events lead to the reformation of the nuclear envelope at mitotic exit.

In another study, an *in vitro* phosphatase assay showed that PP2A dephosphorylates BAF (**Fig. 1.12**). Increased concentrations of purified PP2A actively dephosphorylated recombinant BAF, previously phosphorylated by VRK1 [202]. However, the regulatory subunit required to target PP2A for BAF dephosphorylation was not explored in that study. For instance, what is the effect of depleting B55 or B56 on BAF recruitment to nuclei? What are the BAF sites dephosphorylated by PP2A? How does BAF dephosphorylation by PP2A affect the proper NER? Is BAF dephosphorylation essential for its interaction with other NE proteins? We will also respond to these questions in **Chapter two** of this thesis.

In a previous study, authors performed a genetic screen to identify genes that express proteins implicated in the process of NER during mitotic exit in *C. elegans*. Many genes were found, but authors were interested investigating in the role of the protein LEM4/ Ankle2, as worm embryos with temperature-sensitive mutants of LEM had severe NE defects [202]. Interestingly, the knockdown of LEM4 by RNAi completely abolished the recruitment of BAF to reassembling nuclei. These results and others made the authors conclude that, at mitotic exit, LEM4 binds both VRK1 and PP2A. LEM4 binding inhibits VRK1 and activates PP2A to promote BAF dephosphorylation and its binding to LEM domain proteins during NER [202]. More recently, a study showed that the knockout of Ankle2 by the CRISPR/Cas9 system also abolishes BAF recruitment to reassembling nuclei in HeLa cells [204]. LEM4 also interacts with both the catalytic and scaffolding region of PP2A [204]. However, what is the nature of the protein Ankle2? Is Ankle2 a PP2A regulatory subunit? Is PP2A-Ankle2 involved in regulating NER? Does PP2A bound to Ankle2 possess a phosphatase activity? Does PP2A bound to Ankle2 dephosphorylate BAF? We will be answering these questions and others in **Chapter three** of this thesis.

1.8.C. PP4 also regulates NER by dephosphorylating BAF

The importance of the role of PP2A and PP1 is in dephosphorylating multiple substrates, one of which is dephosphorylating mitotic exit substrates. The wide range of PP2A and PP1 regulatory subunits is essential for increasing substrate specificity and targeting the phosphatase to different cell compartments [122]. However, other phosphatases can function in triggering some events of NER. In human cells, for instance, the protein phosphatase PP4 dephosphorylates BAF for its recruitment to newly formed nuclei during NER. Cells depleted from the catalytic subunit of PP4 increased BAF phosphorylation and produced irregular and wrinkled shaped nuclei [205]. This indicates that PP4 dephosphorylate BAF in human cells and that BAF dephosphorylation is essential for proper NER. We will discuss the results of this study in **Chapter four** of this thesis. We will also discuss some results that might contradict with data from this study in **Chapter two**.

CHAPTER 2

Publication

PP2A-B55 promotes nuclear envelope reformation after mitosis in *Drosophila*

Article published in *JCB* 2018 Dec 3;217(12):4106-4123 PP2A-B55 promotes nuclear envelope reformation after mitosis in *Drosophila*.

Haytham Mehsen[1], Vincent Boudreau[1,2], Damien Garrido[1], Mohammed Bourouh[3], Myreille Larouche[1,2], Paul S. Maddox[1], Andrew Swan[3], and Vincent Archambault[1,2]

1 Institute for Research in Immunology and Cancer, Université de Montréal, Montréal, Québec, Canada.

2 Département de Biochimie et Médecine Moléculaire, Université de Montréal, Montréal, Québec, Canada.

3 Department of Biology, University of Windsor, Windsor, Ontario, Canada.

Corresponding Author: Vincent Archambault

2.1 Abstract

As a dividing cell exits mitosis and daughter cells enter interphase, many proteins must be dephosphorylated. The protein phosphatase 2A (PP2A) with its B55 regulatory subunit plays a crucial role in this transition, but the identity of its substrates and how their dephosphorylation promotes mitotic exit are largely unknown. We conducted a maternal-effect screen in *Drosophila* to identify genes that function with PP2A-B55/Tws in the cell cycle. We found that eggs that receive reduced levels of Tws and of components of the nuclear envelope (NE) often fail development, concomitant with NE defects following meiosis and in syncytial mitoses. Our mechanistic studies using *Drosophila* cells indicate that PP2A-Tws promotes nuclear envelope reformation (NER) during mitotic exit by dephosphorylating BAF and suggests that PP2A-Tws targets additional NE components including Lamin and Nup107. This work establishes *Drosophila* as a powerful model to

further dissect the molecular mechanisms of NER and suggests additional roles of PP2A-Tws in the completion of meiosis and mitosis.

2.2 Introduction

The roles of kinases in mitosis have been extensively characterized in the last decades. Cyclin B-CDK1 triggers entry into mitosis [206]. Phosphorylation of multiple substrates by this enzyme alters their activities to promote chromosome condensation, nuclear envelope breakdown and spindle assembly [207]. Other kinases, including Aurora A and Polo, peak in activity when cells enter mitosis and promote this transition [208, 209]. The onset of chromosome segregation, concomitant with the degradation of mitotic cyclins, marks the beginning of mitotic exit. While some phosphorylated substrates are degraded by the proteasome, thousands of sites on hundreds of proteins are dephosphorylated in an orderly manner during mitotic exit to ensure proper return to G1 [45, 210]. Although phosphatases are equally important as kinases, their roles in the cell cycle have been much less studied. Which proteins must be dephosphorylated, at which sites and by which phosphatases for correct mitotic exit to take place is still poorly understood.

Phosphatases are increasingly recognized as highly regulated and selective enzymes in the coordination of cell division [211]. While the number of catalytic phosphatase subunits is inferior to the number of kinases, many phosphatases are regulated by a myriad of associated subunits and posttranslational modifications. The trimeric Protein Phosphatase 2A (PP2A) is composed of a catalytic subunit C, a scaffold subunit A and a regulatory subunit B [212]. Several alternative types of B subunits,

generally termed B, B', B'' and B''', can modulate PP2A, by conferring substrate specificity and directing PP2A to different sub-cellular locations. In vertebrates, 4 subtypes of B-type subunits co-exist: B55α, β, γ and δ. B55α and B55δ are ubiquitously expressed and have been shown to play important roles in cell division. PP2A-B55 enzymes efficiently dephosphorylate CDK substrates [84-86]. In *Xenopus*, depletion of B55δ from interphase egg extracts accelerates mitotic entry [85]. In human cells, silencing B55α delays nuclear envelope reformation, chromosome decondensation and interferes with spindle function in cytokinesis [88]. Genetic work in mice has provided evidence for functions of B55α and B55δ in mitotic exit [213]. In *Drosophila*, the sole B-type PP2A subunit is encoded by *twins* (*tws*). Mutations in *tws* are lethal and lead to anaphase defects in larval neuroblasts [214]. Thus, PP2A-B55 plays an important role in mitotic exit *in vivo* across animal species.

PP2A-B55 activity is cell-cycle regulated: low in early mitosis and high in late M-phase and interphase [85]. This regulation depends on Greatwall (Gwl) kinase, which is activated by CDK1 at mitotic entry and phosphorylates Endosulfine proteins (ENSA and Arpp19 in vertebrates, Endos in *Drosophila*). Once phosphorylated by Gwl, Endosulfines act as selective competitive inhibitors of PP2A-B55 [215-217]. Endosulfines are substrates of PP2A-B55 which have very high affinity for the enzyme but are dephosphorylated inefficiently, transiently inhibiting PP2A-B55 with respect to its other substrates [101]. This inhibition of PP2A-B55 promotes the phosphorylation state of CDK1 substrates. At mitotic exit, PP1 initiates Gwl inactivation [218, 219]. Endosulfines are eventually dephosphorylated by PP2A-B55, which then becomes active towards other substrates [101]. The delay between Cyclin B-CDK1 inactivation and PP2A-B55 activation allows an orderly sequence of events in mitotic exit in human cells, with PP2A-B55 acting only after chromosome segregation [87].

PP2A-B55 regulates spindle function in cytokinesis and promotes chromosome decondensation and nuclear envelope reformation (NER) [71, 87, 88]. However, the important substrates of PP2A-B55 in these functions, and the mechanistic impact of their dephosphorylation are largely unknown. The reassembly of interphase nuclei after mitosis is an orderly process that requires the reconstruction of a nuclear envelope around chromatin [122, 220, 221]. Proteins of the nuclear lamina and nuclear pores are assembled in a step-wise manner on chromatin-binding adaptors including Barrier-to-Autointegration Factor (BAF). In *C. elegans*, BAF recruitment to reassembling nuclei has been shown to depend on PP2A, although the mechanism of this regulation is still unclear [202]. Little is known about the mechanisms of NER in *Drosophila*.

In this study, we have used *Drosophila* to search for essential functions of PP2A-B55/Tws in the cell cycle. We conducted a maternal-effect genetic screen to identify enhancer mutations of a partial loss of PP2A-Tws function. We hypothesized that we would identify factors that function with PP2A-Tws in mitotic exit, as an entry point towards a better mechanistic understanding of this process. We found genetic interactions that pointed towards an important role of PP2A-Tws in NER. We followed up with functional and biochemical studies to dissect the roles of PP2A-Tws in NER. Our results suggest that PP2A-Tws dephosphorylates multiple proteins including BAF and Lamin to promote the reassembly of nuclei after mitosis.

2.3 Results

2.3.A. A maternal-effect genetic screen for interactors of PP2A-Tws.

To identify genes that collaborate with PP2A-Tws in the cell cycle, we conducted a genetic screen in *Drosophila*. We exploited the fact that female meiosis and the first embryonic cell cycles are sensitive to genetic alterations in the cell cycle machinery. Oogenesis and early embryogenesis rely on maternally deposited mRNAs and proteins (**Fig. 2.1.A**) Several genes that encode cell cycle regulators or effectors were identified from maternal-effect lethal mutants [222]. We used flies that are heterozygous for a strong hypomorphic allele of *tws* (*tws*^{P}) [223]. These flies are viable and fertile, but are sensitized to partial loss of function in genes that collaborate with PP2A-Tws. We hypothesized that genes of which the loss of a single allele is maternal-effect synthetic-lethal in the *tws*^{P}/+ background may function in a common mechanism with PP2A-Tws in the cell cycle (**Fig. 2.1.B, C**). Similarly, we previously identified mutations in *tws* as heterozygous enhancers of *gwl*^{Scant}, which encodes a constitutively active form of Gwl, a kinase that antagonizes PP2A-Tws [89].

We screened through a collection of deletions on the 2nd and 3rd chromosomes, mostly obtained from the Drosdel isogenic deficiency kit [224]. Most of them are large genomic deletions, and together they cover nearly 70% of the genome. Each line was crossed with the *tws*^{P}*/TM6B* line to generate *Df/+, tws*^{P}/+ females that were subjected to fertility tests. Deletions that, when combined with *tws*^{P}, resulted in a hatching rate below 50% were selected for further analysis. In parallel to the screen against *tws*^{P}, we similarly screened against a null allele of *microtubule star* (*mts*$^{XE\text{-}2258}$), which encodes the catalytic subunit of PP2A [225]. The genetic interactors of *tws* and *mts* overlapped only partially,

suggesting that the mutant allele in *mts* also sensitizes eggs or embryos in PP2A-dependent functions that rely on regulatory subunits other than Tws. Not surprisingly, deletions uncovering *mts* interacted with *tws,* and deletions uncovering *tws* interacted with *mts*, probably because halving the levels of both Tws and Mts simultaneously further compromises the levels of PP2A-Tws holoenzyme. An overview of the primary results is shown in (**Fig. 2.1.D**). The complete dataset is presented in **Table 1**.

Finer mapping with overlapping deletions, followed by the testing of candidate genes included in the uncovered genomic intervals, led us to the identification of individual genes for which mutation of one allele in combination with one mutant allele of *tws* or *mts* strongly decreases the viability of embryos in a maternal effect (**Fig. 2.2.A**). As expected, we recovered an interaction between *tws* and *polo*, which encodes a mitotic kinase, as previously found [89]. A strong interaction was found between *tws* and *CycB3*, which encodes the mitotic Cyclin B3, required for anaphase [226]. Interestingly, we also found interactions between *tws* and *lamin* (*lam; Dm_0*), which encodes the Lamin protein, a structural component of the nuclear lamina, around which the nuclear envelope is assembled during mitotic exit [122].

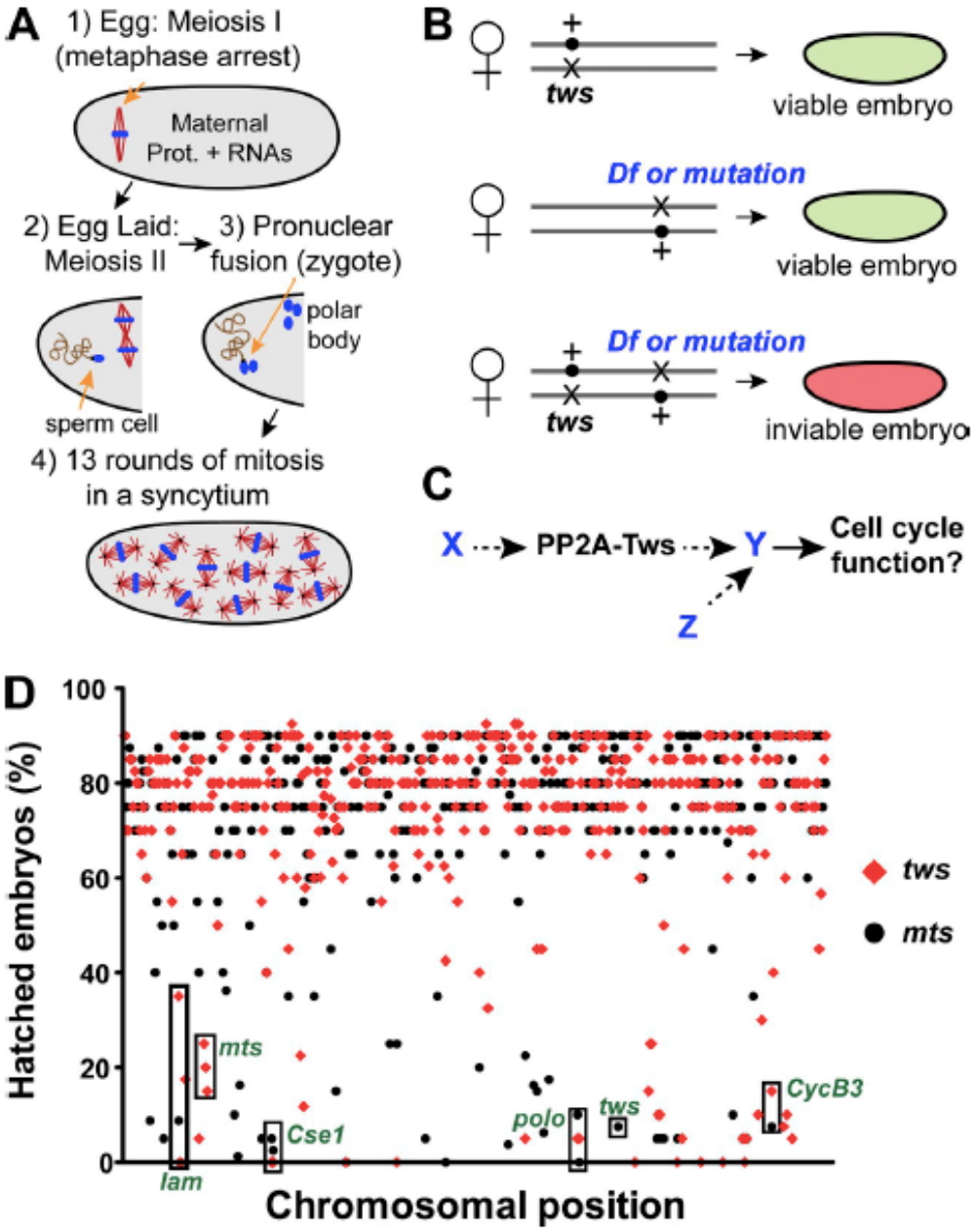

Figure 2.1 A maternal-effect second-site noncomplementation screen for interactors of PP2A-Tws. A. Completion of meiosis in the egg and early embryogenesis in *Drosophila* depends on maternally provided mRNAs and proteins. B. Design of the screen. Genetic deletions (deficiencies, *Df*) were combined with a mutant allele of *tws* (tws^{P}) or *mts* ($mts^{XE\text{-}2258}$) in one cross. Heterozygosity for either tws^{P} (or $mts^{XE\text{-}2258}$) or the *Df* (or mutation) allows viability and fertility, but heterozygosity for both results in females whose eggs fail to hatch. C. Genes identified in this screen could function upstream (X),

downstream (Y) or in parallel (Z) to PP2A-Tws in the cell cycle. D. Overview of primary results. Names of particular genes found to interact genetically with *tws* and *mts* are indicated on data points corresponding to deficiencies that uncovered them. Experiment in D was performed by Vincent Boudreau. Drawings in A and B were done by Vincent Archambault.

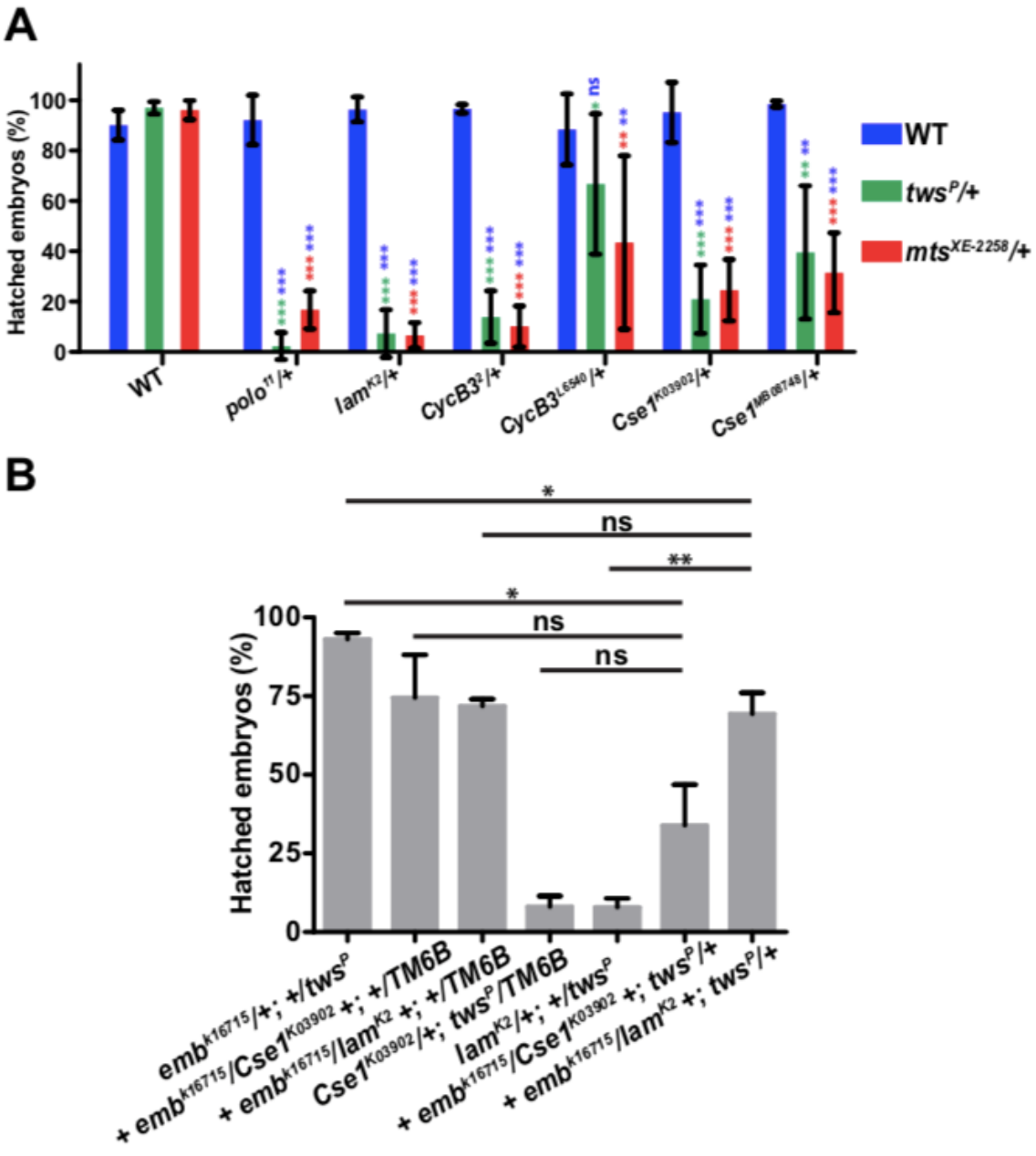

Figure 2.2. Genetic interactions of PP2A-Tws identified. A. Genetic interactions between *tws*, *mts* and hits identified in the screen. The percentages of embryos hatching

from females of the indicated genotypes were quantified. Genotypes are the combination of what is labeled under the graph and what is indicated by the color code. Error bars: S.D. *P=0.0132, **0.0056<P<0.0068, ***0.0001<P<0.0009, from two-tailed *t*-test between the double mutant and the single tws^{P} (green symbols) or $mts^{XE-2258}$ (red symbols) mutants, or between the double mutant and the single mutant allele of the identified interactor (blue). B. Genetic interactions between nucleo-cytoplasmic transport factors and *tws*. Introduction of one hypomorphic allele of *embargoed/Crm1* (emb^{k16715}) in lam^{K2}/+; tws^{P}/+ females or $cse1^{k03902}$/+; tws^{P}/+ females rescues the development of embryos they produce. Percentages of hatching of embryos from females of the indicated genotypes were scored. Error bars: S.D. *0.0239<P<0.0417, **P=0.0014, from two-tailed *t*-test. Experiment in B was performed by Vincent Boudreau.

2.3.B. Eggs and embryos with reduced PP2A-Tws and Lamin incur nuclear envelope defects and abort development.

We hypothesized that the genetic interaction between *tws* and *lamin* might reflect a role of PP2A-Tws in NER during mitotic exit. To confirm the genetic interaction between *tws* and *lamin*, we tested different alleles of both genes. Three hypomorphic alleles of *tws* were tested and all of them enhanced alleles of *lamin* in the following strength order: tws^{aar1} > tws^{P} > tws^{aar2}. Reciprocally, all 3 alleles of *lamin* tested enhanced alleles of *tws* in the following strength order: lam^{K2} ≈ lam^{A25} > lam^{04643} (**Fig. 2.3.A**). To begin exploring the cellular basis for the lethality observed, we examined embryos aged between 0 and 2 hours from lam^{K2}/+; tws^{P}/+ mothers. Western blots confirmed that mothers heterozygous for the tws^{P} and lam^{K2} mutations produced embryos with lower levels of Tws and Lamin (**Fig. 2.3.B**). Immunofluorescence revealed that the majority of embryos undergoing mitotic development have severe defects (**Fig. 2.3.C**). Nuclei are often mispositioned and have abnormal sizes and shapes. Centrosomes are frequently disjoined from nuclei

(quantified in **Fig. 2.3.D**). Chromatin masses are seen free in the cytoplasm, often attached to nuclear envelope fragments, as if shredded. All these phenotypes could result from a weakness or defect in the nuclear envelope. Time-lapse imaging of syncytial embryos from *lam*^{K2}/+*; tws*^{P}/+ mothers also expressing GFP-Polo as a marker of mitotic structures [227] reveals that the disintegration of nuclei/centrosome units leads to further disorganization including spindle fusions and uneven nuclear spacing (Movies S1-S2). Embryos laid by *tws*^{P}/+ or *lam*^{K2}/+ mutants displayed only minor developmental defects such as occasional centrosome detachment from nuclei (Figures **2.4** and **2.3.D**).

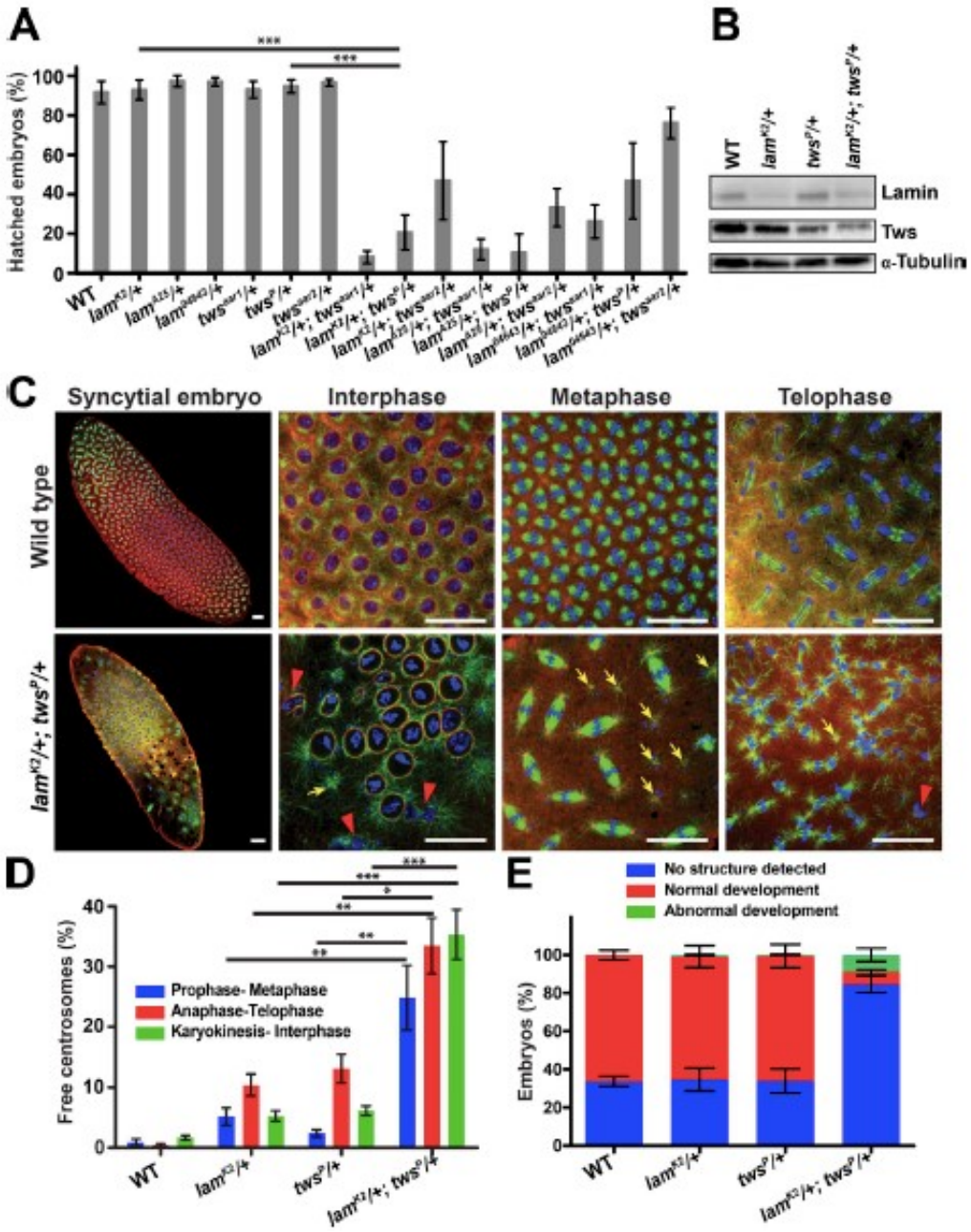

Figure 2.3. Collaboration between PP2A-Tws and Lamin is required for syncytial embryonic development. A. Genetic interactions between different alleles of *tws* and *lam*. Percentages of hatching of embryos from females of the indicated genotypes were scored. Error bars: S.E.M. ***P<0.0001, from two-tailed *t*-test. B. Western blots from embryos showing how protein levels are affected by the maternal genotypes. C. Phenotypes in embryos revealed by immunofluorescence against α-Tubulin (green), γ-Tubulin and Lamin (red), and DNA (DAPI, blue). In embryos from $lam^{K2}/+; tws^{P}/+$ females, several defects are observed: aberrant nuclear distribution (left), interphase nuclei of

abnormal shapes and sizes, centrosome detachments (yellow arrows), broken nuclei (red arrowheads). All scale bars: 20 μm. D. Quantification of free centrosomes observed at different cell cycle stages in embryos of the indicated genotypes. E. Quantification of global embryonic development for the indicated genotypes. Error bars: S.E.M. *P=0.0165, **0.0021<P<0.0027, ***P<0.0001, from two-tailed *t*-test.

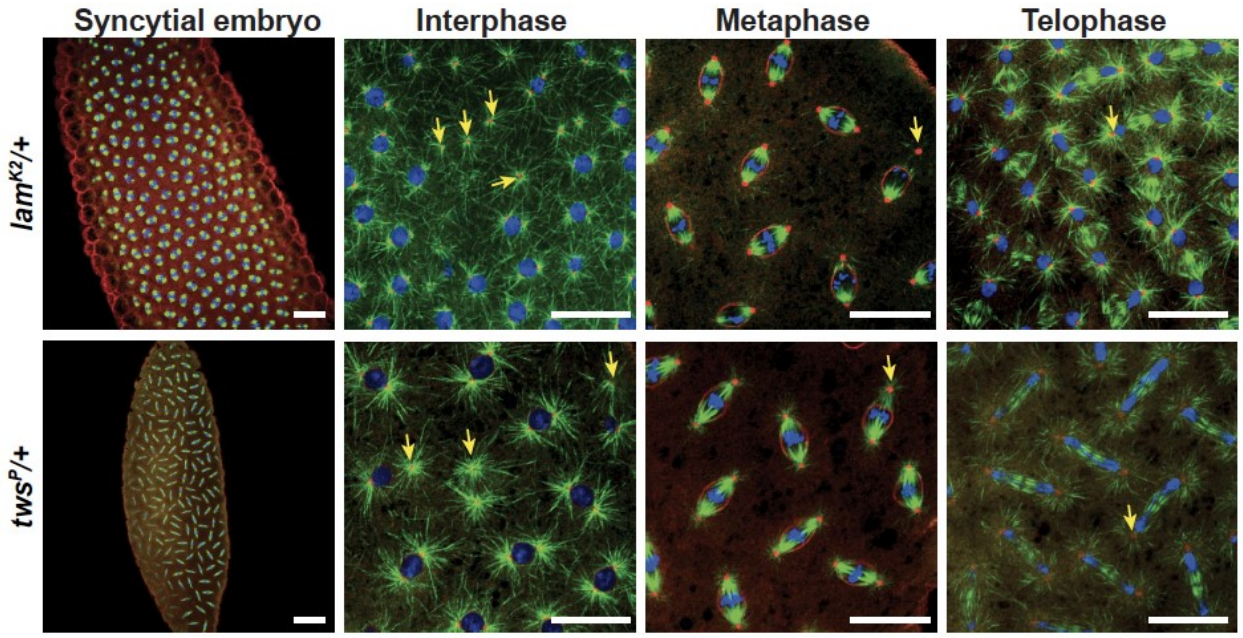

Figure 2.4. Embryos from females heterozygous for *lam*^{K2} or *tws*^{P} alleles alone show only minor developmental defects. Immunofluorescence against α-Tubulin (green), γ-Tubulin and Lamin (red), and DNA (DAPI, blue). Arrows indicate detached centrosomes. All scale bars: 20 μm.

Although major defects are prevalent in *lam*^{K2}/+; *tws*^{P}/+ derived embryos where mitotic nuclei are detected at the cortex, we found that the majority of eggs laid do not reach that stage (**Fig. 2.3.E**). We therefore investigated potential earlier defects, as early as meiosis. Normally, an oocyte arrests in metaphase of meiosis I until it is laid by the mother. Ovulation triggers completion of meiosis I, and meiosis II immediately follows with

two spindles attached together at one pole. At the end of meiosis II, four haploid nuclei assemble a nuclear envelope around decondensed chromatin, in post-meiotic interphase. If the egg has been fertilized, the innermost nucleus generally becomes the female pronucleus and it joins the male pronucleus before the first mitosis occurs. The other three nuclei eventually come together and undergo NEBD, chromatin condenses and associates with a microtubule array as a polar body (**Fig. 2.1.A**). If the egg is not fertilized, all four post-meiotic nuclei assemble into a polar body. We collected eggs/embryos aged between 0 and 20 minutes and analyzed them by immunofluorescence after fixation using a protocol allowing deep staining. We found *lam*^{K2}*/+; tws*^{P}*/+* eggs at all stages of meiosis, with similar frequencies to single-mutant eggs (**Fig. 2.5.A-I**). However, in eggs from *lam*^{K2}*/+; tws*^{P}*/+* mothers, we found that NE structures as detected by Lamin staining were often absent or of irregular shape (**Fig. 2.5.F, G, and J**). These results suggest that when levels of PP2A-Tws and Lamin are halved, the assembly of post-meiotic interphase nuclei is compromised. Using FISH against the X-chromosome, we found that most eggs from *lam*^{K2}*/+; tws*^{P}*/+* mothers form a zygotic nucleus containing at least one X-chromosome, indicating that a female pronucleus contributed to zygote formation (data not shown). Therefore, while nuclear envelope formation is compromised, pronuclear apposition can still occur, suggesting that the failure of embryos to develop is due primarily to defects that happen after meiosis, in the early mitotic divisions.

To explore the specificity of the genetic link between Lamin and PP2A-Tws, we tested for potential genetic interactions between *lam*^{K2} and different mutant alleles of various phosphatase subunits (Table 2). Strong genetic interactions were found only between *lam*^{K2} and *tws* or *mts* mutant alleles, suggesting that PP2A-Tws plays a particularly important role in relation to Lamin.

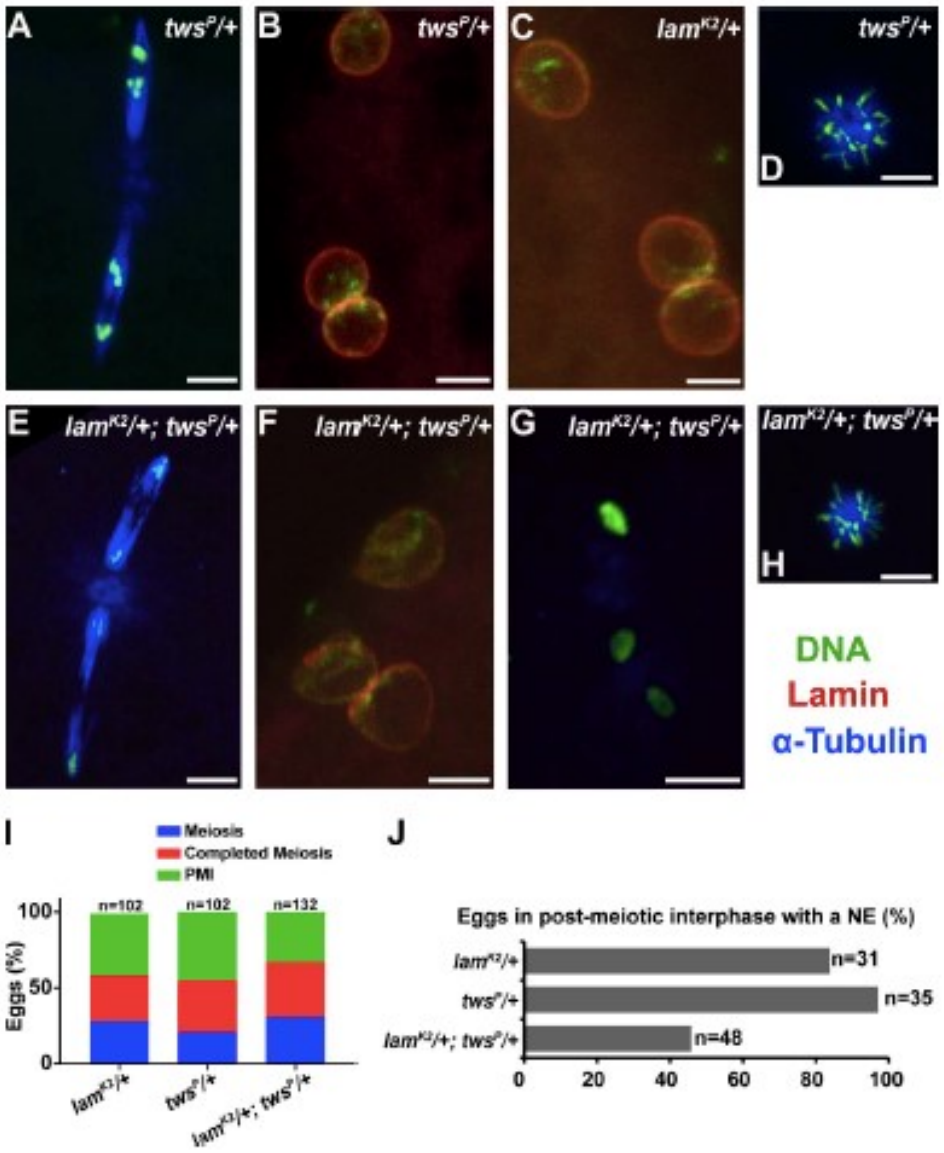

Figure 2.5. PP2A-Tws and Lamin cooperate for nuclear envelope reformation in meiosis. Eggs were collected for 0 to 20 min, fixed in methanol and stained for α -Tubulin (Blue), DNA (Green) and Lamin (Red). A-D. Representative images from *lam*^{K2}/+ or *tws*^{P}/+ eggs. A. Meiotic spindles in anaphase II. B,C. Post-meiotic interphase; 3 nuclei are shown with nuclear envelopes present around each nucleus. D. a polar body is formed after completion of meiosis. E-H. Representative images from *lam*^{K2}/+; *tws*^{P}/+ double eggs. E. Normal meiotic spindles in anaphase II. F,G. Several *lam*^{K2}/+; *tws*^{P}/+ eggs in post-meiotic interphase show either 3 nuclei with faint and irregular nuclear envelopes (F compared to B and C) or 3 nuclei without nuclear envelopes (G). H. The majority of eggs from *lam*^{K2}/+;

tws^{P}/+ mothers are able to complete meiosis normally, indicated by the formation of a polar body. I. Eggs from *lam*^{K2}/+; *tws*^{P}/+ mothers complete meiosis. Phenotypes observed were classified as either in meiosis, in post-meiotic interphase (PMI) or completed meiosis (indicated by the formation of a polar body). J. Quantification of the fraction of eggs in post-meiotic interphase with detectable nuclear envelopes. For data in I and J, numbers were pooled from two separate stainings and scorings done with eggs cumulated after multiple collections with immediate fixations. All scale bars: 5 μm. Experiments in this figure were performed by Mohammed Bourouh.

2.3.C. CDK phosphorylation consensus sites in Lamin control its solubility.

Based on these results, we hypothesized that PP2A-Tws could dephosphorylate Lamin to promote its function at the nuclear envelope. The regulation of lamins by phosphorylation is complex and not completely understood, but their phosphorylation at CDK sites has been shown to promote lamina disassembly in various systems [136, 167, 228]. In *Drosophila* Lamin, 6 of the 7 minimal CDK motifs (S/T-P) were so far found to be phosphorylated [228]. To begin testing if phosphorylation at CDK sites is required for the dispersal of *Drosophila* Lamin in mitosis, we mutated all 7 CDK sites into Ala (7A) or Asp (7D) residues (**Fig. 2.6.A**). We then made stable cell lines allowing inducible expression of RFP-Lamin$^{WT,\ 7A\ or\ 7D}$ and imaged cell division. While RFP-Lamin^{WT} localizes to the NE in interphase, it becomes dispersed throughout the cell in mitosis (**Fig. 2.6.B** top). By contrast, RFP-Lamin^{7A} fails to disperse in mitosis, forming an elongating mass around the presumptive chromosome mass that is successfully split into two nucleus-like structures as the cell divides (**Fig. 2.6.B** bottom). These results suggest that phosphorylation of Lamin at CDK consensus sites is required for normal dispersion of Lamin in mitosis.

However, we observed that RFP-Lamin^{7D} also fails to become dispersed in mitosis (data not shown), possibly because the 7 Asp substitutions do not fully mimic the effect of phosphorylation.

To test biochemically if phosphorylation of Lamin at CDK sites promotes its dispersion in the cell, we made cells expressing the different forms of Myc-Lamin. Cells were lysed and extracts were centrifuged to separate a soluble fraction (supernatant) from an insoluble fraction (pellet) containing the chromatin. Lysates were analyzed by Western blots. While 40% of Myc-Lamin^{WT} is soluble, 80% of Myc-Lamin^{7D} is soluble under these conditions (**Fig. 2.6.C, D**). Myc-Lamin^{7A} behaves similarly to Myc-Lamin^{WT} in these extracts from asynchronous cells. These results suggest that phosphorylation at CDK consensus sites in Lamin may disrupt an interaction that promotes lamina assembly. Treating cells with okadaic acid (OA), which inhibits a subset of phosphatases including PP2A, increased the solubility of Myc-Lamin^{WT}, consistent with the idea that PP2A-Tws promotes lamina assembly (**Fig. 2.6.C, D**). However, Myc-Lamin^{7A} was similarly affected by OA, suggesting that phosphorylation outside CDK sites on Lamin can also disrupt the lamina (see below).

Finally, we used genetics to test if Cyclin B-CDK1 antagonizes the collaboration between PP2A-Tws and Lamin in embryos. We found that introduction of a *CycB* mutant allele in *lam^{K2}/+; tws^{P}/+* females partially rescues their fertility, suggesting that PP2A-Tws promotes NER partly by dephosphorylating Cyclin B-CDK1 sites, possibly on Lamin (**Fig. 2.6.E**).

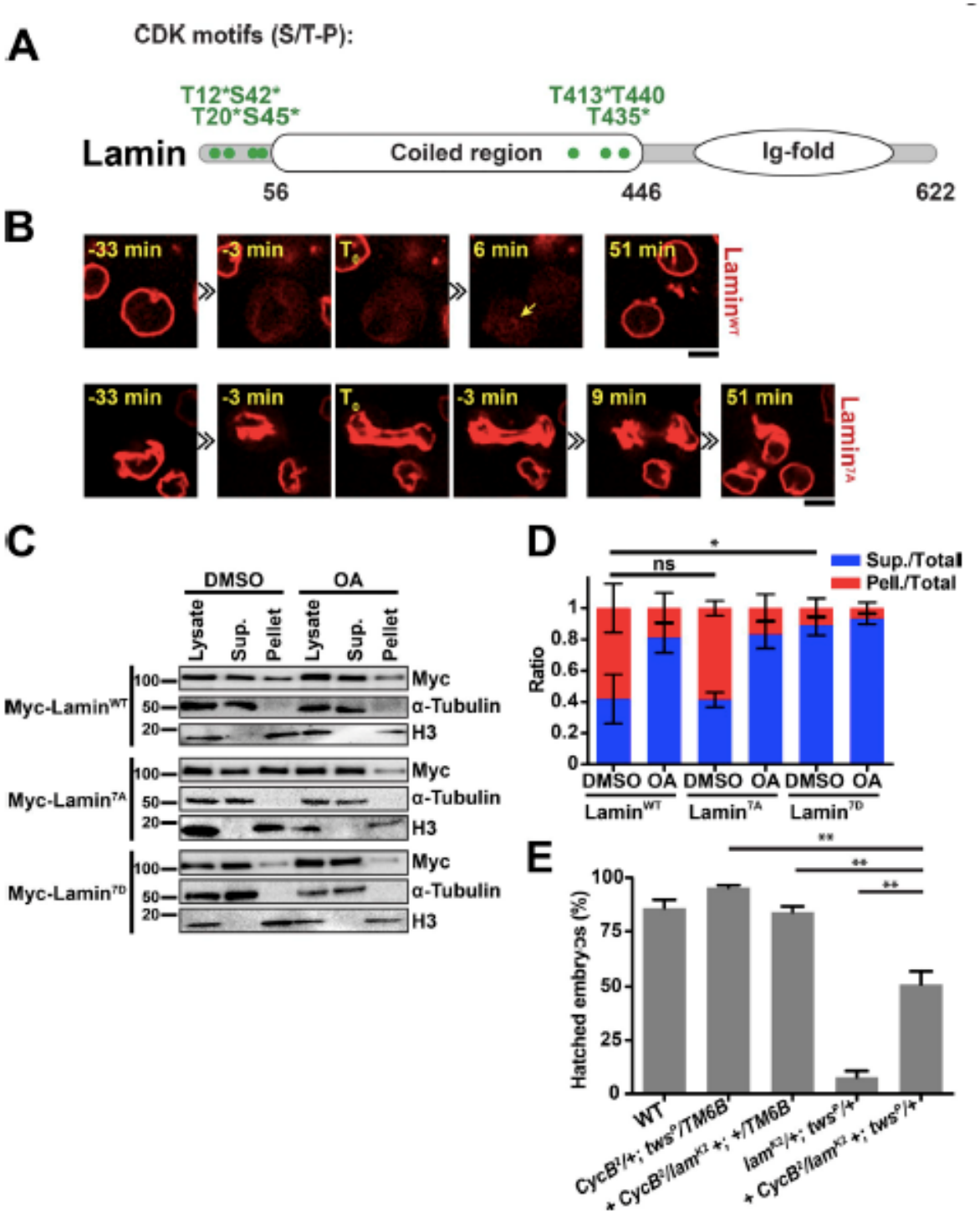

Figure 2.6. Phosphorylation at CDK phosphorylation consensus sites in Lamin may promote its dispersion in mitosis. A. All 7 minimal CDK phosphorylation consensus sites, shown here in a schematic Lamin structure (adapted from [229]), were mutated into Ala or Asp residues. *phosphorylation sites observed experimentally [228]. B. Cells

expressing RFP-Lamin^{WT} or RFP-Lamin^{7A} were filmed on a spinning-disk confocal microscope. T_0 was defined as the beginning of the cell's elongation as it divides. While RFP-Lamin^{WT} becomes dispersed in mitosis and starts being recruited at 6 min (yellow arrow), RFP-Lamin^{7A} is never dispersed as the cells progress through mitosis. C. Mutation of all CDK consensus sites into Asp in Lamin (Myc-Lamin^{7D}) increases its solubility. Stable cell lines expressing the indicated proteins were treated as indicated before being lysed and the insoluble material was pelleted (see Materials & Methods). Fractions were analyzed by Western blot. D. Quantification of relative Western blots signals from soluble and insoluble fractions from 3 independent experiments as in B. Error bars: S.D. *P=0.0437, from two-tailed *t*-test. E. Introduction of one null allele of *CycB* (*CycB*^{2}) in *Lam*^{K2}*/+; tws*^{P}*/+* females rescue the development of embryos they produce. Percentages of hatching of embryos from females of the indicated genotypes were scored. Erroμr bars: S.D. ** 0.0051<P<0.0095, from two-tailed *t*-test. Experiment in E was performed by Vincent Boudreau.

2.3.D. PP2A-Tws promotes the recruitment of Lamin and Nup107 to nascent nuclei during mitotic exit.

The genetic and biochemical results described above suggested that PP2A-Tws might promote Lamin reassembly on nuclei at the end of mitosis. To test this idea, we generated a *Drosophila* D-Mel2 cell line that stably expresses GFP-Lamin and mCherry-α-Tubulin and examined the effect of Tws depletion by RNAi on the reassembly of GFP-Lamin. Silencing of Tws was confirmed by Western blot (**Fig. 2.7.A**). In control cells (transfected with KAN dsRNA), GFP-Lamin starts to enrich on reforming nuclei 5 to 10 min after anaphase spindle elongation. By contrast, in Tws-depleted cells, GFP-Lamin appears later, 20 to 25 min after spindle elongation (**Fig. 2.7.B-C**). We conclude that PP2A-Tws promotes the recruitment of Lamin during NER.

We wondered if PP2A-Tws specifically promotes the recruitment of Lamin in NER or if it also affects other components of the NE. We examined Nup107, a component of the Nup107-Nup160 subcomplex whose recruitment at the NE nucleates nuclear pore complex assembly and does not depend on Lamins in human cells [122, 195]. Moreover, human Nup107 is phosphorylated in mitosis and is efficiently dephosphorylated by PP2A-B55 [91, 230]. As for GFP-Lamin, the recruitment of GFP-Nup107 is delayed upon Tws depletion (**Fig. 2.7.D-E**). We also tested mutations in *Nup107* and found that they genetically interact with *tws*, like mutations in *lamin*, with similar embryonic phenotypes (**Fig. 2.8**). These results could reflect a role of PP2A-Tws in the dephosphorylation of both Lamin and Nup107 to promote their recruitment to the nuclear envelope. Alternatively, PP2A-Tws could dephosphorylate a factor upstream of both Lamin and Nup107, to promote NER.

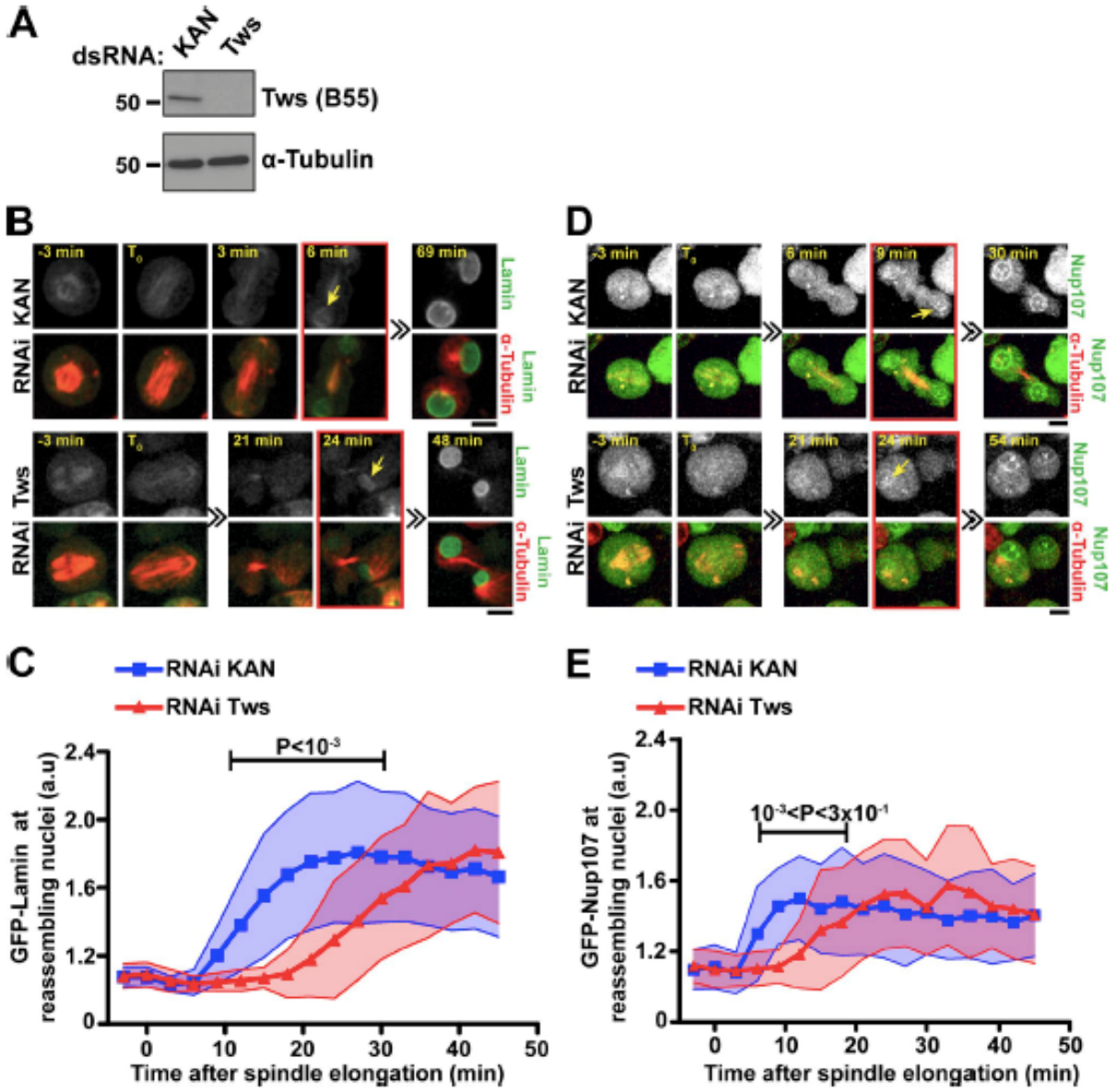

Figure 2.7. PP2A-Tws is required for timely recruitment of Lamin and Nup107 to reassembling nuclei during mitotic exit. A. Western blots showing the RNAi depletion of Tws. B, D. Live imaging of cells expressing GFP-Lamin (B) or GFP-Nup107 (D), and mCherry-Tubulin was performed after transfection with dsRNA against Tws or the bacterial KAN gene (non-target control). Red frames and yellow arrows indicate the onset of recruitment of GFP-Lamin or Nup107-GFP to reassembling nuclei. C, E. Quantification of GFP-Lamin or GFP-Nup107 recruitment on reassembling nuclei from the experiments in B and D. The fluorescence intensity in a fixed-size area at reassembling nuclei was

quantified for each time point. Between 29 and 45 cells were quantified in each condition. Shaded areas indicate the standard deviation. P values are from a two-tailed *t*-test.

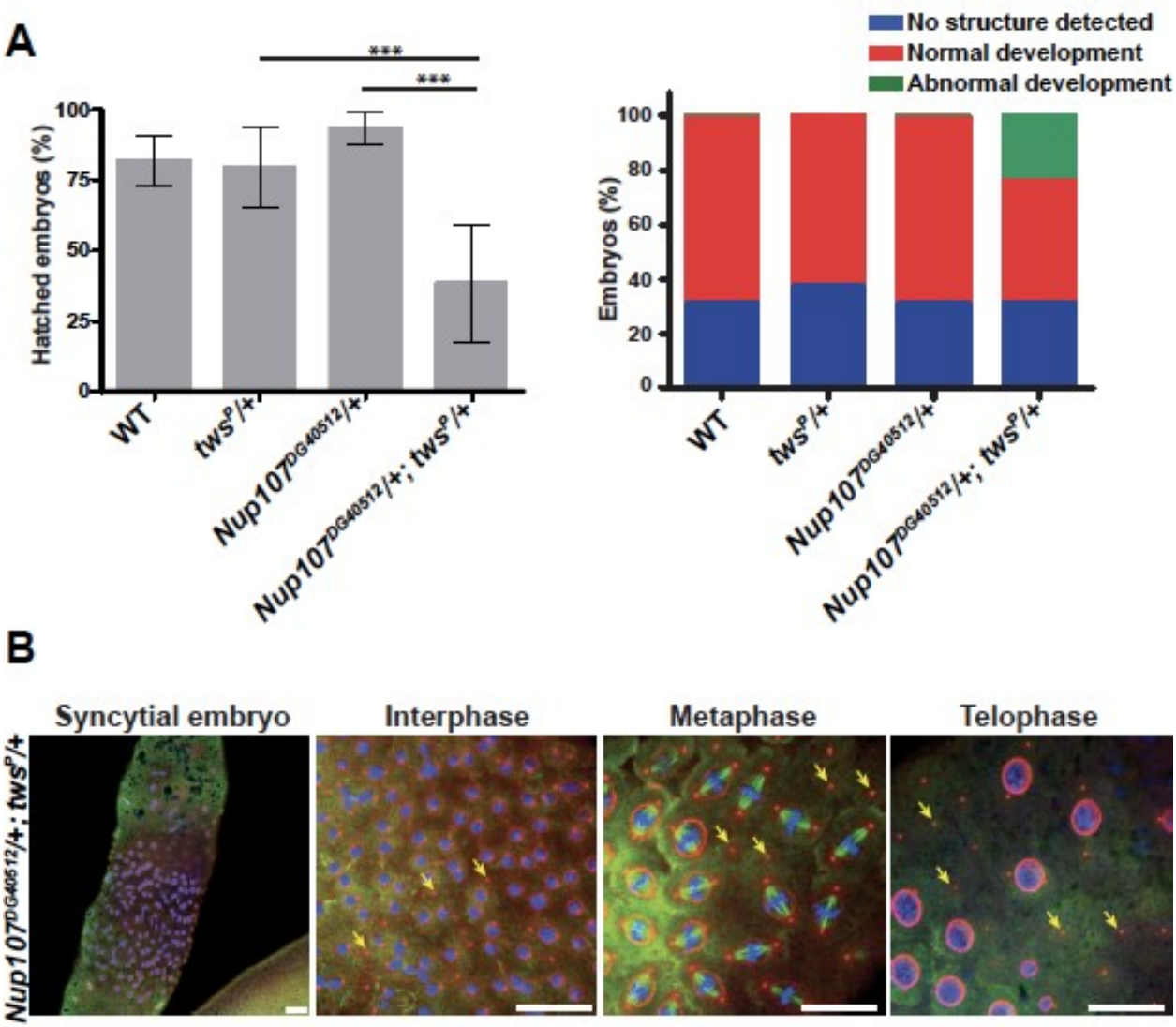

Figure 2.8. Collaboration between PP2A-Tws and Nup107 is required for syncytial embryonic development. A. Genetic interaction between *tws* and *Nup107*. Left: percentages of hatching of embryos from females of the indicated genotypes were scored. Error bars: S.D. ***P<0.0001, from two-tailed *t*-test. Right: quantification of embryonic development defects for the indicated genotypes. B. Immunofluorescence against α-Tubulin (green), γ-Tubulin and Lamin (red), and DNA (DAPI, blue). Arrows indicate detached centrosomes. All scale bars: 20 μm. In embryos from *Nup107^{DG40512}/+; tws^{P}/+* females, nuclei are unevenly distributed and centrosome detachments (arrows) are observed.

2.3.E. PP2A-Tws promotes the recruitment of the upstream factor BAF to nascent nuclei during mitotic exit.

In light of the above results, we searched for a protein that could be regulated by PP2A-Tws upstream of Lamin and Nup107 during NER. We became interested in BAF, as its human ortholog may be the first protein to be recruited in the NER cascade [122]. BAF is a conserved protein that interacts with both DNA and LEM-domain proteins of the nuclear envelope in interphase [158]. In human cells and in *C. elegans*, BAF becomes dispersed in the cytoplasm in early mitosis and is recruited back on DNA in telophase, where it holds chromosomes together allowing the formation of the NE around a single nucleus [161, 231]. Moreover, the recruitment of BAF to chromatin during telophase has been shown to depend on PP2A in *C. elegans* and HeLa cells, although the identity of the regulatory subunit(s) of PP2A involved was unclear [202].

To examine the dynamics of *Drosophila* BAF in cell division, we made a stable cell line expressing GFP-BAF and mCherry-Tubulin. We found that *Drosophila* BAF is nuclear in interphase and becomes dispersed in the cell in mitosis. During mitotic exit, GFP-BAF is quickly recruited to chromatin, starting 4 min after spindle elongation (**Fig. 2.9.A** top, **2.9.B**). We tested if this recruitment of BAF depends on PP2A-Tws. Depletion of Tws results in a delay in GFP-BAF recruitment during NER. In addition, the recruitment pattern is altered. In control cells, GFP-BAF is initially strongly recruited all over the chromosomes while they still appear condensed (early phase), and GFP-BAF then becomes restricted to the nuclear periphery (late phase). Similar BAF dynamics were observed in human cells [161, 231]. Instead, in Tws-depleted cells, GFP-BAF recruitment is immediately restricted to the nuclear periphery and never reaches the peak intensity seen in control cells (**Fig. 2.9.A** bottom, **2.9.B**). We conclude that PP2A-Tws promotes the timely recruitment of BAF

to chromosomes during mitotic exit. Moreover, PP2A-Tws appears to be specifically required for the early phase of intense BAF recruitment to segregated chromosomes at the onset of NER. Further evidence that PP2A-Tws regulates the loading of BAF on reassembling nuclei comes from our observation that depletion of Endos, which selectively inhibits PP2A-Tws in early mitosis [217], advances the recruitment of BAF (**Fig. 2.10).**

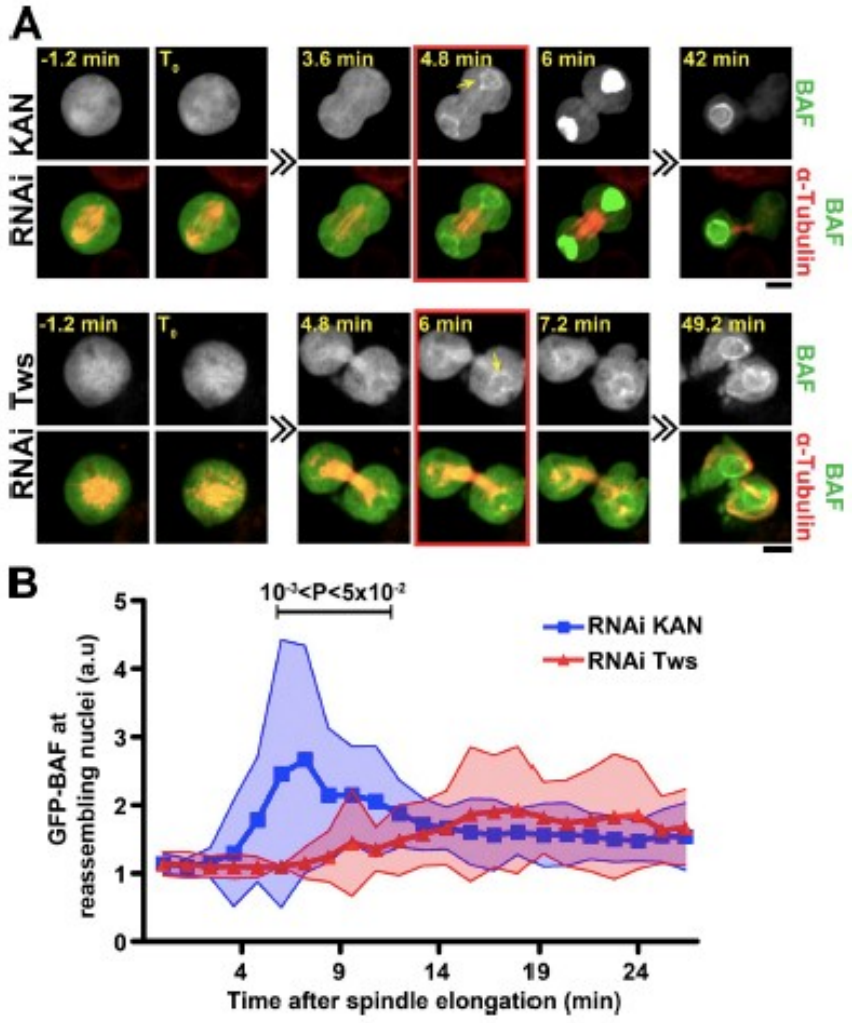

Figure 2.9. PP2A-Tws is required for timely recruitment of BAF to reassembling nuclei during mitotic exit. A. Live imaging of cells expressing GFP-BAF and mCherry-Tubulin was performed after transfection with dsRNA against Tws or the bacterial KAN gene (non-target control). B. Quantification of GFP-BAF recruitment on reassembling nuclei from the experiments in A. The fluorescence intensity in a fixed-size area at reassembling nuclei was quantified for each time point. For RNAi KAN and RNAi Tws, 26 and 25 cells were quantified, respectively. Shaded areas indicate the standard deviation. P values are from a two-tailed *t*-test.

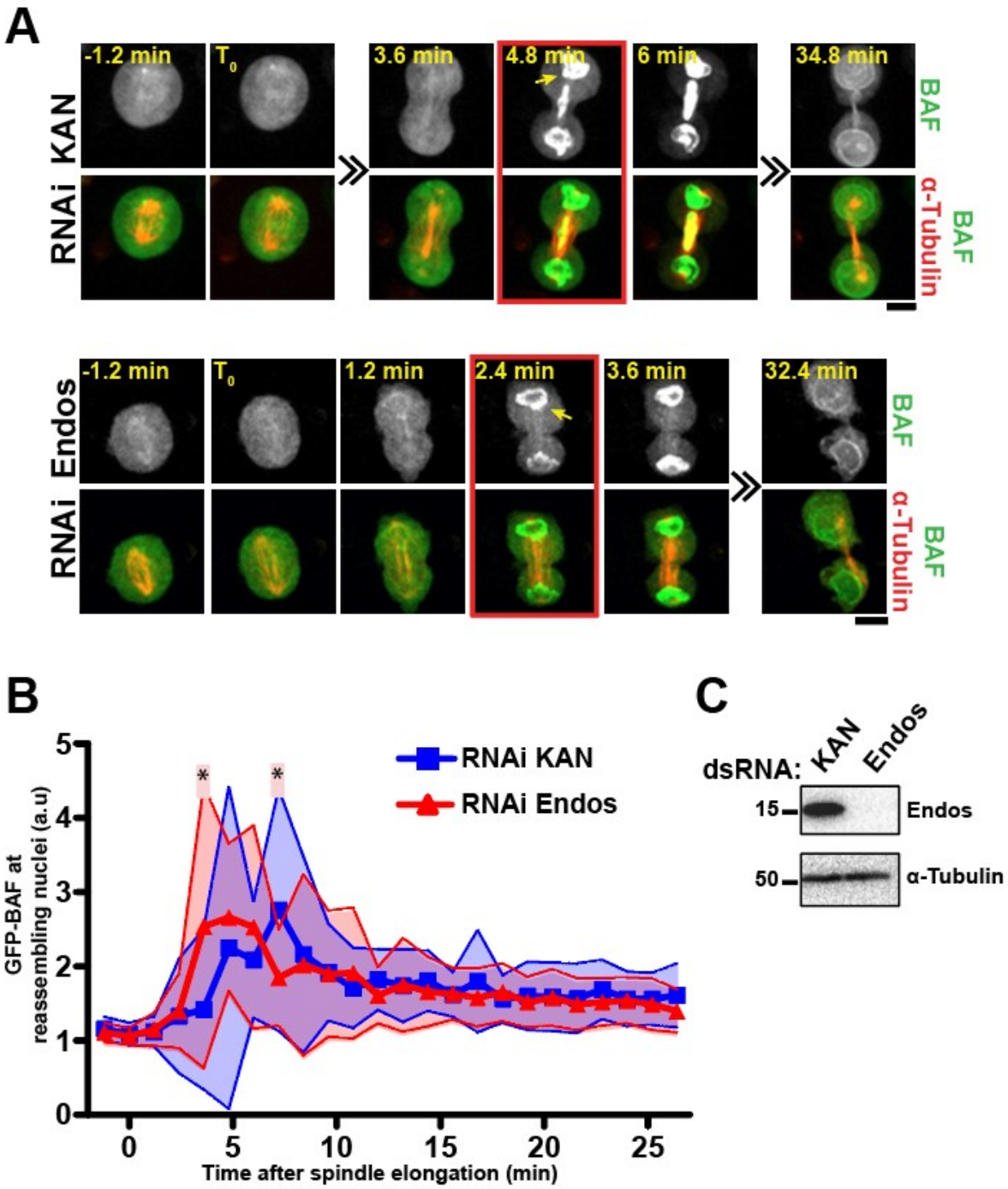

Figure 2.10. Depletion of Endos advances the recruitment of BAF on reassembling nuclei after mitosis. A. Live imaging of cells expressing GFP-BAF and mCherry-Tubulin was performed after transfection with dsRNA against Endos or the bacterial KAN gene (non-target control). B. Quantification of GFP-BAF recruitment on reassembling nuclei from the experiments in A. The fluorescence intensity in a fixed-size area at reassembling

nuclei was quantified for each time point. For RNAi KAN and RNAi Endos, 17 and 21 cells were quantified, respectively. Shaded areas indicate the standard deviation. *P<0.05 from two-tailed *t*-test. C. Western blots showing the RNAi depletion of Endos.

In *C. elegans*, the release of BAF from chromatin in mitosis is triggered by the phosphorylation of BAF by the VRK-1 kinase [232]. Although *Drosophila* BAF is known to be required for normal cell cycle progression and NE organization in somatic cells, its regulation in mitosis has not been explored [162]. However, in oogenesis, BAF is phosphorylated in prophase by the NHK-1 kinase, the ortholog of VRK-1 [181]. As a result, chromosomes detach from the NE before it breaks down, forming a compact structure called the karyosome. Disruption of NHK-1-dependent phosphorylation of BAF results in persistent association between chromosomes and the NE, ensuing meiotic defects and female sterility [181]. We hypothesized that the role of NHK-1 in phosphorylating BAF to trigger its release from chromatin in female meiosis may also be important in mitosis in *Drosophila*. To test this, we mutated the 3 known NHK-1 phosphorylation sites in BAF [181] into alanine residues (BAF^{3A}, **Fig. 2.11.A**). GFP-BAF^{3A} remains on chromosomes in mitosis, unlike GFP-BAF^{WT}, suggesting that phosphorylation of BAF by NHK-1 is required for BAF dispersal in mitosis (**Fig. 2.12.A**, **C** top, and **Fig. 2.11.B**). By contrast, the phosphomimetic GFP-BAF^{3D} was defective in its recruitment to chromosomes during mitotic exit compared to GFP-BAF^{WT} and its dynamics was similar to GFP-BAF^{WT} after depletion of Tws (**Fig. 2.11.C**, compare with **Fig. 2.9.A**). These results suggest that PP2A-Tws promotes the recruitment of BAF on reassembling nuclei by dephosphorylating NHK-1 sites on BAF.

We next tested if the Tws-dependent recruitment of BAF on chromosomes is sufficient for the recruitment of Lamin. In cells expressing both GFP-BAF^{WT} and RFP-

Lamin, we found that depletion of Tws delays the recruitment of RFP-Lamin during NER, as expected (**Fig. 2.12.A, B**). By contrast, no delay of Lamin recruitment is observed in cells expressing GFP-BAF^{3A} depleted of Tws (**Fig. 2.12.C, D**). These results suggest that dephosphorylation of BAF by PP2A-Tws promotes Lamin recruitment during NER. However, the fact that GFP-BAF^{3A} does not retain Lamin on chromosomes throughout mitosis indicates that Lamin recruitment is not solely dependent on BAF dephosphorylation and is likely regulated by additional mechanisms. One of these mechanisms may be the direct dephosphorylation of Lamin by PP2A-Tws, as proposed above.

The above results suggest that the observed genetic interaction between *tws* and *lamin* in embryos may partly reflect a role of PP2A-Tws in the dephosphorylation of BAF at NHK-1 sites, and that this dephosphorylation is required for Lamin recruitment to the reassembling nuclear envelope. Thus, we hypothesized that weakening NHK-1 function in *lam^{K2}/+; tws^{P}/+* females might rescue their fertility. Interestingly, the introduction of a single copy of either one of two mutant alleles of *nhk-1* in *lam^{K2}/+; tws^{P}/+* females rescues the viability of the embryos they produce (**Fig. 2.12.E**). This result suggests that PP2A-Tws plays a critical role in antagonizing NHK-1 to promote NER after female meiosis and in syncytial mitoses.

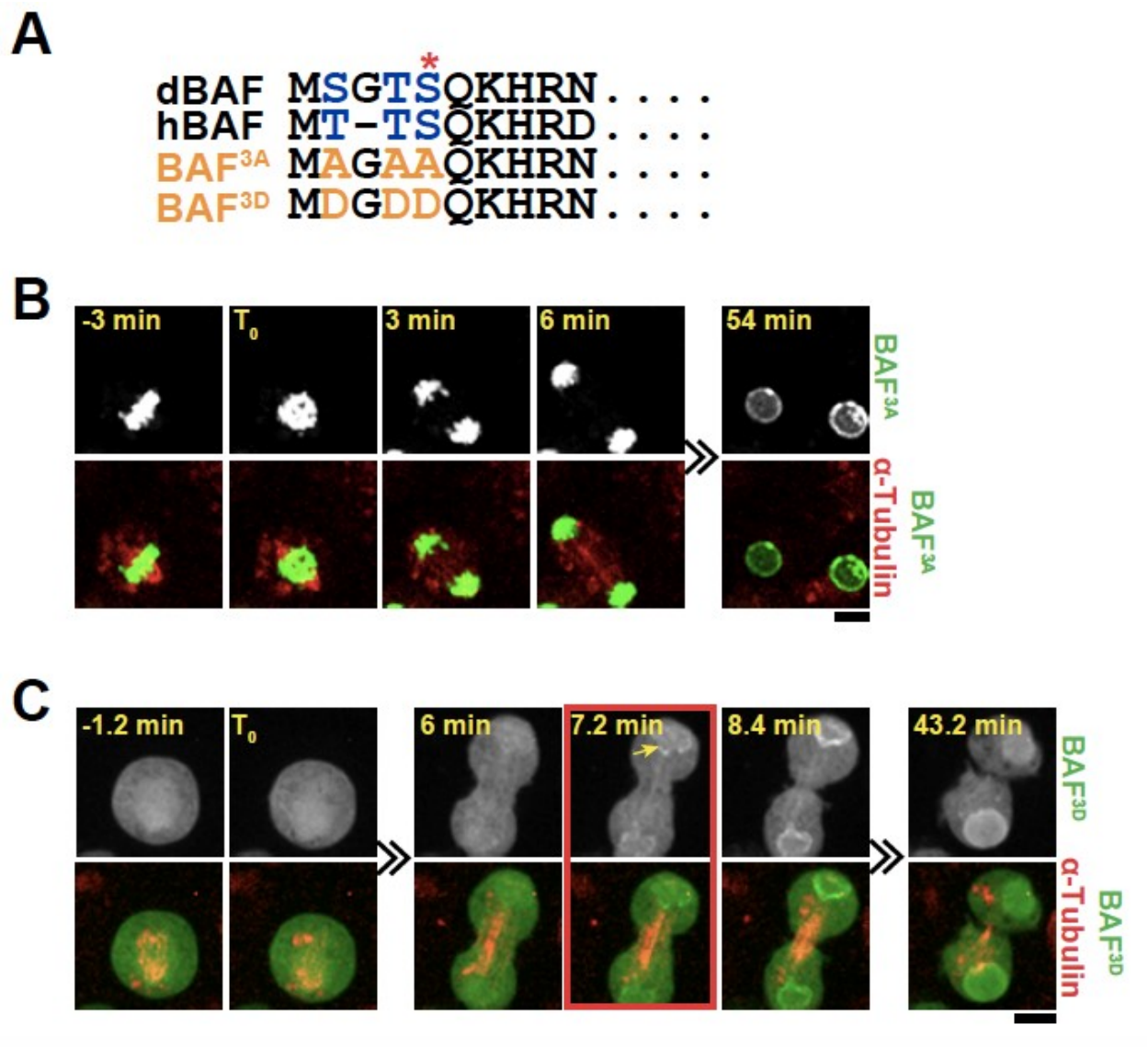

Figure 2.11. Phosphorylation of BAF at NHK-1 sites controls its localization in mitosis. A. The conserved NHK-1 phosphorylation sites mutated in BAF. The red asterisk indicates major phosphorylation site at Ser5 [181]. B-C. Live imaging of cells expressing GFP-BAF^{3A} and mCherry-Tubulin (B) or GFP-BAF^{3D} and mCherry-Tubulin (C). See **Fig. 2.10** for comparison with GFP-BAF^{WT}.

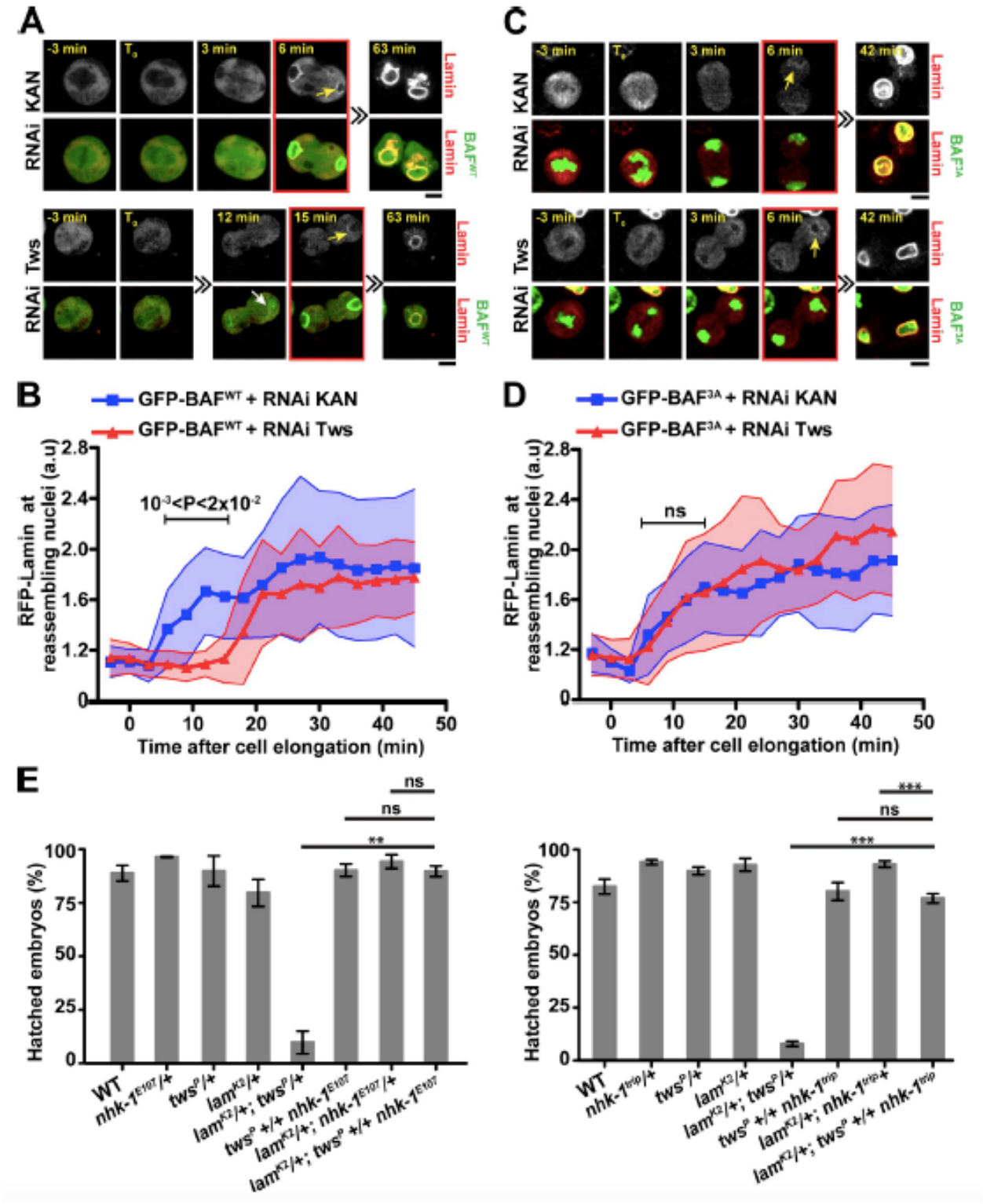

Figure 2.12. The recruitments of BAF and Lamin to reassembling nuclei depend on BAF dephosphorylation. A, C. Live imaging in cells expressing RFP-Lamin and GFP-BAF^{WT} (A) or GFP-BAF^{3A} (C) was performed after transfection with dsRNA against Tws

or the bacterial KAN gene (non-target control). Red frames and yellow arrows indicate the onset of recruitment of RFP-Lamin to segregated chromosomes. The white arrow indicates BAF^{WT} recruitment. B, D. Quantification of RFP-Lamin recruitment from the experiments in A and C. The fluorescence intensity in a fixed-size area at reassembling nuclei was quantified for each time point. Between 20 and 35 cells were quantified in each condition. Shaded areas indicate the standard deviation. E. Introduction of one copy of mutant alleles of *nhk-1* in lam^{K2}/+; tws^{P}/+ females rescues the development of embryos they produce. Percentages of hatching of embryos from females of the indicated genotypes were scored. Error bars: S.D. **P=0.0012, ***P<0.0001, from two-tailed *t*-test. Experiment in E (left) was performed by Damien Garrido.

2.3.F. Dephosphorylation of BAF promotes its association with Lamin.

In vertebrates, BAF associates with Lamin via multiple LEM-domain proteins [122]. In human cells, these interactions are negatively regulated by the phosphorylation of BAF by NHK-1 [158]. Using co-immunoprecipitation, we confirmed that *Drosophila* BAF associates with Lamin. We used this assay to investigate how the BAF-Lamin association is regulated (**Fig. 2.13.A**). Treatment of cells with OA abolishes the association between GFP-BAF and Myc-Lamin, consistent with the idea that PP2A-Tws promotes the association between BAF and Lamin during NER (**Fig. 2.13.A**, lanes 2 vs 1).

To test if the BAF-Lamin association is negatively regulated by NHK-1, we transfected cells with dsRNA against NHK-1 (or against KAN as a negative control). The efficiency of the dsRNA against NHK-1 was verified by monitoring the depletion of a PrA-tagged form of NHK-1 by Western blot (**Fig. 2.13.B**). We found that silencing NHK-1 tends to promote the BAF-Lamin association (**Fig. 2.13.A** lanes 4 vs 1), and even partially rescues this association in OA-treated cells (lanes 5 vs 2). Treating the cells with RO-3306, a CDK1 inhibitor that prevents mitotic entry, reinforces the association between BAF

and Lamin, consistent with the idea that NHK-1 phosphorylates BAF in mitosis (**Fig. 2.13.A**). These results suggest that the BAF-Lamin association is negatively regulated by NHK-1 in mitosis.

To test if the disruption of the BAF-Lamin association by OA treatment depends on the NHK-1 phosphorylation sites on BAF, we performed co-purifications using BAF^{3A} (**Fig. 2.13.C**). Unlike BAF^{WT} which fails to associate with Lamin upon OA treatment (**Fig. 2.13.C,** lanes 4 vs 3), BAF^{3A} associates with Lamin even in the presence of OA (**Fig. 2.13.C**, lanes 6 vs 5). Conversely, BAF^{3D} fails to associate with Lamin even without OA treatment (**Fig. 2.13.C**, lanes 7 and 8). These results suggest that NHK-1, by its known ability to phosphorylate BAF, disrupts the BAF-Lamin association and that OA-sensitive phosphatase activity, likely including PP2A-Tws, counteracts this phosphorylation to promote the BAF-Lamin association in addition to promoting the earlier recruitment of BAF to chromatin. We did not observe a decrease in BAF-Lamin association upon Tws RNAi (data not shown). This result is expected because Tws RNAi delays Lamin recruitment by only 10-15 minutes (**Fig. 2.12.B**), and as *Drosophila* cells in culture are notoriously difficult to synchronize, the assay uses asynchronous cultures where most cells are in interphase.

To explore when and where PP2A-Tws may regulate BAF in the cell, we used a proximal ligation assay (PLA), which monitors proximity between two proteins, as when they interact. A cell line stably expressing GFP-BAF and Myc-Tws was used, with primary antibodies against GFP and Myc. We detected abundant PLA foci between GFP-BAF and Myc-Tws (**Fig. 2.14.A**). The PLA signal is specific as it is not detected in cells expressing only GFP-BAF or Myc-Tws or neither protein. Moreover, no PLA signal is detected in cells expressing both fusion proteins if either primary antibody is left out (data not shown). Interestingly, the number of PLA signal foci per cell is significantly higher in late mitosis

and cytokinesis than in interphase and early mitosis. In addition, foci are mostly present in the cytoplasm (**Fig. 2.14.A**). These results are in agreement with a function of PP2A-Tws in the dephosphorylation of cytoplasmic BAF to promote its subsequent recruitment to the reassembling nuclei during mitotic exit.

We used an *in vitro* assay to test the dephosphorylation kinetics of a BAF peptide phosphorylated at Ser5 (BAF-pS5, **Fig. 2.11.A**). This site is equivalent to the known major NHK-1 site in human BAF, and its dephosphorylation was shown to promote BAF binding to DNA and LEM proteins at the NE [181, 182]. As enzymes, we used PP2A obtained by immunoprecipitation of Flag-tagged regulatory subunits. We found that PP2A-Tws can dephosphorylate BAF-pS5 (**Fig. 2.14.B**). This reaction is slower than the dephosphorylation of well-documented PP2A-B55 sites in human PRC1 (PRC1-pT481 and PRC1-pT602) [87]. This result is expected because PP2A-B55 enzymes are known to dephosphorylate pThr residues more rapidly than pSer residues in their substrates [91, 92]. For comparison, we tested the ability of PP2A-Wdb/B56 to dephosphorylate the same sites, normalizing activities for the amount of the PP2A catalytic subunit (Mts), present in the reaction as quantified by Western blot. Consistent with results in human cells, PP2A-Wdb was capable of dephosphorylating PRC1-pT602 much better than PRC1-pT481 [87]. Very little activity of PP2A-Wdb was detected on BAF-pS5. These results confirm that Tws confers specificity to PP2A for its dephosphorylation of BAF at its major NHK-1 site.

Although our results strongly suggest that BAF is a target of PP2A-Tws, Lamin and Nup107 could also be its targets, as discussed above. We tested the ability of these proteins, tagged with GFP, to associate with Myc-tagged Tws, using co-IP. BAF, Lamin and Nup107 all associated specifically with Tws (**Fig. 2.14.C-D**). These results suggest that PP2A-Tws targets multiple proteins to promote NER.

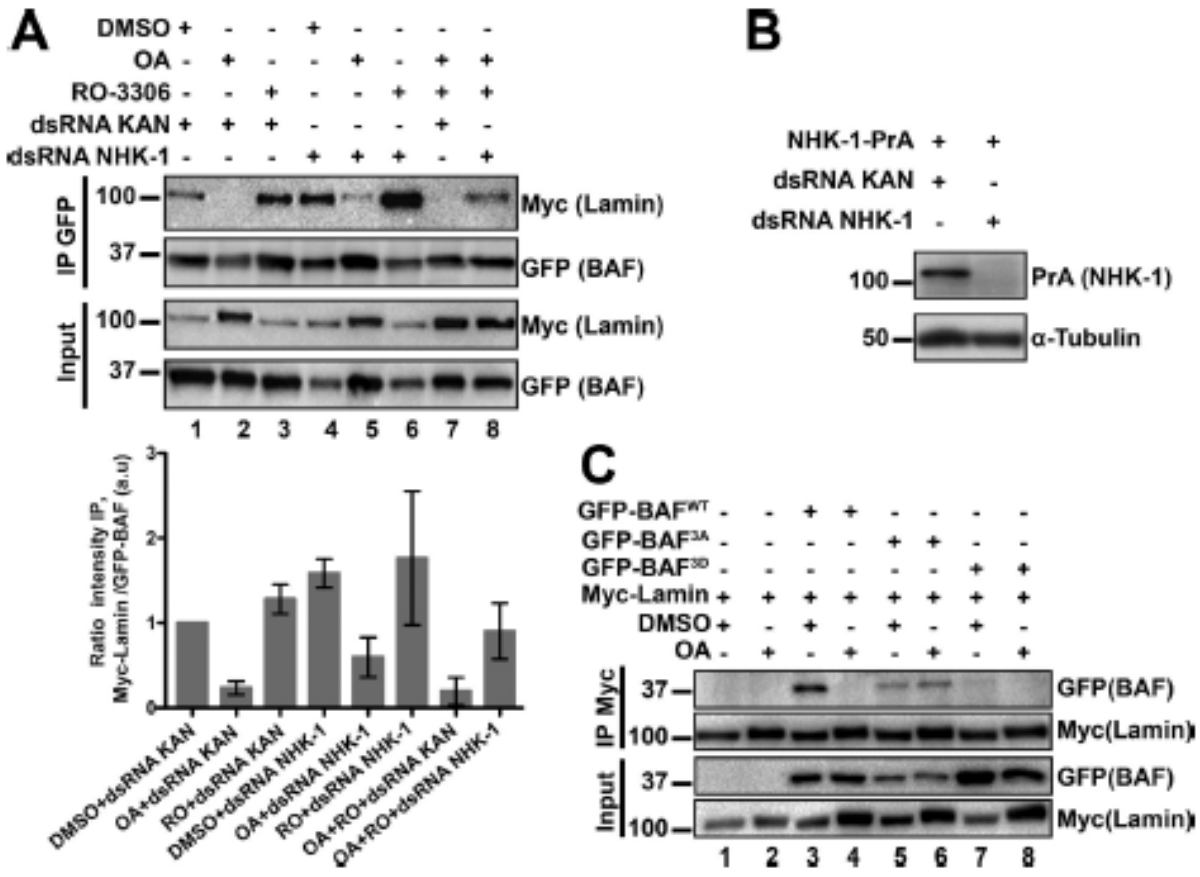

Figure 2.13. The association between BAF and Lamin is regulated by mitotic kinases and phosphatases. A. Cells stably expressing GFP-BAF and Myc-Lamin were submitted to different treatments as indicated followed by immunoprecipitation against GFP and Western blots. The ratios between co-immunoprecipitated Myc-Lamin and GFP-BAF, averaged between three experiments, is shown below. Error bars: S.E.M. B. The efficiency of the dsRNA against NHK-1 was verified by transfecting cells stably expressing NHK-1-PrA followed by Western blot. C. Disruption of the BAF-Lamin association requires NHK-1 phosphorylation sites in BAF (experiment as in A).

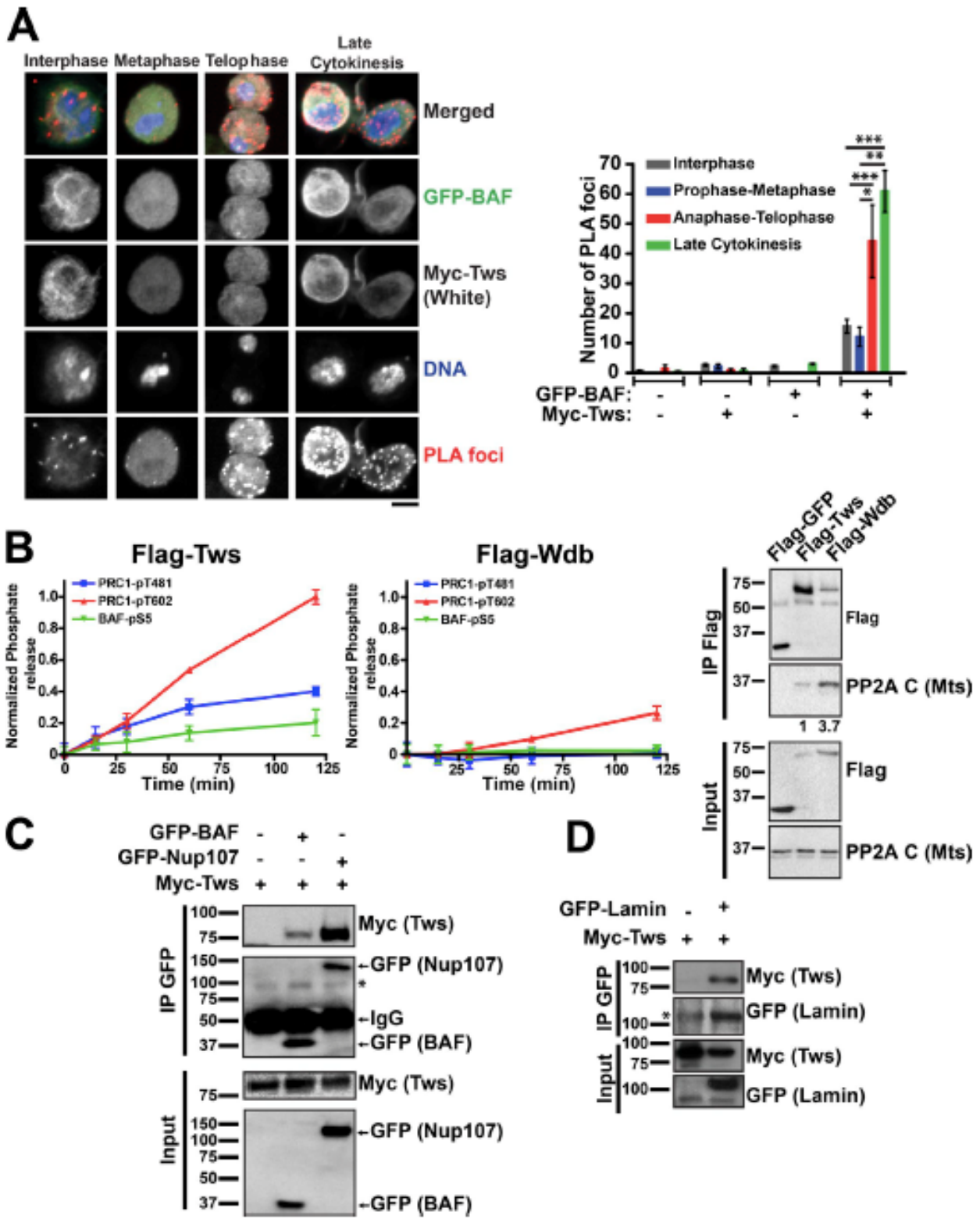

Figure 2.14. Tws associates with BAF during mitotic exit and PP2A-Tws dephosphorylates BAF. A. Proximal Ligation Assay (PLA). Left: Cells transfected with

Myc-Tws and GFP-BAF were submitted to PLA using antibodies against Myc and GFP (red foci). Immunofluorescence for Myc was done in parallel and DNA was stained with DAPI. Right: Quantification of PLA foci per cell. Cells expressing only Myc-Tws or GFP-BAF were analyzed as controls. Error bars: S.E.M. *P=0.0488; **P=0.0082; ***P=0.0002, from two-tailed *t*-test. B. PP2A-Tws dephosphorylates a BAF peptide *in vitro*. Flag-Tws, Flag-Wdb or Flag-GFP were immunoprecipitated and incubated with the indicated phosphopeptides for different times. Left: Phosphate release was measured as described in Materials and Methods. Error bars: standard deviation. Right: Immunoprecipitation products were analyzed by Western blotting. The relative quantification of the Mts band intensities is shown below the blot. All results shown were obtained in the same, representative experiment. Error bars: S.D. from triplicates. C-D. Cells transfected with the indicated proteins were submitted to co-IP against GFP followed by Western blot analysis. * indicates a background band in co-IP product, probably corresponding to a dimer of IgG heavy chain.

2.4 Discussion

The molecular mechanisms mediating an orderly mitotic exit and return into interphase are much less understood than the mechanisms of mitotic entry. Moreover, while phosphatases are known to play crucial roles in promoting the mitosis to interphase transition, their specific contributions to the various events of this process remain largely unknown. Here, we have used the *Drosophila* system to search for and dissect the molecular events controlled by the PP2A-B55/Tws phosphatase in the cell cycle. Second-site noncomplementation (SSNC) screens have been used in various model organisms to identify functionally linked genes [233]. This work builds on the power of SSNC maternal-effect screens in *Drosophila* to identify close collaboration between genes in cell cycle regulation [89, 234, 235].

Our genetic screen uncovered a strong link between PP2A-Tws and NER at the end of M-phase. We found that simultaneously reducing the levels of Tws and Lamin in eggs using heterozygous mutations in mothers causes major defects in NER after meiosis II or after mitosis for embryos that initiated syncytial nuclear divisions. This result is striking considering that Lamin is not an essential protein in several cell types. Hypomorphic *lamin* mutants develop to adulthood, despite showing nuclear migration defects in photoreceptors and being female sterile [138]. In *lamin* null mutants, neuroblasts continue to proliferate in the absence of detectable Lamin [236]. In mice, the orthologous B-type lamins are dispensable for cell viability and proliferation, at least in keratinocytes; however, B-type lamins are essential in neurons [237]. In general, B-type lamins may play a crucial role in structuring nuclei and withstanding force in cells where nuclear migration/positioning is essential. Such cell types include *Drosophila* eggs, where pronuclei must converge before fusing, and syncytial embryos, where nuclei migrate towards the cortex.

Using cells in culture, we found that PP2A-Tws promotes the recruitment of several nuclear envelope components after mitosis, namely BAF, Lamin and Nup107. In *Drosophila* oogenesis, BAF phosphorylation by NHK-1 promotes the detachment of chromatin from the germinal vesicle during karyosome formation [181]. In this work, we found that BAF requires NHK-1 phosphorylation sites to dissociate from chromatin during NEBD, as in *C. elegans* [202, 232]. Our genetic, biochemical and imaging results suggest that phosphorylation of BAF by NHK-1 is reversed by PP2A-Tws to promote its recruitment on chromatin at the onset of NER (**Fig. 2.15**). This is consistent with results in *C. elegans* that showed a role for PP2A in this process, although the relevant phosphorylation sites in BAF were not investigated and the PP2A adaptor subunit involved was unclear [202].

Recent work shows that BAF plays a crucial role in holding chromosomes together just after anaphase to promote the assembly of the NE around a single nucleus [161]. Our findings suggest that PP2A-Tws dephosphorylates BAF to promote this function. Our results also suggest that regulation of BAF phosphorylation by NHK-1 and PP2A-Tws regulates its ability to form complexes with Lamin. In vertebrates, BAF is known to interact with lamins via LEM domain proteins at the NE [122]. Human BAF phosphorylation by VRK1/NHK-1 decreases its ability to interact with a LEM domain [182]. LEM domain proteins have also been shown to be phosphorylated to negatively regulate their ability to interact with BAF in *Xenopus* extracts [172, 238]. Thus, PP2A-B55 could dephosphorylate LEM proteins to further promote their association with BAF during NER, and this possibility should be investigated.

By inducing the recruitment of BAF on reassembling nuclei, PP2A-Tws likely promotes the recruitment of multiple downstream NE components. Nevertheless, PP2A-Tws likely has other targets in NER, possibly including Lamin and Nup107 (**Fig. 2.15**). Both proteins contain multiple CDK phosphorylation motifs, and PP2A-B55 enzymes have been shown to dephosphorylate many such sites efficiently [84-86]. Moreover, we observed that Lamin and Nup107 both associate with Tws. We found that mutation of all CDK consensus sites in Lamin prevents lamina disassembly in mitosis and, although the attempted phospho-mimetic mutation of all sites did not disrupt lamina assembly in live cells, it increases Lamin solubility in cell lysates. The CDK sites on Lamin are grouped in 2 clusters flanking the coiled region, and some of these sites have already been shown to negatively regulate homotypic interactions of Lamin (**Fig. 2.6.A**) [228]. We have not explored the effect of mutating CDK sites in Nup107. However, Nup107 is rapidly dephosphorylated at multiple sites during mitotic exit in human cells [210] and

dephosphorylation of at least one CDK site in Nup107 was shown to depend on PP2A-B55 [91]. However, although PP2A-B55 is capable of dephosphorylating several CDK sites, many of these sites are probably regulated mainly by another phosphatase *in vivo*. Moreover, numerous examples of PP2A-B55-dependent, non-CDK sites were recently identified [91]. This is further exemplified here by the dephosphorylation of BAF by PP2A-Tws at a NHK-1 site, which cannot be a CDK site as it lacks the proline residue in position +1. Nevertheless, with its positively charged amino-acid residues in positions +2 to +4 (**Fig. 2.11**), this site resembles the recently defined PP2A-B55 consensus motif [91] and a consensus motif for sites lacking a Pro residue at position +1 but that are rapidly dephosphorylated during mitotic exit [210].

Overall, PP2A-B55 appears to target multiple proteins, dephosphorylating them at various sites that depend on multiple kinases, to promote NER cooperatively. A recent phosphoproteomic study found that several proteins of the nuclear envelope are particularly prone to rapid dephosphorylation during mitotic exit, in a process that likely involves other phosphatases [210]. Much work remains to be done to fully dissect the mechanisms at play. The fact that NER is only delayed and not completely prevented when PP2A-Tws is silenced in cell culture could be due to an incomplete inactivation of PP2A-Tws inherent to the RNAi approach. Alternatively, other phosphatases may partially compensate for the loss of PP2A-Tws activity. Protein phosphatase 4 (PP4) may function in this way as it has been shown to dephosphorylate BAF in human cells [205]. In addition, Protein Phosphatase 1 enzymes likely contribute to NER in *Drosophila* as they promote this process through multiple mechanisms in vertebrates, including the dephosphorylation of Lamin B [220, 239].

Our screen results point at other functions of PP2A-Tws in the completion of M phase that remain to be explored, although some of the genetic interactions identified could reflect roles of PP2A-Tws unrelated to mitotic regulation. Our preliminary, unpublished results suggest that the genetic interaction between *tws* and *CycB3* reflects their collaboration in the completion of meiosis (**Fig 2.2.A**). Interestingly, we uncovered genetic interactions between *tws* and genes that encode nucleo-cytoplasmic transport factors. Mutations in the gene for Cse1/CAS, which transports importin β back to the cytoplasm to promote its function in nuclear import, enhances *tws*-dependent embryonic lethality (**Fig. 2.2.A**) [240]. Conversely, mutations in *embargoed (emb)*, which encodes the nuclear export factor Crm1, rescues *tws*-dependent embryonic lethality (**Fig. 2.2.B**) [241]. These results suggest that active nuclear import plays an important role in NER or other aspects of interphase nuclear formation after mitosis and/or meiosis, presumably by promoting the nuclear localization of crucial enzymes or structural factors. The identities of rate-limiting factors for NER and for the return of nuclei to interphase, and the regulation of their nucleo-cytoplasmic transport in this process are important open questions that should be the topic of future investigations.

In this work, we have used a genetic strategy to search for the roles of PP2A-Tws in the cell cycle *in vivo*. We found that PP2A-Tws promotes NER and we have begun to dissect the molecular mechanisms at play. This study opens the door to the use of *Drosophila* to gain a better mechanistic understanding of NER. Moreover, it will be a

powerful system to further dissect the functions of PP2A-Tws and other phosphatases in the coordination of mitotic exit.

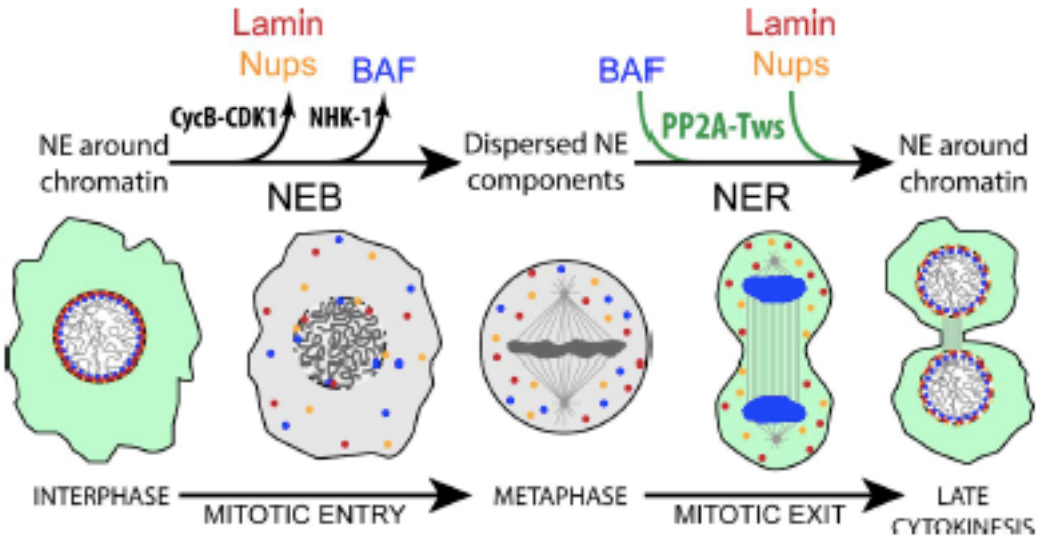

Figure 2.15. Model for the role of PP2A-Tws in promoting NER after mitosis. As the cell enters mitosis, Cyclin B-CDK1 phosphorylates Lamin (red) and probably other proteins including Nup107 (Nups are in yellow) to induce NEBD. NHK-1 phosphorylates BAF (blue), inducing its dissociation from chromatin. As the cell exits mitosis, PP2A-Tws dephosphorylates BAF, inducing its rapid recruitment to condensed chromatin in late anaphase (green: PP2A-Tws active). Lamin and Nup107 are likely also dephosphorylated by PP2A-Tws to promote their assembly in NEs. When the NE is reformed, BAF becomes restricted to the inner periphery of the nucleus. Figure made by Vincent Archambault.

2.5 Materials and Methods

2.5.A. Plasmids and mutagenesis

Plasmids were generated by using the Gateway recombination system (Invitrogen). The cDNA of each gene was cloned in a pDONOR221 entry vector before being recombined into destination vectors containing copper-inducible (pMT) or constitutive (pAC5) promoters. The following plasmids were generated: pAC5-GFP-Lamin^{WT}, pAC5-Myc-Lamin^{WT}, pAC5-Myc-Lamin^{7A}, pAC5-Myc-Lamin^{7D}, pMT-RFP-Lamin^{WT}, pMT-RFP-

Lamin^{7A}, pAC5-mCherry-Tubulin, pMT-GFP-Nup107, pAC5-Myc-Nup107, pMT-GFP-BAF^{WT}, pMT-GFP-BAF^{3A}, pMT-GFP-BAF^{3D}, pAC5-Myc-BAF^{WT}, pAC5-Myc-Tws, pAC5-GFP-Tws, pAC5-Flag-Tws, pAC5-Flag-Wdb, pAC5-Flag-GFP, pAC5-NHK-1-PrA. Amino acid substitution mutants were generated using QuikChange Lightning Site-Directed Mutagenesis Kit (Agilent) as described by the manufacturer protocol. cDNAs for plasmids expressing Lamin mutants were generated by BioBasic.

2.5.B. Fly culture, genetic screen, and fertility tests

Fly culture was done according to standard procedures. For the genetic screen, a collection of 417 lines containing most Drosdel deficiencies and a few additional ones (obtained from Marc Therrien) covering most of chromosomes II and III was used (see Table 1 for the complete list). Each line was crossed to the *y w; tws^{P}/TM6B* or *mts$^{XE-2258}$/CyO* lines. Flies heterozygous for both the deletion and the *tws^{P}* or *mts$^{XE-2258}$* mutation were selected based on the absence of balancer chromosomes and their fertility was tested (see below). Table 3 provides a list of all mutant alleles used in this study, their molecular lesion and their origin. Flies expressing GFP-Polo were from Claudio Sunkel.

For fertility tests shown in Figures **2.6.E**, **2.12.E** left, **2.2.B** and Table 2, 3 to 5 virgin females of 1 to 4 days of age were crossed with 3 to 5 Oregon R males per tube and kept at 25°C for one day. Flies were then transferred to tubes containing grape juice agar with yeast paste. After one day, flies were transferred again to new tubes. Twenty-four hours later, the percentage of hatched embryos was counted. Approximately 100 embryos were counted each time and this scoring was repeated at least 3 times. For experiments shown in Figures **2.3.A**, **2.12.E** right, and **2.8**, the fertility of 5 to 10 single virgin females crossed with 3 to 5 Oregon R males was scored. For the genetic screen (Figure **2.1.D** and Table

1), the fertility of a group of 3 to 5 females (not necessarily virgins) crossed to 3 to 5 Oregon R males was scored on 3 consecutive days and numbers were pooled.

2.5.C. Embryo and egg immunostaining

For immunofluorescence shown in Figures **2.3.C**, **2.4** and **2.8**, females were kept to lay embryos on grape juice agar for two hours at 25°C. Embryos were immediately dechorionated and fixed as described [235]. The following primary antibodies were used for staining: anti-Lamin Dm0 from mouse (1:100; DSHB Hybridoma Product ADL84.12, by P.A. Fisher), anti-α-Tubulin YL1/2 from rat (1:50; #6160, Abcam), anti-γ-Tubulin GTU-88 from mouse (1:50; #T5326, Sigma). After an overnight incubation of primary antibodies at 4°C, embryos were incubated with secondary antibodies coupled to Alexa-488 (1:200; Invitrogen) or Cy3 (1:200; Jackson) for two hours at room temperature. DNA was marked with DAPI. Embryos were mounted using Vectashield (Vector laboratories). Images were generated using the LSM 700 confocal microscope (Zeiss), using the 63 X oil objective, and treated using Photoshop.

For examining meiosis (**Fig. 2.5**), females were kept to lay eggs on an agar plate for 20 minutes after which eggs were dechorionated and washed in a solution of 0.7% NaCl, 0.05% Triton-X. Eggs were then fixed in a solution of 1 heptane : 1 methanol before being washed in 100% methanol, and rehydrated sequentially in a 90%, 70% and 50% methanol followed by a wash in Phosphate Buffer Saline (PBS) + 0.2% Tween. Eggs were then incubated with 1:100 anti-Lamin ADL 67.10 from mouse (Developmental Studies Hybridoma Bank), 1:2000 rat anti-α-Tubulin YL1/2 (Sigma) and Oligreen (Invitrogen). Secondary Alexa-conjugated antibodies were used 1:1000. Eggs were then mounted using 1,2,3,4-Tetrahydronaphthalene (Sigma). Images were taken on an Olympus

FV1000 scanning confocal microscope with 60X water objective lens.

2.5.D. *Drosophila* cell culture and drug treatments

D-Mel2 cells were cultured in Express Five medium (Invitrogen) supplemented with glutamine, penicillin and streptomycin. Stable cell lines were generated in a selection medium containing 10 µg/ml of blasticidin. Expression of transgenes under a copper-inducible promotes was induced by adding $CuS0_4$ (300 µM) to the media for at least 8 hours. For phosphatase inhibition, cells were treated with 100 nM okadaic acid (Bioshop) for 30 minutes before being lysed for immunoprecipitation. For CDK1 inhibition, cells were treated with 10 µM RO-3306 (Tocris Bioscience) for 1 hour and 30 minutes before being lysed.

2.5.E. Transient transfections

D-Mel2 cells of 70% to 80% confluence in six well plates or 25-cm^2 flasks were transfected with 2.5 µg or 5 µg of plasmids respectively using the X-tremeGene HP DNA transfection reagent (Roche) as described by the manufacturer's instructions. Cells were cultured between 24 and 72 hours at 25°C before being assayed. For RNAi, cells of 60 to 70% confluence were plated in 6-well plates and transfected with 25 µg dsRNA for Tws, NHK-1 or Endos, along with the Transfast reagent (Promega). dsRNA against the bacterial resistance gene kanamycin (KAN) was used as a non-target control. Cells were incubated at 25°C for 72 to 96 hours before being analyzed.

2.5.F. Time-lapse microscopy

Time-lapse fluorescence imaging of cultured cells and embryos was performed on a Spinning-Disk confocal system (Yokogawa CSU-X1 5000) mounted on a fluorescence microscope (Zeiss Axio Observer.Z1) using a 63X oil objective an Axiocam 506 mono camera (Zeiss).

2.5.G. Proximal-ligation assay (PLA)

D-Mel2 cells stably expressing GFP-Tws and myc-BAF^{WT} were fixed using 37% formaldehyde (Sigma), after which cells were blocked then incubated with anti-GFP from rabbit (1:200; Invitrogen) and anti-Myc 9E10 from mouse (1:200; Santa Cruz Biotechnology, Inc.) for one hour at room temperature. PLA was performed using the Duolink starter kits (Sigma) as described by the manufacturer. The Duolink anti-rabbit plus and anti-mouse minus probes were used. During the amplification step, cells were incubated with secondary antibodies coupled to Alexa-488 from rabbit (1:200; Invitrogen), Cy3 from mouse (1:200; Jackson), and Alexa-566 from mouse for two hours at room temperature. DAPI was used to stain DNA. Images were taken using a LSM 700 confocal microscopy, and treated using Photoshop.

2.5.H. Immunoprecipitation and western blotting

For each sample, between 4 and 20 million cells transfected as above were harvested and washed in PBS containing protease inhibitors: 1 mM PMSF, 10 µg/ml aprotinin and 10 µg/ml leupeptin. Cells were lysed in 75 mM K-HEPES pH 7.5, 150 mM NaCl, 1 mM DTT, 2 mM $MgCl_2$, 2 mM EGTA, 1% Triton X-100, with protease inhibitors as above. Lysates were centrifuged at 14 600 rpm for 10 min at 4°C. Clarified lysates were incubated with anti-GFP from rabbit (Invitrogen) on a wheel for 1 hour at 4°C and then incubated with 15 to 20 µl of Protein A-conjugated Dynabeads suspension (Life Technologies) for another 45 min at 4°C. Beads were washed in 1 ml of lysis buffer 4 X 5 min and eluted directly in Laemmli sample buffer for SDS-PAGE. Primary antibodies used in Western blotting were anti-GFP from rabbit (Invitrogen), anti-Myc 9E10 from mouse (Santa Cruz Biotechnology, Inc.), anti-Lamin Dm0 (DSHB Hybridoma Product ADL84.12), anti-α-Tubulin DM1A from mouse (Sigma), anti-Tws from rabbit (Thermo Fisher Scientific), anti-H3 from rabbit (NEB), anti-Endos from rabbit (custom made by Thermo Fisher Scientific), anti-Flag M2 from mouse (Sigma), peroxidase AffiniPure Goat anti-mouse IgG (Jackson), and peroxidase-conjugated AffiniPure Goat anti-rabbit IgG (Jackson). For analyzing protein levels of mutant embryos of Figure **2.3**, embryos from Oregon R and single and double mutant females were collected as described above and washed with PBS solution containing protease inhibitors before being crushed and clarified by centrifugation at 14 600 rpm for 10 min at 4°C. Before SDS-PAGE, protein levels in supernatants were quantified using the Bradford protein assay kit (Biorad). The same masses of total proteins were loaded for all samples and proteins were analyzed by immunoblotting.

2.5.I. Phosphatase assay

Approximately 200 million D-mel2 cells stably expressing either Flag-Tws, Flag-Wdb or Flag-GFP were collected and centrifuged at 1500 rpm for 5 min at 4°C. Pellets were suspended in Tris buffer saline containing protease inhibitors: 1 mM PMSF, 10 µg/ml aprotinin and 10 µg/ml leupeptin. Cells were lysed in buffer containing 20 mM Tris-HCl pH 7.5, 150 mM NaCl, 2 mM EGTA, 0.5% NP-40, 1 mM DTT, and the protease inhibitors as above and incubated on a wheel for 15 min at 4°C, before being centrifuged at 4600 rpm for 15 min at 4°C. Supernatants were incubated with anti-Flag antibody for 75 min on a wheel at 4°C and with Protein G-conjugated Dynabeads (Life Technologies) for an additional 45 min. Beads were washed 4 X 5 min with lysis buffer before being used as sources of enzymes for the phosphatase assay. The following peptides were used as substrates: BAF-pS5: MSGTpSQKHRNFVAEPMGNK; PRC1-pT481; SKRRGLAPNpTPGKARKLNTTT; PRC1-pT602: LSKASKSDATSGILNSpTNIQS (all synthesized by Biobasic). The 2X reaction solutions contained 400 µM of peptides, 20 mM Tris pH 7.5, 5 mM $MgCl_2$, 1 mM EGTA, 20 mM β-mercaptoethanol, and 1,45 mg/ml of bovine serum albumin. For the phosphatase reactions, equal volumes of 2X reaction solution and washed bead suspensions were combined and incubated at room temperature in 96-well plates. Reactions were stopped by the addition of 90 mM $HClO_4$. Phosphate release was revealed by the addition of one volume of 1 M malachite green solution. The absorbance was then measured at a wavelength of 620 nm using a plate reader (Tecan Infinite 200 PRO). For results presented in Figure **2.14.B**, the colorimetric measurements obtained with Flag-GFP for each time points were subtracted from the measurements obtained with Flag-Tws and Flag-Wdb. Values for T_0 were also subtracted

from both series. All values were normalized by fixing the highest value obtained to 1 (the activity associated with Flag-Tws on PRC1-pT602 peptide after 2 hours). In addition, activities were normalized for the amount of PP2A catalytic subunit (Mts) present in the reactions by dividing the activities associated with Flag-Wdb by the ratio of the Mts band intensities from the Flag-Wdb IP/Flag-Tws IP purified complexes.

2.6 Tables

Bloomington stock #	Name	Cyto. bk points	Balancer	% Hatching with *tws*^{P}/+	% Hatching with *mts*$^{XE-2258}$/+	Validated interacting gene
24626	Df(2L)ED50001	21A1;21B1	SM6a	90	90	
9353	Df(2L)ED5878	21B1;21B3	SM6a	70	75	
8901	Df(2L)ED19	21B3;21B7	SM6a	70	80	
24958	Df(2L)BSC454	21B7;21B8	SM6a	85	88	
8672	Df(2L)BSC106	21B7;21C2	Tg	85	85	
8673	Df(2L)BSC107	21C2;21E2	CyO	75	75	
8908	Df(2L)ED94	21E2;21E3	SM6a	83	70	
24118	Df(2L)ED105	21E2;22A1	SM6a	80	70	
7492	Df(2L)Exel6005	22A3;22B1	CyO	80	75	
26540	Df(2L)BSC688	22B1;22D6	SM6a	70	80	
24959	Df(2L)BSC455	22D5;22E1	SM6a	65	85	
9176	Df(2L)ED136	22F4;23A3	SM6a	75	83	
7744	Df(2L)Exel6277	23A2;23B1	CyO	70	75	
26544	Df(2L)BSC692	23B3;23B7	SM6a	60	60	
9610	Df(2L)BSC180	23B7;23C3	CyO	83	83	
8904	Df(2L)ED4651	23B8;23F3	SM6a	85	9	
6965	Df(2L)BSC31	23E5;23F4-5	CyO	70	80	
6507	Df(2L)drm-P2	23F3;24A2	SM6b	80	80	
23677	Df(2L)BSC292	23F6;24A2	CyO	80	40	
24123	Df(2L)ED247	24A2;24C3	SM6a	85	55	
7495	Df(2L)Exel6009	24C3;24C8	CyO	80	88	
7790	Df(2L)Exel8010	24C8;24D4	CyO	85	75	
9600	Df(2L)BSC165	24D4;24D8	CyO	85	50	
23680	Df(2L)BSC295	24D4;24F3	CyO	80	5	
744	Df(2L)M24F-B	24E2;24F6	SM1	75	75	
9270	Df(2L)ED250	24F4;25A7	Cy[1]	85	80	
24124	Df(2L)ED7853	25A3;25B10	SM6a	80	75	
1164	Df(2L)tkv3	25A4;25D5	SM1	70	70	
9605	Df(2L)BSC172	25B10;25C1	CyO	55	65	
8835	Df(2L)BSC110	25C1;25C4	CyO	75	50	
8674	Df(2L)BSC109	25C4;25C8	CyO	90	90	
7497	Df(2L)Exel6011	25C8;25D5	CyO	80	85	
7498	Df(2L)Exel6012	25D5;25E6	CyO	35	9	*lam*
9560	Df(2L)BSC169	25E5;25F3	CyO	0	0	*lam*
9343	Df(2L)ED334	25F2;26B2	SM6a	65	75	

9181	Df(2L)ED285	25F5;26A3	SM6a	88	90	
9182	Df(2L)ED292	25F5;26B2	SM6a	18	90	
9272	Df(2L)ED347	25F5;26B5	SM6a	80	65	
9183	Df(2L)ED299	26B1;26B2	SM6a	83	75	
9187	Df(2L)ED354	26B1;26B5	SM6a	83	83	
9341	Df(2L)ED385	26B1;26D7	SM6a		65	
6338	Df(2L)BSC6	26D3-E1;26F4-7	SM6a	75	85	
24378	Df(2L)BSC354	26D7;26E3	CyO	85	90	
9615	Df(2L)BSC188	26F1;27A2	CyO	83	55	
24126	Df(2L)ED441	27A1;27E1	SM6a	5	40	
23676	Df(2L)BSC291	27D6;27F2	CyO	85	90	
9060	Df(2L)ED489	27E4;28B1	SM6a	75	75	
9708	Df(2L)BSC233	27F3;28D2	CyO	25	inviable	*mts*
7147	Df(2L)BSC41	28A4-B1;28D3-9	CyO	20	inviable	*mts*
9502	Df(2L)BSC142	28C3;28D3	CyO	15	inviable	*mts*
7807	Df(2L)Exel7034	28E1;28F1	CyO	75	75	
9704	Df(2L)BSC227	28E8;29B1	CyO	80	80	
8836	Df(2L)BSC111	28F5;29B1	CyO	78	85	
24132	Df(2L)ED629	29B4;29E4	SM6a	80	65	
9631	Df(2L)BSC204	29D5;29F8	CyO	65	65	
8906	Df(2L)ED678	29F5;30B12	SM6a	50	55	
24133	Df(2L)ED690	30B3;30E4	SM6a	80	70	
6478	Df(2L)BSC17	30C3--30F1	SM6a	80	90	
9715	Df(2L)BSC240	30C7;30F2	CyO	88	40	
8469	Df(2L)BSC50	30F4-5;31B1-4	SM6a	90	75	
26541	Df(2L)BSC689	30F5;31B1	CyO	90	36	
9503	Df(2L)BSC143	31B1;31D9	CyO	90	65	
9635	Df(2L)BSC208	31D7;31D11	CyO	90	90	
9637	Df(2L)BSC209	31D7;31E1	CyO	80	80	
24135	Df(2L)ED8142	31E1;32A4	SM6a	80	70	
9642	Df(2L)BSC214	31F5;32B4	CyO	75	10	
9641	Df(2L)BSC213	32B1;32C1	CyO	75	70	
9505	Df(2L)BSC145	32C1;32C1	CyO	75	1	
9716	Df(2L)BSC241	32C1;32F2	CyO	65	16	
9718	Df(2L)BSC244	32F2;33B6	CyO	80	65	
24109	Df(2L)ED761	33A2;33E5	SM6a	80	75	
8907	Df(2L)ED775	33B8;34A3	SM6a	90	85	
23662	Df(2L)BSC277	34A1;34B2	CyO	75	85	
6999	Df(2L)BSC30	34A3;34B7-9	SM6a	80	90	
26865	Df(2L)BSC768	34A9;34B8	SM6a	88	50	
27383	Df(2L)BSC812	34B11;34E1	SM6a	90	70	
9594	Df(2L)BSC159	34B4;34C4	Dp(2;2)Cam5	80	90	
23152	Df(2L)BSC252	34D1;34F1	CyO	90	75	
9061	Df(2L)ED793	34E4;35B4	SM6a	90	90	
6963	Df(2L)ED3	35B2;35D1	SM6a	80	90	
8946	Df(2L)ED1050	35B8;35D4	SM6a	90	90	
1491	Df(2L)r10	35D1-36A7	CyO	55	5	

26542	Df(2L)BSC690	35D4;35D4	CyO	70	90	
7521	Df(2L)Exel6038	35D6;35E2	CyO	75	85	
23663	Df(2L)BSC278	35E1;35F1	CyO	40	40	
27353	Df(2L)BSC781	35F1;36A1	CyO	80	90	
24113	Df(2L)ED1102	35F12;36A10	SM6a	83	88	
3180	Df(2L)H20	36A8-9;36E1-2	CyO	0	5	*Cse1*
24114	Df(2L)ED1161	36A10;36C9	SM6a	0	3	*Cse1*
9507	Df(2L)BSC148	36C8;36E3	CyO	65	80	
7839	Df(2L)Exel7070	36E2;36E6	CyO	88	75	
23156	Df(2L)BSC256	36E3;36F2	CyO	80	90	
7840	Df(2L)Exel8038	36E5;36F5	CyO	75	75	
9508	Df(2L)BSC149	36F5;36F10	CyO	75	75	
8935	Df(2L)ED1203	36F7;37C5	SM6a	60	80	
24116	Df(2L)ED1272	37C5;38A2	SM6a	90	70	
8679	Df(2L)ED1303	37E5;38C6	SM6a	75	85	
9269	Df(2L)ED1315	38B4;38F5	SM6a	45	35	
9682	Df(2L)ED1378	38F1;39D2	SM6a	90	70	
9266	Df(2L)ED1473	39B4;40A5	Cy[1]	93	92	
9340	Df(2L)ED1466	39E3;40A5	Cy[1]	90	75	
9510	Df(2L)BSC151	40A5;40E5	CyO	90	85	
25705	Df(2R)BSC630	41D3;41F11	CyO	60	80	
8044	Df(2R)ED1552	42A11;42C7	SM6a	90	80	
8045	Df(2R)ED1612	42A13;42E6	SM6a	23	88	
9683	Df(2R)ED1484	42A2;42A14	SM6a	82	75	
9062	Df(2R)ED1673	42E1;43D3	SM6a	12	60	
8931	Df(2R)ED1715	43A4;43F1	SM6a	58	75	
8941	Df(2R)ED1725	43E4;44B5	SM6a	83	65	
24335	Df(2R)BSC267	44A4;44C4	CyO	88	60	
9157	Df(2R)ED1770	44D5;45B4	SM6a	65	60	
9063	Df(2R)ED1791	44F7;45F1	SM6a	75	75	
23665	Df(2R)BSC280	45C4;45F4	CyO	60	12	
9410	Df(2R)BSC132	45F6;46B4	SM6a	75	60	
7867	Df(2R)Exel9016	46B1;46B2	CyO	83	85	
23682	Df(2R)BSC298	46B2;46C7	CyO	70	90	
9539	Df(2R)BSC152	46C1;46D6	CyO	60	80	
23686	Df(2R)BSC303	46E1;46F3	CyO	73	75	
23666	Df(2R)BSC281	46F1;47A9	CyO	77	85	
25428	Df(2R)BSC595	47A3;47F1	CyO	80	70	
8910	Df(2R)ED2219	47D6;48B6	SM6a	83	85	
9626	Df(2R)BSC199	48C5;48E4	CyO	77	45	
26551	Df(2R)BSC699	48D7;48E6	SM6a	63	90	
24929	Df(2R)BSC425	48F1;49A1	CyO	73	88	
7543	Df(2R)Exel6061	48F1;49A6	CyO	70	15	
23688	Df(2R)BSC305	49A4;49A10	CyO	71	75	
30585	Df(2R)BSC880	49A9;49E1	SM6a	75	70	
1642	Df(2R)wg135	49B2;49F1	CyO	90	90	
24989	Df(2R)BSC485	49B10;49E6	CyO	60	75	

7869	Df(2R)Exel7121	49B5;49B12	CyO	75	83	
442	Df(2R)CX1	49C1;49C4;50C23;50D1	SM1	0	0	
7544	Df(2R)Exel6062	49E6;49F1	CyO	88	90	
7871	Df(2R)Exel8057	49F1;49F10	CyO	90	65	
23169	Df(2R)BSC273	49F4;50A13	CyO	83	75	
23170	Df(2R)BSC274	50A7;50B4	CyO	80	65	
23690	Df(2R)BSC307	50B6;50C18	CyO	80	80	
24385	Df(2R)BSC361	50C3;50F1	CyO	90	80	
24407	Df(2R)BSC383	50C6;50D2	CyO	80	75	
7875	Df(2R)Exel7130	50D4;50E4	CyO	85	75	
8913	Df(2R)ED2354	50E6;51B1	SM6a	85	15	
7749	Df(2R)Exel6284	51B1;51C2	CyO	85	83	
24933	Df(2R)BSC429	51C2;51D1	CyO	88	85	
25741	Df(2R)BSC651	51C5;51E2	CyO	83	90	
9064	Df(2R)ED2426	51E2;52B1	SM6a	75	80	
8914	Df(2R)ED2436	51F11;52D11	SM6a	80	75	
8915	Df(2R)ED2457	52D11;52E7	SM6a	80	55	
7885	Df(2R)Exel9060	52E11;52F1	HV	85	85	
29661	Df(2R)ED2487	52E6;53C4	SM6a	75	75	
23692	Df(2R)BSC309	52F11;53B1	CyO	80	80	
25078	Df(2R)BSC550	53C1;53C6	CyO	90	80	
7546	Df(2R)Exel6064	53C11;53D11	CyO	90	65	
7888	Df(2R)Exel7144	53C8-53D2	CyO	55	75	
9278	Df(2R)ED2747	53D11;53F8	SM6a	80	85	
24356	Df(2R)BSC331	53D14;54A1	CyO	80	80	
6916	Df(2R)ED1	53E4;53F8	SM6a	88	90	
7548	Df(2R)Exel6066	53F8;54B6	CyO	90	78	
24379	Df(2R)BSC355	54B16;54C3	CyO	80	25	
9596	Df(2R)BSC161	54B2;54B17	CyO	85	88	
7890	Df(2R)Exel7149	54C10;54D5	CyO	63	65	
24371	Df(2R)BSC347	54D2;54E9	CyO	70	60	
6780	Df(2R)14H10W	54E5;55B7	SM6a	0	25	
9066	Df(2R)ED3610	54F1;55C8	Cy		91	
8918	Df(2R)ED3683	55C2;56C4	SM6a	85	85	
7551	Df(2R)Exel6069	56B5;56C11	CyO	80	70	
9423	Df(2R)BSC135	56C11;56D5	CyO	80	75	
9067	Df(2R)ED3728	56D10;56E2	SM6a	75	85	
6647	Df(2R)BSC22	56D7;E3;56F9;12	SM6a	80	70	
27354	Df(2R)BSC782	56D8;56D14	SM6a	80	80	
30588	Df(2R)BSC883	56E1;56F11	SM6a	75	88	
25678	Df(2R)BSC594	56E1;56F9	CyO	75	75	
7896	Df(2R)Exel7162	56F11;56F16	CyO	70		
6609	Df(2R)BSC19	56F12;14;57A4	SM6a	80		
26553	Df(2R)BSC701	56F15;57A9	SM6a	70	60	
26554	Df(2R)BSC702	57A2;57B3	SM6a	65	85	
9267	Df(2R)ED3791	57B1;57D4	Cy[1]	83	85	
2605	Df(2R)Pu-D17	57B4;58B2	SM1	85	85	

27582	Df(2R)BSC821	57D10;57E6	SM6a	70	80	
26516	Df(2R)BSC664	57D12;58A3	SM6a	75	5	
30590	Df(2R)BSC885	57D2;57D10	SM6a	90	80	
25430	Df(2R)BSC597	58A2;58F1	SM6a	63	80	
7903	Df(2R)Exel7173	58D4;58E5	CyO	80	88	
25431	Df(2R)BSC598	58F3;59A1	SM6a	90	85	
27359	Df(2R)BSC787	58F4;59B1	SM6a	85	88	
3909	Df(2R)59AD	59A1;59D4	SM1	80	80	
29988	Df(2R)BSC865	59A4;59B7	Dp(2;2)Cam16	73	35	
25432	Df(2R)BSC599	59B1;59B3	SM6a	70	65	
27356	Df(2R)BSC784	59B4;59B6	SM6a	90	90	
26866	Df(2R)BSC769	59B7;59D9	SM6a	80	90	
26513	Df(2R)BSC661	59D8;59F5	SM6a	63	75	
9424	Df(2R)BSC136	59F5;60B6	SM6a	43	0	
24380	Df(2R)BSC356	60B8;60C4	SM6a	85	80	
27352	Df(2R)BSC780	60C2;60D14	SM6a	60	80	
25437	Df(2R)BSC604	60D4;60E11	SM6a	80	75	
2528	Df(2R)gsb	60E9;10;60F1;2	CyO	90	90	
4961	Df(2R)Kr10	60E10;60F5	CyO	85	85	
25441	Df(2R)BSC608	60E11;60F2	SM6a	75	90	
24758	Df(2R)ED50004	60F5;60F5	SM6a	55	90	
741	Df(2R)M41A10	H38R-H46	SM1	5	13	
8047	Df(3L)ED201	61B1;61C1	TM6C,Sb	80	65	
24386	Df(3L)BSC362	61C1;61C7	TM6C,Sb	80	75	
8050	Df(3L)ED4196	61C7;62A2	TM2 (Ubx)	70	75	
8053	Df(3L)ED207	61C9;62A6	TM2 (Ubx)	80	80	
23674	Df(3L)BSC289	61F6;62A9	TM6C,Sb	90	90	
5411	Df(3L)Aprt-32	62B1;62E3	TM6 (Ubx)	85	75	
9693	Df(3L)BSC181	62A11;62B7	TM6C,Sb	75	80	
27372	Df(3L)BSC800	62A9;62A9	TM6C,Sb	90	90	
8096	Df(3L)ED4287	62B4;62E5	TM6C,Sb	90	80	
8976	Df(3L)BSC119	62E7;62F5	TM6B,Tb	80	83	
6755	Df(3L)BSC23	62E8;63B5-6	TM2 (Ubx)	90	75	
3650	Df(3L)M21	62F;63D	In(3LR)T33^{L}r19^{R}	40	20	
7571	Df(3L)Exel6092	62F5;63A3	TM6B,Tb	88	75	
26523	Df(3L)BSC671	63A2;63B11	TM6C,Sb	75	85	
26524	Df(3L)BSC672	63A7;63B12	TM6C,Sb	70	70	
8058	Df(3L)ED4293	63C1;63C1	TM6C,Sb	93	90	
8059	Df(3L)ED208	63C1;63F5	TM6C,Sb	33	90	
24392	Df(3L)BSC368	63F1;64A4	TM6C,Sb	90	90	
8060	Df(3L)ED4341	63F6;64B9	TM6C,Sb	80	80	
8061	Df(3L)ED210	64B9;64C13	TM6C,Sb	90	90	
3096	Df(3L)ZN47	64C;65C	TM3,Sb	90		
24395	Df(3L)BSC371	64C1;64E1	TM6C,Sb	90	80	
7586	Df(3L)Exel6107	64E5;64F5	TM6B,Tb	90	90	
24914	Df(3L)BSC410	64E7;65B3	TM6C,Sb	88	90	
24915	Df(3L)BSC411	65A2;65C1	TM6C,Sb	83	88	

7588	Df(3L)Exel6109	65C3;65D3	TM6B,Tb	85	90	
6867	Df(3L)BSC27	65D4-5;65E4-6	TM6B,Tb	80	65	
9701	Df(3L)BSC224	65D5;65E6	TM6C,Sb	90	85	
6964	Df(3L)BSC33	65E10-F1;65F2-6	TM2 (Ubx)	75	10	
8974	Df(3L)BSC117	65E9;65F5	TM6B,Tb	85	78	
7929	Df(3L)Exel8104	65F7;66A4	TM6B,Tb	88	80	
24399	Df(3L)BSC375	66A3;66A19	TM6C,Sb	85	87	
24412	Df(3L)BSC388	66A8;66B11	TM6C,Sb	93	75	
7591	Df(3L)Exel6112	66B5;66C8	TM6B,Tb	85	85	
24413	Df(3L)BSC389	66C12;66D8	TM6C,Sb	93	55	
27576	Df(3L)BSC815	66C3;66D4	TM6C,Sb	70	75	
8066	Df(3L)ED4421	66D12;67B3	TM6C,Sb	90	90	
27577	Df(3L)BSC816	66D9;66D12	TM6C,Sb	80	70	
3650	Df(3L)M21	62F;63D	In(3LR)T33^{1}f19^{R}	5	23	
7079	Df(3L)BSC35	66F1-2;67B2-3	TM3,Sb	75	75	
8970	Df(3L)BSC113	67B1;67B5	TM6B,Tb	88	88	
8975	Df(3L)BSC118	67B11;67C5	TM6B,Tb	80	80	
24415	Df(3L)BSC391	67B7;67C5	TM6C,Sb	90	80	
24416	Df(3L)BSC392	67C4;67D1	TM6C,Sb	80	16	
26525	Df(3L)BSC673	67C7;67D10	TM6C,Sb	80	85	
9355	Df(3L)ED4457	67E2;68A7	TM6C,Sb	45	15	
8068	Df(3L)ED4470	68A6;68E1	TM6C,Sb	70	70	
8069	Df(3L)ED4475	68C13;69B4	TM6C,Sb	70	65	
26828	Df(3L)BSC730	68F7;69E6	TM6C,Sb	45	80	
8070	Df(3L)ED4483	69A5;69D3	TM6C,Sb	75	6	
8072	Df(3L)ED4486	69C4;69F6	TM6C,Sb	83	70	
6457	Df(3L)BSC12	69F6-70A1;70A1-2	TM3,Sb	85	88	
8097	Df(3L)ED4502	70A3;70C10	TM6C,Sb	70	18	
9214	Df(3L)ED4536	70C11;70D3	TM6C,Sb	70	80	
9072	Df(3L)ED4528	70C15;70D2	TM6C,Sb	83	90	
9074	Df(3L)ED4534	70C15;70D3	TM6C,Sb	90	90	
8073	Df(3L)ED4543	70C6;70F4	TM6C,Sb	75	75	
8074	Df(3L)ED217	70F4;71E1	TM6C,Sb	75	80	
8075	Df(3L)ED218	71B1;71E1	TM6C,Sb	75	90	
27888	Df(3L)BSC845	71D3;72A1	TM6C,Sb	85	85	
24947	Df(3L)BSC443	72B1;72E4	TM6C,Sb	70	75	
8077	Df(3L)ED220	72D4;72F1	TM6C,Sb	75	80	
8078	Df(3L)ED4606	72D4;73C4	TM6C,Sb	70	90	
8099	Df(3L)ED4685	73D5;74E2	TM6C,Sb	75	80	
27347	Df(3L)BSC775	75A2;75E4	TM6C,Sb	75	80	
9697	Df(3L)BSC220	75F1;76A1	TM6C,Sb	80	80	
8086	Df(3L)ED228	76A1;76D3	TM6C,Sb	85	88	
6646	Df(3L)BSC20	76A7-B1;76B4-5	TM6B,Tb	90	75	
8088	Df(3L)ED4858	76D3;77C1	TM2 (Ubx)	5	10	*polo*
2052	Df(3L)rdgC-co2	77A1;77D1	TM6C,Sb	5	0	*polo*
27369	Df(3L)BSC797	77C3;78A1	TM6C,Sb	80	88	
24952	Df(3L)BSC448	77C6;77E4	TM6C,Sb	75	90	

7588	Df(3L)Exel6109	65C3;65D3	TM6B,Tb	85	90	
6867	Df(3L)BSC27	65D4-5;65E4-6	TM6B,Tb	80	65	
9701	Df(3L)BSC224	65D5;65E6	TM6C,Sb	90	85	
6964	Df(3L)BSC33	65E10-F1;65F2-6	TM2 (Ubx)	75	10	
8974	Df(3L)BSC117	65E9;65F5	TM6B,Tb	85	78	
7929	Df(3L)Exel8104	65F7;66A4	TM6B,Tb	88	80	
24399	Df(3L)BSC375	66A3;66A19	TM6C,Sb	85	87	
24412	Df(3L)BSC388	66A8;66B11	TM6C,Sb	93	75	
7591	Df(3L)Exel6112	66B5;66C8	TM6B,Tb	85	85	
24413	Df(3L)BSC389	66C12;66D8	TM6C,Sb	93	55	
27576	Df(3L)BSC815	66C3;66D4	TM6C,Sb	70	75	
8066	Df(3L)ED4421	66D12;67B3	TM6C,Sb	90	90	
27577	Df(3L)BSC816	66D9;66D12	TM6C,Sb	80	70	
3650	Df(3L)M21	62F;63D	In(3LR)T33^{1}f19^{R}	5	23	
7079	Df(3L)BSC35	66F1-2;67B2-3	TM3,Sb	75	75	
8970	Df(3L)BSC113	67B1;67B5	TM6B,Tb	88	88	
8975	Df(3L)BSC118	67B11;67C5	TM6B,Tb	80	80	
24415	Df(3L)BSC391	67B7;67C5	TM6C,Sb	90	80	
24416	Df(3L)BSC392	67C4;67D1	TM6C,Sb	80	16	
26525	Df(3L)BSC673	67C7;67D10	TM6C,Sb	80	85	
9355	Df(3L)ED4457	67E2;68A7	TM6C,Sb	45	15	
8068	Df(3L)ED4470	68A6;68E1	TM6C,Sb	70	70	
8069	Df(3L)ED4475	68C13;69B4	TM6C,Sb	70	65	
26828	Df(3L)BSC730	68F7;69E6	TM6C,Sb	45	80	
8070	Df(3L)ED4483	69A5;69D3	TM6C,Sb	75	6	
8072	Df(3L)ED4486	69C4;69F6	TM6C,Sb	83	70	
6457	Df(3L)BSC12	69F6-70A1;70A1-2	TM3,Sb	85	88	
8097	Df(3L)ED4502	70A3;70C10	TM6C,Sb	70	18	
9214	Df(3L)ED4536	70C11;70D3	TM6C,Sb	70	80	
9072	Df(3L)ED4528	70C15;70D2	TM6C,Sb	83	90	
9074	Df(3L)ED4534	70C15;70D3	TM6C,Sb	90	90	
8073	Df(3L)ED4543	70C6;70F4	TM6C,Sb	75	75	
8074	Df(3L)ED217	70F4;71E1	TM6C,Sb	75	80	
8075	Df(3L)ED218	71B1;71E1	TM6C,Sb	75	90	
27888	Df(3L)BSC845	71D3;72A1	TM6C,Sb	85	85	
24947	Df(3L)BSC443	72B1;72E4	TM6C,Sb	70	75	
8077	Df(3L)ED220	72D4;72F1	TM6C,Sb	75	80	
8078	Df(3L)ED4606	72D4;73C4	TM6C,Sb	70	90	
8099	Df(3L)ED4685	73D5;74E2	TM6C,Sb	75	80	
27347	Df(3L)BSC775	75A2;75E4	TM6C,Sb	75	80	
9697	Df(3L)BSC220	75F1;76A1	TM6C,Sb	80	80	
8086	Df(3L)ED228	76A1;76D3	TM6C,Sb	85	88	
6646	Df(3L)BSC20	76A7-B1;76B4-5	TM6B,Tb	90	75	
8088	Df(3L)ED4858	76D3;77C1	TM2 (Ubx)	5	10	*polo*
2052	Df(3L)rdgC-co2	77A1;77D1	TM6C,Sb	5	0	*polo*
27369	Df(3L)BSC797	77C3;78A1	TM6C,Sb	80	88	
24952	Df(3L)BSC448	77C6;77E4	TM6C,Sb	75	90	

7588	Df(3L)Exel6109	65C3;65D3	TM6B,Tb	85	90	
6867	Df(3L)BSC27	65D4-5;65E4-6	TM6B,Tb	80	65	
9701	Df(3L)BSC224	65D5;65E6	TM6C,Sb	90	85	
6964	Df(3L)BSC33	65E10-F1;65F2-6	TM2 (Ubx)	75	10	
8974	Df(3L)BSC117	65E9;65F5	TM6B,Tb	85	78	
7929	Df(3L)Exel8104	65F7;66A4	TM6B,Tb	88	80	
24399	Df(3L)BSC375	66A3;66A19	TM6C,Sb	85	87	
24412	Df(3L)BSC388	66A8;66B11	TM6C,Sb	93	75	
7591	Df(3L)Exel6112	66B5;66C8	TM6B,Tb	85	85	
24413	Df(3L)BSC389	66C12;66D8	TM6C,Sb	93	55	
27576	Df(3L)BSC815	66C3;66D4	TM6C,Sb	70	75	
8066	Df(3L)ED4421	66D12;67B3	TM6C,Sb	90	90	
27577	Df(3L)BSC816	66D9;66D12	TM6C,Sb	80	70	
3650	Df(3L)M21	62F;63D	In(3LR)T33^{1}f19^{R}	5	23	
7079	Df(3L)BSC35	66F1-2;67B2-3	TM3,Sb	75	75	
8970	Df(3L)BSC113	67B1;67B5	TM6B,Tb	88	88	
8975	Df(3L)BSC118	67B11;67C5	TM6B,Tb	80	80	
24415	Df(3L)BSC391	67B7;67C5	TM6C,Sb	90	80	
24416	Df(3L)BSC392	67C4;67D1	TM6C,Sb	80	16	
26525	Df(3L)BSC673	67C7;67D10	TM6C,Sb	80	85	
9355	Df(3L)ED4457	67E2;68A7	TM6C,Sb	45	15	
8068	Df(3L)ED4470	68A6;68E1	TM6C,Sb	70	70	
8069	Df(3L)ED4475	68C13;69B4	TM6C,Sb	70	65	
26828	Df(3L)BSC730	68F7;69E6	TM6C,Sb	45	80	
8070	Df(3L)ED4483	69A5;69D3	TM6C,Sb	75	6	
8072	Df(3L)ED4486	69C4;69F6	TM6C,Sb	83	70	
6457	Df(3L)BSC12	69F6-70A1;70A1-2	TM3,Sb	85	88	
8097	Df(3L)ED4502	70A3;70C10	TM6C,Sb	70	18	
9214	Df(3L)ED4536	70C11;70D3	TM6C,Sb	70	80	
9072	Df(3L)ED4528	70C15;70D2	TM6C,Sb	83	90	
9074	Df(3L)ED4534	70C15;70D3	TM6C,Sb	90	90	
8073	Df(3L)ED4543	70C6;70F4	TM6C,Sb	75	75	
8074	Df(3L)ED217	70F4;71E1	TM6C,Sb	75	80	
8075	Df(3L)ED218	71B1;71E1	TM6C,Sb	75	90	
27888	Df(3L)BSC845	71D3;72A1	TM6C,Sb	85	85	
24947	Df(3L)BSC443	72B1;72E4	TM6C,Sb	70	75	
8077	Df(3L)ED220	72D4;72F1	TM6C,Sb	75	80	
8078	Df(3L)ED4606	72D4;73C4	TM6C,Sb	70	90	
8099	Df(3L)ED4685	73D5;74E2	TM6C,Sb	75	80	
27347	Df(3L)BSC775	75A2;75E4	TM6C,Sb	75	80	
9697	Df(3L)BSC220	75F1;76A1	TM6C,Sb	80	80	
8086	Df(3L)ED228	76A1;76D3	TM6C,Sb	85	88	
6646	Df(3L)BSC20	76A7-B1;76B4-5	TM6B,Tb	90	75	
8088	Df(3L)ED4858	76D3;77C1	TM2 (Ubx)	5	10	*polo*
2052	Df(3L)rdgC-co2	77A1;77D1	TM6C,Sb	5	0	*polo*
27369	Df(3L)BSC797	77C3;78A1	TM6C,Sb	80	88	
24952	Df(3L)BSC448	77C6;77E4	TM6C,Sb	75	90	

24953	Df(3L)BSC449	77F2;78C2	TM6C,Sb	88	90	
25116	Df(3L)BSC553	78A2;78C2	TM6C,Sb	90	75	
24923	Df(3L)BSC419	78C2;78D8	TM6C,Sb	90	80	
8101	Df(3L)ED4978	78D5;79A2	TM6C,Sb	90	70	
9700	Df(3L)BSC223	79A3;79B3	TM6C,Sb	65	70	
24955	Df(3L)BSC451	79B2;79F5	TM6C,Sb	80	75	
8089	Df(3L)ED230	79C2;80A4	TM6C,Sb	70	90	
8102	Df(3L)ED5017	80A4;80C2	TM6C,Sb	80	90	
2597	Df(3R)10-65	81F;81F	TM3,Sb	90	80	
9196	Df(3R)ED5021	81F6;82A5	TM6C,Sb	70	75	
9197	Df(3R)ED5046	81F6;82D2	TM6C,Sb	75	80	
9226	Df(3R)ED5100	81F6;82E7	TM6C,Sb	88	85	
9075	Df(3R)ED5020	82A1;82A5	TM6C,Sb	90	90	
8091	Df(3R)ED5092	82A1;82E7	TM6C,Sb	65	75	
8093	Df(3R)ED5095	82C5;82E7	TM6C,Sb	80	80	
8967	Df(3R)ED5147	82E7;83A1	TM6C,Sb	70	90	
8965	Df(3R)ED5156	82F8;83A4	TM6C,Sb	83	85	
25077	Df(3R)BSC549	83A6;83B6	TM6C,Sb	75	90	
8103	Df(3R)ED5177	83B4;83B6	TM6C,Sb	85	88	
9199	Df(3R)ED5187	83B7;83B8	TM6C,Sb	85	70	
24968	Df(3R)BSC464	83B7;83E1	TM6C,Sb	75	8	
7443	Df(3R)BSC47	83B7-C1;83C6-D1	TM3,Sb	80	75	
8681	Df(3R)ED5196	83B9;83D2	TM6C,Sb	83	90	
26533	Df(3R)BSC681	83E2;83E5	TM6C,Sb	75	85	
26836	Df(3R)BSC738	83E5;84A1	TM6C,Sb	85	90	
24971	Df(3R)BSC467	83F1;84B2	TM6C,Sb	85	90	
25724	Df(3R)BSC633	84B2;84C3	TM6C,Sb	80	83	
8685	Df(3R)ED7665	84B4;84E11	TM6C,Sb	80	70	
8682	Df(3R)ED5230	84E6;85A5	TM6C,Sb	90	80	
9338	Df(3R)ED5296	84F6;85C3	TM6C,Sb	0	80	
9203	Df(3R)ED5331	85C3;85D1	TM6C,Sb	80	90	
9202	Df(3R)ED5327	85D1;85D1	TM6C,Sb	88	80	
9204	Df(3R)ED5339	85D1;85D11	TM6C,Sb	60	90	
24980	Df(3R)BSC476	85D16;85D24	TM6C,Sb	75	75	
8919	Df(3R)ED5429	85D19;85F8	TM2 (Ubx)	70	60	
7731	Df(3R)Exel6264	85D24;85E5	TM6B,Tb	90	65	
25011	Df(3R)BSC507	85D6;85D15	TM6C,Sb	90	80	
9227	Df(3R)ED5428	85E1;85F8	TM6C,Sb	15		
9080	Df(3R)ED5454	85E5;85F12	TM6C,Sb	25		
9078	Df(3R)ED5438	85E5;85F8	TM6C,Sb	25	sterile	
7633	Df(3R)Exel6154	85E9;85F1	TM6B,Tb	85	70	
7634	Df(3R)Exel6155	85F1;85F10	TM6B,Tb	80	70	
9082	Df(3R)ED5474	85F11;86B1	TM6C,Sb	inviable	5	*tws*
9081	Df(3R)ED5472	85F16;86B1	TM6C,Sb	10	10	
9215	Df(3R)ED5495	85F16;86C7	TM6C,Sb	10	5	
25696	Df(3R)BSC621	85F5;85F14	TM6C,Sb	80	80	*tws?*
24983	Df(3R)BSC479	86A3;86C7	TM6C,Sb	50	5	

7638	Df(3R)Exel6159	86C3;86C7	TM6B,Tb	70	70	
7956	Df(3R)Exel7305	86C6;86C7	TM6B,Tb	85	85	
7957	Df(3R)Exel7306	86C7;86D5	TM6B,Tb	90	88	
25126	Df(3R)BSC568	86C7;86D7	TM6C,Sb	85	65	
8957	Df(3R)ED5514	86C7;86E11	TM6C,Sb	80	80	
9084	Df(3R)ED5518	86C7;86E13	TM6C,Sb	85	70	
24973	Df(3R)BSC469	86D8;87A2	TM6C,Sb	85	75	
8029	Df(3R)ED5577	86F9;87B13	TM6C,Sb	0	5	
24990	Df(3R)BSC486	87B10;87E9	TM6C,Sb	80	90	
9087	Df(3R)ED5610	87B11;87D7	TM6C,Sb	80	90	
9085	Df(3R)ED5554	87B5;87B11	TM6C,Sb	5	25	
9086	Df(3R)ED5591	87B7;87C7	TM6C,Sb	45	90	
8921	Df(3R)ED5623	87E3;88A4	TM2 (Ubx)	85	88	
8959	Df(3R)ED5622	87F10;88A4	TM6C,Sb	80	70	
9090	Df(3R)ED5644	88A4;88C9	TM6C,Sb	85	90	
23714	Df(3R)ED10555	88C9;88D8	TM3,Sb	75	75	
24137	Df(3R)ED5664	88D1;88E3	TM6C,Sb	85	75	
9152	Df(3R)ED5705	88E12;89A5	TM2 (Ubx)	80	90	
24138	Df(3R)ED10566	88E2;88E5	TM6C,Sb	80	90	
26839	Df(3R)BSC741	88E8;88F1	TM6C,Sb	75	80	
25019	Df(3R)BSC515	88F6;89A8	TM6C,Sb	0	75	
7983	Df(3R)Exel7328	89A12;89B6	TM6B,Tb	85	80	
26580	Df(3R)BSC728	89A8;89B2	TM6C,Sb	5	70	
3678	Df(3R)sbd45	89B4;89B10	TM6 (Ubx)	75	80	
1467	Df(3R)P115,	89B7-89E7	TM1 (Sb)	90	80	
9482	Df(3R)ED10642	89B17;89D5	TM6C,Sb	80	80	
7737	Df(3R)Exel6270	89B18;89D8	TM6B,Tb	90	90	
8104	Df(3R)ED5780	89E11;90C1	TM2 (Ubx)	80	45	
26846	Df(3R)BSC748	89E5;89E11	TM6C,Sb	80	90	
27362	Df(3R)BSC790	90B6;90E2	TM6C,Sb	80	70	
9207	Df(3R)ED5785	90C2;90D1	TM6C,Sb	75	85	
25740	Df(3R)BSC650	90C6;91A2	TM6C,Sb	75	80	
9208	Df(3R)ED5815	90F4;91B8	TM6C,Sb	90	75	
6962	Df(3R)ED2	91A5;91F1	TM6C,Sb	0	85	
8683	Df(3R)ED5911	91C5;91F4	TM6C,Sb	85	90	
24139	Df(3R)ED5938	91D4;92A11	TM6C,Sb	75		
8964	Df(3R)ED6025	92A11;92E2	TM6C,Sb	60	68	
25021	Df(3R)BSC517	92C1;92F13	TM2 (Ubx)	80	75	
9501	Df(3R)BSC141	92F2;93A1	TM6B,Tb	70	75	
7413	Df(3R)BSC43	92F7-93A1;93B3-6	TM2 (Ubx)	75	10	
27580	Df(3R)BSC819	93A2;93B8	TM6C,Sb	90	90	
7739	Df(3R)Exel6272	93A4;93B13	TM6B,Tb	85	75	
9485	Df(3R)ED10838	93C1;93D4	TM2 (Ubx)	85	80	
24140	Df(3R)ED6058	93D4;93F6	TM6C,Sb	70	90	
8923	Df(3R)ED6085	93F14;94B5	TM2 (Ubx)	70	75	
9091	Df(3R)ED6090	94A1;94C1	TM3,Ser	5	5	
8924	Df(3R)ED6093	94A2;94C4	TM2 (Ubx)	0	5	

8684	Df(3R)ED6096	94B5;94E7	TM6C,Sb	5	5	
25694	Df(3R)BSC619	94D10;94E13	TM6C,Sb		50	
9497	Df(3R)BSC137	94F1;95A4	TM6B,Tb	70	90	
24993	Df(3R)BSC489	94F3;95D1	TM6C,Sb	70	60	
150341	Df(3R)ED6155	95B1-95D11	TM6C,Sb	65	35	
7675	Df(3R)Exel6196	95C12;95D8	TM6B,Tb	85	90	
28827	Df(3R)ED10893	95C8;95E1	TM6C,Sb	90	88	
9347	Df(3R)ED6187	95D10;96A7	TM2 (Ubx)	10	75	
7676	Df(3R)Exel6197	95D8;95E1	TM6B,Tb	90	75	
24996	Df(3R)BSC492	95E7;96B17	TM6C,Sb	30	75	
24343	Df(3R)BSC317	95F2;95F11	TM6C,Sb	80	80	
2363	Df(3R)crb87-5	95F6-8;96A18-20	TM3, Ser	65	80	
25728	Df(3R)BSC638	95F8;95F14	TM6C,Sb	85	90	
7678	Df(3R)Exel6199	95F8;96A2	TM6B,Tb	85	80	
7948	Df(3R)Exel7357	96A2;96A13	TM6B,Tb	80	80	
9211	Df(3R)ED6220	96A7;96C3	TM6C,Sb	15	8	*CycB3*
24965	Df(3R)BSC461	96B15;96D1	TM6C,Sb	40	80	
7680	Df(3R)Exel6201	96C2;96C4	TM6B,Tb	90	90	
7681	Df(3R)Exel6202	96D1;96D1	TM6B,Tb	85	90	
7682	Df(3R)Exel6203	96E2;96E6	TM6B,Tb	90	85	
24909	Df(3R)BSC321	96E6;96E9	TM6C,Sb	75	90	
9500	Df(3R)BSC140	96F1;96F10	TM6B,Tb	90	75	
8105	Df(3R)ED6232	96F10;97D2	TM6C,Sb	8	90	
9478	Df(3R)ED6235	97B9;97D12	TM6C,Sb	60	90	
9210	Df(3R)ED6255	97D2;97F1	TM6C,Sb	10	40	
25001	Df(3R)BSC497	97E6;98B5	TM6C,Sb		80	
29667	Df(3R)ED6280	98B6;98B6	TM6C,Sb	90	90	
25390	Df(3R)BSC567	98B6;98E5	TM6C,Sb	5	85	
7688	Df(3R)Exel6210	98E1;98F5	TM6B,Tb	80	80	
29997	Df(3R)BSC874	98E1;99A1	TM6C,Sb	75	75	
27378	Df(3R)BSC806	98F1;98F10	TM6C,Sb	75	80	
25005	Df(3R)BSC501	98F10;99B9	TM6C,Sb	80	90	
8961	Df(3R)ED6310	98F12;99B2	TM6C,Sb	90	75	
3547	Df(3R)L127	99B5-99F1	TM6 (Ubx)	90	75	
25075	Df(3R)BSC547	99B5;99C2	TM6C,Sb	80	90	
25695	Df(3R)BSC620	99C5;99D3	TM6C,Sb	75	80	
2352	Df(3R)X3F	99D2;99E1	TM3,Sb	80	60	
25006	Df(3R)BSC502	99D3;99D8	TM6C,Sb	90	90	
2234	Df(3R)R133	99E1-3Rt	TM3,Sb	75	70	
25007	Df(3R)BSC503	99E3;99F6	TM6C,Sb	70	90	
25008	Df(3R)BSC504	99F4;100A2	TM6C,Sb	75	70	
7997	Df(3R)Exel7378	99F8;100A5	TM6B,Tb	80	80	
24142	Df(3R)ED6346	100A5;100B1	TM6C,Sb	45	90	
27365	Df(3R)BSC793	100B5;100C4	TM6C,Sb	57	90	
24143	Df(3R)ED6361	100C7;100E3	TM6C,Sb	70	75	
24144	Df(3R)ED6362	100E1;100E3	TM6C,Sb	85	80	
24516	Df(3R)ED50003	100E1;100F5	TM6C,Sb	90	80	

Table 1. Complete results from the genetic deletion screen. Percentages of embryos hatching from females heterozygous for each deletion and heterozygous for *tws*^{P} or *mts*$^{XE-2258}$ are shown. For each deletion, its Bloomington stock number, its name, its cytological breakpoints and its balancer chromosome are indicated. Interacting genes that were validated with mutant alleles are indicated next to the deletion(s) that uncovered them. One deletion (labeled *tws*?) that should uncover *tws* did not genetically interact with *tws*^{P} or *mts*$^{XE-2258}$. This could occur if the deletion additionally uncovers a suppressor gene, of if its breakpoints differ from those published in the databases.

Mutant	% Hatching	S.D.	% Hatching with *lam*^{K2}/+	S.D.
Wild type	84	16	94	5
tws^{P}/+	91	7	9	5
tws^{aar1}/+	85	5	9	7
Pp2A-29B^{EP2332}/+	97	3	89	5
wdb^{07}/+	96	3	70	33
wdb^{KG04556}/+	95	6	96	8
wrd^{A131}/+ *	92	1	94	6
wrd^{MI00407}/+	98	3	84	9
Mob4$^{EY\Delta L3}$/+	91	8	65	15
Mob3^{G17981}/+	98	3	92	1
cka^{05836}/+	98	4	98	3
cka^{2}/+	92	5	93	6
cka^{4}/+	95	9	96	3
Strip^{e04482}/+	99	1	93	6
mts$^{XE-2258}$/+	88	8	3	0,3
mts^{EY12638}/+	96	2	87	6
mts^{2496}/+	88	5	7	7
mts^{s5286}/+	91	8	7	5
PP1-87B^{BG-3}/+	89	5	88	9
PP1-87B^{1}/+	79	5	88	10
PP4-19C^{G11307}/+ *	91	4	79	10
sds22^{e00975}/+	93	0,5	86	3
PPP4R2r^{EP307}/+	100	0	70	10
Pp1alpha-96A^{2}/+	88	9	89	3
flw^{1}/+ *	94	6	63	18
Pp1-13C^{MI13024}/+ *	93	5	80	5
flfl^{795}/+	95	5	71	5

Table 2. A screen for genetic interactions between *lamin* and genes encoding various phosphatase subunits. Percentages of embryos hatching from females heterozygous for each of the indicated mutant alleles only (left) or additionally heterozygous for *lam*^{K2} deletion (right) are shown, along with standard deviations (S.D.).

Values indicating strong interactions are green. All values were obtained from the same experiment, except for those marked with an asterisk (*) which were quantified separately.

Mutants	Source	Molecular lesion (according to Flybase)
lam^{K2}	Bloomington stock 25093	Addition of the nucleotides CTGC between G460 and A461 results in a frameshift after amino acid 153.
lam^{A25}	Bloomington stock 25092	Deletion of the nucleotides GATCC and TCTACCA results in a frameshift after amino acid 611. The deletion removes the C-terminal CaaX box.
lam^{04643}	Bloomington stock 11384	P{PZ} insertion in the first intron, 258bp upstream of the translation start site.
tws^{aar1}	David Glover	Unknown nature of the allele.
tws^{P}	David Glover	Insertion of P{lacW} into a tip of the second intron, 4bp downstream from an exon-intron boundary.
tws^{aar2}	David Glover	Imprecise excision of P-element in tws^{aar1} flies.
CycB^{2}	Bloomington stock 6630	Imprecise excision of P-element resulting in small deletion removing the region encoding α-helix 1, a conserved element of the cyclin box.
nhk-1^{E107}	Hiroyuki Ohkura	Imprecise excision of P{EP}*nhk-1*^{EP863} generates a 1.1kb deletion of the genomic region corresponding to the kinase domain of ball and is therefore considered a kinase-null mutation.
nhk-1^{trip}	Hiroyuki Ohkura	Nonsense mutation (AAA to TGA) resulting in truncation of the noncatalytic region.
mts$^{XE-2258}$	David Glover	16bp deletion, bases -7 to 9, that spans the translation start site. The next in-frame methionine does not occur for another 66 amino acids.
polo^{11}	David Glover	Breakpoint allele: is In(3L)77B1-3;77E1-2.
CycB3^{2}	Bloomington stock 6635	Deletion from 5' UTR, including the region encoding α-helix 1, a conserved element of the cyclin box essential for cdc2 binding.
CycB3^{L6540}	Bloomington stock 10337	Insertion of P{lacW} in 5'UTR of *CycB3*.
Cse1^{K03902}	Bloomington stock 10536	Insertion of The P{lacW} 71bp upstream of the ATG start of *Cas*.
Cse1^{MB08748}	Bloomington stock 26129	Insertion of Mi{ET1} at the 3rd exon of *Cas*.
emb^{k16715}	Bloomington stock 11195	Insertion of P{lacW} 400bp 5' of the transcription start site.
Nup107^{DG40512}	Bloomington stock 21784	Insertion of P{wHy} at the 5' UTR of *Nup107*.
Pp2A-29B^{EP2332}	Bloomington stock 17044	Insertion of P{EP} within *Pp2A-29B*.
wdb^{07}	Bloomington stock 9813	Insertion of P{UASp-YFP.Rab30.T21N} within *wdb*.
wdb^{KG94556}	Bloomington stock 13820	Insertion of P{SUPor-P} within *wdb*.
wrd^{A131}	Bloomington stock 16046	Insertion of PBac{5HPw+} within *wrd*.

wrd^{MI00407}	Bloomington stock 30989	Insertion of Mi{MIC} within *wrd*.
Mob4^{EYΔL3}	Bloomington stock 36311	357 bp deletion resulting from the imprecise excision of P{EPgy2}*Mob4*^{EY23407}
Mob3^{G17981}	Bloomington stock 28097	Insertion of P{EP} in the 5' UTR of *mob3*.
cka^{05836}	Bloomington stock 11451	Insertion in the 5' untranslated region.
cka^{2}	Marc Therien	Imprecise excision of the insertion in *Cka*^{05836}
Strip^{e04482}	Bloomington stock 18264	Insertion of PBac{RB} withing *Strip*.
cka^{4}	Marc Therien	Imprecise excision of the insertion in *Cka*^{05836}
mts^{EY12638}	Bloomington stock 20763	Insertion of P{EPgy2} in the first intron of *mts*.
mts^{2496}	Bloomington stock 11193	Insertion of P{PZ} in the 5' UTR of *mts*.
mts^{s5286}	Bloomington stock 10464	Insertion of P{lacW} in the *mts* region; precise position is not indicated.
PP1-87B^{BG-3}	Bloomington stock 23696	Deletion with a breakpoint 165bp upstream of the ATG initiation site. This removes the TATA box and other upstream sequences. Extent of deletion unknown.
PP1-87B^{1}	Bloomington stock 6207	Amino acid replacement: G220S.
PP4-19C^{G11307}	Bloomington stock 26629	Insertion of P{EP} witing *PP4-19C*.
sds22^{e00975}	Bloomington stock 17908	Insertion of PBAC{RB} in the 5' UTR of *sdsd22*.
PPP4R2r^{EP307}	Bloomington stock 10106	Insertion of P{EP} in the 5' UTR of *PPP4R2r*.
Pp1alpha-96A^{2}	Bloomington stock 23698	Imprecise excision of the insertion in *Pp1α-96A*^{GS11179}, resulting in a 1.7kb deletion, which removes the proximal promoter region, transcription start site and exons 1-3 of Pp1α-96A.
flw^{1}	Bloomington stock 46	Amino acid replacement: V284A.
Pp1-13C^{MI13024}	Bloomington stock 59649	Insertion of Mi{MIC} within *Pp1-13C*.
flfl^{795}	Bloomington stock 66535	Amino acid change leading to a premature stop codons at positions 324.

Table 3. Mutant alleles used in this study, their source and their molecular lesion.

CHAPTER 3

Deciphering the functions of Ankle2 during mitotic exit

3.1 Abstract

Chapter 2 presented evidence that PP2A-B55 dephosphorylates the small NE protein BAF. When dephosphorylated, BAF binds to DNA and shapes the nucleus for the recruitment of downstream nuclear proteins such as the nuclear lamina protein Lamin B and the nucleoporin Nup107. In this chapter, I am presenting progress I accomplished at the end of my project in dissecting the role of the protein LEM4/Ankle2, which was previously shown to regulate BAF recruitment to reassembling nuclei in human cells and *C. elegans*. However, the nature of Ankle2 and the molecular mechanism by which it promotes BAF functions during NER are still not well known. I first confirm that the function of Ankle2 in recruiting BAF to reassembling nuclei is conserved in *Drosophila*. I also show that Ankle2 is required for proper mitotic progression during fly embryo development. Using biochemical assays and mass spectrometry, I demonstrate that Ankle2 forms a complex with PP2A-A and PP2A-C that has phosphatase activity. This study sheds light on a role of a new protein that is important for the reformation of the nuclear envelope and mitotic progression. More efforts are being made now in our lab to reach a full picture of the nature and the role of Ankle2 in *Drosophila*.

I want to emphasize that this Chapter contains unfinished work, with either preliminary results or experiments that should be confirmed with further repetition. In this context, one could argue that this part should not be included in my thesis, though I decided to include it as it contains exciting findings that are worth showing. Also, since senior authors contributed to writing the published paper shown in Chapter 2, this 3rd Chapter was a chance to write in my own words. This Chapter contains data from experiments performed in collaboration with Laia Jordana, a new Ph.D. student I

supervised in our laboratory. Laia is currently working on this project to decipher the different molecular mechanisms by which Ankle2 regulate NER and mitosis.

3.2 Introduction

In a previous study, we show that the depletion of Tws didn't lead to a complete failure in the reassembly of NE proteins at NER, suggesting that other phosphatases are also implicated in the regulation of NER [242]. Interestingly, a study in *C. elegans* showed that the protein LEM4 might be required for proper NER [202]. Ankle2 (LEM4 in human cells) is a member of the LEM domain protein family as it contains a LEM domain in its N-terminal region [202]. However, LEM4 lacks an N-terminal LEM domain in *C. elegans* (**Fig. 3.1**). Worm embryos with LEM4 mutations show irregularly shaped nuclei with an abnormal organization of Lamin and nucleoporins, and these phenotypes were rescued upon LEM4 overexpression [202]. Similar phenotypes were also observed when Ankle2 (LEM4) in HeLa cells was depleted by RNAi [202] or knocked-out by CRISPR/Cas9 [204], suggesting that the role LEM4 is conserved through evolution. Also, an RNAi screen using fly S2 cells, shows that the depletion of Ankle2 decreased the cell mitotic index, cell count, and nuclear size [243]. Intriguingly, depletion of LEM4 in worm embryos expressing GFP-BAF strongly abolished BAF recruitment to reassembling nuclei [202]. A similar phenotype was also observed in human cells when Ankle2 was either knocked down by RNAi [202] or knocked out by CRISPR/Cas9 [204]. These results suggest that Ankle2/LEM4 is required for proper NER by its role in BAF recruitment on reassembling nuclei at mitotic exit. This requirement seems to be independent of the Ankle2 LEM domain, as the overexpression of an Ankle2 fragment lacking a LEM domain rescued BAF recruitment to

reassembling nuclei in cells with Ankle2 knockout [204]. In addition, Ankle2 forms a complex with both the catalytic and scaffolding subunits of PP2A [202, 204]. These subunits could not interact with an Ankle2 lacking the first 241 amino acid and another lacking the last 110 amino acids. Interestingly, these two Ankle2 fragments were not able to rescue BAF recruitment to reassembling nuclei during NER [204]. These results indicate that PP2A binding to Ankle2 is crucial for BAF recruitment on reforming nuclei at mitotic exit. In addition, in human cells, LEM4 interacts with and inhibit VRK1 from phosphorylating BAF in *vitro* [202]. These results and others in these studies propose a model where, at mitotic exit, LEM4 interacts with VRK1 and PP2A. This interaction inhibits VRK1 and activates PP2A to dephosphorylate BAF and induce its interaction with LEM domain proteins found on the INM during NER [202, 204, 244]. However, is Ankle2 a PP2A regulatory subunit and what is the role of Ankle2 in BAF dephosphorylation during NER are questions that need to be answered.

Ankle2 localization is still under investigation. One of the few studies investigating Ankle2 localization shows that Ankle2 is found mostly cytoplasmic and weakly localizes to the NE in interphase U2OS cells [245]. Another study using fly larvae brain cells shows that Ankle2 colocalizes with ER proteins [244]. However, the localization of Ankle2 during cell division is not yet explored. Also, the function of Ankle2 at the ER is still unknown.

At the developmental level, Ankle2 seems to have a function in brain development both in humans and flies. A large mutant screen identified an Ankle2 mutation that resulted in fly adults with abnormal development of sensory organs and loss of thoracic bristles [246]. Also, larvae with this mutation had smaller brains, mainly because cell proliferation in these brains was strongly affected [246]. These observations are in accordance with data that shows a decrease in cell counts and the mitotic index seen in fly cells depleted

from Ankle2 [243]. Interestingly, the role of Ankle2 in brain development is also conserved in humans, as the genome of a family with microcephaly contained a deleted variant of *Ankle2* [246]. Also, *Ankle2* expression was downregulated in brain tissues from patients with Parkinson [247]. Hence, it seems that studying more about the role of this protein is of great interest not only for fundamental cell biology but also for clinical research.

In this study, we used *Drosophila* embryos and cells in culture to investigate the role of Ankle2 during cell division. We found that Ankle2 is in complex with PP2A and have preliminary data that shows that PP2A-Ankle2 can dephosphorylate two phospho-peptides *in vitro.* Ankle2 depletion leads to a failure of BAF recruitment to newly formed nuclei in cells, and an arrest in metaphase of the first mitotic division in fly eggs. Our results suggest a role for PP2A-Ankle2 in regulating NER and proper mitotic progression.

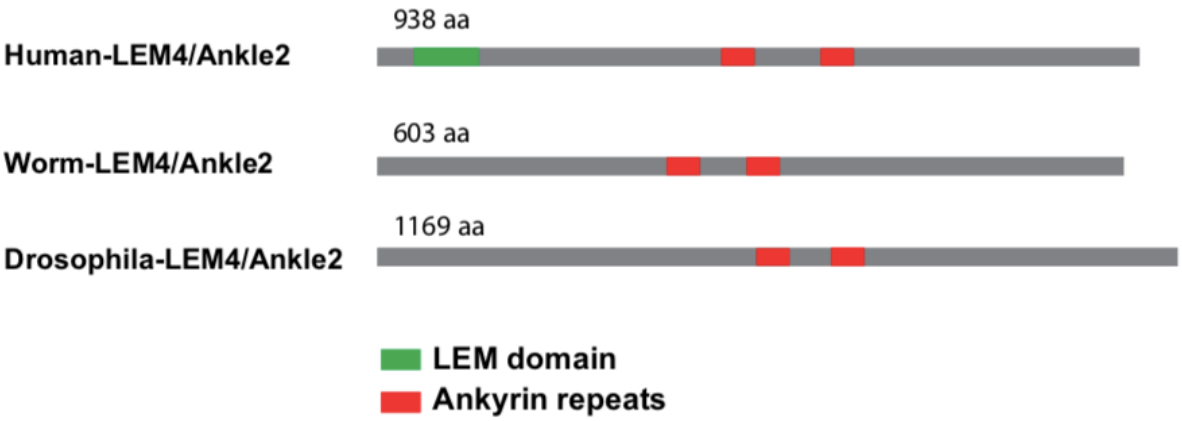

Figure 3.1 Schematic representation of the protein structure of LEM4/Ankle2 in Human, worm and *Drosophila*. The alignment was based on [202]. The length of the *Drosophila*-Lem4/Ankle2 was taken from [248].

3.3 Results

3.3.A. *Drosophila* Ankle2 promotes NER by regulating BAF and Lamin B recruitment to reassembling nuclei

Mutations in *Lem4* in *C. elegans* lead to the formation of improperly shaped nuclei. However, whether Ankle2 promote NER was not tested. First, we wanted to test if *Ankle2* genetically interacts with genes coding for NE proteins. To do so, I crossed female flies heterozygous for an *Ankle2* mutation (*Ankle2*^{A}) with male flies heterozygous for two *lamin* mutations (*lam*^{K2} and *lam*^{A25}). Double mutant female flies were kept to lay eggs, and the percentage of hatched eggs was determined. Wild type flies and single female mutants were used as negative controls. I found that the percentage of hatching eggs from *Ankle2A*/+; *lam*^{K2}/+ and *Ankle2A*/+; *lam*^{A25}/+ females was lower when compared with hatching percentages of eggs from single mutants (*Ankle2*^{A}/+, *lam*^{K2}/+, and *lam*^{A25}/+) females and wild type females (**Fig. 3.2**). These data show that *Ankle2* genetically interacts with *lam* and suggest that Ankle2 collaborates with Lamin, presumably in promoting the integrity of the NE.

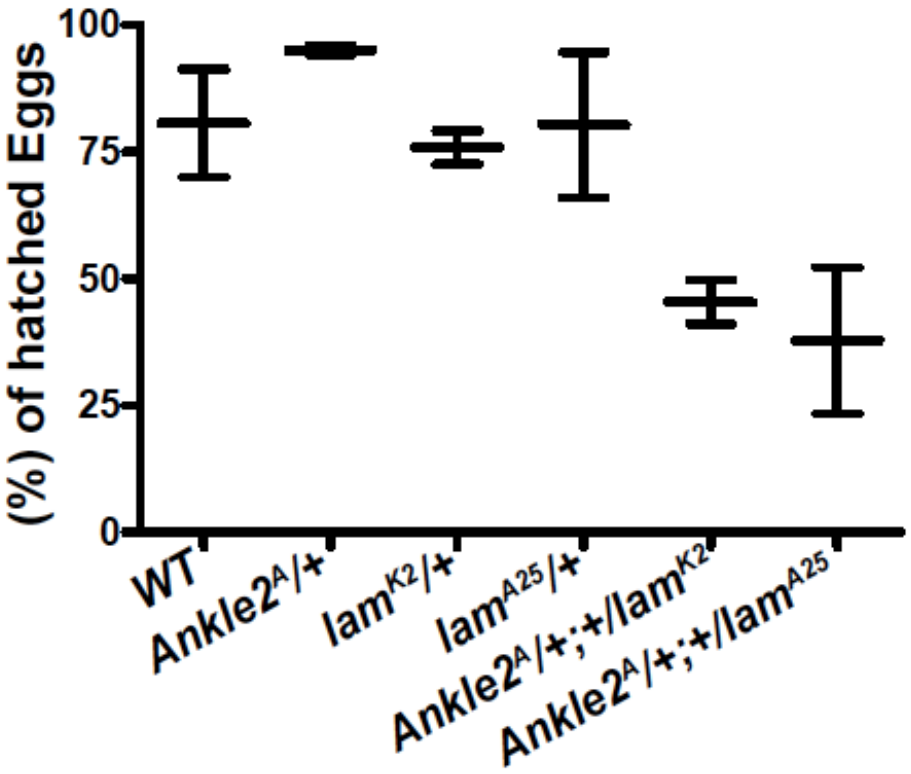

Figure 3.2 Genetic interaction between an allele of *Ankle2* and different alleles of *lamin.* The percentage of hatched eggs from females with the indicated genotypes was determined from two experiments. Error bars: range. This experiment was performed by Laia Jordana and me.

Ankle2 knockdown by RNAi and knockout by CRISPR/Cas9 in HeLa cells abolished the recruitment of BAF on reassembling nuclei at mitotic exit [204]. To test if this is the case for fly Ankle2, I generated Ankle2 dsRNA to deplete Ankle2 in cells stably expressing GFP-BAF and mcherry-α-Tubulin. In cells transfected with KAN dsRNA (control), GFP-BAF is soluble in the cytoplasm after NEBD. After spindle elongation at anaphase onset (T=0), GFP-BAF recruits to chromatin after 3.6 min and concentrates more on chromatin after 4.8 min, and then to the NE at a later time (**Fig. 3.3.A**). In contrast, in cells transfected with dsRNA Ankle2, GFP-BAF fails to recruit to reassembling nuclei after spindle elongation but instead forms aggregates in the cell cytoplasm (**Fig. 3.3.A**).

Following quantification, the intensity of GFP-BAF at reassembling nuclei in Ankle2 depleted cells is very low after spindle elongation (**Fig. 3.3.B).** These results indicate that Ankle2 promotes the recruitment of BAF to reassembling nuclei at mitotic exit.

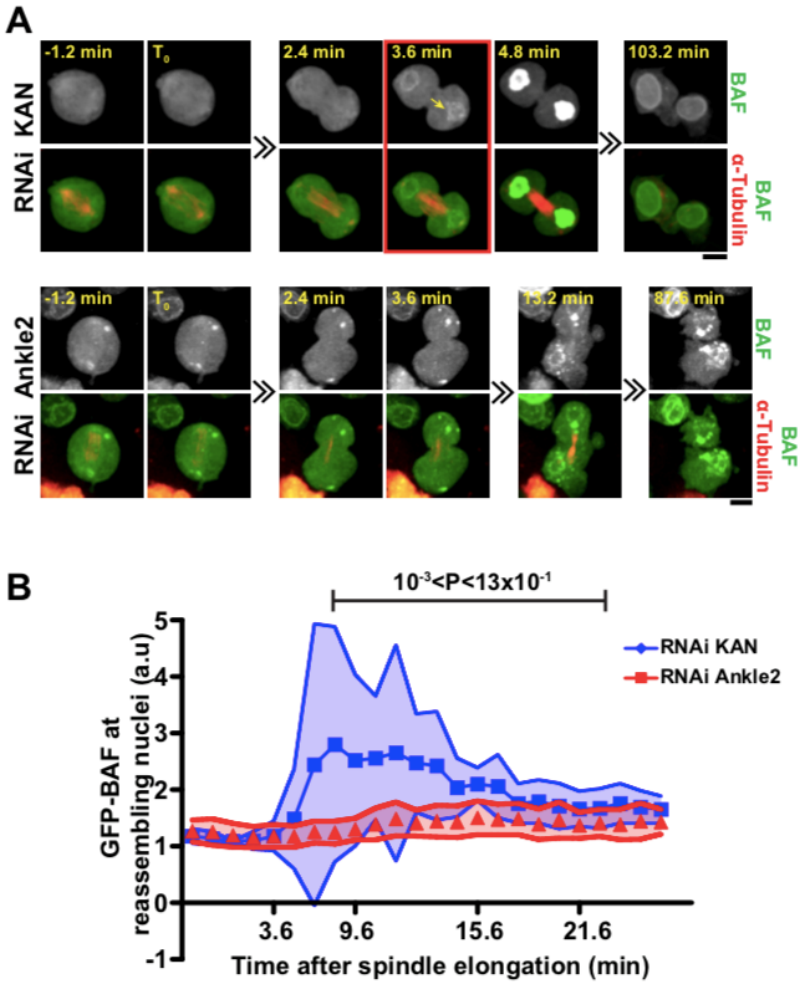

Figure 3.3 Ankle2 depletion leads to an abolishment in GFP-BAF recruitment to reassembling nuclei at mitotic exit. A. Live-imaging of cells stably expressing GFP-BAF and mcherry-α-Tubulin transfected with either dsRNA against Ankle2 or dsRNA against the bacterial resistant gene KAN (control). Time=0 was taken as the time where spindle elongation takes place. An image was taken each 1.2 min. The red square is the time where BAF is recruited after spindle elongation. The yellow arrow shows the recruitment of GFP-BAF. Scale bar is 5 μm. **B.** Quantification of the fluorescence intensity of GFP-BAF at reassembling nuclei at each time point. For RNAi Kan and RNAi Ankle2,

15 and 20 cells were quantified, respectively. The shaded area indicates the standard deviation. P values are from a two-tailed *t*-test.

To test whether the abolishment of BAF at reassembling nuclei after Ankle2 depletion affects the recruitment of other NE proteins to nuclei, I depleted Ankle2 in cells expressing GFP-BAF and RFP-Lamin B. As expected, the depletion of Ankle2 leads to an abolishment in GFP-BAF recruitment to newly formed nuclei (**Fig 3.4**). Interestingly, the recruitment RFP-Lamin B appeared to be delayed by several minutes upon Ankle2 depletion in the dividing cells examined (**Fig. 3.4**). However, the quantification of this phenotype is still lacking. Laia Jordana in our laboratory will repeat these experiments and quantified the fluorescence. These results suggest that Ankle2 is also required for the timely reassembly of other NE proteins during NER.

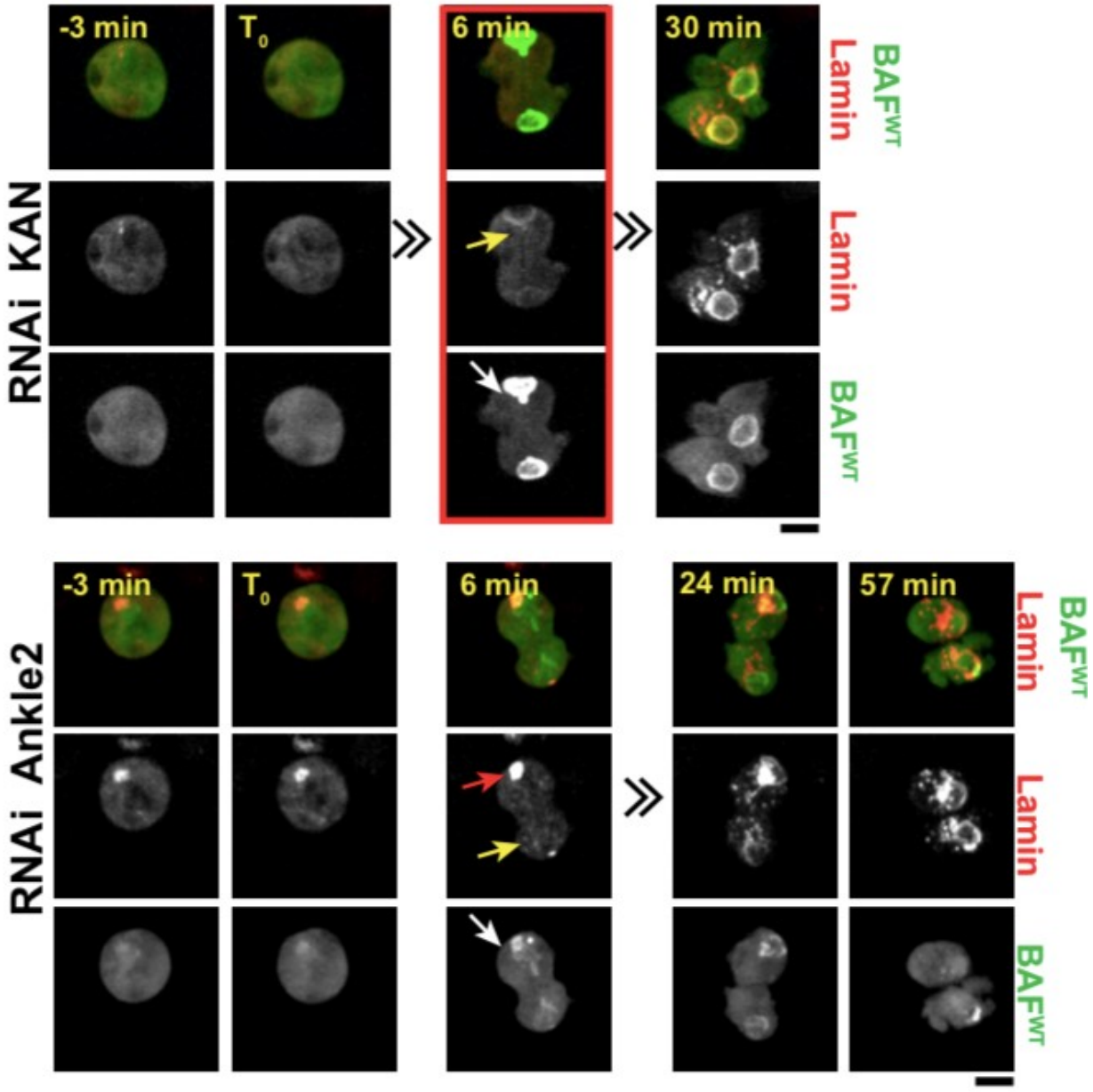

Figure 3.4 Ankle2 depletion leads to delay in RFP-Lamin B to newly formed nuclei recruitment at mitotic exit. Live imaging of cells stably expressing GFP-BAF and RFP-Lamin B transfected with either dsRNA Ankle2 or dsRNA KAN (control). Time=0 was taken as the time where spindle elongation takes place. An image was taken each 3 min. The red square is the time where BAF and Lamin B are recruited after spindle elongation. The yellow arrow shows GFP-BAF localization and the white arrow shows RFP-Lamin localization. The red arrow shows an aggregate of Lamin B. Scale bar is 5 μm.

3.3.B. Ankle2 is required for the maintenance of nuclear integrity

A screen was recently performed to identify proteins which, when depleted, cause micronucleation. In this study, HeLa cells were first depleted from more than 1295 proteins that are known to be important during mitosis and then treated with nocodazole (inhibitor of microtubule polymerization) and reversine (inhibitor of the spindle assembly checkpoint). This drug combination will enable cells with defective spindles to exit mitosis. Following treatment and time-lapse microscopy, the depletion of BAF gave the highest percentage of cells with micronuclei [161]. However, the effect of Ankle2 depletion on the formation of micronucleated cells was not tested in that study. To test this, cells expressing GFP-Lamin B and mcherry-α-tubulin were depleted from Ankle2 and treated with nocodazole and reversine. When analyzed by live imaging, I observed that cells depleted from Ankle2 and treated with both inhibitors contained more micronuclei than control cells (**Fig. 3.5.A-B**). Laia repeated that experiment and Dmel cells were fixed and immunostained for Lamin B and a DNA marker (DAPI). Surprisingly, cells transfected with dsRNA Ankle2, even without drug treatment, showed about 25% increase in the percentage of micronuclei when compared with the control cells (RNAi Kan, data not shown). Most of the micronuclei observed in cells depleted from Ankle2 lacked a lamin staining. These were excluded from the previous experiment as the DNA in cells was not marked. These results indicate that Ankle2 is required for maintaining nuclear integrity, probably by regulating BAF recruitment at newly formed nuclei during NER.

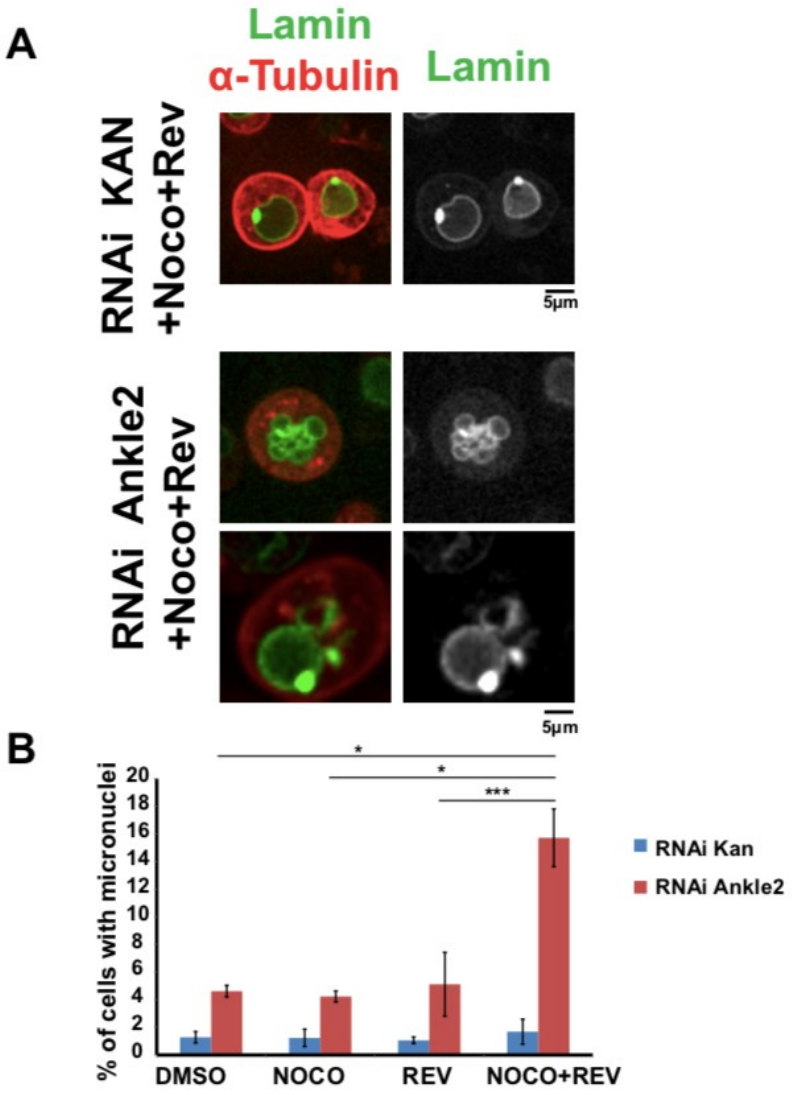

Figure 3.5 Ankle2 is required for nuclear integrity. A. Cells stably expressing GFP-Lamin B and mcherry-α-Tubulin transfected with either dsRNA against Ankle2 or dsRNA against the bacterial resistant gene KAN (control) and treated with nocodazole and reversine. Cells depleted from Ankle2 and treated with both inhibitors form micronuclei. Scale bar is 5 μm. **B.** Quantification of cells with micronuclei transfected with either dsRNA Ankle2 or dsRNA KAN and treated with different inhibitors as shown. The experiment was done three times, and, in each experiment, more than 500 cells were quantified per condition. Error bars represent standard deviation. *0.0051<P<0.0095, ***P<0.0001 from a two-tailed *t*-test

3.3.C. Ankle2 promotes the progression of mitosis during early embryo development

I then wanted to investigate the role on Ankle2 *in vivo* during syncytial embryo development. In a fruit fly ovary, and following egg ovulation, the egg arrests in the metaphase I of the first meiotic division. After the female lays the egg, meiosis continues within twenty minutes till the formation of four meiotic products near the egg cortex [22]. When the egg is fertilized, the male pronucleus and one of the fourth female meiotic products come in close proximity without fusing [22]. Then, NEBD takes place, and the genetic content of both pronuclei divide separately during the first mitosis. After that, thirteen cycles of quick nuclear divisions, which lasts for two hours, take place in a syncytium [22]. The three other female meiotic products combine to form a polar body. Most of the RNAs and proteins required for these rapid divisions are contributed by the mother fly.

Before looking at the phenotypes resulting from Ankle2 depletion in fly embryos, I wanted to test whether Ankle2 depletion affects embryo survival. For this, I crossed male flies with a *UAS-dsRNA Ankle2* with female flies expressing Gal4 under the effect of a maternal α promoter (mat- α-Gal4), which expresses the transgene in the germline. As a negative control, female flies with the mat-α-Gal4 driver were crossed with Oregon R (wild type). Eggs laid by females from the F1 generation were counted, and the percentage of hatched eggs was determined. Interestingly, none of the eggs depleted from Ankle2 hatched (**Fig. 3.6.A**), indicating that Ankle2 is indispensable for embryo survival. Ankle2 depletion was confirmed by immunoblotting (**Fig. 3.6.B**).

I next wanted to identify the phenotypes that could explain this strong embryonic lethality. For this, females from the F1 generation of the above crosses were kept to lay eggs for 2 hours (enough time to monitor the whole thirteen nuclear division stage) and fixed with formaldehyde, allowing examination of mitosis nuclei near the cortex, using immunofluorescence. However, no structures were detected, suggesting that defects occurred earlier in development, when structures are deeper in the egg or embryo. To investigate this hypothesis, I kept females from the F1 generation to lay eggs for 1-2 hours, fixed then with methanol, which allows deeper immunofluorescence observation, and looked at the phenotypes. Most of the Ankle2 depleted eggs that I observed successfully completed meiosis, as indicated by the presence of a polar body near the egg cortex (**Fig. 3.6.C**). Some eggs also showed normal meiotic divisions, indicating that Ankle2 is not essential for the completion of meiosis (data not shown). Intriguingly, the vast majority of these eggs were blocked in metaphase of the first or second mitosis, compared to controls that progressed normally with successive mitoses (**Fig. 3.6.D**). These results suggest that Ankle2 is essential for normal mitotic progression during early embryo development.

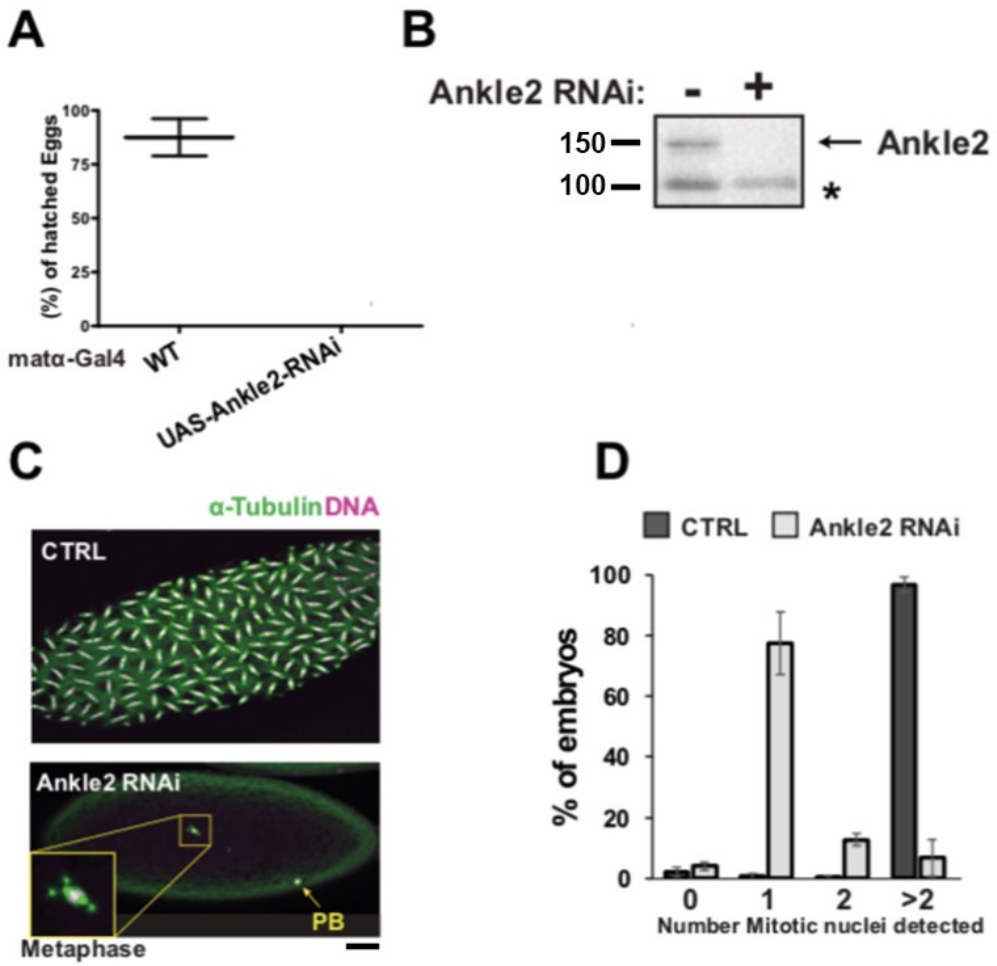

Figure 3.6 Ankle2 is essential for proper mitotic progression in fly embryos. A. The percentage of hatched eggs depleted from Ankle2 was determined and compared with the control (eggs from females only expressing the Gal4 driver). The quantification is an average of two experiments. Error bars: range **B.** Confirmation of Ankle2 depletion by immunoblotting. Eggs were crushed, and proteins were extracted and loaded on a protein gel. The membrane was blotted with anti-Ankle2 antibody. (*) is a non-specific band and used as a loading control. **C.** Eggs depleted form Ankle2 aging between 1-2 hours are arrested at the first metaphase of the first mitotic division. PB: Polar body. Normal embryo development was seen in the CTRL (eggs from females only expressing the Gal4 driver). Scale bar is 20 μm **D.** Quantification of embryos with 0,1,2 or more than 2 mitotic nuclei. This experiment was done three times**.** Error bars represent standard deviation. All experiments of this figure were done by Laia Jordana and me.

3.3.D. Ankle2 localizes to the ER during interphase and concentrates on the NE during NEBD

I next wanted to investigate the localization of Ankle2 during mitosis, as this was never explored before [245]. To do so, I generated fly cells stably expressing GFP-Ankle2 and mcherry-α-tubulin. As seen in [245], GFP-Ankle2 localizes mostly in the cytoplasm and weakly to the NE in interphase cells (**Fig. 3.7.A**). In cells I have analyzed, GFP-Ankle2 formed cytoplasmic foci in interphase cells, which suggests that GFP-Ankle2 associates with structures in the cytoplasm (**Fig. 3.7.A**). However, surprisingly, the GFP-Ankle2 signal concentrates at the NE during NEBD, and then became cytoplasmic and partially nuclear at mitotic exit (**Fig. 3.7.A**). The concentration of GFP-Ankle2 to the NE during prometaphase was not expected, especially after I have seen that Ankle2 is critical for proper GFP-BAF recruitment to newly formed nuclei at mitotic exit. Since no previous study visualized N-terminal tagged Ankle2 localization, I reasoned that the N-terminal GFP tag might affect the proper Ankle2 localization. For this reason, I looked at cells stably expressing Ankle2-GFP and mcherry-α-tubulin. Ankle2-GFP showed a similar localization dynamics as GFP-Ankle2 (**Fig. 3.7.B**). These results show that Ankle2 localizes to the NE during NEBD, but the function of Ankle2 during NEBD has not been explored yet.

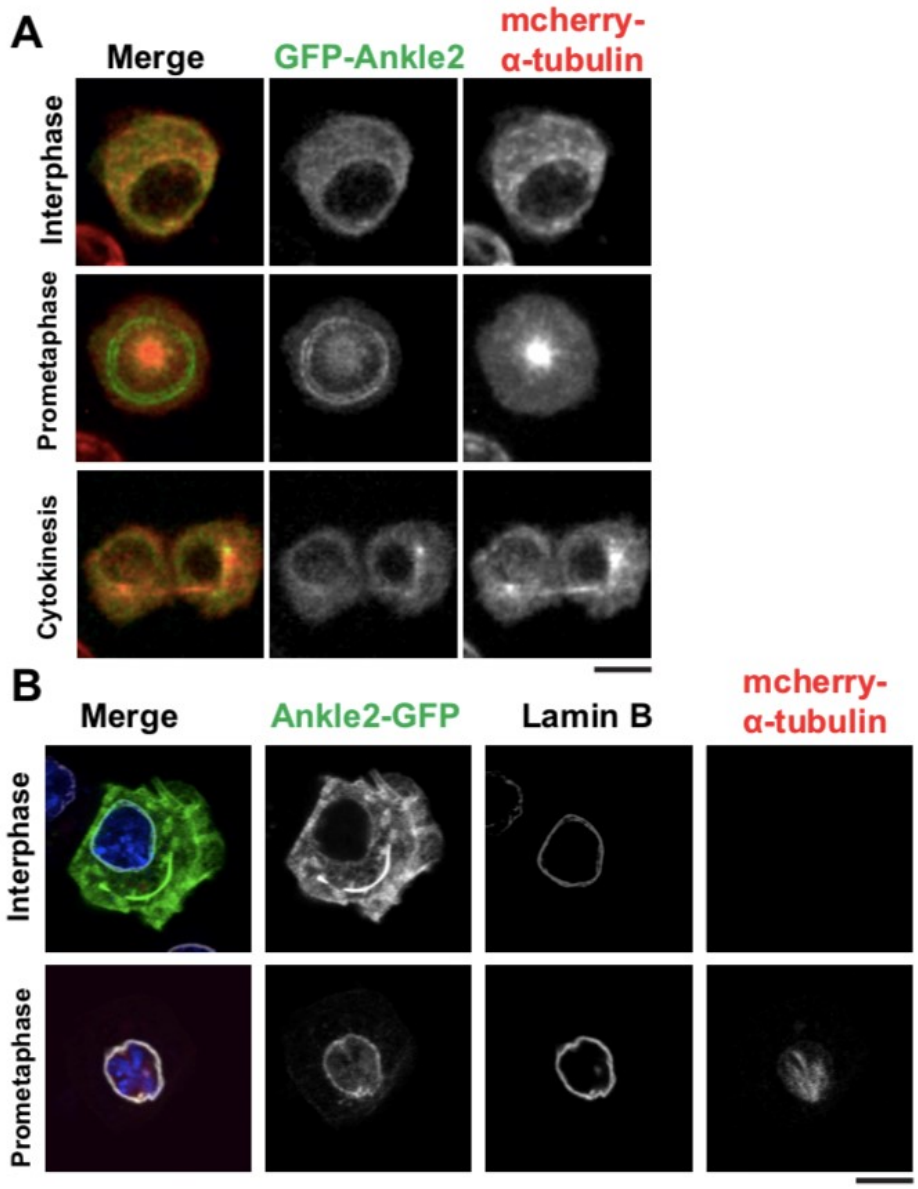

Figure 3.7 Ankle2 localizes cytoplasmic structures during interphase cells and concentrates on the nuclear envelope during NEBD. A. Live-imaging of cells expressing GFP-Ankle2 and mcherry-α-Tubulin**.** In interphase cells, GFP-Ankle2 localizes to cytoplasmic structures and is weakly nuclear. In prometaphase cells, GFP-Ankle2 concentrates on the nuclear envelope during NEBD. In a cytokinetic cell, GFP-Ankle2 is present in the cytoplasm and weekly to the nuclear envelope. **B.** Cells expressing Ankle2-GFP and mcherry-α-Tubulin were fixed and stained with Lamin B and DNA. Similar localizations as cells expressing GFP-Ankle2 were also noticed. Scale bar is 5 μm. The experiment in **A** was done by me, and of the experiment in **B** was done by Laia Jordana

As seen in interphase cells, both GFP tagged versions of Ankle2 localize to cytoplasmic structures. In a study using HeLa cells, both endogenous and GFP-tagged LEM4 localized to the ER [202]. I wanted to test whether this also applies to *Drosophila* Ankle2. To do so, cells stably expressing Ankle2-GFP were fixed and stained for a known ER protein called calnexin. Interestingly, a clear colocalization signal was seen between both GFP-tagged Ankle2 and this ER protein (**Fig. 3.8.A**). Interestingly, a recent study showed a clear colocalization between Ankle2 and ER proteins in fly brain cells and a localization of Ankle2 to the NE during NEBD [244]. To investigate this possibility in fly cells, I purified Ankle2 from cells stably expressing GFP-tagged Ankle2 and submitted the purification products for mass spectrometry analysis at IRIC's proteomics platform. Flag-GFP cells were used as a negative control. A fraction of the purified product was migrated on a gel, and the gel was then silver stained (**Fig. 3.8.B**). Interestingly, I found several ER proteins such as Vap33, Sec16β, Tango5, and GammaCOP, that co-purified with both GFP-tagged Ankle2, but not with Flag-GFP (**Fig. 3.8.A**). Laia Jordana repeated the same experiment, but this time by purifying both GFP-tagged Ankle2 forms. The same Ankle2 protein interactors were identified using mass spectrometry. Taken together, these results indicate that Ankle2 associates with the ER, however the mechanism by which Ankle2 binds ER proteins and its role at that cellular component need to be investigated.

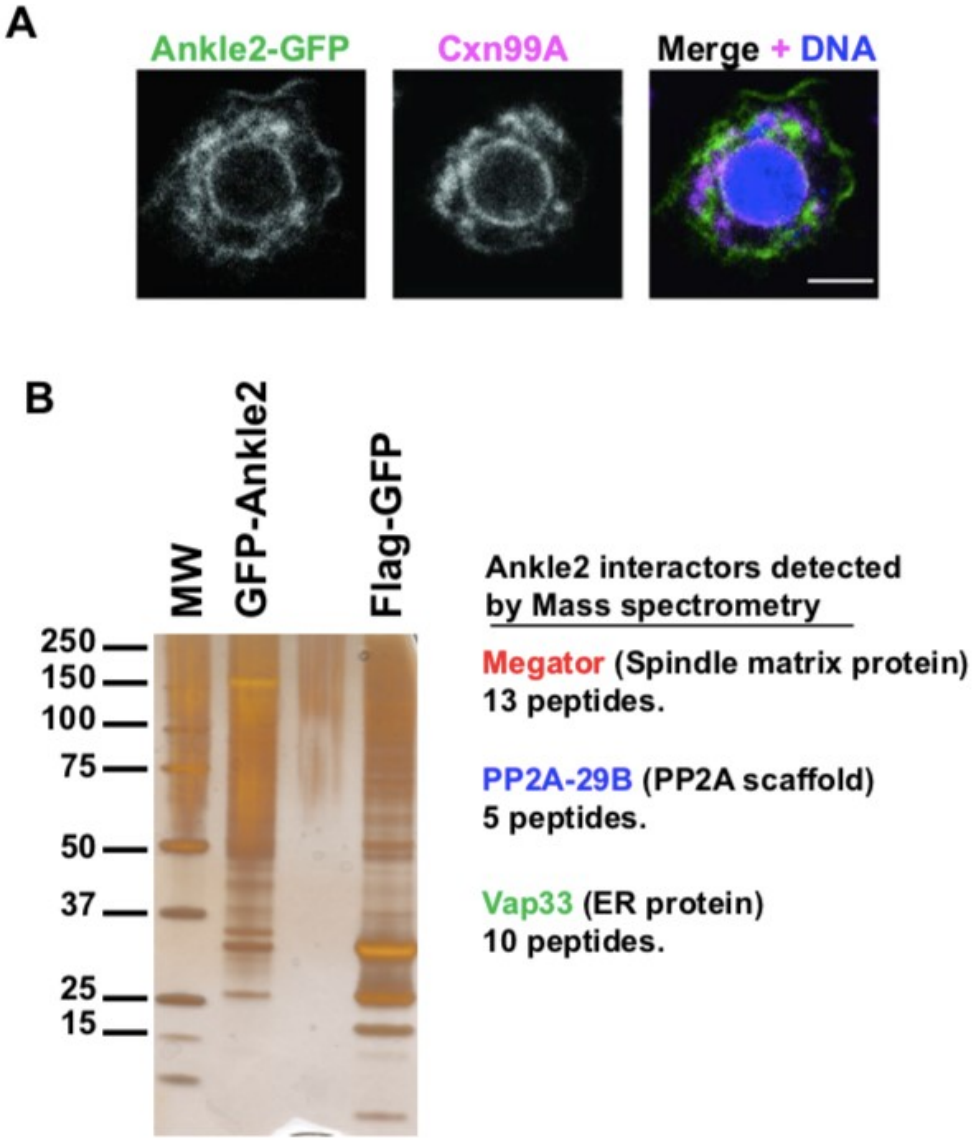

Figure 3.8 Ankle2 protein partners identified using mass spectrometry. A. Cells expressing Ankle2-GFP were fixed and stained for the ER protein Cx99A and DNA. A clear colocalization of the two proteins can be noticed. Scale bar is 5 μm. This experiment was done by Laia Jordana. **B.** GFP-Ankle2 was purified using GFP Chromotek beads from fly cells stably expressing this tagged protein. A small fraction of the purified products was loaded on a gel and silver stained. The remaining fraction analyzed by mass spectrometry. Some Ankle2 binding partners are listed along with their identified peptide count. Cells expressing Flag-GFP were used as negative control.

3.3.E. Ankle2 may function as a PP2A regulatory subunit

Previous studies showed that Ankle2 associates with the PP2A complex in human cells [202, 204]. I asked whether fly Ankle2 is also found in a common complex with PP2A. When I went back to our mass spectrometry results of purified Ankle2, I found that both the PP2A catalytic and the scaffolding subunits co-purified with both GFP-tagged Ankle2, suggesting that these proteins are found in a common complex (**Fig. 3.8.B**). However, no peptides of Tws were identified with both tagged forms of Ankle2. To confirm the purification results, I purified both GFP-tagged Ankle2 from stable cell lines expressing these tagged proteins and blotted the purification products using anti-Mts and ant-Tws antibodies. Flag-GFP and GFP-Tws were also purified from cells and used as negative and positive controls, respectively. Interestingly, Mts but not Tws was co-purified with GFP-tagged forms of Ankle2 (**Fig. 3.9.A**). The fact that Ankle2 copurified with both the catalytic and scaffolding subunits of PP2A, without detection of a known PP2A regulatory subunit, is consistent with the idea that Ankle2 may function as a PP2A regulatory subunit.

If Ankle2 is a PP2A regulatory subunit, it should work in a common pathway with Mts, and genes expressing these proteins should interact with each other. To test this possibility, I crossed female flies heterozygous for an *Ankle2* mutation (*Ankle2*^{A}) with males flies heterozygous for an *mts* (*mts*$^{XE-2258}$) or two *tws* mutations (*tws*^{P} and *tws*^{aar1}). Double mutant female flies from the F1 generation were kept to lay eggs, and the percentage of hatched eggs was determined. Wild type flies and single female mutant flies from the F1 were used as negative controls. After egg counting, I found that the percentage of eggs from *Ankle2*^{A}/+; *mts*$^{XE-2258}$/+ females was low (about 20%) when compared with the hatching percentage of eggs from single mutants (*Ankle2*^{A}/+ and *mts*$^{XE-2258}$/+) females and wild type females (**Fig. 3.9.B)**. Surprisingly, the hatching egg

percentage from *Ankle2A*/+; *tws*^{P}/+ and *Ankle2A*/+; *tws*^{aar1}/+ females was high compared with the percentage of hatched eggs from single mutants (*Ankle2A*/+, *tws*^{P}/+, and *tws*^{aar1}/+) females and wild type females (**Fig. 3.9.B**). These results indicate that *Ankle2* genetically interacts with *mts* but not with *tws*. These results suggest that Ankle2 collaborates with PP2A and are consistent with the idea that Ankle2 may function as a PP2A regulatory subunit.

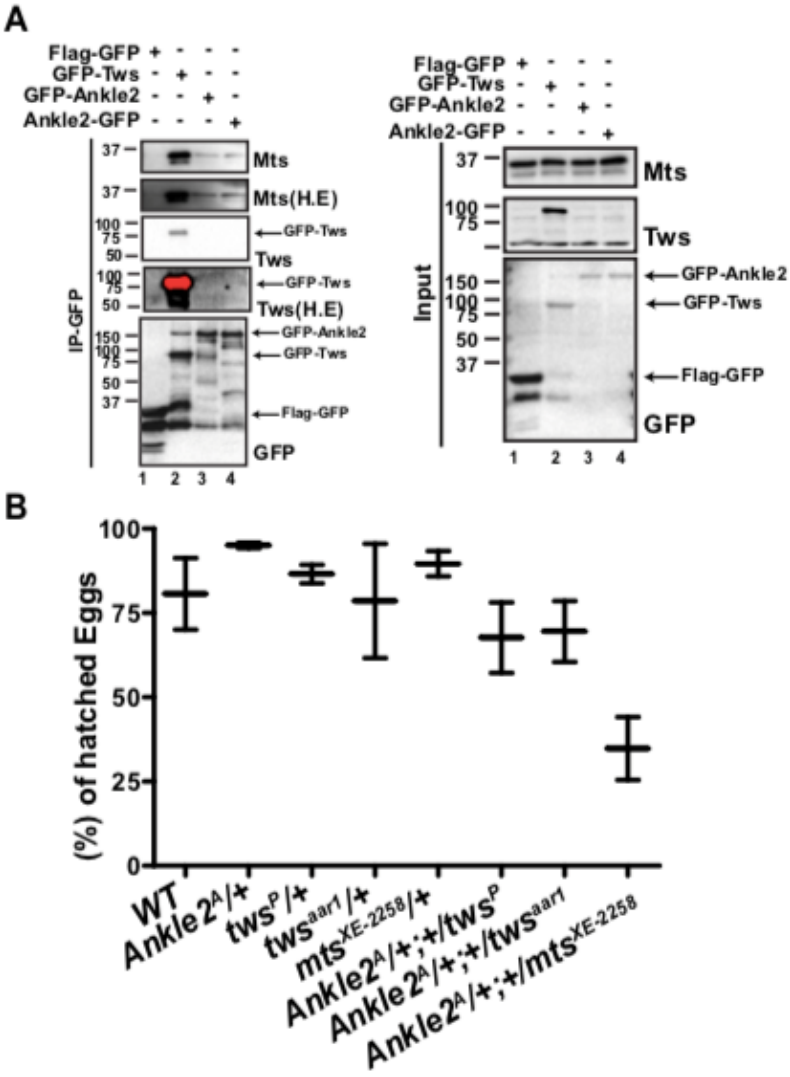

Figure 3.9 Ankle2 is a potential regulatory subunit of PP2A A. GFP-Ankle2 and Ankle2-GFP was purified and blotted for Mts and Tws. Purifications from cells expressing Flag-GFP and Tws-GFP were used as controls. As observed in the figure, Mts was co-

purified with Tws, and both GFP-tagged Ankle2 versions. This experiment was done three times. Red spots on the blot represent saturated signals. **B.** Genetic interaction between and *Ankle2* allele and an *mts* allele, but not with *tws* alleles. The percentage of hatched eggs from females with the indicated genotypes was determined from two experiments. Error bars: range. These experiments were performed by Laia Jordana and me.

3.3.F. Ankle2 may not associate with BAF in fly cells

Ankle2 was found to be in complex with BAF in human cells, though the association between these two proteins is weaker than that between BAF and LEM2 [204]. Although no LEM domain is present in the *Drosophila* Ankle2(**Fig. 3.1**), I wanted to test if Ankle2 associates with BAF in fly cells. For this, I purified myc-BAF from cells transiently expressing myc-BAF and either Flag-GFP, GFP-Tws, GFP-Ankle2, and Ankle2-GFP. Cells only expressing GFP-tagged Flag, Tws, and Ankle2 were used as negative controls. I then blotted the purified products using an anti-GFP antibody. A small amount of GFP-tagged Ankle2 was co-purified with BAF, compared with the positive control (GFP-Tws, **Fig. 3.10**). No GFP signal was seen in all negative controls suggesting that the interactions I see are specific. Unfortunately, I couldn't reproduce these results after trying the same assay for two times. Therefore, there is a possibility of a possible interaction between Ankle2 and BAF, but of low affinity. However, the conditions which I am using to do the experiment do not allow me to conclude either way.

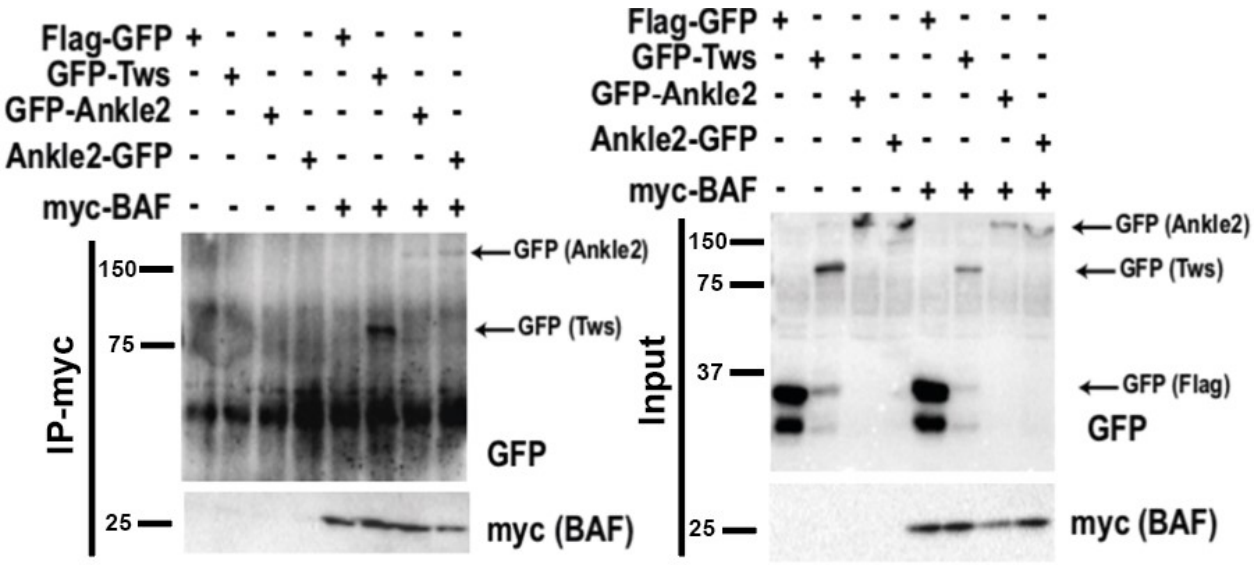

Figure 3.10 Ankle2 and BAF may not be found in a common complex. Fly cells were co-transfected with either GFP-Ankle2 or Ankle2-GFP and myc-BAF. Myc-BAF was purified used magnetic beads, and the purified products were blotted with anti-GFP antibody. Cells transfected with only Flag-GFP, GFP-Tws, both versions of GFP-tagged Ankle2, or co-transfected with either Flag-GFP or GFP-Tws and myc-BAF were used as controls. The results of this experiment were only seen once, hence a confirmation of these results is required using different conditions.

3.3.G. The Ankle2-PP2A complex possesses a phosphatase activity

Since I showed that Ankle2 is present in a common complex with PP2A, I hypothesized that this complex possesses a phosphatase activity. To test this hypothesis, Flag-tagged forms of Ankle2 were purified from stable cell lines expressing these proteins. Flag-GFP and Flag-Tws were also purified from cells and used as negative and positive controls, respectively. I then incubated the purified products with the following phospho-peptides derived from human proteins: PRC1-pT48, BAF-pS5, and Knl1-pT875. The sites

in the former two peptides are known to be dephosphorylated by PP2A-B55 [242], while that that on the protein Knl1, a kinetochore binding partner of SAC proteins, is known to be dephosphorylated by PP2A-B56 in HeLa cells [249]. After two hours of incubation, I noticed that PP2A-Tws was able to dephosphorylate all three peptides (**Fig. 3.11.A**). Interestingly, Flag-tagged forms of Ankle2 were able to dephosphorylate Knl1-pT875, partially PRC1-pT48, but not BAF-pS5. However, while Mts was detected in the Flag-Tws purification product, it was not detectable in the Flag-Ankle2 or Ankle2-Flag purification products (**Fig. 3.11.B**). This could explain why Ankle2-associated phosphatase activity was much lower than that of Tws in this experiment (**Fig. 3.11.A**). These preliminary results suggest that PP2A-Ankle2 has phosphatase activity.

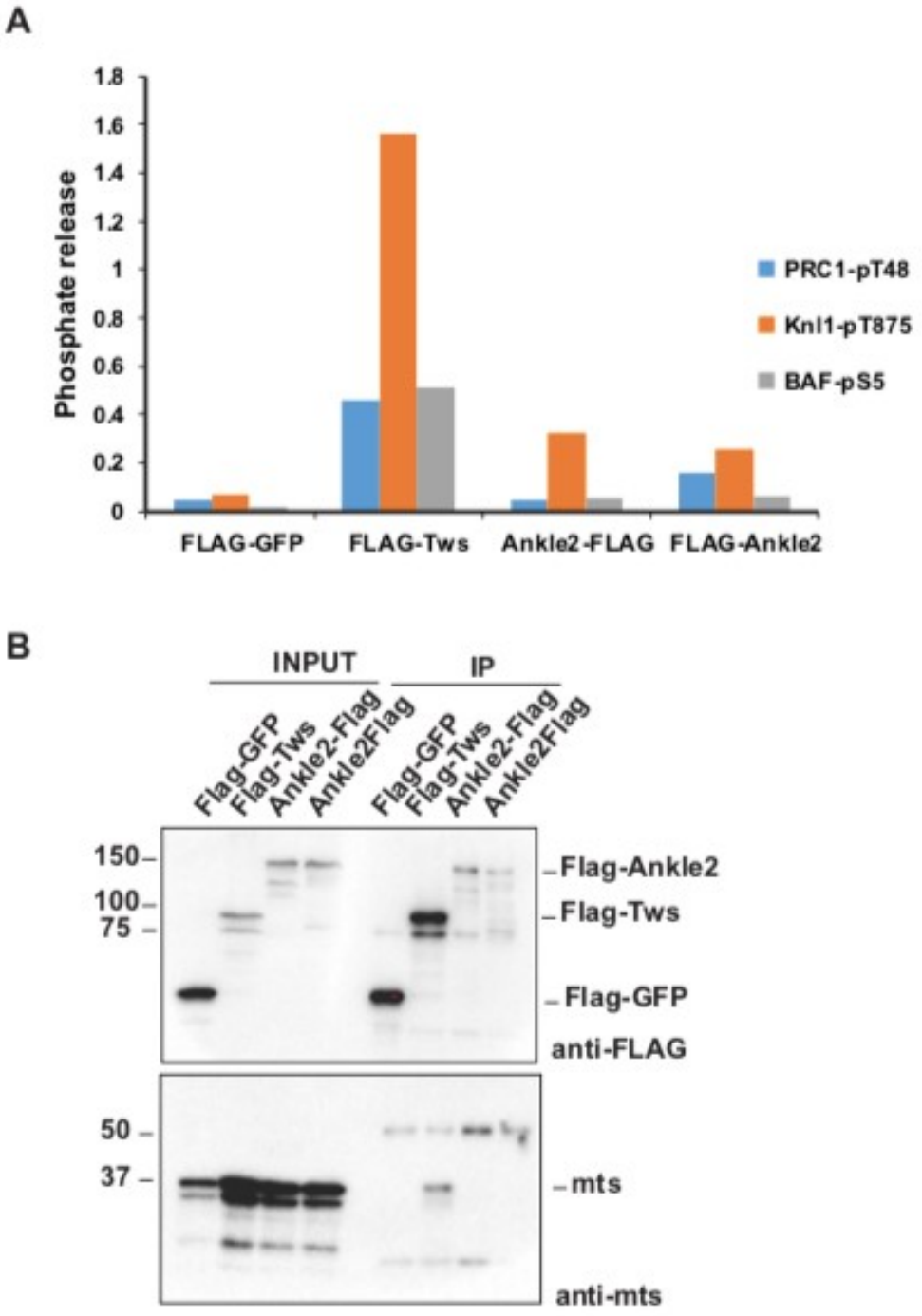

Figure 3.11 PP2A-Ankle2 possesses a phosphatase activity. A. The amount of phosphate released when three phosphopeptides were incubated with Flag-GFP, Flag-Tws, Ankle2-Flag, or Flag-Ankle2 purified from fly cells. **B.** Protein samples from the purified products and the input were loaded on gels and membranes were blotted with

either anti-Flag or anti-Mts antibodies. This experiment was done by me and by Laia Jordana.

3.4 Discussion

The role of different phosphatases in the process of NER and in mitotic exit is incompletely understood. Our recent study using *Drosophila* shows that PP2A-B55 plays a crucial role during NER. The depletion of Tws (B55 in flies) leads to a delay in the recruitment of several vital NE proteins. However, other phosphatases seem important in promoting NER, since a complete failure of NER was not observed following Tws depletion. Several studies show that the protein LEM4/Ankle2 contributes to the process of NER. Nevertheless, little is known about the nature of this protein and the mechanisms by which Ankle2 regulates NER. Here, I show that Ankle2 is a potential PP2A regulatory subunit that is also essential in recruiting different NE proteins such as BAF and Lamin B. The recruitment of other NE proteins to reassembled nuclei might also depend on Ankle2 function. I also show that PP2A-Ankle2 is necessary both for NER in D-Mel cells and proper mitotic progression in embryos.

For its contribution to NER, I have preliminary data showing that *Ankle2* genetically interacts with *lamin*. It seems that removing half of Ankle2 and Lamin B is deleterious for fly development. This was expected since we know that PP2A-Ankle2 promotes BAF recruitment to reassembling nuclei and we show that the dephosphorylation of BAF is important for Lamin B recruitment [242]. It would be interesting to examine the different phenotypes in embryos from females heterozygous for *Ankle2* and *lamin* mutations.

The contribution of Ankle2 in NER was observed when Ankle2 is depleted in cells expressing GFP-BAF and RFP-Lamin B. As seen in human cells [204], the recruitment of

GFP-BAF was abolished, and that of RFP-Lamin was delayed during NER [204]. Since we have shown that BAF associates with Lamin B [242], I expected that the abolishment of BAF recruitment would also lead to a Lamin B recruitment failure during NER upon Ankle2 depletion. My preliminary results show that Lamin B recruitment to reforming nuclei at NER is delayed but not abolished upon Ankle2 depletion (**Fig. 3.4**), though more cells should be quantified for confirmation. This result suggests that either Ankle2 is required for Lamin B recruitment, probably by regulating PP2A-B55 activity, or that Lamin B recruitment to reassembling nuclei does not depend solely on its binding to BAF but can also bind other NE proteins. It was already shown that lamins associate with proteins of the NPC [200, 201]. Therefore, Lamin B might associate with some Nups for its recruitment to newly formed nuclei. More experiments should be done to examine whether Ankle2 depletion affects the localization of Nups to the NE during NER.

Moreover, Ankle2 depletion in cells treated with some mitotic inhibitors leads to an increase in the percentage of cells with micronuclei. These results were also noticed in human cells, depleted from BAF [161]. In that study, the effect of these inhibitors on cells was tested. For instance, the treatment of HeLa cells with nocodazole increased the percentage of cells with depolymerized microtubules [161]. When I looked at fly cells, I did not observe a similar phenotype. However, I was not surprised by that observation as I knew that nocodazole is not efficient in depolymerizing microtubules in fly cells. However, and although I did not see such effect, it was evident that these inhibitors were functioning in these cells (**Fig. 3.5**) since I noticed an apparent increase in the percentage of cells with micronuclei only upon treatment with both inhibitors and Ankle2 depletion. Performing live imaging on these cells could confirm if there might by a small effect on microtubule depolymerization. In addition, marking DNA in Ankle2 depleted Dmel cells without inhibitor

treatment revealed more micronucleated structures seen in Ankle2 lacking a nuclear envelope. These structures were not visible and therefore could not be scored in the quantifications shown in **Figure 3.5**, as Laia Jordana noticed a 25% increase in micronuclei in Ankle2 depleted cells when she stained for DNA, compared to 4% only in **Figure 3.5**. Several reasons could explain the increase in micronuclei percentage upon Ankle2 depletion. The first reason is that, since BAF dephosphorylation was necessary for shaping a nucleus, BAF might not be dephosphorylated following Ankle2 depletion, which might lead to failure of BAF to shape a nucleus, and thus the nucleus becomes fragmented. It would be interesting to test whether cells expressing a phospho-mimetic BAF mutant, as used in [242], will show an increase in the percentage of cells with micronuclei. A depletion of endogenous BAF would also be required. Another explanation is that Ankle2 depletion doesn't impair NER but might induce apoptosis. It is known that apoptosis is often correlated with micronuclei formation [250]. Hence, it is important to test whether micronuclei formation upon Ankle2 depletion is linked to apoptosis by staining Ankle2 depleted cells with anti-caspase antibodies.

Next, I wanted to study the role of Ankle2 *in vivo* using the fly model. Ankle2 RNAi was expressed in the female germline using the UAS system. Since Ankle2 function is essential for promoting proper NER, I expected to see a failure or defects of nuclear divisions during syncytial embryo development when Ankle2 is absent. I was surprised to see that no nuclear divisions took place at that stage of development. When I looked at eggs depleted from Ankle2 during meiosis, I noticed that meiosis completed normally, but eggs were mostly blocked at the metaphase of the first mitotic division (**Fig. 3.6.C-D**). A similar phenotype was never seen either in human cells [204] or *C. elegans* [202] when Ankle2 was depleted, suggesting that Ankle2 plays a specific or particularly important role

in mitotic progression in fly embryos. In other studies, a similar mitotic arrest phenotype is either when genes expressing *Drosophila* proteins of the APC complex such as morula (APC2) or fizzy (Cdc20) are mutated [251, 252] or in the case of DNA damage [253]. In embryos from females with *fizzy* mutants (*CDC20* in flies), precursors of the dorsal peripheral nervous system were arrested at metaphase [251]. A similar arrest was also seen in nurse cells of flies with morula mutations [252]. My experiment indicates that Ankle2 might have a role in regulating APC activity. APC activation during different phases of the cell cycle is phosphorylation dependent. The APC activator, Cdc20, only binds and activates a phosphorylated APC complex at the end of mitosis [254]. In addition, Cdh1 bound-APC can ubiquitinate some substrates when the APC is phosphorylated and ubiquitinate other substrates when the APC is dephosphorylated [255]. Therefore, Ankle2 bound to PP2A might function in dephosphorylating some APC complex proteins for its activation. Many experiments are still needed to investigate that hypothesis.

The crucial scientific question that I am trying to answer in this study is whether Ankle2 is a potential PP2A regulatory subunit. The first requirement for Ankle2 to be a regulatory subunit is to be in complex with PP2A and not with other PP2A regulatory subunits. Many studies showed that Ankle2 is in complex with PP2A [202, 204]. However, whether other PP2A subunits were also present in that complex was not examined. Our Ankle2 purification confirmed that Ankle2 is in complex with both the catalytic and the scaffolding subunits of PP2A (**Fig. 3.8**). I did not detect Tws or any other PP2A regulatory subunit peptides in the purification samples. Also, I confirmed the Ankle2-PP2A association by western blotting, but no Tws was detected (**Fig. 3.9.A**). As we know that PP2A regulatory subunits are mutually exclusive in the PP2A holoenzymes [256], this result is consistent with the idea that Ankle2 function as PP2A regulatory subunit.

Moreover, a genetic interaction between *Ankle2* and *mts* (PP2A catalytic subunit in fruit flies) exists but is absent between *Ankle2* and *tws* (**Fig. 3.9.B**). These results suggest that PP2A and Ankle2 act together to promote a specific molecular mechanism where Tws is not involved. More experiments are needed to reproduce these results and to test whether no interaction exists between *Ankle2* and genes expressing other PP2A regulatory subunits.

The second requirement needed for Ankle2 to be a potential PP2A regulatory subunit is the ability of the PP2A-Ankle2 complex to dephosphorylate substrates. I found that when the PP2A-Ankle2 complex is purified, two phospho-peptides, phospho-PRC1 and a phospho-Knl1, which are known to be dephosphorylated by PP2A-B55, were also dephosphorylated This could indicate that PP2A-Ankle2 dephosphorylates these peptides, or that there is a small amount of PP2A-Tws purified with Ankle2 that is able to dephosphorylate these peptides. Depleting Tws by RNAi could be done to confirm that only PP2A-Ankle2 is responsible for dephosphorylating these peptides. Also, I noticed that PP2A-Ankle2 did not dephosphorylate a phospho-BAF peptide *in vitro*. This could be explained by the possibility PP2A-Ankle2 does not dephosphorylate BAF or that enough PP2A catalytic protein was not purified with Ankle2 to dephosphorylate the peptide. I think that with the results we have, both possibilities are plausible. For the first possibility, PP2A-Ankle2 might not directly dephosphorylate BAF. It is still unclear whether Ankle2 is found in complex with BAF (**Fig. 3.10**). However, this result was seen using cells in culture. If the interaction between Ankle2 and BAF is taking place during mitotic exit, then it might be difficult to see this interaction knowing that a small fraction of these cells is undergoing mitosis, and it is impossible to synchronize these cells efficiently. Therefore, to test whether that interaction between Ankle2 exists, this experiment should be done using fly

embryos during nuclear divisions. In this context, nuclei in embryos are in continuous divisions, and an interaction (if it exists) may be more clearly noticed. As another explanation, Ankle2 might not interact with BAF, due to the absence of a LEM domain in the N-terminal region of Ankle2. Another possibility that explains why PP2A-Ankle2 did not dephosphorylate the phospho-BAF peptide is the low amount of mts copurified with Ankle2. Many optimizations should be done to increase the amount of purified Mts before the phosphatase assay is done.

Also, a PP2A regulatory subunit often targets the PP2A dimeric complex to specific subcellular localization such as in the case of the regulatory subunit PR72/RSA-1 which targets PP2A to centrosomes in *C. elegans* [257], and B56 which sends the PP2A dimeric complex to the cytoplasm and the nucleus of human cells [258]. According to my results, Ankle2 localizes in the cytoplasm and NE in interphase cells and unexpectedly concentrates on the NE during NEBD and then to the cytoplasm during NER (**Fig. 3.7**). Ankle2 localization to NE during NEBD might suggest that Ankle2 plays a role during this process. In my purification results, Ankle2 purified with the Megator, a spindle matrix protein [259]. Whether Ankle2 is required for targeting Megator inside the spindle region during NEBD is unknown. In addition, I have some results that show that Ankle2 colocalizes with the ER. This was also seen before in *Drosophila* and HeLa cells [244, 245]. However, it is still unknown whether Ankle2 and PP2A colocalize in the cell and, more specifically, in the ER. Performing immunofluorescence in cells by staining for the scaffolding or catalytic subunits of PP2A might provide us with an answer.

Finally, a structural analysis is required to test whether Ankle2 is a regulatory subunit of PP2A. As discussed in **Chapter 1**, the B56 subunit contains a structural motif called a HEAT repeat composed of two alpha-helices linked by a short loop [75]. On the

other hand, the structure of the B55 regulatory subunit consists of seven β-propellers and a β-hairpin-like structure [75]. X-ray crystallography or nuclear magnetic resonance (NMR) analysis of Ankle2 can indicate whether it contains a similar structure as the B55 or B56 subunits.

The above results enable me to suggest a model in which Ankle2 in complex with PP2A localizes to the ER and dephosphorylate BAF and other NE proteins. This leads to the recruitment of BAF to chromatin and the initiation of the NER cascade (**Fig. 3.12**). It also suggests that PP2A-Ankle2 is required for APC function and mitotic progression. More experiments are indeed needed to test this model. This study will be necessary for identifying the role of Ankle2 in NER and other processes during cell division. This also confirms that phosphatases other than PP2A-B55 are implicated in NER and could be studied using the *Drosophila* model.

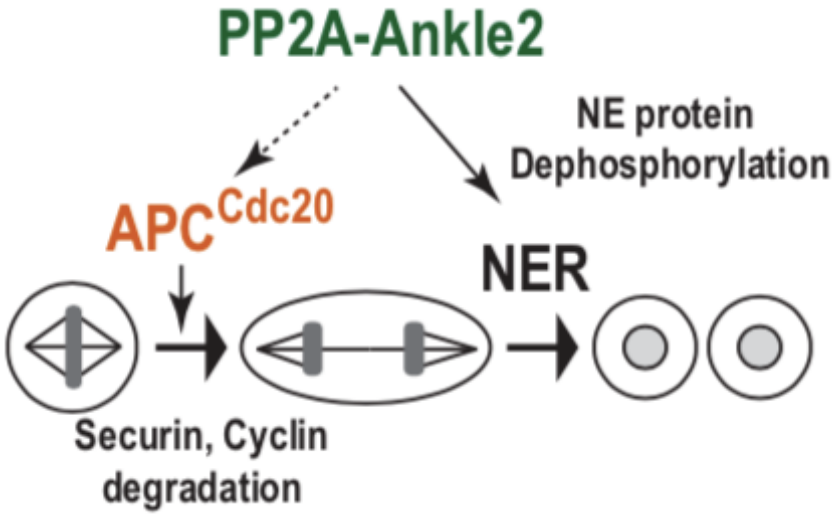

Figure 3.12 A model that describes the role of PP2A-Ankle2 for promoting proper mitotic progression and NER. During exit from mitosis, Ankle2 in complex with PP2A might be responsible for regulating the APC bound to Cdc20 complex activity to induce

securin and cyclin degradation leading to proper mitotic progression. Also, PP2A-Ankle2 promotes NER possibly by dephosphorylating BAF and other NE proteins. Figure by Vincent Archambault.

3.5 Materials and Methods

3.5.A. Plasmids

Plasmids were generated using the Gateway recombination system (Invitrogen). The cDNA of each gene was cloned in a pDON OR221 entry vector before being recombined into destination vectors containing copper-inducible (pMT) or constitutive (pAC5) promoters. The following plasmids were generated: pMT-GFP-Ankle2, pMT-Ankle2-GFP, pMT-Flag-Ankle2, pMT-Ankle2-Flag. The following plasmids were already generated and used in [242]: pMT-GFP-BAF, pAC5-GFP-Lamin B, pMT-RFP-Lamin B, pAC5-Flag-Tws, pAC5-Flag-GFP, pAC5- mcherry-α-Tubulin, pAC5-myc-BAF.

3.5.B. Fly culture and fertility tests

Fly culture was done according to standard procedures. For fertility tests in **Figures 3.1 and 3.8**, three to five virgin females of the corresponding genotype were crossed with three males of either the corresponding mutation or wild type Oregon R in normal food fly tubes. Flies were kept at 25°C for 10 days, after which virgin females from there crosses were selected based on the absence of balancer chromosomes. Each of these females was placed in a grape juice agar tube with yeast paste and were kept to lay eggs for 1 day at 25°C. After 1 day, flies were transferred again for two consecutive days to new agar tubes. Tubes containing laid eggs were kept at 25°C for 1 day, and later, the percentage of hatched eggs was determined. The scoring of egg hatching was repeated two times, and the numbers were pooled. Same procedure was done in the experiment of **Figure**

3.5, but three to five virgins were placed in a grape juice agar tube instead of one. Mutant fly lines were obtained from the Bloomington *Drosophila* Stock Center (Bloomington, IN), David Glover (University of Cambridge, Cambridge, England), and Hugo Bellen (Baylor College of Medicine, Houston, Texas).

3.5.C. Fly egg and cell immunostaining

For the immunofluorescence shown in Fig. 3.5, females were kept to lay eggs in cages on grape juice agar for either 20 min or 1 hour at 25°C. For the 1 to 2 hours collection, grape juice agar plates were left without flies for 1 hour at 25°C. Eggs were then dechorionated by a quick wash using 100% bleach. Then, eggs were washed with water and then with an embryo washing buffer containing 0.5% Triton X-100 and 7% NaCl. Eggs were then transferred to tubes containing 1:1of heptane: methanol and were then shaken vigorously. Then, heptane was removed, and more methanol was added. Eggs were then incubated at 4°C overnight for fixation. After fixation, eggs were rehydrated by adding incubating them with varying percentages of methanol as follows: 90% methanol: 1X Phosphate-buffered saline (PBS), 75%, 50%, and 25%. Eggs were then rinsed and incubated with a solution of PBS+ 0.2% Triton X-100 (PBT). Then, eggs were blocked by incubating them in a solution PBT+5% BSA 1 hour at room temperature. Then, eggs were incubated with a solution containing the anti-α-Tubulin YL1/2 from rat (1:500; #6160, Abcam) antibody and [800µg/ml] of RNAseA at 4°C overnight. Eggs were then incubated with a solution containing the secondary antibody anti-rat-Alexa-488 (1:200; Invitrogen) and 10ug/ml propidium iodide (PI) for 2 hours at room temperature. Finally, eggs were mounted using 1,2,3,4-Tetrahydronaphthalene (Sigma). Images were taken on a Leica

SP8 confocal microscope using the 63X oil objective lens. Images were processed using Adobe photoshop.

For cell immunostaining, cells were fixed using a solution containing 37% formaldehyde, PIPES 0.2M pH 6.8, HEPES 0.2M pH 7, EGTA 0.5M pH 6.8, and MgSO4 1M. Cells were then washed with PBS then blocked with a solution of PBT+5% BSA. Then, cells were incubated with the antibodies: anti-Lamin Dm0 from mouse (1:100; DSHB Hybridoma Product ADL84.12, by P.A. Fisher), anti- Cnx99A from mouse (1:100, DSHB Hybridoma product, by Munro, S.).

3.5.D. *Drosophila* cell culture and drug treatments

D-Mel2 cells were cultured in Express Five medium (Invitrogen) containing penicillin, streptomycin, and glutamine (PSG). To express transgenes under a copper-inducible promoter, a concentration of 300 μM of CuS04 was added to the media for 8 hours. For inhibitor treating: cells were treated with 200 ng/ml of nocodazole and 320 nM of reversine as used in [161], and were incubated for 20 hours at 25 ^{0}C. For the generation of stable cell lines, 70 % to 80% confluent D-Mel2 cells were first seeded in a six-well plate before being transfected with 5 μg plasmids, using the X-tremeGene HP DNA transfection reagent (Roche) as instructed by the manufacturer. After 48 hours in culture, cells were treated with 1 ug/ml of Blasticidine and were passed every two days until the stable cell line is acquired. For RNAi, 60% to 70% D-Mel2 cells were seeded in a six-well plate before being transfected with 25 μg dsRNA for Ankle2 in the presence of the Transfast reagent (Promega). Cells were transfected with dsRNA against the bacterial resistance gene KAN and were used as a negative control. Cells were incubated at 25°C for 72–96 h before being analyzed.

3.5.E. Time-lapse microscopy

A fraction of cultured cells was platted into a small 8 well plate and was placed on a spinning-disk confocal system (CSU-X1 5000; Yokogawa) mounted on a fluorescence microscope (Axio Observer.Z1; Zeiss) using a 63X oil objective an Axiocam 506 mono camera (Zeiss).

3.5.F. Immunoprecipitation and Western blotting

For each cell line, two T75 flasks of cells were used, and cells were collected and washed in PBS containing protease inhibitors (1 mM PMSF, 10 µg/ml aprotinin, and 10 µg/ml leupeptin). Cells were then lysed in a solution containing 75 mM K-Hepes pH 7.5, 150 mM KCl, 2 mM EGTA, 2 mM $MgCl_2$, 0.5% Triton X-100, 5% Glycerol, 1 mM DTT, 1 mM PMSF, 10 µg/ml aprotinin, and 10 µg/ml leupeptin. Lysates were then centrifuged at a speed of 14600 rpm for 8 min at 4°C. Clear lysates were incubated with ChromoTek GFP-Trap beads (Chromotek) for 2 hours at 4°C. Beads were then washed in lysis buffer for 4 × 5 min and eluted directly in Laemmli sample buffer for SDS-PAGE. Antibodies used for western blotting: anti-Myc 9E10from mouse (1:2000, Santa Cruz Biotechnology, Inc.), anti- GFP from rabbit (1:1000, Invitrogen), anti-Tws from rabbit (1:1000, Thermo Fisher Scientific), anti-Mts from mouse (1:1000, Thermo Fisher Scientific), anti-Cyclin A from mouse (1:2000, DSHB Hybridoma Product, by C.F. Lehner), anti-Cyclin B from mouse (1:2000, DSHB Hybridoma Product by by P.H. O'Farrell), anti-Cyclin B3 from rabbit (1:2000, ThermoFisher scientific, custom made), anti-Ankle2 from rabbit (1:2000, ThermoFisher scientific, custom made), anti-actin from mouse (1:5000, EMD Millipore), anti-Flag from mouse (1:1000, Sigma), peroxidase-conjugated AffiniPure Goat anti–

mouse IgG (Jackson), and peroxidase-conjugated AffiniPure Goat anti–rabbit IgG (Jackson).

3.5.G. Protein purification and Mass spectrometry

For each cell line, two T175 flasks of cells were used, and the same purification procedure explained above was used. 10% of the total sample volume was loaded on a gel for silver-nitrate staining, while 90% was sent for mass spectrometry analysis.

3.5.H. Phosphatase assay

The same procedures were followed as described in [242].

CHAPTER 4

Discussion and Perspectives

An important scientific question I was trying to answer in my project is the role of PP2A in regulating crucial events of mitotic exit. More specifically, I was trying to identify substrates which when failed to be dephosphorylated by PP2A can lead to various mitotic exit defects. After analyzing different hits from our screen, I was interested in studying the role of PP2A-B55 during NER and this is what was shown and discussed in **Chapter Two**. Also, a similar role of PP2A-Ankle2 was demonstrated and discussed in **Chapter Three**. However, results from our screen suggest that other functions of PP2A are still unidentified. In this chapter, I first discuss results from **Chapters Two** and **Three** that were not discussed. I compare my results to other studies in the cell cycle field and examine their findings. In another part of this chapter, I raise different questions regarding new PP2A functions and give ideas to test these questions. Finally, I discuss different approaches where PP2A can be considered a target in cancer treatment.

4.1. PP2A and the nuclear envelope reformation

Many studies over the past decades highlighted the importance of the kinase CDK1-cyclin B and other kinases during NEBD at mitotic entry [132, 136, 137, 165, 170, 173, 180, 184]. However, few efforts were made to identify phosphatases that counteract kinase activity and dephosphorylate nuclear envelope protein complexes to promote NER. In the past few years, a growing interest in discovering the roles of protein phosphatases in promoting mitotic exit in different model organisms is observed [45, 75, 129, 260]. Recently, close attention to discovering a function of the phosphatases PP2A-B55 and PP1 is noticed. In my project, I wanted to study the role of PP2A-B55 in NER using *Drosophila*. In **Chapter Two** of this thesis, I have interesting findings that show an important role of PP2A-B55 in promoting NER [242]. I found that PP2A-B55

dephosphorylate BAF *in vitro*. When dephosphorylated, other nuclear envelope proteins such as Lamin B are recruited to the nuclear vicinity to complete NER. This is in accordance with a study that identified a role of PP2A in dephosphorylating BAF [202]. However, whether PP2A-B55 is responsible for that role was not extensively studied in that paper. Also, a clear mechanistic explanation of the role of PP2A in BAF dephosphorylation was still missing in that study. Another study using human cells suggested a role for PP4 in dephosphorylating BAF [205]. Fertility tests for *Drosophila* females with heterozygous mutations for genes coding for Lamin B and several PP4 subunits suggest no genetic interaction (**Chapter 2, Table 2**). Although other pieces of evidence contradict our findings, their results could still suggest that PP4 dephosphorylate BAF in human cells, but not in *Drosophila*. However, it would be difficult to explain this fact when looking from an evolutionary perspective.

In **Chapter Two,** my results suggest that BAF dephosphorylation by PP2A-B55 is required for recruiting nuclear envelope proteins such as Lamin B and Nup107 during NER. We also provide pieces of evidence that PP2A-B55 might dephosphorylate these proteins *in vivo*. Eggs laid by females heterozygous for a *tws*, *lamin*, and *CycB* mutation hatched normally compared to those laid by females heterozygous for a double *tws* and *lamin* mutation (**Chapter 2, Fig. 2.6.E**). Since the introduction of a heterozygous *CycB* mutation partially rescued embryo hatching, one could imagine that, in that context, Lamin B was over phosphorylated in the presence of low levels of PP2A-Tws, which leads to a failure of embryo hatching. A low hatching percentage was also seen from females heterozygous for a *tws* and *Nup107* mutation ((**Chapter 2, Fig. 2.8.A**), suggesting that PP2A-Tws also dephosphorylates Nup107 *in vivo*. However, we could not find clear biochemical evidence that PP2A-B55 dephosphorylate Lamin B and Nup107. The

increase in solubility of Lamin B when cells are treated with OA (**Chapter 2, Fig. 2.13.A-C**) could suggest that PP1 is a Lamin B phosphatase. This is in accordance with other biochemical evidence that confirms that hypothesis [239]. Also, the fact that BAF and Lamin B interaction is lost upon OA treatment (**Chapter 2, Fig. 2.13.A-C**), but not Tws depletion could also suggest a role of PP1 in dephosphorylating Lamin B. However, we did not find any evidence that confirms this hypothesis (**Chapter 2, Table 2**)**.** It would be interesting to test whether the depletion of PP1 or its regulatory subunits could affect the recruitment of Lamin B to reassembling nuclei during mitotic exit. Regarding the role of PP2A-B55 in dephosphorylating Nup107 or other nucleoporins, we observed a strong interaction between PP2A-Tws and Nup107 (**Chapter 2, Fig. 2.14.C**). It would be interesting to test if PP2A-B55 can dephosphorylate a phospho-Lamin B or phospho-Nup107 peptide *in vitro.*

In Chapter Two, we confirm previous studies that show that CDK1-cyclin B is not the only Lamin B kinase. A phospho-deficient Lamin B protein mutated on all 7 possible CDK1-cyclin B phosphorylation sites becomes soluble when cells expressing this mutant were treated with OA (**Chapter 2, Fig. 2.6.C**). This either shows that other kinases phosphorylate Lamin B as discussed in [132] or that these kinases phosphorylate Lamin B interacting proteins which affects Lamin B solubility . Also, and despite other studies suggesting that PP2A-B55 mainly dephosphorylates sites phosphorylated by CDK1-cyclin B [85], our results provide strong evidence that PP2A-B55 dephosphorylates sites phosphorylated by other kinases such as those phosphorylated on BAF and Lamin B.

Taken together, our results in **Chapter Two** are consistent with several scientific findings in the field about the role of PP2A-B55 in promoting NER. Other experiments are still needed to identify more PP2A-B55 substrates that are required for NER during mitotic

exit.

Our results in Chapter **Two** show that PP2A-B55 promotes NER during mitotic exit. However, a complete failure of the recruitment of nuclear envelope proteins was not observed upon B55 depletion. This was also observed before in human cells [88]. This suggests a role of other phosphatases in promoting NER. I became interested in studying about Ankle2/LEM4, as its loss by either RNAi or CRISPR in *C. elegans* or human cells lead to a complete failure in BAF recruitment to reassembling nuclei during NER [202, 204]. Other results in these studies suggest that Ankle2/LEM4 is a PP2A regulatory subunit [204]. My findings confirm that the role of Ankle2 is also conserved in *Drosophila*. Our current model suggests that PP2A-Ankle2 bound to the ER is crucial for regulating NER at least by dephosphorylating BAF. In the phosphatase assay shown in **Chapter Two, section 2.3.F**, PP2A-B55 dephosphorylated the BAF-pS5 peptide, although results from that chapter and from [181] suggest that the two other BAF phospho-sites might be important for BAF functions. It is still under debate whether PP2A-Ankle2 can dephosphorylate the other sites not dephosphorylated by PP2A-B55. BAF recruitment to reassembling nuclei is a two-step process, in which first it binds chromatin through its DNA binding capability and then binds LEM domain proteins [161]. Since Ankle2 depletion leads to a complete abolishment of BAF recruitment during NER, one could imagine that BAF dephosphorylation by PP2A-Ankle2 is crucial for BAF DNA binding capability, and PP2A-B55 is important for its binding to LEM domain proteins. Another explanation that favors that hypothesis is Ankle2 localization to the ER. As discussed in **Chapter one, section 1.8**, the ER is an important factor during NER. Hence, one could imagine that PP2A-Ankle2 bound to the ER might be the first phosphatase in contact with NE proteins during NER and can thus dephosphorylate BAF to induce its binding to DNA. To test this

hypothesis, it would be necessary to identify the region by which Ankle2 binds to ER proteins. Then, one can test whether expressing an Ankle2 lacking that region leads to a destruction of the PP2A-Ankle2 complex and an improper BAF recruitment to newly assembling nuclei.

When analyzing the genetic screen results in **Chapter 2, Table1**, we found that a female with a female heterozygous for a t*ws* or *mts* mutation and a chromosomal deletion laid eggs with a low hatching percentage. This deletion covers a chromosomal region containing the gene *ote*, which codes for the protein Otefin, a known *Drosophila* LEM domain protein [156]. As discussed in **Chapter One, section 1.6.D.a**, LEM domain proteins interact with BAF or chromatin through a phosphorylation-dependent manner [168, 172]. CDK1-cyclin B and other kinases were shown to phosphorylate LEM domain proteins during mitosis [170-172], though the nature of the phosphatase(s) that dephosphorylate(s) these proteins is still unknown. Results from the screen suggest that PP2A-Tws and Otefin are found in a common pathway. Also, preliminary mass spectrometry results from Myreille Larouche, a Ph.D. student in our laboratory show that the level of phospho-Otefin increases in cells either depleted from Tws or treated with OA. These results suggest that PP2A-Tws can either directly or indirectly dephosphorylate Otefin. Other experiments are still needed to examine the role of PP2A-B55 in regulating Otefin functions during the cell cycle.

Results from this study and other studies show that NER in cells of different organisms is a complex process that cannot be regulated by only one phosphatase. However, PP2A in complex with different regulatory subunits is crucial in promoting NER (**Fig. 4.1**). The future challenge is to identify substrates of the nuclear envelope that are only regulated by PP2A bound to a specific regulatory subunit.

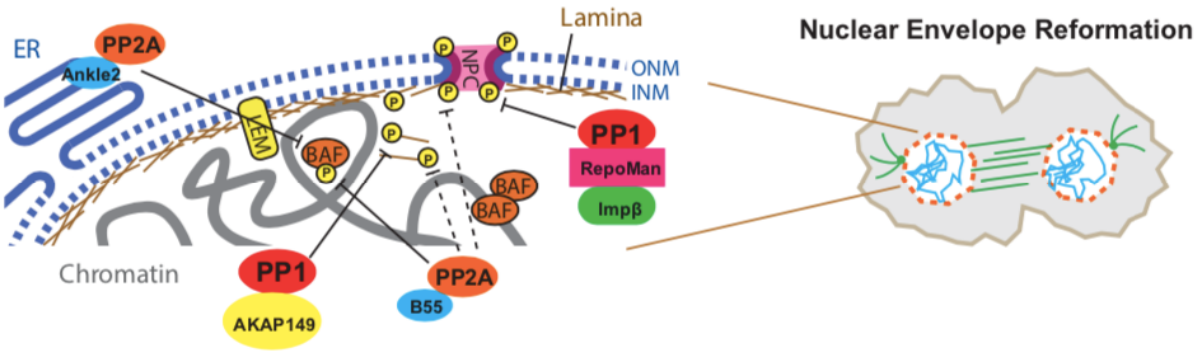

Figure 4.1: The model for the regulation of nuclear envelope reassembly. Our results suggest that PP2A-B55 dephosphorylate BAF and other nuclear envelope proteins. Also, our and other findings suggest that PP2A-Ankle2 localized to the ER is able to dephosphorylate BAF during NER at mitotic exit.

4.2 PP2A cellular functions that are still missing

In **Chapters Two and Three**, we highlighted the importance of PP2A in regulating the process of NER at mitotic exit. Nevertheless, PP2A regulates other functions during mitotic exit. In **Chapter One**, **section 1.5.A.b**, I discussed the roles of PP2A-B55 during mitotic exit. PP2A-B55 seems to play crucial roles during cytokinesis through its function in dephosphorylating PRC1 in human cells [87]. I have results that suggest that the role of PP2A-B55 during cytokinesis is also conserved in *Drosophila*. In fly cells expressing GFP-Lamin B, mcherry-α-tubulin and depleted from Tws, the percentage of binucleated cells was 30% more than that of control cells (**Fig. 4.2.A**). Also, the central spindle

structure in cells depleted from Tws was more dispersed compared to control cells which had an hourglass-like structure (**Fig. 4.2.B**). These results suggest that PP2A-Tws is important for the formation of a proper central spindle during cytokinesis, failure of which leads to cytokinetic defects and cell binucleation. More experiments are still needed to investigate the role of PP2A-Tws during cytokinesis in flies and identify the substrates regulated by PP2A-Tws during cytokinesis.

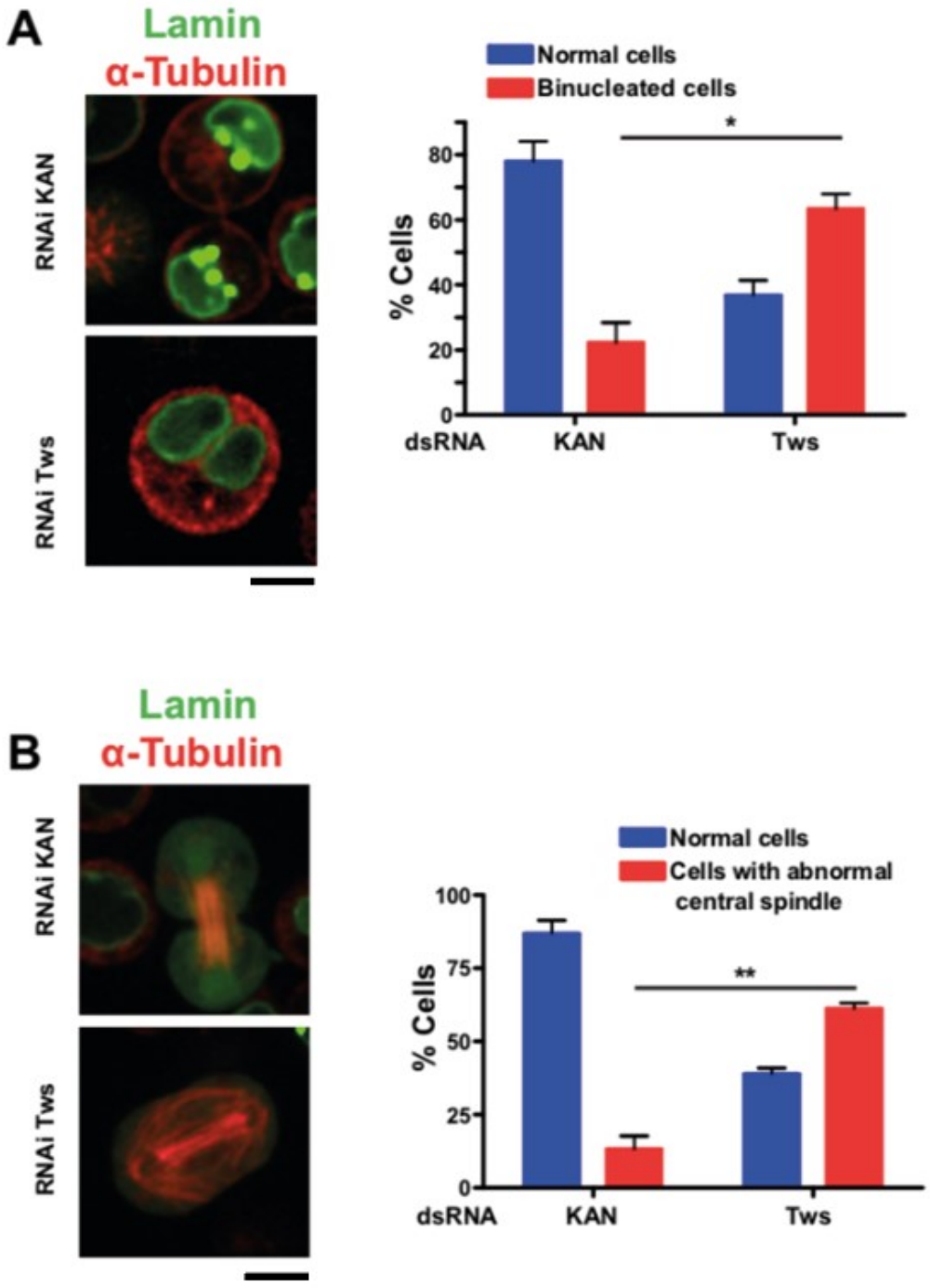

Figure 4.2 PP2A-Tws is required during cytokinesis in *Drosophila* cells.
A. Left. Cells expressing GFP-Lamin B and mcherry-α-tubulin were transfected with either dsRNA Kan or Tws and live imaging was performed. These two images were taken at the end of cytokinesis. Scale bar is 5 μm. Right. The percentage of normal and binucleated at the end of cytokinesis was quantified in both conditions. Error bars present standard

deviation. **P=0.0061, from a two-tailed *t*-test. B. Left. Live imaging of cells transfected with either dsRNA KAN or Tws during cytokinesis. In control cells, the central spindle adopts an hourglass-like structure compared to being more dispersed when Tws is depleted. Scale bar is 5 μm. Right. The percentage of normal and cells with dispersed central spindle during cytokinesis was quantified in both conditions. Error bars present standard deviation. *P=0.32 from a two-tailed *t*-test.

Although the majority of studies highlighted the importance of PP2A in regulating events of mitotic exit, PP2A can also contribute to other cellular processes. Recently, interest has been growing in understanding the role of PP2A in regulating mRNA translation to proteins [261]. At the beginning of this process in eukaryotic cells, a pre-initiation complex, composed of the 40S ribosome and several protein initiation proteins, forms and scans the mRNA for the start codon [262]. After start codon recognition, the pre-initiation complex joins with the 60S ribosomes and translation initiates [262]. Studies showed that the functions of many of the translation initiation proteins are regulated by kinases such as the mTOR kinase [263], S6 kinase, eEF2 kinase, and others [261]. Interestingly, a study using human cells shows that translation initiation protein eIF4G1 is phosphorylated by CDK1-cyclin B [264]. When phosphorylated on Ser1232, eIF4G1 loses the ability to bind RNA [264]. The phosphorylation of translation initiation proteins is also conserved in other systems. Another study using plants demonstrates that CDK1 phosphorylates eIF4A on Thr164 within the RNA-binding domain [265]. This might suggest a mechanism by which CDK1 negatively regulates translation during cell division. Recent studies demonstrated that several phosphatases are necessary to regulate essential functions of translation initiation proteins [261]. For instance, depletion of the PP1 in human cells decreased the dephosphorylation of the translation initiation protein

eIF2α on Ser51 [266]. The dephosphorylation of eIF2α by PP1 seems to be crucial for cell response to stress [266]. Also, PP2A seems to be involved in regulating the functions of translation initiation proteins. For example, a study using Neuro-2A cells shows that PP2A dephosphorylates eIF4B [267]. When dephosphorylated by PP2A, the affinity of eIF4B and BC RNA translational repressors decreases, thus allowing eIF4B to bind the 40S ribosome and initiate translation [267]. In addition, a study using HEK293 cells showed that PP2A directly binds and dephosphorylates eIF4E [268]. Treating these cells with OA or depleting PP2A by RNAi increased eIF4E phosphorylation levels [268]. These studies and others suggest an important role of PP2A in dephosphorylating translation initiation proteins. However, the nature of the trimeric PP2A complex involved in this process is unknown.

When looking at other hits in our screen, I found that females with *tws* mutation and deletion in regions containing genes coding for eukaryotic translation initiation proteins laid eggs with low egg hatching percentage. Some of the deleted regions contained the genes that expressed the proteins eIF4A, eIF3f2, eIF3k, and eIF6. To test this possibility, genetic interaction must be first confirmed by performing fertility tests for females with a *tws* mutation and mutations in genes coding for translation initiation proteins. Also, it is known that maternal mRNA translation is very active during syncytial embryo development [269]. Thus, the role of PP2A during translation could be studied using embryos at this early developmental stage. Moreover, depleting B55 by RNAi could be performed to test its effect on the interaction between translation initiation proteins. Also, *in vitro* phosphatase assays could be conducted to determine if PP2A-B55 can dephosphorylate phospho-peptides of translation initiation proteins. This will provide new insights on a role of PP2A-B55 in regulating mechanisms that are not only implicated in

events of mitotic exits but in other cellular processes.

PP2A might also be involved in mechanisms of development. A mutation in the gene coding for Ankle2 leads to the formation of a smaller brain [244] and defects in the formation of sensory organs [246]. Also, a family suffering from microcephaly carries different mutations in *Ankle2* [246]. These results suggest a role for Ankle2 in brain development. A recent study using *Drosophila* proposed a mechanistic explanation of this role. When Ankle2 levels decrease, the BAF phosphorylating kinase, NHK-1, is dispersed in the cytoplasm of fly neuroblasts compared to being nuclear in control neuroblasts. These results were also confirmed when using human fibroblasts [244]. Interestingly, cytoplasmic NHK-1 leads to a decrease in the phosphorylation levels of aPKC and spindle alignment defects. Also, in flies with the *Ankle2* mutation, the localization of the Par-6 complex, which is essential for asymmetric divisions of neuroblasts, is disrupted [244]. These results highlight the importance of Ankle2 during the early stages of fly development. Since a mutation of NHK-1 rescues the phenotypes associated with the *Ankle2* mutation, it remains to be seen whether the phosphorylation state of BAF is affected in these neuroblasts. It is also important to identify the mechanism by which the localization of the Par-6 complex is disrupted. It is known that Par-6 is phosphorylated by aPKC [270]. One hypothesis could be that aPKC is activated when it is either phosphorylated by NHK-1 or dephosphorylated by PP2A-Ankle2 during the division of neuroblasts. More experiments are still needed to test that hypothesis.

4.3 PP2A and cancer treatment

In **Chapter One, section 1.5.A.d**, I discussed that PP2A is considered a tumor suppressor gene [118], and its level of gene expression is abnormal in various cancer types [120]. I also discussed that targeting mitotic exit regulatory proteins might be a promising approach for identifying new cancer drugs [112]. Therefore, since PP2A-B55 is an essential regulator of mitotic exit, it presents an important target for cancer drug discovery. Over the past decade, great efforts have been made to identify PP2A-activating drugs (PADs). One promising PAD is the drug FTY720, a sphingosine analog, that binds the PP2A endogenous inhibitor, SET, and prevents its interaction with PP2A, thus leading to PP2A premature activation [271]. Studies show that SET binds to the PP2A catalytic subunit and inhibits its activity [272]. Treatment of acute myeloid leukemia cell line HL-60 with FTY720 restored PP2A activity and reduced cell proliferation by 50% [271]. The activation of PP2A by FTY720 showed important results in treating lung cancer [273], B-cell malignancies [274], and myelogenous leukemia [275]. It would be interesting to test the effect of this drug on the process of NER.

Scientists also developed a drug that can inhibit the interaction between MASTL (Greatwall in human cells) and ENSA. Such a compound will prevent MASTL phosphorylation of ENSA and thus prevents PP2A-B55 inhibition. An active MASTL was successfully purified and an inhibitor was already discovered [276]. Treatment of human cells with the MASTL kinase inhibitor GKI-1 leads to a decrease in ENSA phosphorylation [276]. However, the ability of this drug to prevent PP2A-B55 inactivation was not tested in that study. It remains to be seen whether treating cells with MASTL inhibitors will lead to PP2A-B55 constitutive activation, mitotic collapse and cancer cell death.

One of the disadvantages of cancer drug therapy is that drugs target both cancerous and normal cells [277]. This will lead to loss of body tissues and vital body functions. Therefore, researchers nowadays are putting efforts to find strategies to kill cancerous cells without affecting normal cells. It is known that specific surface markers are found on cancerous cells and absent from normal cells [278]. Viruses are known to recognize specific cell surface receptors. This receptor recognition mechanism is important for viral entry to the cell [279]. Many encouraging results have emerged from using viral gene delivery mechanisms in cancer treatment [279]. A virus is engineered in a way that recognizes a specific cell surface receptor of a specific cancerous cell type. When this virus enters the cell, it integrates its genome in the genome of the host cell. Genetic material integrated is expressed using the host cell machinery [279]. Expressing a mutant form of a gene or an shRNA that leads to a depletion of a host gene can lead to the death of these cancerous cells [279]. Nowadays, scientists are using nanotechnology to develop means for gene delivery [280]. This approach is new and seems like a promising one to cancer treatment. As seen in **Chapter Three**, the depletion of Ankle2 leads to the abolishment of BAF recruitment to reassembling nuclei and cells with micronuclei. When they persist in the cell, micronuclei can trigger an innate immune response which leads to the lysis of the defective cell [281]. This mainly happens through a mechanism that depends on the cyclic GMP-AMP synthase (cGAS), a nucleic acid sensor that binds DNA [281]. In a micronucleated cell, cGAS is active and activate Type I Interferon response via a protein called Stimulator of Interferon Genes (STING) [281]. This will activate an immune response that will eliminate the micronucleated cell.

In our laboratory, we are trying to identify proteins that when depleted will lead to micronuclei formation in cells. The results of this project can be used by other groups that

are currently developing DNA delivery techniques to cancerous cells in a way that can deplete proteins leading for micronucleation in these cells.

References:

1. Kumar, M., Pushpa, K., and Mylavarapu, S.V. (2015). Splitting the cell, building the organism: Mechanisms of cell division in metazoan embryos. IUBMB Life *67*, 575-587.
2. Morgan, D. (2007). The Cell Cycle: Principles of Control, (London: New Science Press).
3. Barnum, K.J., and O'Connell, M.J. (2014). Cell cycle regulation by checkpoints. Methods Mol Biol *1170*, 29-40.
4. Zetterberg, A., Larsson, O., and Wiman, K.G. (1995). What is the restriction point? Current opinion in cell biology *7*, 835-842.
5. Firat-Karalar, E.N., and Stearns, T. (2014). The centriole duplication cycle. Philos Trans R Soc Lond B Biol Sci *369*.
6. McIntosh, J.R. (2016). Mitosis. Cold Spring Harb Perspect Biol *8*.
7. Cassimeris, L., and Skibbens, R.V. (2003). Regulated assembly of the mitotic spindle: a perspective from two ends. Curr Issues Mol Biol *5*, 99-112.
8. Sablin, E.P. (2000). Kinesins and microtubules: their structures and motor mechanisms. Curr Opin Cell Biol *12*, 35-41.
9. Terasaki, M., Campagnola, P., Rolls, M.M., Stein, P.A., Ellenberg, J., Hinkle, B., and Slepchenko, B. (2001). A new model for nuclear envelope breakdown. Mol Biol Cell *12*, 503-510.
10. Cheeseman, I.M. (2014). The kinetochore. Cold Spring Harb Perspect Biol *6*, a015826.
11. D'Avino, P.P., Giansanti, M.G., and Petronczki, M. (2015). Cytokinesis in animal cells. Cold Spring Harb Perspect Biol *7*, a015834.
12. Tolwinski, N.S. (2017). Introduction: *Drosophila*-A Model System for Developmental Biology. J Dev Biol *5*.
13. Zykova, T.Y., Levitsky, V.G., Belyaeva, E.S., and Zhimulev, I.F. (2018). Polytene Chromosomes - A Portrait of Functional Organization of the *Drosophila* Genome. Curr Genomics *19*, 179-191.
14. Fernandez-Moreno, M.A., Farr, C.L., Kaguni, L.S., and Garesse, R. (2007). *Drosophila melanogaster* as a model system to study mitochondrial biology. Methods Mol Biol *372*, 33-49.
15. Reiter, L.T., and Bier, E. (2002). Using *Drosophila* melanogaster to uncover human disease gene function and potential drug target proteins. Expert Opin Ther Targets *6*, 387-399.
16. Hartwell, L.H., Hood, L., Goldberg, M. L., Reynolds, A. E., Silver, L. M., and Veres, R. C (2004). Genetics from Genes to Genomes, Volume second edition, (McGraw-Hill.).
17. Hales, K.G., Korey, C.A., Larracuente, A.M., and Roberts, D.M. (2015). Genetics on the Fly: A Primer on the *Drosophila* Model System. Genetics *201*, 815-842.
18. Phelps, C.B., and Brand, A.H. (1998). Ectopic gene expression in *Drosophila* using GAL4 system. Methods *14*, 367-379.
19. Elliott, D.A., and Brand, A.H. (2008). The GAL4 system : a versatile system for the expression of genes. Methods Mol Biol *420*, 79-95.

20. St Johnston, D. (2002). The art and design of genetic screens: *Drosophila* melanogaster. Nat Rev Genet *3*, 176-188.
21. Gratz, S.J., Rubinstein, C.D., Harrison, M.M., Wildonger, J., and O'Connor-Giles, K.M. (2015). CRISPR-Cas9 Genome Editing in *Drosophila*. Curr Protoc Mol Biol *111*, 31 32 31-20.
22. Loppin, B., Dubruille, R., and Horard, B. (2015). The intimate genetics of *Drosophila* fertilization. Open Biol *5*.
23. Stafstrom, J.P., and Staehelin, L.A. (1984). Dynamics of the nuclear envelope and of nuclear pore complexes during mitosis in the *Drosophila* embryo. Eur J Cell Biol *34*, 179-189.
24. Garcia, K., Duncan, T., and Su, T.T. (2007). Analysis of the cell division cycle in *Drosophila*. Methods *41*, 198-205.
25. Hunt, T., Nasmyth, K., and Novak, B. (2011). The cell cycle. Philos Trans R Soc Lond B Biol Sci *366*, 3494-3497.
26. Malumbres, M., and Barbacid, M. (2005). Mammalian cyclin-dependent kinases. Trends Biochem Sci *30*, 630-641.
27. Lim, S., and Kaldis, P. (2013). Cdks, cyclins and CKIs: roles beyond cell cycle regulation. Development *140*, 3079-3093.
28. Chang, E.J., Begum, R., Chait, B.T., and Gaasterland, T. (2007). Prediction of cyclin-dependent kinase phosphorylation substrates. PLoS One *2*, e656.
29. Atherton-Fessler, S., Parker, L.L., Geahlen, R.L., and Piwnica-Worms, H. (1993). Mechanisms of p34cdc2 regulation. Mol Cell Biol *13*, 1675-1685.
30. Pavletich, N.P. (1999). Mechanisms of cyclin-dependent kinase regulation: structures of Cdks, their cyclin activators, and Cip and INK4 inhibitors. J Mol Biol *287*, 821-828.
31. Yuan, K., and O'Farrell, P.H. (2015). Cyclin B3 is a mitotic cyclin that promotes the metaphase-anaphase transition. Curr Biol *25*, 811-816.
32. Bourouh, M., Dhaliwal, R., Rana, K., Sinha, S., Guo, Z., and Swan, A. (2016). Distinct and Overlapping Requirements for Cyclins A, B, and B3 in *Drosophila* Female Meiosis. G3 (Bethesda) *6*, 3711-3724.
33. Karasu, M.E., Bouftas, N., Keeney, S., and Wassmann, K. (2019). Cyclin B3 promotes anaphase I onset in oocyte meiosis. J Cell Biol *218*, 1265-1281.
34. Wilmes, G.M., Archambault, V., Austin, R.J., Jacobson, M.D., Bell, S.P., and Cross, F.R. (2004). Interaction of the S-phase cyclin Clb5 with an "RXL" docking sequence in the initiator protein Orc6 provides an origin-localized replication control switch. Genes Dev *18*, 981-991.
35. Porter, L.A., and Donoghue, D.J. (2003). Cyclin B1 and CDK1: nuclear localization and upstream regulators. Prog Cell Cycle Res *5*, 335-347.
36. Morgan, D.O. (1995). Principles of CDK regulation. Nature *374*, 131-134.
37. Poon, R.Y., and Hunter, T. (1995). Dephosphorylation of Cdk2 Thr160 by the cyclin-dependent kinase-interacting phosphatase KAP in the absence of cyclin. Science *270*, 90-93.
38. Cheng, A., Kaldis, P., and Solomon, M.J. (2000). Dephosphorylation of human cyclin-dependent kinases by protein phosphatase type 2C alpha and beta 2 isoforms. J Biol Chem *275*, 34744-34749.
39. Sherr, C.J., and Roberts, J.M. (1999). CDK inhibitors: positive and negative regulators of G1-phase progression. Genes Dev *13*, 1501-1512.

40. Nakayama, K., and Nakayama, K. (1998). Cip/Kip cyclin-dependent kinase inhibitors: brakes of the cell cycle engine during development. Bioessays *20*, 1020-1029.
41. Cardozo, T., and Pagano, M. (2004). The SCF ubiquitin ligase: insights into a molecular machine. Nat Rev Mol Cell Biol *5*, 739-751.
42. Orlicky, S., Tang, X., Willems, A., Tyers, M., and Sicheri, F. (2003). Structural basis for phosphodependent substrate selection and orientation by the SCFCdc4 ubiquitin ligase. Cell *112*, 243-256.
43. Castro, A., Bernis, C., Vigneron, S., Labbe, J.C., and Lorca, T. (2005). The anaphase-promoting complex: a key factor in the regulation of cell cycle. Oncogene *24*, 314-325.
44. Alfieri, C., Chang, L., Zhang, Z., Yang, J., Maslen, S., Skehel, M., and Barford, D. (2016). Molecular basis of APC/C regulation by the spindle assembly checkpoint. Nature *536*, 431-436.
45. Wurzenberger, C., and Gerlich, D.W. (2011). Phosphatases: providing safe passage through mitotic exit. Nat Rev Mol Cell Biol *12*, 469-482.
46. Dephoure, N., Zhou, C., Villen, J., Beausoleil, S.A., Bakalarski, C.E., Elledge, S.J., and Gygi, S.P. (2008). A quantitative atlas of mitotic phosphorylation. Proc Natl Acad Sci U S A *105*, 10762-10767.
47. Petrone, A., Adamo, M.E., Cheng, C., and Kettenbach, A.N. (2016). Identification of Candidate Cyclin-dependent kinase 1 (Cdk1) Substrates in Mitosis by Quantitative Phosphoproteomics. Mol Cell Proteomics *15*, 2448-2461.
48. Hershko, A. (1999). Mechanisms and regulation of the degradation of cyclin B. Philos Trans R Soc Lond B Biol Sci *354*, 1571-1575; discussion 1575-1576.
49. Adhikari, D., Liu, K., and Shen, Y. (2012). Cdk1 drives meiosis and mitosis through two different mechanisms. Cell Cycle *11*, 2763-2764.
50. Malumbres, M. (2014). Cyclin-dependent kinases. Genome Biol *15*, 122.
51. Hayles, J., Fisher, D., Woollard, A., and Nurse, P. (1994). Temporal order of S phase and mitosis in fission yeast is determined by the state of the p34cdc2-mitotic B cyclin complex. Cell *78*, 813-822.
52. Follette, P.J., and O'Farrell, P.H. (1997). Cdks and the *Drosophila* cell cycle. Curr Opin Genet Dev *7*, 17-22.
53. Furuno, N., den Elzen, N., and Pines, J. (1999). Human cyclin A is required for mitosis until mid prophase. J Cell Biol *147*, 295-306.
54. Vasquez, R.J., Gard, D.L., and Cassimeris, L. (1999). Phosphorylation by CDK1 regulates XMAP215 function in vitro. Cell Motil Cytoskeleton *43*, 310-321.
55. Chou, Y.H., Bischoff, J.R., Beach, D., and Goldman, R.D. (1990). Intermediate filament reorganization during mitosis is mediated by p34cdc2 phosphorylation of vimentin. Cell *62*, 1063-1071.
56. Jiang, W., Jimenez, G., Wells, N.J., Hope, T.J., Wahl, G.M., Hunter, T., and Fukunaga, R. (1998). PRC1: a human mitotic spindle-associated CDK substrate protein required for cytokinesis. Mol Cell *2*, 877-885.
57. Mollinari, C., Kleman, J.P., Jiang, W., Schoehn, G., Hunter, T., and Margolis, R.L. (2002). PRC1 is a microtubule binding and bundling protein essential to maintain the mitotic spindle midzone. J Cell Biol *157*, 1175-1186.

58. Kraft, C., Herzog, F., Gieffers, C., Mechtler, K., Hagting, A., Pines, J., and Peters, J.M. (2003). Mitotic regulation of the human anaphase-promoting complex by phosphorylation. EMBO J *22*, 6598-6609.
59. Rudner, A.D., and Murray, A.W. (2000). Phosphorylation by Cdc28 activates the Cdc20-dependent activity of the anaphase-promoting complex. J Cell Biol *149*, 1377-1390.
60. Bettencourt-Dias, M., Giet, R., Sinka, R., Mazumdar, A., Lock, W.G., Balloux, F., Zafiropoulos, P.J., Yamaguchi, S., Winter, S., Carthew, R.W., et al. (2004). Genome-wide survey of protein kinases required for cell cycle progression. Nature *432*, 980-987.
61. Archambault, V., and Glover, D.M. (2009). Polo-like kinases: conservation and divergence in their functions and regulation. Nat Rev Mol Cell Biol *10*, 265-275.
62. Kachaner, D., Garrido, D., Mehsen, H., Normandin, K., Lavoie, H., and Archambault, V. (2017). Coupling of Polo kinase activation to nuclear localization by a bifunctional NLS is required during mitotic entry. Nat Commun *8*, 1701.
63. Wolfe, B.A., Takaki, T., Petronczki, M., and Glotzer, M. (2009). Polo-like kinase 1 directs assembly of the HsCyk-4 RhoGAP/Ect2 RhoGEF complex to initiate cleavage furrow formation. PLoS Biol *7*, e1000110.
64. Hu, C.K., Ozlu, N., Coughlin, M., Steen, J.J., and Mitchison, T.J. (2012). Plk1 negatively regulates PRC1 to prevent premature midzone formation before cytokinesis. Mol Biol Cell *23*, 2702-2711.
65. Ellinger-Ziegelbauer, H., Karasuyama, H., Yamada, E., Tsujikawa, K., Todokoro, K., and Nishida, E. (2000). Ste20-like kinase (SLK), a regulatory kinase for polo-like kinase (Plk) during the G2/M transition in somatic cells. Genes Cells *5*, 491-498.
66. Qian, Y.W., Erikson, E., and Maller, J.L. (1998). Purification and cloning of a protein kinase that phosphorylates and activates the polo-like kinase Plx1. Science *282*, 1701-1704.
67. Tsvetkov, L., and Stern, D.F. (2005). Phosphorylation of Plk1 at S137 and T210 is inhibited in response to DNA damage. Cell Cycle *4*, 166-171.
68. Tsvetkov, L.M., Tsekova, R.T., Xu, X., and Stern, D.F. (2005). The Plk1 Polo box domain mediates a cell cycle and DNA damage regulated interaction with Chk2. Cell Cycle *4*, 609-617.
69. Willems, E., Dedobbeleer, M., Digregorio, M., Lombard, A., Lumapat, P.N., and Rogister, B. (2018). The functional diversity of Aurora kinases: a comprehensive review. Cell Div *13*, 7.
70. Bird, A.W., and Hyman, A.A. (2008). Building a spindle of the correct length in human cells requires the interaction between TPX2 and Aurora A. J Cell Biol *182*, 289-300.
71. Afonso, O., Matos, I., Pereira, A.J., Aguiar, P., Lampson, M.A., and Maiato, H. (2014). Feedback control of chromosome separation by a midzone Aurora B gradient. Science *345*, 332-336.
72. Satinover, D.L., Leach, C.A., Stukenberg, P.T., and Brautigan, D.L. (2004). Activation of Aurora-A kinase by protein phosphatase inhibitor-2, a bifunctional signaling protein. Proc Natl Acad Sci U S A *101*, 8625-8630.

73. Carmena, M., Pinson, X., Platani, M., Salloum, Z., Xu, Z., Clark, A., Macisaac, F., Ogawa, H., Eggert, U., Glover, D.M., et al. (2012). The chromosomal passenger complex activates Polo kinase at centromeres. PLoS Biol *10*, e1001250.
74. Kapuy, O., He, E., Uhlmann, F., and Novak, B. (2009). Mitotic exit in mammalian cells. Mol Syst Biol *5*, 324.
75. Moura, M., and Conde, C. (2019). Phosphatases in Mitosis: Roles and Regulation. Biomolecules *9*.
76. Janssens, V., and Goris, J. (2001). Protein phosphatase 2A: a highly regulated family of serine/threonine phosphatases implicated in cell growth and signalling. Biochem J *353*, 417-439.
77. Juanes, M.A., Khoueiry, R., Kupka, T., Castro, A., Mudrak, I., Ogris, E., Lorca, T., and Piatti, S. (2013). Budding yeast greatwall and endosulfines control activity and spatial regulation of PP2A(Cdc55) for timely mitotic progression. PLoS Genet *9*, e1003575.
78. Merigliano, C., Marzio, A., Renda, F., Somma, M.P., Gatti, M., and Verni, F. (2017). A Role for the Twins Protein Phosphatase (PP2A-B55) in the Maintenance of *Drosophila* Genome Integrity. Genetics *205*, 1151-1167.
79. Qadota, H., Matsunaga, Y., Bagchi, P., Lange, K.I., Carrier, K.J., Pols, W.V., Swartzbaugh, E., Wilson, K.J., Srayko, M., Pallas, D.C., et al. (2018). Protein phosphatase 2A is crucial for sarcomere organization in Caenorhabditis elegans striated muscle. Mol Biol Cell *29*, 2084-2097.
80. Pinto, B.S., and Orr-Weaver, T.L. (2017). *Drosophila* protein phosphatases 2A B' Wdb and Wrd regulate meiotic centromere localization and function of the MEI-S332 Shugoshin. Proc Natl Acad Sci U S A *114*, 12988-12993.
81. Groves, M.R., Hanlon, N., Turowski, P., Hemmings, B.A., and Barford, D. (1999). The structure of the protein phosphatase 2A PR65/A subunit reveals the conformation of its 15 tandemly repeated HEAT motifs. Cell *96*, 99-110.
82. Cho, U.S., and Xu, W. (2007). Crystal structure of a protein phosphatase 2A heterotrimeric holoenzyme. Nature *445*, 53-57.
83. Xu, Y., Chen, Y., Zhang, P., Jeffrey, P.D., and Shi, Y. (2008). Structure of a protein phosphatase 2A holoenzyme: insights into B55-mediated Tau dephosphorylation. Mol Cell *31*, 873-885.
84. Mayer-Jaekel, R.E., Ohkura, H., Ferrigno, P., Andjelkovic, N., Shiomi, K., Uemura, T., Glover, D.M., and Hemmings, B.A. (1994). *Drosophila* mutants in the 55 kDa regulatory subunit of protein phosphatase 2A show strongly reduced ability to dephosphorylate substrates of p34cdc2. J Cell Sci *107 (Pt 9)*, 2609-2616.
85. Mochida, S., Ikeo, S., Gannon, J., and Hunt, T. (2009). Regulated activity of PP2A-B55 delta is crucial for controlling entry into and exit from mitosis in Xenopus egg extracts. EMBO J *28*, 2777-2785.
86. Castilho, P.V., Williams, B.C., Mochida, S., Zhao, Y., and Goldberg, M.L. (2009). The M phase kinase Greatwall (Gwl) promotes inactivation of PP2A/B55delta, a phosphatase directed against CDK phosphosites. Mol Biol Cell *20*, 4777-4789.
87. Cundell, M.J., Bastos, R.N., Zhang, T., Holder, J., Gruneberg, U., Novak, B., and Barr, F.A. (2013). The BEG (PP2A-B55/ENSA/Greatwall) pathway ensures cytokinesis follows chromosome separation. Mol Cell *52*, 393-405.
88. Schmitz, M.H., Held, M., Janssens, V., Hutchins, J.R., Hudecz, O., Ivanova, E., Goris, J., Trinkle-Mulcahy, L., Lamond, A.I., Poser, I., et al. (2010). Live-cell

imaging RNAi screen identifies PP2A-B55alpha and importin-beta1 as key mitotic exit regulators in human cells. Nat Cell Biol *12*, 886-893.
89. Wang, P., Pinson, X., and Archambault, V. (2011). PP2A-twins is antagonized by greatwall and collaborates with polo for cell cycle progression and centrosome attachment to nuclei in *drosophila* embryos. PLoS Genet *7*, e1002227.
90. Wang, F., Zhu, S., Fisher, L.A., Wang, W., Oakley, G.G., Li, C., and Peng, A. (2018). Protein interactomes of protein phosphatase 2A B55 regulatory subunits reveal B55-mediated regulation of replication protein A under replication stress. Sci Rep *8*, 2683.
91. Cundell, M.J., Hutter, L.H., Nunes Bastos, R., Poser, E., Holder, J., Mohammed, S., Novak, B., and Barr, F.A. (2016). A PP2A-B55 recognition signal controls substrate dephosphorylation kinetics during mitotic exit. J Cell Biol *214*, 539-554.
92. Hein, J.B., Hertz, E.P.T., Garvanska, D.H., Kruse, T., and Nilsson, J. (2017). Distinct kinetics of serine and threonine dephosphorylation are essential for mitosis. Nat Cell Biol *19*, 1433-1440.
93. Castro, A., and Lorca, T. (2018). Greatwall kinase at a glance. J Cell Sci *131*.
94. Vigneron, S., Gharbi-Ayachi, A., Raymond, A.A., Burgess, A., Labbe, J.C., Labesse, G., Monsarrat, B., Lorca, T., and Castro, A. (2011). Characterization of the mechanisms controlling Greatwall activity. Mol Cell Biol *31*, 2262-2275.
95. Mochida, S. (2014). Regulation of alpha-endosulfine, an inhibitor of protein phosphatase 2A, by multisite phosphorylation. FEBS J *281*, 1159-1169.
96. Okumura, E., Morita, A., Wakai, M., Mochida, S., Hara, M., and Kishimoto, T. (2014). Cyclin B-Cdk1 inhibits protein phosphatase PP2A-B55 via a Greatwall kinase-independent mechanism. J Cell Biol *204*, 881-889.
97. Kim, M.Y., Bucciarelli, E., Morton, D.G., Williams, B.C., Blake-Hodek, K., Pellacani, C., Von Stetina, J.R., Hu, X., Somma, M.P., Drummond-Barbosa, D., et al. (2012). Bypassing the Greatwall-Endosulfine pathway: plasticity of a pivotal cell-cycle regulatory module in *Drosophila melanogaster* and *Caenorhabditis elegans*. Genetics *191*, 1181-1197.
98. Lorca, T., and Castro, A. (2013). The Greatwall kinase: a new pathway in the control of the cell cycle. Oncogene *32*, 537-543.
99. Wang, P., Galan, J.A., Normandin, K., Bonneil, E., Hickson, G.R., Roux, P.P., Thibault, P., and Archambault, V. (2013). Cell cycle regulation of Greatwall kinase nuclear localization facilitates mitotic progression. J Cell Biol *202*, 277-293.
100. Hegarat, N., Vesely, C., Vinod, P.K., Ocasio, C., Peter, N., Gannon, J., Oliver, A.W., Novak, B., and Hochegger, H. (2014). PP2A/B55 and Fcp1 regulate Greatwall and Ensa dephosphorylation during mitotic exit. PLoS Genet *10*, e1004004.
101. Williams, B.C., Filter, J.J., Blake-Hodek, K.A., Wadzinski, B.E., Fuda, N.J., Shalloway, D., and Goldberg, M.L. (2014). Greatwall-phosphorylated Endosulfine is both an inhibitor and a substrate of PP2A-B55 heterotrimers. Elife *3*, e01695.
102. Wang, P., Larouche, M., Normandin, K., Kachaner, D., Mehsen, H., Emery, G., and Archambault, V. (2016). Spatial regulation of greatwall by Cdk1 and PP2A-Tws in the cell cycle. Cell Cycle *15*, 528-539.
103. Bertram, J.S. (2000). The molecular biology of cancer. Mol Aspects Med *21*, 167-223.
104. Knudson, A.G., Jr. (1974). Heredity and human cancer. Am J Pathol *77*, 77-84.

105. Loeb, L.A., and Harris, C.C. (2008). Advances in chemical carcinogenesis: a historical review and prospective. Cancer Res *68*, 6863-6872.
106. Fortunato, A., Boddy, A., Mallo, D., Aktipis, A., Maley, C.C., and Pepper, J.W. (2017). Natural Selection in Cancer Biology: From Molecular Snowflakes to Trait Hallmarks. Cold Spring Harb Perspect Med *7*.
107. Hanahan, D., and Weinberg, R.A. (2011). Hallmarks of cancer: the next generation. Cell *144*, 646-674.
108. Lee, E.Y., and Muller, W.J. (2010). Oncogenes and tumor suppressor genes. Cold Spring Harb Perspect Biol *2*, a003236.
109. Mathers, C.D., Boerma, T., and Ma Fat, D. (2009). Global and regional causes of death. Br Med Bull *92*, 7-32.
110. Williams, G.H., and Stoeber, K. (2012). The cell cycle and cancer. J Pathol *226*, 352-364.
111. Canavese, M., Santo, L., and Raje, N. (2012). Cyclin dependent kinases in cancer: potential for therapeutic intervention. Cancer Biol Ther *13*, 451-457.
112. Manchado, E., Guillamot, M., and Malumbres, M. (2012). Killing cells by targeting mitosis. Cell Death Differ *19*, 369-377.
113. Weaver, B.A. (2014). How Taxol/paclitaxel kills cancer cells. Mol Biol Cell *25*, 2677-2681.
114. Sinha, D., Duijf, P.H.G., and Khanna, K.K. (2019). Mitotic slippage: an old tale with a new twist. Cell Cycle *18*, 7-15.
115. Orr, G.A., Verdier-Pinard, P., McDaid, H., and Horwitz, S.B. (2003). Mechanisms of Taxol resistance related to microtubules. Oncogene *22*, 7280-7295.
116. Wang, Z., Wan, L., Zhong, J., Inuzuka, H., Liu, P., Sarkar, F.H., and Wei, W. (2013). Cdc20: a potential novel therapeutic target for cancer treatment. Curr Pharm Des *19*, 3210-3214.
117. Garcia, L., Garcia, F., Llorens, F., Unzeta, M., Itarte, E., and Gomez, N. (2002). PP1/PP2A phosphatases inhibitors okadaic acid and calyculin A block ERK5 activation by growth factors and oxidative stress. FEBS Lett *523*, 90-94.
118. Van Hoof, C., and Goris, J. (2004). PP2A fulfills its promises as tumor suppressor: which subunits are important? Cancer Cell *5*, 105-106.
119. Schonthal, A.H. (2001). Role of serine/threonine protein phosphatase 2A in cancer. Cancer Lett *170*, 1-13.
120. Ruvolo, P.P., Qui, Y.H., Coombes, K.R., Zhang, N., Ruvolo, V.R., Borthakur, G., Konopleva, M., Andreeff, M., and Kornblau, S.M. (2011). Low expression of PP2A regulatory subunit B55alpha is associated with T308 phosphorylation of AKT and shorter complete remission duration in acute myeloid leukemia patients. Leukemia *25*, 1711-1717.
121. Remmerie, M., and Janssens, V. (2019). PP2A: A Promising Biomarker and Therapeutic Target in Endometrial Cancer. Front Oncol *9*, 462.
122. Schellhaus, A.K., De Magistris, P., and Antonin, W. (2016). Nuclear Reformation at the End of Mitosis. J Mol Biol *428*, 1962-1985.
123. Rodrigues, N.T., Lekomtsev, S., Jananji, S., Kriston-Vizi, J., Hickson, G.R., and Baum, B. (2015). Kinetochore-localized PP1-Sds22 couples chromosome segregation to polar relaxation. Nature *524*, 489-492.
124. Vagnarelli, P., and Earnshaw, W.C. (2012). Repo-Man-PP1: a link between chromatin remodelling and nuclear envelope reassembly. Nucleus *3*, 138-142.

125. Takagi, M., Nishiyama, Y., Taguchi, A., and Imamoto, N. (2014). Ki67 antigen contributes to the timely accumulation of protein phosphatase 1gamma on anaphase chromosomes. J Biol Chem *289*, 22877-22887.
126. Booth, D.G., Takagi, M., Sanchez-Pulido, L., Petfalski, E., Vargiu, G., Samejima, K., Imamoto, N., Ponting, C.P., Tollervey, D., Earnshaw, W.C., et al. (2014). Ki-67 is a PP1-interacting protein that organises the mitotic chromosome periphery. Elife *3*, e01641.
127. Landsverk, H.B., Kirkhus, M., Bollen, M., Kuntziger, T., and Collas, P. (2005). PNUTS enhances in vitro chromosome decondensation in a PP1-dependent manner. Biochem J *390*, 709-717.
128. Steen, R.L., Martins, S.B., Tasken, K., and Collas, P. (2000). Recruitment of protein phosphatase 1 to the nuclear envelope by A-kinase anchoring protein AKAP149 is a prerequisite for nuclear lamina assembly. J Cell Biol *150*, 1251-1262.
129. Chen, F., Archambault, V., Kar, A., Lio, P., D'Avino, P.P., Sinka, R., Lilley, K., Laue, E.D., Deak, P., Capalbo, L., et al. (2007). Multiple protein phosphatases are required for mitosis in *Drosophila*. Curr Biol *17*, 293-303.
130. Hetzer, M.W. (2010). The nuclear envelope. Cold Spring Harb Perspect Biol *2*, a000539.
131. Beck, M., and Hurt, E. (2017). The nuclear pore complex: understanding its function through structural insight. Nat Rev Mol Cell Biol *18*, 73-89.
132. Fields, A.P., and Thompson, L.J. (1995). The regulation of mitotic nuclear envelope breakdown: a role for multiple lamin kinases. Prog Cell Cycle Res *1*, 271-286.
133. Gerace, L., and Burke, B. (1988). Functional organization of the nuclear envelope. Annu Rev Cell Biol *4*, 335-374.
134. WEI, M.G., TONG, X.J., CHEN, B., ZHANG, B., LIU, Z.F., DING, M.X., and ZHAI, Z.H. (1996). Assembly of lamins in vitro Cell. Cell research *6*, 11-22.
135. Stuurman, N. (1997). Identification of a conserved phosphorylation site modulating nuclear lamin polymerization. FEBS Lett *401*, 171-174.
136. Peter, M., Nakagawa, J., Doree, M., Labbe, J.C., and Nigg, E.A. (1990). In vitro disassembly of the nuclear lamina and M phase-specific phosphorylation of lamins by cdc2 kinase. Cell *61*, 591-602.
137. Peter, M., Heitlinger, E., Haner, M., Aebi, U., and Nigg, E.A. (1991). Disassembly of in vitro formed lamin head-to-tail polymers by CDC2 kinase. EMBO J *10*, 1535-1544.
138. Patterson, K., Molofsky, A.B., Robinson, C., Acosta, S., Cater, C., and Fischer, J.A. (2004). The functions of Klarsicht and nuclear lamin in developmentally regulated nuclear migrations of photoreceptor cells in the *Drosophila* eye. Mol Biol Cell *15*, 600-610.
139. Broers, J.L., Ramaekers, F.C., Bonne, G., Yaou, R.B., and Hutchison, C.J. (2006). Nuclear lamins: laminopathies and their role in premature ageing. Physiol Rev *86*, 967-1008.
140. Stuurman, N., Delbecque, J.P., Callaerts, P., and Aebi, U. (1999). Ectopic overexpression of *Drosophila* lamin C is stage-specific lethal. Exp Cell Res *248*, 350-357.
141. Gonzalez-Aguilera, C., and Askjaer, P. (2012). Dissecting the NUP107 complex: multiple components and even more functions. Nucleus *3*, 340-348.

142. D'Angelo, M.A., and Hetzer, M.W. (2008). Structure, dynamics and function of nuclear pore complexes. Trends Cell Biol *18*, 456-466.
143. Mason, D.A., and Goldfarb, D.S. (2009). The nuclear transport machinery as a regulator of *Drosophila* development. Semin Cell Dev Biol *20*, 582-589.
144. Strambio-De-Castillia, C., Niepel, M., and Rout, M.P. (2010). The nuclear pore complex: bridging nuclear transport and gene regulation. Nat Rev Mol Cell Biol *11*, 490-501.
145. Schooley, A., Vollmer, B., and Antonin, W. (2012). Building a nuclear envelope at the end of mitosis: coordinating membrane reorganization, nuclear pore complex assembly, and chromatin de-condensation. Chromosoma *121*, 539-554.
146. Rout, M.P., and Aitchison, J.D. (2001). The nuclear pore complex as a transport machine. J Biol Chem *276*, 16593-16596.
147. Matreyek, K.A., Yucel, S.S., Li, X., and Engelman, A. (2013). Nucleoporin NUP153 phenylalanine-glycine motifs engage a common binding pocket within the HIV-1 capsid protein to mediate lentiviral infectivity. PLoS Pathog *9*, e1003693.
148. Beaudet, D., Akhshi, T., Phillipp, J., Law, C., and Piekny, A. (2017). Active Ran regulates anillin function during cytokinesis. Mol Biol Cell *28*, 3517-3531.
149. Tessier, T.M., Dodge, M.J., Prusinkiewicz, M.A., and Mymryk, J.S. (2019). Viral Appropriation: Laying Claim to Host Nuclear Transport Machinery. Cells *8*.
150. Raghunayakula, S., Subramonian, D., Dasso, M., Kumar, R., and Zhang, X.D. (2015). Molecular Characterization and Functional Analysis of Annulate Lamellae Pore Complexes in Nuclear Transport in Mammalian Cells. PLoS One *10*, e0144508.
151. Hampoelz, B., Mackmull, M.T., Machado, P., Ronchi, P., Bui, K.H., Schieber, N., Santarella-Mellwig, R., Necakov, A., Andres-Pons, A., Philippe, J.M., et al. (2016). Pre-assembled Nuclear Pores Insert into the Nuclear Envelope during Early Development. Cell *166*, 664-678.
152. Starr, D.A., and Han, M. (2002). Role of ANC-1 in tethering nuclei to the actin cytoskeleton. Science *298*, 406-409.
153. Starr, D.A., and Fischer, J.A. (2005). KASH 'n Karry: the KASH domain family of cargo-specific cytoskeletal adaptor proteins. Bioessays *27*, 1136-1146.
154. Goldberg, M.W., and Allen, T.D. (1995). Structural and functional organization of the nuclear envelope. Curr Opin Cell Biol *7*, 301-309.
155. Wagner, N., and Krohne, G. (2007). LEM-Domain proteins: new insights into lamin-interacting proteins. Int Rev Cytol *261*, 1-46.
156. Barton, L.J., Wilmington, S.R., Martin, M.J., Skopec, H.M., Lovander, K.E., Pinto, B.S., and Geyer, P.K. (2014). Unique and shared functions of nuclear lamina LEM domain proteins in *Drosophila*. Genetics *197*, 653-665.
157. Ye, Q., Callebaut, I., Pezhman, A., Courvalin, J.C., and Worman, H.J. (1997). Domain-specific interactions of human HP1-type chromodomain proteins and inner nuclear membrane protein LBR. J Biol Chem *272*, 14983-14989.
158. Margalit, A., Brachner, A., Gotzmann, J., Foisner, R., and Gruenbaum, Y. (2007). Barrier-to-autointegration factor--a BAFfling little protein. Trends Cell Biol *17*, 202-208.
159. Segura-Totten, M., Kowalski, A.K., Craigie, R., and Wilson, K.L. (2002). Barrier-to-autointegration factor: major roles in chromatin decondensation and nuclear assembly. J Cell Biol *158*, 475-485.

160. Umland, T.C., Wei, S.Q., Craigie, R., and Davies, D.R. (2000). Structural basis of DNA bridging by barrier-to-autointegration factor. Biochemistry *39*, 9130-9138.
161. Samwer, M., Schneider, M.W.G., Hoefler, R., Schmalhorst, P.S., Jude, J.G., Zuber, J., and Gerlich, D.W. (2017). DNA Cross-Bridging Shapes a Single Nucleus from a Set of Mitotic Chromosomes. Cell *170*, 956-972 e923.
162. Furukawa, K., Sugiyama, S., Osouda, S., Goto, H., Inagaki, M., Horigome, T., Omata, S., McConnell, M., Fisher, P.A., and Nishida, Y. (2003). Barrier-to-autointegration factor plays crucial roles in cell cycle progression and nuclear organization in *Drosophila*. J Cell Sci *116*, 3811-3823.
163. Guttinger, S., Laurell, E., and Kutay, U. (2009). Orchestrating nuclear envelope disassembly and reassembly during mitosis. Nat Rev Mol Cell Biol *10*, 178-191.
164. Gong, D., Pomerening, J.R., Myers, J.W., Gustavsson, C., Jones, J.T., Hahn, A.T., Meyer, T., and Ferrell, J.E., Jr. (2007). Cyclin A2 regulates nuclear-envelope breakdown and the nuclear accumulation of cyclin B1. Curr Biol *17*, 85-91.
165. Ward, G.E., and Kirschner, M.W. (1990). Identification of cell cycle-regulated phosphorylation sites on nuclear lamin C. Cell *61*, 561-577.
166. Stuurman, N., Sasse, B., and Fisher, P.A. (1996). Intermediate filament protein polymerization: molecular analysis of *Drosophila* nuclear lamin head-to-tail binding. J Struct Biol *117*, 1-15.
167. Heald, R., and McKeon, F. (1990). Mutations of phosphorylation sites in lamin A that prevent nuclear lamina disassembly in mitosis. Cell *61*, 579-589.
168. Dechat, T., Gotzmann, J., Stockinger, A., Harris, C.A., Talle, M.A., Siekierka, J.J., and Foisner, R. (1998). Detergent-salt resistance of LAP2alpha in interphase nuclei and phosphorylation-dependent association with chromosomes early in nuclear assembly implies functions in nuclear structure dynamics. EMBO J *17*, 4887-4902.
169. Dreger, M., Otto, H., Neubauer, G., Mann, M., and Hucho, F. (1999). Identification of phosphorylation sites in native lamina-associated polypeptide 2 beta. Biochemistry *38*, 9426-9434.
170. Nikolakaki, E., Meier, J., Simos, G., Georgatos, S.D., and Giannakouros, T. (1997). Mitotic phosphorylation of the lamin B receptor by a serine/arginine kinase and p34(cdc2). J Biol Chem *272*, 6208-6213.
171. Courvalin, J.C., Segil, N., Blobel, G., and Worman, H.J. (1992). The lamin B receptor of the inner nuclear membrane undergoes mitosis-specific phosphorylation and is a substrate for p34cdc2-type protein kinase. J Biol Chem *267*, 19035-19038.
172. Hirano, Y., Segawa, M., Ouchi, F.S., Yamakawa, Y., Furukawa, K., Takeyasu, K., and Horigome, T. (2005). Dissociation of emerin from barrier-to-autointegration factor is regulated through mitotic phosphorylation of emerin in a xenopus egg cell-free system. J Biol Chem *280*, 39925-39933.
173. Chase, D., Serafinas, C., Ashcroft, N., Kosinski, M., Longo, D., Ferris, D.K., and Golden, A. (2000). The polo-like kinase PLK-1 is required for nuclear envelope breakdown and the completion of meiosis in Caenorhabditis elegans. Genesis *26*, 26-41.
174. Lenart, P., Petronczki, M., Steegmaier, M., Di Fiore, B., Lipp, J.J., Hoffmann, M., Rettig, W.J., Kraut, N., and Peters, J.M. (2007). The small-molecule inhibitor BI 2536 reveals novel insights into mitotic roles of polo-like kinase 1. Curr Biol *17*, 304-315.

175. de Castro, I.J., Gil, R.S., Ligammari, L., Di Giacinto, M.L., and Vagnarelli, P. (2018). CDK1 and PLK1 coordinate the disassembly and reassembly of the nuclear envelope in vertebrate mitosis. Oncotarget *9*, 7763-7773.
176. Kettenbach, A.N., Schweppe, D.K., Faherty, B.K., Pechenick, D., Pletnev, A.A., and Gerber, S.A. (2011). Quantitative phosphoproteomics identifies substrates and functional modules of Aurora and Polo-like kinase activities in mitotic cells. Sci Signal *4*, rs5.
177. Portier, N., Audhya, A., Maddox, P.S., Green, R.A., Dammermann, A., Desai, A., and Oegema, K. (2007). A microtubule-independent role for centrosomes and aurora a in nuclear envelope breakdown. Dev Cell *12*, 515-529.
178. Tseng, L.C., and Chen, R.H. (2011). Temporal control of nuclear envelope assembly by phosphorylation of lamin B receptor. Mol Biol Cell *22*, 3306-3317.
179. Lusk, C.P., Waller, D.D., Makhnevych, T., Dienemann, A., Whiteway, M., Thomas, D.Y., and Wozniak, R.W. (2007). Nup53p is a target of two mitotic kinases, Cdk1p and Hrr25p. Traffic *8*, 647-660.
180. Miller, M.W., Caracciolo, M.R., Berlin, W.K., and Hanover, J.A. (1999). Phosphorylation and glycosylation of nucleoporins. Arch Biochem Biophys *367*, 51-60.
181. Lancaster, O.M., Cullen, C.F., and Ohkura, H. (2007). NHK-1 phosphorylates BAF to allow karyosome formation in the *Drosophila* oocyte nucleus. J Cell Biol *179*, 817-824.
182. Nichols, R.J., Wiebe, M.S., and Traktman, P. (2006). The vaccinia-related kinases phosphorylate the N' terminus of BAF, regulating its interaction with DNA and its retention in the nucleus. Mol Biol Cell *17*, 2451-2464.
183. Bengtsson, L., and Wilson, K.L. (2006). Barrier-to-autointegration factor phosphorylation on Ser-4 regulates emerin binding to lamin A in vitro and emerin localization in vivo. Mol Biol Cell *17*, 1154-1163.
184. Molitor, T.P., and Traktman, P. (2014). Depletion of the protein kinase VRK1 disrupts nuclear envelope morphology and leads to BAF retention on mitotic chromosomes. Mol Biol Cell *25*, 891-903.
185. Ohsugi, M., Adachi, K., Horai, R., Kakuta, S., Sudo, K., Kotaki, H., Tokai-Nishizumi, N., Sagara, H., Iwakura, Y., and Yamamoto, T. (2008). Kid-mediated chromosome compaction ensures proper nuclear envelope formation. Cell *132*, 771-782.
186. Hetzer, M., Meyer, H.H., Walther, T.C., Bilbao-Cortes, D., Warren, G., and Mattaj, I.W. (2001). Distinct AAA-ATPase p97 complexes function in discrete steps of nuclear assembly. Nat Cell Biol *3*, 1086-1091.
187. Ramadan, K., Bruderer, R., Spiga, F.M., Popp, O., Baur, T., Gotta, M., and Meyer, H.H. (2007). Cdc48/p97 promotes reformation of the nucleus by extracting the kinase Aurora B from chromatin. Nature *450*, 1258-1262.
188. Anderson, D.J., and Hetzer, M.W. (2008). Reshaping of the endoplasmic reticulum limits the rate for nuclear envelope formation. J Cell Biol *182*, 911-924.
189. Stavru, F., Hulsmann, B.B., Spang, A., Hartmann, E., Cordes, V.C., and Gorlich, D. (2006). NDC1: a crucial membrane-integral nucleoporin of metazoan nuclear pore complexes. J Cell Biol *173*, 509-519.
190. Hallberg, E., Wozniak, R.W., and Blobel, G. (1993). An integral membrane protein of the pore membrane domain of the nuclear envelope contains a nucleoporin-like region. J Cell Biol *122*, 513-521.

191. Anderson, D.J., and Hetzer, M.W. (2007). Nuclear envelope formation by chromatin-mediated reorganization of the endoplasmic reticulum. Nat Cell Biol *9*, 1160-1166.
192. Haraguchi, T., Kojidani, T., Koujin, T., Shimi, T., Osakada, H., Mori, C., Yamamoto, A., and Hiraoka, Y. (2008). Live cell imaging and electron microscopy reveal dynamic processes of BAF-directed nuclear envelope assembly. J Cell Sci *121*, 2540-2554.
193. Dabauvalle, M.C., Muller, E., Ewald, A., Kress, W., Krohne, G., and Muller, C.R. (1999). Distribution of emerin during the cell cycle. Eur J Cell Biol *78*, 749-756.
194. Chaudhary, N., and Courvalin, J.C. (1993). Stepwise reassembly of the nuclear envelope at the end of mitosis. J Cell Biol *122*, 295-306.
195. Clever, M., Funakoshi, T., Mimura, Y., Takagi, M., and Imamoto, N. (2012). The nucleoporin ELYS/Mel28 regulates nuclear envelope subdomain formation in HeLa cells. Nucleus *3*, 187-199.
196. Mitchell, J.M., Mansfeld, J., Capitanio, J., Kutay, U., and Wozniak, R.W. (2010). Pom121 links two essential subcomplexes of the nuclear pore complex core to the membrane. J Cell Biol *191*, 505-521.
197. Baur, T., Ramadan, K., Schlundt, A., Kartenbeck, J., and Meyer, H.H. (2007). NSF- and SNARE-mediated membrane fusion is required for nuclear envelope formation and completion of nuclear pore complex assembly in Xenopus laevis egg extracts. J Cell Sci *120*, 2895-2903.
198. Vietri, M., Schink, K.O., Campsteijn, C., Wegner, C.S., Schultz, S.W., Christ, L., Thoresen, S.B., Brech, A., Raiborg, C., and Stenmark, H. (2015). Spastin and ESCRT-III coordinate mitotic spindle disassembly and nuclear envelope sealing. Nature *522*, 231-235.
199. Newport, J.W., Wilson, K.L., and Dunphy, W.G. (1990). A lamin-independent pathway for nuclear envelope assembly. J Cell Biol *111*, 2247-2259.
200. Al-Haboubi, T., Shumaker, D.K., Koser, J., Wehnert, M., and Fahrenkrog, B. (2011). Distinct association of the nuclear pore protein Nup153 with A- and B-type lamins. Nucleus *2*, 500-509.
201. Lussi, Y.C., Hugi, I., Laurell, E., Kutay, U., and Fahrenkrog, B. (2011). The nucleoporin Nup88 is interacting with nuclear lamin A. Mol Biol Cell *22*, 1080-1090.
202. Asencio, C., Davidson, I.F., Santarella-Mellwig, R., Ly-Hartig, T.B., Mall, M., Wallenfang, M.R., Mattaj, I.W., and Gorjanacz, M. (2012). Coordination of kinase and phosphatase activities by Lem4 enables nuclear envelope reassembly during mitosis. Cell *150*, 122-135.
203. Vagnarelli, P., Hudson, D.F., Ribeiro, S.A., Trinkle-Mulcahy, L., Spence, J.M., Lai, F., Farr, C.J., Lamond, A.I., and Earnshaw, W.C. (2006). Condensin and Repo-Man-PP1 co-operate in the regulation of chromosome architecture during mitosis. Nat Cell Biol *8*, 1133-1142.
204. Snyers, L., Erhart, R., Laffer, S., Pusch, O., Weipoltshammer, K., and Schofer, C. (2018). LEM4/ANKLE-2 deficiency impairs post-mitotic re-localization of BAF, LAP2alpha and LaminA to the nucleus, causes nuclear envelope instability in telophase and leads to hyperploidy in HeLa cells. Eur J Cell Biol *97*, 63-74.
205. Zhuang, X., Semenova, E., Maric, D., and Craigie, R. (2014). Dephosphorylation of barrier-to-autointegration factor by protein phosphatase 4 and its role in cell mitosis. J Biol Chem *289*, 1119-1127.

206. Lindqvist, A., Rodriguez-Bravo, V., and Medema, R.H. (2009). The decision to enter mitosis: feedback and redundancy in the mitotic entry network. J Cell Biol *185*, 193-202.
207. Morgan, D.O. (2007). The Cell Cycle: Principles of Control, (London: New Science Press).
208. Archambault, V., Lepine, G., and Kachaner, D. (2015). Understanding the Polo Kinase machine. Oncogene *34*, 4799-4807.
209. Carmena, M., Ruchaud, S., and Earnshaw, W.C. (2009). Making the Auroras glow: regulation of Aurora A and B kinase function by interacting proteins. Curr Opin Cell Biol *21*, 796-805.
210. McCloy, R.A., Parker, B.L., Rogers, S., Chaudhuri, R., Gayevskiy, V., Hoffman, N.J., Ali, N., Watkins, D.N., Daly, R.J., James, D.E., et al. (2015). Global Phosphoproteomic Mapping of Early Mitotic Exit in Human Cells Identifies Novel Substrate Dephosphorylation Motifs. Mol Cell Proteomics *14*, 2194-2212.
211. Rogers, S., McCloy, R., Watkins, D.N., and Burgess, A. (2016). Mechanisms regulating phosphatase specificity and the removal of individual phosphorylation sites during mitotic exit. Bioessays *38 Suppl 1*, S24-32.
212. Wlodarchak, N., and Xing, Y. (2016). PP2A as a master regulator of the cell cycle. Crit Rev Biochem Mol Biol *51*, 162-184.
213. Manchado, E., Guillamot, M., de Carcer, G., Eguren, M., Trickey, M., Garcia-Higuera, I., Moreno, S., Yamano, H., Canamero, M., and Malumbres, M. (2010). Targeting mitotic exit leads to tumor regression in vivo: Modulation by Cdk1, Mastl, and the PP2A/B55alpha,delta phosphatase. Cancer Cell *18*, 641-654.
214. Mayer-Jaekel, R.E., Ohkura, H., Gomes, R., Sunkel, C.E., Baumgartner, S., Hemmings, B.A., and Glover, D.M. (1993). The 55 kd regulatory subunit of *Drosophila* protein phosphatase 2A is required for anaphase. Cell *72*, 621-633.
215. Mochida, S., Maslen, S.L., Skehel, M., and Hunt, T. (2010). Greatwall phosphorylates an inhibitor of protein phosphatase 2A that is essential for mitosis. Science *330*, 1670-1673.
216. Gharbi-Ayachi, A., Labbe, J.C., Burgess, A., Vigneron, S., Strub, J.M., Brioudes, E., Van-Dorsselaer, A., Castro, A., and Lorca, T. (2010). The substrate of Greatwall kinase, Arpp19, controls mitosis by inhibiting protein phosphatase 2A. Science *330*, 1673-1677.
217. Rangone, H., Wegel, E., Gatt, M.K., Yeung, E., Flowers, A., Debski, J., Dadlez, M., Janssens, V., Carpenter, A.T., and Glover, D.M. (2011). Suppression of scant identifies Endos as a substrate of greatwall kinase and a negative regulator of protein phosphatase 2A in mitosis. PLoS Genet *7*, e1002225.
218. Heim, A., Konietzny, A., and Mayer, T.U. (2015). Protein phosphatase 1 is essential for Greatwall inactivation at mitotic exit. EMBO Rep *16*, 1501-1510.
219. Ma, S., Vigneron, S., Robert, P., Strub, J.M., Cianferani, S., Castro, A., and Lorca, T. (2016). Greatwall dephosphorylation and inactivation upon mitotic exit is triggered by PP1. J Cell Sci *129*, 1329-1339.
220. de Castro, I.J., Gokhan, E., and Vagnarelli, P. (2016). Resetting a functional G1 nucleus after mitosis. Chromosoma *125*, 607-619.
221. LaJoie, D., and Ullman, K.S. (2017). Coordinated events of nuclear assembly. Curr Opin Cell Biol *46*, 39-45.
222. Glover, D.M. (1989). Mitosis in *Drosophila*. J Cell Sci *92 (Pt 2)*, 137-146.

223. Uemura, T., Shiomi, K., Togashi, S., and Takeichi, M. (1993). Mutation of twins encoding a regulator of protein phosphatase 2A leads to pattern duplication in *Drosophila* imaginal discs. Genes Dev *7*, 429-440.
224. Ryder, E., Ashburner, M., Bautista-Llacer, R., Drummond, J., Webster, J., Johnson, G., Morley, T., Chan, Y.S., Blows, F., Coulson, D., et al. (2007). The DrosDel deletion collection: a *Drosophila* genomewide chromosomal deficiency resource. Genetics *177*, 615-629.
225. Wassarman, D.A., Solomon, N.M., Chang, H.C., Karim, F.D., Therrien, M., and Rubin, G.M. (1996). Protein phosphatase 2A positively and negatively regulates Ras1-mediated photoreceptor development in *Drosophila*. Genes & Development *10*, 272-278.
226. Yuan, K., and O'Farrell, P.H. (2015). Cyclin B3 is a mitotic cyclin that promotes the metaphase-anaphase transition. Curr Biol *25*, 811-816.
227. Moutinho-Santos, T., Sampaio, P., Amorim, I., Costa, M., and Sunkel, C.E. (1999). In vivo localisation of the mitotic POLO kinase shows a highly dynamic association with the mitotic apparatus during early embryogenesis in *Drosophila*. Biol Cell *91*, 585-596.
228. Machowska, M., Piekarowicz, K., and Rzepecki, R. (2015). Regulation of lamin properties and functions: does phosphorylation do it all? Open Biol *5*.
229. Lyakhovetsky, R., and Gruenbaum, Y. (2014). Studying lamins in invertebrate models. Adv Exp Med Biol *773*, 245-262.
230. Glavy, J.S., Krutchinsky, A.N., Cristea, I.M., Berke, I.C., Boehmer, T., Blobel, G., and Chait, B.T. (2007). Cell-cycle-dependent phosphorylation of the nuclear pore Nup107-160 subcomplex. Proc Natl Acad Sci U S A *104*, 3811-3816.
231. Haraguchi, T., Koujin, T., Segura-Totten, M., Lee, K.K., Matsuoka, Y., Yoneda, Y., Wilson, K.L., and Hiraoka, Y. (2001). BAF is required for emerin assembly into the reforming nuclear envelope. J Cell Sci *114*, 4575-4585.
232. Gorjanacz, M., Klerkx, E.P., Galy, V., Santarella, R., Lopez-Iglesias, C., Askjaer, P., and Mattaj, I.W. (2007). Caenorhabditis elegans BAF-1 and its kinase VRK-1 participate directly in post-mitotic nuclear envelope assembly. EMBO J *26*, 132-143.
233. Hawley, R.S., and Gilliland, W.D. (2006). Sometimes the result is not the answer: the truths and the lies that come from using the complementation test. Genetics *174*, 5-15.
234. White-Cooper, H., Carmena, M., Gonzalez, C., and Glover, D.M. (1996). Mutations in new cell cycle genes that fail to complement a multiply mutant third chromosome of *Drosophila*. Genetics *144*, 1097-1111.
235. Archambault, V., Zhao, X., White-Cooper, H., Carpenter, A.T., and Glover, D.M. (2007). Mutations in *Drosophila* Greatwall/Scant Reveal Its Roles in Mitosis and Meiosis and Interdependence with Polo Kinase. PLoS Genet *3*, e200.
236. Osouda, S., Nakamura, Y., de Saint Phalle, B., McConnell, M., Horigome, T., Sugiyama, S., Fisher, P.A., and Furukawa, K. (2005). Null mutants of *Drosophila* B-type lamin Dm(0) show aberrant tissue differentiation rather than obvious nuclear shape distortion or specific defects during cell proliferation. Dev Biol *284*, 219-232.
237. Yang, S.H., Chang, S.Y., Yin, L., Tu, Y., Hu, Y., Yoshinaga, Y., de Jong, P.J., Fong, L.G., and Young, S.G. (2011). An absence of both lamin B1 and lamin B2 in

keratinocytes has no effect on cell proliferation or the development of skin and hair. Hum Mol Genet *20*, 3537-3544.
238. Hirano, Y., Iwase, Y., Ishii, K., Kumeta, M., Horigome, T., and Takeyasu, K. (2009). Cell cycle-dependent phosphorylation of MAN1. Biochemistry *48*, 1636-1643.
239. Thompson, L.J., Bollen, M., and Fields, A.P. (1997). Identification of protein phosphatase 1 as a mitotic lamin phosphatase. J Biol Chem *272*, 29693-29697.
240. Tekotte, H., Berdnik, D., Torok, T., Buszczak, M., Jones, L.M., Cooley, L., Knoblich, J.A., and Davis, I. (2002). Dcas is required for importin-alpha3 nuclear export and mechano-sensory organ cell fate specification in *Drosophila*. Dev Biol *244*, 396-406.
241. Collier, S., Chan, H.Y., Toda, T., McKimmie, C., Johnson, G., Adler, P.N., O'Kane, C., and Ashburner, M. (2000). The *Drosophila* embargoed gene is required for larval progression and encodes the functional homolog of schizosaccharomyces Crm1. Genetics *155*, 1799-1807.
242. Mehsen, H., Boudreau, V., Garrido, D., Bourouh, M., Larouche, M., Maddox, P.S., Swan, A., and Archambault, V. (2018). PP2A-B55 promotes nuclear envelope reformation after mitosis in *Drosophila*. J Cell Biol *217*, 4106-4123.
243. Billmann, M., Horn, T., Fischer, B., Sandmann, T., Huber, W., and Boutros, M. (2016). A genetic interaction map of cell cycle regulators. Mol Biol Cell *27*, 1397-1407.
244. Link, N., Chung, H., Jolly, A., Withers, M., Tepe, B., Arenkiel, B.R., Shah, P.S., Krogan, N.J., Aydin, H., Geckinli, B.B., et al. (2019). Mutations in ANKLE2, a ZIKA Virus Target, Disrupt an Asymmetric Cell Division Pathway in *Drosophila* Neuroblasts to Cause Microcephaly. Dev Cell.
245. Kaufmann, T., Kukolj, E., Brachner, A., Beltzung, E., Bruno, M., Kostrhon, S., Opravil, S., Hudecz, O., Mechtler, K., Warren, G., et al. (2016). SIRT2 regulates nuclear envelope reassembly through ANKLE2 deacetylation. J Cell Sci *129*, 4607-4621.
246. Yamamoto, S., Jaiswal, M., Charng, W.L., Gambin, T., Karaca, E., Mirzaa, G., Wiszniewski, W., Sandoval, H., Haelterman, N.A., Xiong, B., et al. (2014). A *drosophila* genetic resource of mutants to study mechanisms underlying human genetic diseases. Cell *159*, 200-214.
247. Mastroeni, D., Sekar, S., Nolz, J., Delvaux, E., Lunnon, K., Mill, J., Liang, W.S., and Coleman, P.D. (2017). ANK1 is up-regulated in laser captured microglia in Alzheimer's brain; the importance of addressing cellular heterogeneity. PLoS One *12*, e0177814.
248. Thurmond, J., Goodman, J.L., Strelets, V.B., Attrill, H., Gramates, L.S., Marygold, S.J., Matthews, B.B., Millburn, G., Antonazzo, G., Trovisco, V., et al. (2019). FlyBase 2.0: the next generation. Nucleic Acids Res *47*, D759-D765.
249. Espert, A., Uluocak, P., Bastos, R.N., Mangat, D., Graab, P., and Gruneberg, U. (2014). PP2A-B56 opposes Mps1 phosphorylation of Knl1 and thereby promotes spindle assembly checkpoint silencing. J Cell Biol *206*, 833-842.
250. Decordier, I., Cundari, E., and Kirsch-Volders, M. (2005). Influence of caspase activity on micronuclei detection: a possible role for caspase-3 in micronucleation. Mutagenesis *20*, 173-179.
251. Dawson, I.A., Roth, S., and Artavanis-Tsakonas, S. (1995). The *Drosophila* cell cycle gene fizzy is required for normal degradation of cyclins A and B during mitosis

and has homology to the CDC20 gene of Saccharomyces cerevisiae. J Cell Biol *129*, 725-737.
252. Reed, B.H., and Orr-Weaver, T.L. (1997). The *Drosophila* gene morula inhibits mitotic functions in the endo cell cycle and the mitotic cell cycle. Development *124*, 3543-3553.
253. Hayashi, M.T., and Karlseder, J. (2013). DNA damage associated with mitosis and cytokinesis failure. Oncogene *32*, 4593-4601.
254. Qiao, R., Weissmann, F., Yamaguchi, M., Brown, N.G., VanderLinden, R., Imre, R., Jarvis, M.A., Brunner, M.R., Davidson, I.F., Litos, G., et al. (2016). Mechanism of APC/CCDC20 activation by mitotic phosphorylation. Proc Natl Acad Sci U S A *113*, E2570-2578.
255. Simpson-Lavy, K.J., Zenvirth, D., and Brandeis, M. (2015). Phosphorylation and dephosphorylation regulate APC/C(Cdh1) substrate degradation. Cell Cycle *14*, 3138-3145.
256. Wu, C.G., Chen, H., Guo, F., Yadav, V.K., McIlwain, S.J., Rowse, M., Choudhary, A., Lin, Z., Li, Y., Gu, T., et al. (2017). PP2A-B' holoenzyme substrate recognition, regulation and role in cytokinesis. Cell Discov *3*, 17027.
257. Schlaitz, A.L., Srayko, M., Dammermann, A., Quintin, S., Wielsch, N., MacLeod, I., de Robillard, Q., Zinke, A., Yates, J.R., 3rd, Muller-Reichert, T., et al. (2007). The C. elegans RSA complex localizes protein phosphatase 2A to centrosomes and regulates mitotic spindle assembly. Cell *128*, 115-127.
258. McCright, B., Rivers, A.M., Audlin, S., and Virshup, D.M. (1996). The B56 family of protein phosphatase 2A (PP2A) regulatory subunits encodes differentiation-induced phosphoproteins that target PP2A to both nucleus and cytoplasm. J Biol Chem *271*, 22081-22089.
259. Lince-Faria, M., Maffini, S., Orr, B., Ding, Y., Claudia, F., Sunkel, C.E., Tavares, A., Johansen, J., Johansen, K.M., and Maiato, H. (2009). Spatiotemporal control of mitosis by the conserved spindle matrix protein Megator. J Cell Biol *184*, 647-657.
260. Kim, H.S., Fernandes, G., and Lee, C.W. (2016). Protein Phosphatases Involved in Regulating Mitosis: Facts and Hypotheses. Mol Cells *39*, 654-662.
261. Kolupaeva, V. (2019). Serine-threonine protein phosphatases: Lost in translation. Biochim Biophys Acta Mol Cell Res *1866*, 83-89.
262. Jackson, R.J., Hellen, C.U., and Pestova, T.V. (2010). The mechanism of eukaryotic translation initiation and principles of its regulation. Nat Rev Mol Cell Biol *11*, 113-127.
263. Guertin, D.A., and Sabatini, D.M. (2007). Defining the role of mTOR in cancer. Cancer Cell *12*, 9-22.
264. Dobrikov, M.I., Shveygert, M., Brown, M.C., and Gromeier, M. (2014). Mitotic phosphorylation of eukaryotic initiation factor 4G1 (eIF4G1) at Ser1232 by Cdk1:cyclin B inhibits eIF4A helicase complex binding with RNA. Mol Cell Biol *34*, 439-451.
265. Bush, M.S., Pierrat, O., Nibau, C., Mikitova, V., Zheng, T., Corke, F.M., Vlachonasios, K., Mayberry, L.K., Browning, K.S., and Doonan, J.H. (2016). eIF4A RNA Helicase Associates with Cyclin-Dependent Protein Kinase A in Proliferating Cells and Is Modulated by Phosphorylation. Plant Physiol *172*, 128-140.

266. Jousse, C., Oyadomari, S., Novoa, I., Lu, P., Zhang, Y., Harding, H.P., and Ron, D. (2003). Inhibition of a constitutive translation initiation factor 2alpha phosphatase, CReP, promotes survival of stressed cells. J Cell Biol *163*, 767-775.
267. Eom, T., Muslimov, I.A., Tsokas, P., Berardi, V., Zhong, J., Sacktor, T.C., and Tiedge, H. (2014). Neuronal BC RNAs cooperate with eIF4B to mediate activity-dependent translational control. J Cell Biol *207*, 237-252.
268. Li, Y., Yue, P., Deng, X., Ueda, T., Fukunaga, R., Khuri, F.R., and Sun, S.Y. (2010). Protein phosphatase 2A negatively regulates eukaryotic initiation factor 4E phosphorylation and eIF4F assembly through direct dephosphorylation of Mnk and eIF4E. Neoplasia *12*, 848-855.
269. Winata, C.L., and Korzh, V. (2018). The translational regulation of maternal mRNAs in time and space. FEBS Lett *592*, 3007-3023.
270. Gunaratne, A., and Di Guglielmo, G.M. (2013). Par6 is phosphorylated by aPKC to facilitate EMT. Cell Adh Migr *7*, 357-361.
271. Pippa, R., Dominguez, A., Christensen, D.J., Moreno-Miralles, I., Blanco-Prieto, M.J., Vitek, M.P., and Odero, M.D. (2014). Effect of FTY720 on the SET-PP2A complex in acute myeloid leukemia; SET binding drugs have antagonistic activity. Leukemia *28*, 1915-1918.
272. Saito, S., Miyaji-Yamaguchi, M., Shimoyama, T., and Nagata, K. (1999). Functional domains of template-activating factor-I as a protein phosphatase 2A inhibitor. Biochem Biophys Res Commun *259*, 471-475.
273. Saddoughi, S.A., Gencer, S., Peterson, Y.K., Ward, K.E., Mukhopadhyay, A., Oaks, J., Bielawski, J., Szulc, Z.M., Thomas, R.J., Selvam, S.P., et al. (2013). Sphingosine analogue drug FTY720 targets I2PP2A/SET and mediates lung tumour suppression via activation of PP2A-RIPK1-dependent necroptosis. EMBO Mol Med *5*, 105-121.
274. Liu, Q., Zhao, X., Frissora, F., Ma, Y., Santhanam, R., Jarjoura, D., Lehman, A., Perrotti, D., Chen, C.S., Dalton, J.T., et al. (2008). FTY720 demonstrates promising preclinical activity for chronic lymphocytic leukemia and lymphoblastic leukemia/lymphoma. Blood *111*, 275-284.
275. Neviani, P., Santhanam, R., Oaks, J.J., Eiring, A.M., Notari, M., Blaser, B.W., Liu, S., Trotta, R., Muthusamy, N., Gambacorti-Passerini, C., et al. (2007). FTY720, a new alternative for treating blast crisis chronic myelogenous leukemia and Philadelphia chromosome-positive acute lymphocytic leukemia. J Clin Invest *117*, 2408-2421.
276. Ocasio, C.A., Rajasekaran, M.B., Walker, S., Le Grand, D., Spencer, J., Pearl, F.M., Ward, S.E., Savic, V., Pearl, L.H., Hochegger, H., et al. (2016). A first generation inhibitor of human Greatwall kinase, enabled by structural and functional characterisation of a minimal kinase domain construct. Oncotarget *7*, 71182-71197.
277. Liu, B., Ezeogu, L., Zellmer, L., Yu, B., Xu, N., and Joshua Liao, D. (2015). Protecting the normal in order to better kill the cancer. Cancer Med *4*, 1394-1403.
278. S, S.F., Szczesna, K., Iliou, M.S., Al-Qahtani, M., Mobasheri, A., Kobolak, J., and Dinnyes, A. (2016). In vitro models of cancer stem cells and clinical applications. BMC Cancer *16*, 738.
279. Wirth, T., and Yla-Herttuala, S. (2014). Gene Therapy Used in Cancer Treatment. Biomedicines *2*, 149-162.

280. Riley, M.K., and Vermerris, W. (2017). Recent Advances in Nanomaterials for Gene Delivery-A Review. Nanomaterials (Basel) *7*.
281. Gekara, N.O. (2017). DNA damage-induced immune response: Micronuclei provide key platform. J Cell Biol *216*, 2999-3001.